

Proteomic characterisation of TDP-43 inclusion pathology in  
amyotrophic lateral sclerosis and frontotemporal dementia



**MACQUARIE**  
University

Thomas James Hedl

Centre for Motor Neuron Disease Research

Department of Biomedical Sciences

Faculty of Medicine and Health Sciences

Macquarie University

A thesis written to fulfil the requirements for the degree of Masters of Research in Medicine and  
Health Sciences at Macquarie University

October 2017

Principal Supervisors: Dr Adam K Walker and Dr Albert Lee



---

# CONTENTS

---

Declaration.....	V
Acknowledgements.....	VII
Abstract.....	VIII
List Of Figures.....	IX
List of Tables.....	X
Abbreviations.....	XI
1. Introduction.....	1
1.1 Introduction.....	1
1.2 Epidemiology/Genetics.....	3
1.3 Symptoms/Subtypes of ALS and FTD.....	7
1.4 Human Pathology.....	10
1.5 Treatment.....	12
1.6 Pathogenesis of ALS and FTD.....	14
1.7 TDP-43.....	20
1.8 Animal Models of ALS and FTD.....	24
1.9 Proteomics in ALS/FTD.....	27
2. Aims.....	29
3. Methods.....	31
3.1 General Reagent Preparation / Materials.....	31
3.2 DNA Preparation.....	34
3.3 Mammalian Cell Culture.....	38
3.4 Cell and Mouse Tissue Lysis/Fractionation.....	42
3.5 Protein Quantification.....	43
3.6 Western blotting.....	43
3.7 Proteomics Optimisation.....	46
3.8 In-gel Tryptic Digestion.....	47
3.9 Liquid Chromatograph Electrospray Mass Spectrometry (LC-ESI-MS/MS).....	49
3.10 Fluorescence Microscopy.....	50
3.11 Data and Statistical Analysis.....	51

4. Results .....	53
4.1 Preliminary Optimisation Experiments .....	53
4.2 Validation of Human TDP-43 pcDNA5/TO Expression by Immunocytochemistry .....	56
4.3 Validation of Human TDP-43 pLenti-C-mGFP Expression by Immunocytochemistry .....	60
4.4 Analysis of Urea-soluble Proteins in NSC-34 Transfected Cells.....	63
4.5 A Greater Number of Proteins are Identified in the Urea-soluble Fraction of Aggregate- Prone Human TDP-43 in Transfected NSC-34 Cells.....	72
4.6 Analysis of Urea-soluble Proteins in TDP-43 Transgenic Mice.....	81
4.7 Comparison of rNLS TDP-43 Transgenic Mice Urea-soluble Exclusive Proteins to Human TDP-43 Mutant Urea-soluble Exclusive Proteins from 30 µg or 150 µg NSC-34 Experiments Implicates Those Involved in TDP-43 Aggregate Pathology .....	91
5. Discussion .....	96
5.1 Involvement of Urea-soluble Proteins Detected in Aggregate-prone $\Delta$ NLS+2KQ and $\Delta$ NLS+4FL Human TDP-43 Transfected NSC-34 Cells in ALS/FTD .....	98
5.2 Involvement of Urea-soluble Proteins detected in rNLS TDP-43 Transgenic in ALS/FTD	101
5.3 Future Directions.....	103
5.4 Concluding Statements.....	106
References .....	108
Appendices .....	120
Appendix A – All proteins identified as either exclusive or shared between the 30 µg Urea-soluble fractions of $\Delta$ NLS, 4FL, $\Delta$ NLS+4FL and $\Delta$ NLS+2KQ human TDP-43 Transfections in NSC-34 Cells .....	120
Appendix B – All proteins identified as either exclusive or shared between the 150 µg Urea-soluble fractions of $\Delta$ NLS+4FL and $\Delta$ NLS+2KQ human TDP-43 Transfections in NSC-34 Cells	153
Appendix C – All proteins identified as exclusive in the Urea-soluble fractions from the NEFH- tTA/tetO-hTDP-43 rNLS transgenic mice .....	182

---

# Declaration

---

I certify that this work contains no material which has been accepted for the award of any other degree or diploma in my name, in any university or other tertiary institution and, to the best of my knowledge and belief, contains no material previously published or written by another person, except where due reference has been made in the text. In addition, I certify that no part of this work will, in the future, be used in a submission in my name, for any other degree or diploma in any university or other tertiary institution without the prior approval of Macquarie University. I also certify that this project has had animal ethics approval (AEC Reference: 2015/042, Expiry Date: 14 December 2017)

I give consent to this copy of my thesis, when deposited in the University Library, being made available for loan and photocopying, subject to the provisions of the Copyright Act 1968.

I also give permission for the digital version of my thesis to be made available on the web, via the University's digital research repository, the Library Search and also through web search engines, unless permission has been granted by the University to restrict access for a period of time.

Thomas James Hedl

Centre for Motor Neuron Disease Research

Department of Biomedical Sciences

Faculty of Medicine and Health Sciences

Macquarie University



---

# Acknowledgements

---

I would like to begin with a tremendous thank-you to my extraordinary supervisors, Dr Adam Walker and Dr Albert Lee. Without your support I would not have been able to come as far as I have. You have been more than just supervisors, you are both wonderful friends and role-models who have guided me to success. I am grateful to have received an education from two brilliant minds in this field, a blessing that will last a life time. Thank-you for being patient with me.

I extend this thanks to all the members of the Walker Neurodegeneration Pathobiology Lab and the Atkin Molecular Neurodegeneration Lab. You have all been fantastic friends and colleagues, providing guidance when I required assistance. To Saarin and Christine, there are no two people who I'd rather have gone through the last few years with, I couldn't ask for better friends.

Finally, I wish to thank my parents. Your guidance throughout my life has led me to where I am today and will most definitely lead me further. Thank-you for making me the person I am today.

---

# Abstract

---

Amyotrophic lateral sclerosis (ALS) and frontotemporal dementia (FTD) are part of a spectrum of adult-onset fatal neurodegenerative diseases. ALS begins in either the upper motor neurons of the motor cortex or the lower motor neurons of the brain-stem and spinal cord, resulting in progressive paralysis. FTD however presents in the frontal and temporal lobes of the brain, causing debilitating changes to personality, language and behaviour. The pathological hallmark of both diseases is the presence of low-solubility protein aggregates (which form large inclusions in affected neurons), usually within the cytoplasm. These inclusions consist of both misfolded non-functional proteins as well as functioning proteins that are sequestered due to abnormal interactions or endogenous aggregate-clearance mechanisms. The major inclusion-forming protein in the vast majority of ALS and approximately half of all FTD cases is the DNA/RNA-binding protein TAR DNA-binding protein of 43 kDa (TDP-43), however the other components of TDP-43 pathology in disease remain largely unknown. The aim of this thesis is to characterise the populations of proteins that are present within ALS/FTD-linked TDP-43 inclusions. Various forms of human TDP-43 (wildtype, cytoplasmic-targeted and post-translational mimetics) were expressed in neuronal NSC-34 and SH-SY5Y cells, and brain tissue from a TDP-43 transgenic mouse model was also used. By developing a biochemical low-solubility protein fractionation method, the types of proteins present with the TDP-43 pathology in these cells and brain samples were isolated for shotgun mass spectrometry proteomics. This approach identified many potential disease-associated as well as previously unidentified proteins that may play a role in ALS/FTD pathology. By identifying the types of proteins that are affected in these terrible diseases, it will be possible to understand the pathways and mechanisms through which they act to ultimately target therapeutics and identify biomarkers for people living with ALS and FTD.

---

# List Of Figures

---

Figure 1:1 – The prevalence of inherited and sporadic cases of ALS/FTD .....	4
Figure 1:2 – Genetic Mutation Overlap Between ALS/FTD .....	6
Figure 1:3 – Classic spectrum of MND .....	8
Figure 1:4 – Locations of the Upper and Lower Motor Neurons.....	10
Figure 1:5 – Major proteins involved in ALS/FTD inclusion pathology.....	14
Figure 1:6 – Protein Structure of TDP-43 .....	20
Figure 1:7 - TDP-43 Mislocalisation and Aggregation in ALS/FTD .....	21
Figure 2:1 – Workflow Demonstrating the Techniques used in this Thesis .....	29
Figure 3:1 – pcDNA 5/TO and pLenti-C-mGFP Plasmid Constructs.....	33
Figure 3:2 – Human TDP-43 Myc Mutants .....	33
Figure 4:1 – 100mm Plate Cell Density Optimisation (48 Hours).....	53
Figure 4:2 – Proteomics Optimisation Gel Processing .....	54
Figure 4:3 – Single vs Triple Gel Processing: Number of Unique Proteins .....	55
Figure 4:4 – NSC-34 cells transfected with 5'myc pcDNA5/TO human TDP-43 constructs .....	58
Figure 4:5 – NSC-34 Cell-line Transfection Efficiency .....	59
Figure 4:6 – SH-SY5Y cells transfected with pLenti-c-mGFP human TDP-43 constructs.....	61
Figure 4:7 – SH-SY5Y Transfection Efficiency .....	62
Figure 4:8 – Total and Myc-tagged TDP-43 in the RIPA-soluble Fraction of NSC-34 Cells .....	64
Figure 4:9 – RIPA Western Blot Quantification of (A) Total and (B) Myc-tagged TDP-43 .....	65
Figure 4:10 – Total and Myc-tagged TDP-43 in the Urea-soluble Fraction of NSC-34 Cells .....	66
Figure 4:11 – Urea Western Blot Quantification of (A) Total and (B) Myc-tagged TDP-43.....	67
Figure 4:12 – All Proteins Identified in Urea-soluble Fractions of NSC-34 Cells Transfected with Human TDP-43 .....	69
Figure 4:13 – Total Protein Counts in RIPA/Urea-soluble Fractions for Untransfected, WT, $\Delta$ NLS+4FL and $\Delta$ NLS+2KQ Human-TDP-43 Replicates.....	73
Figure 4:14 – All Proteins Identified in Urea Fractions of NSC-34 Transfected Cells (150 $\mu$ g) .....	75
Figure 4:15 – Panther Database Gene Ontology of Urea-soluble Proteins Exclusive to the $\Delta$ NLS+4FL and $\Delta$ NLS+2KQ human TDP-43 Transfections .....	77
Figure 4:16 – All Unique Proteins Identified in 30 $\mu$ g Urea-soluble Replicates vs 150 $\mu$ g Urea-soluble Replicates.....	79
Figure 4:17 – Total and Human TDP-43 Expression in the RIPA-soluble Fraction of Control and Double Transgenic (NEFH-tTA/tetO-hTDP-43rNLS) Mouse Cortex.....	82
Figure 4:18 – Total and Human TDP-43 Expression in the Urea-soluble Fraction of Control and Double Transgenic (NEFH-tTA/tetO-hTDP-43 $\Delta$ NLS) Mouse Cortex.....	83
Figure 4:19 –All Proteins Identified in Urea-soluble Fractions Across 5 Biological Replicates of (A) Control Mice and (B) rNLS TDP-43 Transgenic Mice.....	84
Figure 4:20 – All Proteins Identified in the Urea-soluble Fractions of Control and rNLS TDP-43 Transgenic Mice.....	85
Figure 4:21 – Panther Database Gene Ontology of Urea-soluble Proteins Exclusive to the rNLS TDP-43 Transgenic Mice.....	88
Figure 4:22 – Total Urea-soluble Fraction Proteins Exclusive to human TDP-43 $\Delta$ NLS, 4FL, $\Delta$ NLS+4FL and $\Delta$ NLS+2KQ (30 $\mu$ g), $\Delta$ NLS+4FL and $\Delta$ NLS+2KQ (150 $\mu$ g) and rNLS TDP-43 Transgenic Mice.....	92

---

# List of Tables

---

Table 1:1 – Genetic Causes of ALS/FTD.....	5
Table 3:1 – Human TDP-43 Constructs Used in this Thesis.....	35
Table 3:2 – Antibody Dilution Table (WB/ICC).....	45
Table 4:1 – Top 10 Exclusive/Shared Proteins in the Urea-soluble Fractions of $\Delta$ NLS, 4FL, $\Delta$ NLS+4FL, $\Delta$ NLS+2KQ Transfected NSC-34 Cells in the 30 $\mu$ g Experiment .....	71
Table 4:2 – Top 10 Exclusive/Shared Proteins in the Urea-soluble Fractions of $\Delta$ NLS+4FL and $\Delta$ NLS+2KQ Transfected NSC-34 Cells in the 150 $\mu$ g Experiment .....	76
Table 4:3 – Top 10 Exclusive Proteins in the Urea-soluble Fraction of the rNLS TDP-43 Transgenic Mice.....	87
Table 4:4 – Proteins with Increased Relative Abundance in Urea-soluble Fractions of rNLS TDP-43 Transgenic Mice .....	89
Table 4:5 – Proteins with Increased Relative Abundance in Urea-soluble Fractions of rNLS TDP-43 Transgenic Mice .....	90
Table 4:6 – Replicate Presence of Urea-soluble Proteins Found in rNLS TDP-43 Transgenic Mice That Either Overlap with Urea-soluble Proteins in Human TDP-43 Mutants from the 30 $\mu$ g or 150 $\mu$ g Experiments.....	93
Table 5:1 – Urea-Soluble Proteins in Aggregate-prone human TDP-43 Transfected NSC-34 Cells Reflect Involvement in ALS/FTD .....	99
Table 5:2 – Urea-Soluble Proteins in rNLS TDP-43 Transgenic Mice Reflect Involvement in ALS/FTD.....	101

---

# Abbreviations

---

<b>8-OHdG</b>	-	8-hydroxy-2'-deoxyguanosine
<b>ALS</b>	-	Amyotrophic lateral sclerosis
<b>AMP</b>	-	Ampicillin
<b>BCA</b>	-	Bicinchoninic assay
<b>BIP</b>	-	Binding immunoglobulin protein
<b>BSA</b>	-	Bovine serum albumin
<b>bvFTD</b>	-	Behavioural variant frontotemporal dementia
<b>CAM</b>	-	Chloramphenicol
<b>CO<sub>2</sub></b>	-	Carbon dioxide
<b>DAPI</b>	-	4',6-Diamidino-2-Phenylindole, Dihydrochloride
<b>dH<sub>2</sub>O</b>	-	Distilled water
<b>DMEM</b>	-	Dulbecco's Modified Eagle Medium
<b>DNA</b>	-	Deoxyribonucleic acid
<b>DTT</b>	-	Dithiothreitol
<b>ER</b>	-	Endoplasmic reticulum
<b>ERAD</b>	-	Endoplasmic reticulum-associated degradation
<b>FBS</b>	-	Foetal bovine serum
<b>FTD</b>	-	Frontotemporal dementia
<b>FTLD</b>	-	Frontal lobar degeneration
<b>FUS</b>	-	Fused in sarcoma
<b>GFP</b>	-	Green fluorescent protein
<b>GlyR-PrLD</b>	-	Glycine rich prion-like domain
<b>hnRNPs</b>	-	Heterogeneous ribonucleoproteins
<b>IAA</b>	-	Iodoacetamide
<b>ICC</b>	-	Immunocytochemistry
<b>iPSCs</b>	-	Induced pluripotent stem cells
<b>IV</b>	-	Intravenous
<b>LB</b>	-	Luria-Bertani
<b>mGFP</b>	-	Membrane-bound green fluorescent protein
<b>MND</b>	-	Motor neuron disease
<b>NMDA</b>	-	N-methyl-D-aspartate
<b>NEFH</b>	-	Neurofilament heavy chain
<b>NES</b>	-	Nuclear export sequence
<b>NLS</b>	-	Nuclear localisation sequence
<b>PAGE</b>	-	Poly-acrylamide gel electrophoresis
<b>PBP</b>	-	Progressive bulbar palsy
<b>PBS</b>	-	Phosphate-buffered saline
<b>PFA</b>	-	Paraformaldehyde
<b>PFNA</b>	-	Progressive non-fluent aphasia
<b>PLS</b>	-	Primary lateral sclerosis
<b>PMA</b>	-	Progressive muscular atrophy
<b>RRM</b>	-	RNA recognition motif
<b>SCRAPPY</b>	-	Spectral Counting Reporting and Analysis Program

<b>SD</b>	-	Semantic/temporal dementia
<b>SDS</b>	-	Sodium dodecyl sulfate
<b>SWATH-MS</b>	-	Sequential window acquisition of all theoretical mass spectra
<b>TBS</b>	-	Tris-buffered saline
<b>TBST</b>	-	Tris-buffered saline + Tween 20
<b>TCTP</b>	-	Translationally controlled tumour protein
<b>TDP-43</b>	-	Transactive response DNA binding protein 43
<b>TNF</b>	-	Tumour necrosis factor
<b>UPR</b>	-	Unfolded protein response
<b>UPS</b>	-	Ubiquitin proteasome system
<b>VEN</b>	-	von Economo neurons
<b>WB</b>	-	Western blot





# 1. Introduction

---

## 1.1 Introduction

Amyotrophic lateral sclerosis (ALS) is a devastatingly fatal neurodegenerative disorder involving the onset and progression of paralysis, culminating in respiratory failure. It is characterised by the gradual death of both upper and lower motor neurons (UMN/LMN) from the brain and brainstem/spinal cord respectively. Although the terms ALS and motor neuron disease (MND) are used interchangeably, ALS is a type of motor neuron disease along with progressive muscular atrophy (PMA), progressive bulbar palsy (PBP) and primary lateral sclerosis (PLS)<sup>1-3</sup>. Historically there have been difficulties in distinguishing between subtypes of motor neuron degenerative disorders alongside cerebral degenerations such as ALS-related dementia. These difficulties arose due to the phenotypic variability as well as pathological, genetic and clinical overlap of the disorders. This made it difficult to identify whether some were variants of the same disorder or completely different disorders. Ince and colleagues (1998) highlighted these classification difficulties and instead proposed that ALS and ALS-related dementia coincide on a spectrum of disease with overlap rather than as separate entities<sup>4</sup>. The proposal was widely accepted due to the strong genetic, clinical pathological linkages found between ALS and frontotemporal dementia (FTD), all of which are discussed below. Elucidation of the molecular pathways leading to onset and progression of pathogenesis in these disorders will be the next step towards discovery of biomarkers and therapeutics.

### 1.1.1 Amyotrophic lateral sclerosis – A brief history

Amyotrophic lateral sclerosis (ALS), also known as Lou Gehrig's disease in the USA after the famous baseball player, was first described in 1874 by French neurologist, Professor Jean-Martin Charcot<sup>5</sup>. He was renowned for his work in the field of anatomical pathology and is hailed as the father of neurology<sup>6</sup>. At the time of his work there was not yet a clinical distinction between diseases of neurogenic and myopathic origin, which added complexity to the diagnosis of syndromes characterised by muscle atrophy and limb weakness<sup>2, 7</sup>. Charcot's major accomplishment in this field was linking the evidence of limb spasticity (now known as one of the upper motor neuron signs of ALS) to corticospinal tract pathology, as well as linking lower motor neuron degeneration to lower motor neuron signs, such as weakness, in limbs<sup>5, 7, 8</sup>. He was responsible for establishing the current clinicopathologic method for defining ALS, criteria that are still used today and confirmed via autopsy<sup>7</sup>. Others also made early contributions to the field, including Jean Cruveilhier, who was the first individual to describe the pathology that later became known as ALS in 1853<sup>9</sup>.

### 1.1.2 Frontotemporal dementia – A brief history

Frontotemporal dementia (FTD) was first characterised by Arnold Pick in 1892 from a routine autopsy of a patient who had suffered progressive mental deterioration<sup>10</sup>. The pathological hallmark of the disorder is frontotemporal lobar degeneration (FTLD) of neurons in the frontal and temporal lobes of the brain, hence the terms FTD and FTLD are sometimes used interchangeably, although FTD is more correctly known as the clinical term and FTLD as the pathological term<sup>11</sup>. FTLD can only be currently confirmed from an autopsy, similar to the verification protocol for ALS. Although classification is still debated, there are generally considered to be three subtypes of FTD; the semantic variant, the behavioural variant, and non-fluent primary progressive aphasia<sup>11</sup>. The disorder historically known as Pick's disease fits within the latter two, pathologically involving the protein Tau in protein aggregates historically known as Pick bodies. Alois Alzheimer was the first to describe the histopathology of the disease a few years after Pick had observed the link between language deficits that accompanied the asymmetric degeneration of cortical neurons<sup>12-14</sup>.

## 1.2 Epidemiology/Genetics

### 1.2.1 Cases of ALS/FTD

The Australian incidence of ALS is 2.74 new cases per 100,000 people per year<sup>15</sup> in comparison to the worldwide median incidence rate of 1.90<sup>16</sup> calculated from a recent systematic global epidemiological review. However, the incidence rate does vary depending on population demographics, as in European populations this value can be from anywhere between 2-16 per 100,000 people per year<sup>17</sup>, suggesting that the Australian incidence is comparable with other regions of the world. There are currently more than 2000 people living with ALS in Australia, and 60% of these cases are men and 40% are women<sup>18</sup>. Since the onset of ALS generally occurs between 55-65 years of age<sup>19</sup>, it is projected that with the current ageing population, the total number of ALS cases worldwide will increase from 222,801 (in 2015) to 376,674 (in 2040)<sup>20</sup>.

FTD is the fourth most common form of dementia and second most common form of young-onset dementia after Alzheimer's disease<sup>21, 22</sup>. The incidence of FTD is estimated to be 10-30 per 100,000 people per year in those aged between 45-65 years<sup>23, 24</sup>. Up to 40% of FTD patients have measurable motor dysfunction, with 15% of all patients meeting eligibility criteria for both FTD and clinical ALS<sup>25, 26</sup>. Likewise, 50% of ALS patients show some degree of functional loss in cognitive tests dependent on the frontal lobe, with 15% of these cases sufficient enough to warrant an FTD diagnosis in addition to ALS<sup>25</sup>. These findings indicate the clinical overlap between these two disorders

### 1.2.2 Economic Impact

The total estimated cost of ALS to Australia in 2015 was AUD\$2.37 billion, which is approximately AUD\$1.1 million AUD per person living with the disease<sup>18</sup>. The total health system costs are estimated to comprise only \$74.4 million of this<sup>18</sup>. The noticeable gap comes from the numerous factors that are easily overlooked when dealing with an illness. These include costs that come from individuals having to leave their jobs due to either being affected directly by the disorder or the carer responsibilities for someone who is. Additional costs include administrative costs, to incorporate assistance programs, either government or non-government funded, which would aim to provide aid and support in the forms of equipment or transport as well as funerals. Transfer costs would

encompass taxation revenue, welfare and disability payments. Each of these costs for just one individual can add up tremendously on top of the already present burden of disease that one has to live with, a cost that cannot be quantitatively or qualitatively measured with accuracy<sup>18</sup>. Similar to ALS, FTD leads to an eventual requirement for 24-hour care, with associated high-cost to society and families of people living with the disease. These numbers highlight the societal impacts of both of these devastating disorders.

### 1.2.3 Genetics

Approximately 10% of all ALS cases are inherited whilst the remaining 90% of cases are of an apparently sporadic origin<sup>26, 27</sup> (**Figure 1:1A**). In contrast, this distribution differs from FTD cases with approximately 60% being sporadic and 40% resulting from inherited genetic mutation<sup>28</sup> (**Figure 1:1B**).

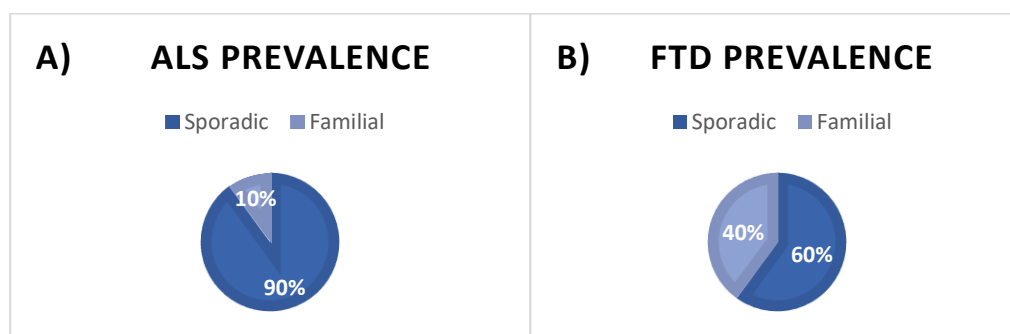


**Figure 1:1 – The prevalence of inherited and sporadic cases of ALS/FTD:** The percentage of cases in both (A) ALS and (B) FTD that are inherited vs sporadic (Adapted from Tan et al. 2017<sup>28</sup>).

Numerous genes have been implicated in increasing susceptibility to and/or causing ALS and FTD when mutated (**Table 1:1**).

**Table 1:1 – Genetic Causes of ALS/FTD:** The different genes that when mutated, contribute to ALS or FTD pathology.

<b>Gene</b>	<b>Protein</b>	<b>Chromosome Location</b>	<b>Disease</b>	<b>Reference</b>
<i>ALS2</i>	Alsin	2q33.1	ALS	29
<i>ALS3*</i>	Unknown	18q21	ALS	30
<i>ALS7*</i>	Unknown	20p13	ALS	31
<i>ANG</i>	Angiogenin	14q11.2	ALS	32, 33
<i>ANXA11</i>	Annexin A11	10q22.3	ALS	34
<i>ATXN2</i>	Ataxin 2	12q24.12	ALS	35
<i>DAO</i>	D-amino-acid oxidase	12q22-23	ALS	36
<i>DCTN1</i>	Dynactin 1	2p13.1	ALS	37
<i>ERBB4</i>	Receptor tyrosine-protein kinase erbB-4	2q34	ALS	38
<i>FIG4</i>	Polyphosphoinositide phosphatase	6q21	ALS	39
<i>HNRNPA1</i>	Heterogeneous nuclear ribonucleoprotein A1	12q13.13	ALS	40
<i>HNRNPA2B1</i>	Heterogeneous Nuclear Ribonucleoprotein A2/B1	7p15.2	ALS	40
<i>MATR3</i>	Matrin 3	5q31.2	ALS	41
<i>NEFH</i>	Neurofilament heavy polypeptide	22q12.2	ALS	42, 43
<i>OPTN</i>	Optineurin	10p13	ALS	44
<i>PDIA1</i>	Protein disulphide-isomerase	17q25	ALS	45, 46
<i>PDIA3</i>	Endoplasmic reticulum resident protein 57	15q15.3	ALS	45, 46
<i>PFN1</i>	Profilin 1	17p13.2	ALS	47
<i>PRPH</i>	Peripherin	12q13.12	ALS	48
<i>SETX</i>	Senataxin	9q34.13	ALS	49
<i>SIGMAR1</i>	Sigma non-opioid intracellular receptor 1	9p13.3	ALS	50
<i>SOD1</i>	Superoxide dismutase 1	21q22.11	ALS	51
<i>SPAST</i>	Spastin	2p22.3	ALS	52
<i>SPG11</i>	Spatascin	15q21.1	ALS	53
<i>UBQLN4</i>	Ubiquilin 4	1q22	ALS	54
<i>VAPB</i>	Vesicle-associated membrane protein-associated protein B/C	20q13.32	ALS	55
<i>C9ORF72</i>	C9ORF72	9p21.2	ALS/FTD	56, 57
<i>CCNF</i>	Cyclin F	16p13.3	ALS/FTD	58
<i>CHCHD10</i>	Coiled-Coil-Helix-Coiled-Coil-Helix Domain Containing 10	22q11.23	ALS/FTD	59
<i>CHMP2B</i>	Charged multivesicular body protein 2B	3p11.2	ALS/FTD	60
<i>FUS</i>	RNA-binding protein FUS/TLS	16p11.2	ALS/FTD	61, 62
<i>SQSTM1</i>	Sequestosome 1	5q35.3	ALS/FTD	63, 64
<i>TARDBP</i>	Transactive response DNA binding protein 43	1p36.22	ALS/FTD	65
<i>TBK1</i>	TANK-binding kinase 1	12q14.2	ALS/FTD	66
<i>TUBA4A</i>	Tubulin alpha-4a	2q35	ALS/FTD	67
<i>UBQLN2</i>	Ubiquilin 2	Xp11.21	ALS/FTD	68
<i>VCP</i>	Valosin-containing protein	9p13.3	ALS/FTD	69, 70
<i>PGRN</i>	Progranulin	17q21.32	FTD	71, 72
<i>MAPT</i>	Microtubule-associated protein Tau	17q21.31	FTD	73
<i>PSEN1</i>	Presenilin 1	14q24.2	FTD	74

Evident from this table, is the genetic overlap between the diseases, robust evidence that supports the 1998 spectrum proposition by Ince and colleagues (1998). There are genetic mutations that are exclusive to each disease, such as *SOD1* in ALS, and *PGRN* and *MAPT* in FTD. In contrast, there are mutations to genes that have been causally linked to both diseases with differing prevalence, such as *FUS* and *TARDBP*, mutations which are more common in ALS, and *VCP* and *CHMP2B* mutations, which are more commonly associated with FTD (**Figure 1:2**).

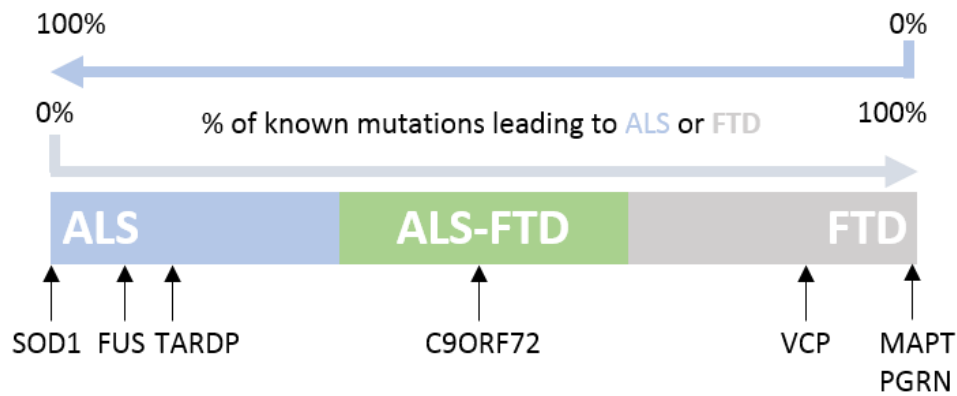


**Figure 1:2 – Genetic Mutation Overlap Between ALS/FTD:** The percentage of known genetic mutations that lead to either ALS or FTD, demonstrating those that are more common or shared in equal proportions between the diseases. (Adapted from Ling et al. 2013)

## 1.3 Symptoms/Subtypes of ALS and FTD

Both ALS and FTD exhibit broad variation in phenotype, age of onset and progression rate. Each of these factors is also influenced by the subtype of disease, genetics as well as environment. Symptoms of ALS can involve UMN or LMN features exclusively or in combination, depending on the subtype<sup>18</sup>. It is not always easy to distinguish between these subtypes. UMN features encompass muscle spasticity, stiffness, slowness, hyperreflexia, such as jaw-jerking, and abnormal gait<sup>75</sup>. LMN features can include, fasciculations, reduced reflexes, limb instability, muscle weakening as well as difficulty breathing<sup>75</sup>. It is common to see signs of both in the same area, for example difficulties with swallowing and speaking with drooling due to spasms, stiffness and muscle-weakening. Cognitive, behavioural and emotional changes may also occur, especially with the presence of associated FTD<sup>76</sup>. Symptoms of FTD include these as well as difficulties with processing language, both in expressing as well as interpreting semantics<sup>11</sup>. In late-stages of both diseases, it is common to see overlap of the clinical phenotypes, and both diseases lead to a requirement for constant care prior to inevitable death, often from pneumonia and respiratory difficulties.

### 1.3.1 MND Subtypes

#### *1.3.1.1 Amyotrophic Lateral Sclerosis (ALS)*

Limb-onset ALS is the most common form of MND, representing more than 70% of all MND cases<sup>77</sup>. Amyotrophic refers to the muscle atrophy associated with the disease, lateral indicates the spinal column involvement and sclerosis refers to scarring or hardening of the tissues that occurs within the spinal cord. Initially patients usually present with LMN signs. As this affects the limbs, they begin to tremor or twitch, accompanied by muscle weakening and stiffness. Symptoms eventually spread encompassing both upper and lower motor neuron signs as both sets of neurons are affected. Survival is approximately 3-5 years after onset of symptoms<sup>18</sup>.

### 1.3.1.2 Progressive bulbar palsy (PBP)

PBP, also known as bulbar-onset ALS, comprises approximately 25% of all MND cases and begins in the bulbar region of the brain, which is composed of the medulla, cerebellum and pons<sup>77, 78</sup>. This region is responsible for many involuntary functions required for life. Onset of PBP involves speech and swallowing deficits, eventually progressing from LMN deterioration to UMN deterioration, and involve symptoms which present initially in cases of limb-onset ALS<sup>78</sup>. Bulbar-onset disease generally results in faster disease progression and survival as short as several months after symptom onset<sup>79</sup>.

### 1.3.1.3 Progressive muscular atrophy (PMA)

PMA onset appears identical to ALS and was thought to exclusively affect only LMNs. Recent results have however implicated UMN features as a later stage of disease progression therefore creating a dilemma where PMA may have to be reclassified<sup>80</sup>. It does differ in the fact that progression of the disease can be significantly slower therefore resulting in a longer survival of up to 10+ years<sup>78, 81, 82</sup>

### 1.3.1.4 Primary lateral sclerosis (PLS)

PLS is an extremely rare case of MND and comprises of less than 2% of all cases. It occurs exclusively in UMN and can only be diagnosed as such with 4 years and no observation of lower motor neuron signs<sup>18</sup>. Survival is generally longer than ALS. Similar to PMA, there is current debate whether or not this subtype exists as a separate entity, therefore diverging from the classic spectrum<sup>78, 81, 82</sup> (**Figure 1:3**). Indeed, PLS may simply represent cases in which progression to full-blown ALS has not yet occurred at the time of death, due to normal variation in rate of disease progression.

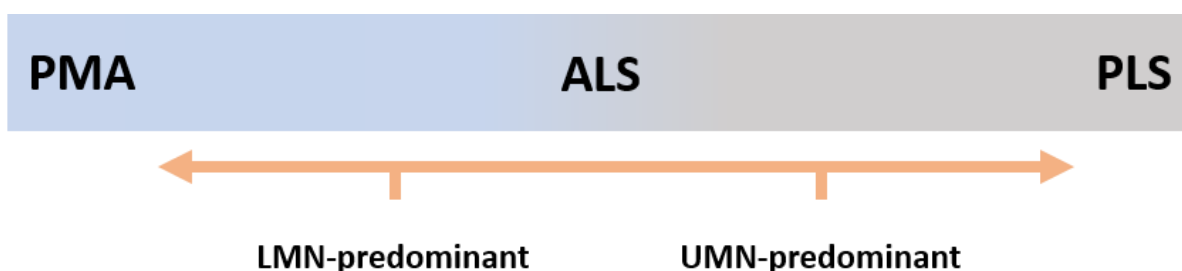


**Figure 1:3 – Classic spectrum of MND:** The classic spectrum of MND illustrating LMN and UMN involvement across ALS, PMA and PLS.

## 1.3.2 FTD

### *1.4.2.1 Behavioural variant frontotemporal dementia (bvFTD)*

The behavioural variant of FTD is the most common type of FTD, accounting for approximately 60% of all FTD patients<sup>83</sup>. In this subtype, people living with FTD often show dramatic and debilitating changes to their personality and behaviour<sup>84</sup>. This often involves divergence from socially-acceptable behaviour, such as breaking the law, sometimes routinely. Eating patterns and consumption can also change along with loss of empathy and, unprovoked emotional outbursts<sup>85-87</sup>.

### *1.4.2.2 Semantic/Temporal dementia (SD)*

Semantic dementia accounts for approximately 20% of all FTD cases<sup>83</sup>. In this variant, people living with FTD lose the ability to understand the meaning of language. The ability to speak and incorporate grammar is retained, however all comprehension is lost<sup>86</sup>. To the observer, this would be equivalent to conversing with an individual who does not speak your language and the person living with FTD may reply with seemingly unintelligible gibberish in later stages of disease.

### *1.4.2.3 Progressive non-fluent aphasia (PNFA)*

Progressive non-fluent aphasia is as prevalent as SD, accounting for 20% of all FTD cases<sup>83</sup>. The symptoms that people living with this form of FTD present with are on the complete opposite side of the spectrum to SD. People living with PNFA are able to comprehend language, but are not able to communicate or express themselves effectively<sup>86</sup>. This is often accompanied with stutters, difficulties pronouncing words and inability to form normal sentence structures.

## 1.4 Human Pathology

### 1.4.1 Amyotrophic lateral sclerosis

As previously discussed, motor neuron cell bodies are present in three areas, the motor cortex in the frontal lobe, the brain stem and the spinal cord. The axons of motor neurons traverse between these areas as well as extend out to muscle fibres all over the body (**Figure 1:4**). In the diseased state these neurons as well as their projections (neurites) exhibit dystrophy and degeneration. This primarily results in a breakdown of axons and synapses before cell bodies, affecting connections to muscle fibres and other neurons prior to cell death. If this process begins in UMNs, the LMNs still innervate the muscle fibres but receive deteriorating and disrupted signal at the synapse from the UMNs<sup>78</sup>. If the process begins in the LMNs, innervation at muscle fibre synapse deteriorates instead, resulting in muscular atrophy<sup>78</sup>. There are many postulated mechanisms behind the cell degeneration, but a pathological hallmark that is seen across all affected cells is the presence of cytoplasmic protein aggregates known as inclusions<sup>88</sup>.

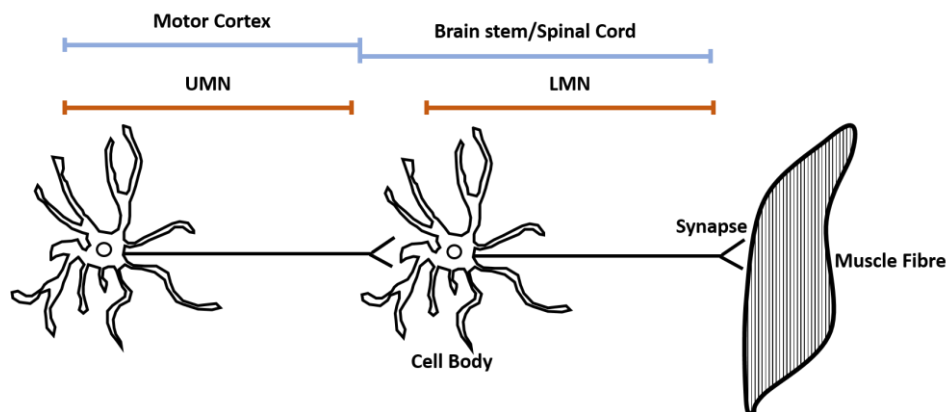


**Figure 1:4 – Locations of the Upper and Lower Motor Neurons:** The extension of the upper and lower motor neurons throughout the brain and spinal cord to muscle fibres all over the body.

### 1.4.2 Frontotemporal Dementia

Neuronal degeneration (FTLD) in FTD occurs in the frontal lobes, anterior temporal lobes, anterior cingulate cortex and insular cortex<sup>84</sup>. Characteristic FTLD demonstrates various pathological features including loss of neurons, gliosis and microvascular changes. In FTLD the main population of cells that seem to be affected are von Economo neurons (VEN), also known as spindle neurons, however overtime there is substantial tissue loss in the described areas<sup>84, 89</sup>. VENs are only present in socially complex animals with large brains and therefore play a crucial yet poorly characterised role in communication between neurons<sup>90, 91</sup>. Like ALS and other neurodegenerative diseases, the pathological hallmark of FTLD is cytoplasmic inclusions in the affected cells. They can occur across cortical layers along with or without the presence of long and short dystrophic neurites.<sup>28</sup>

## 1.5 Treatment

The diagnosis for both ALS and FTD currently operates via the exclusion principle, thus eliminating unlikely diseases based on the symptoms a patient is exhibiting. As with most neurodegenerative disorders they are diagnosed by symptom progression and development over an extended period of time, with confirmation usually not until autopsy. Prognosis is generally poor, as with the most common forms of each disease, death usually occurs at 3-5 years of symptom onset for ALS and 8 years for FTD, however some patients may die within only several months of symptom onset<sup>78, 84</sup>.

There are currently no drugs approved for the specific treatment of FTD, although drugs such as anti-psychotics may be prescribed. There are only two drugs that are FDA approved for the treatment of ALS, namely riluzole and edaravone. Although not very effective, the drugs have been shown to mildly prolong survival.

### 1.5.1 Riluzole

Riluzole until recently has been the only FDA-approved drug for the treatment of ALS. It was approved for use in the US in 1995 after findings in a large cohort of patients demonstrated an increased survival<sup>92</sup>. Since then its effectiveness as a treatment has been shown across numerous models and patient cohorts. Overall however, the drug only increases total life expectancy by 2-3 months on average, rendering it mildly effective, and the drug does not improve quality of life of individual people living with ALS<sup>93</sup>. Riluzole is a glutamate antagonist, however the mechanistic action of the drug is widely disputed<sup>77, 94</sup>. It has been shown to trigger presynaptic inhibition and release of glutamate, inactivate damaged voltage gated sodium channels and noncompetitively bind to N-methyl-D-aspartate (NMDA) receptors as an antagonist<sup>95, 96</sup>. The drug is administered orally through either a tablet or liquid.

### 1.5.2 Edaravone

Edaravone is not a new drug to the market, prior to being available for ALS patients it was used for patients who had suffered from stroke<sup>97</sup>. The mechanism of action is still poorly understood, it is known to be an antioxidant and has recently been shown to suppress oxidative stress and inflammation in the microglia of mice<sup>98,99</sup>. This has implicated it as a promising drug in the treatment of neurodegenerative disorders, however in the context of ALS it has not been as fruitful. Despite failing two clinical trials for the treatment of ALS, edaravone was approved after significant findings in a defined sub-set of patients in a third trial<sup>100-102</sup>. It is administered intravenously (IV), with treatment sessions taking approximately an hour, a more invasive and time-consuming approach than riluzole. However, oral formulation is currently under development and has been tested in mice, with 62% less bioavailability than IV<sup>99</sup>. The drug appears to slow symptom progression rather than extending survival or combating the condition, and was only effective in patients starting treatment early in disease course. Therefore, the widespread usefulness of edaravone for ALS therapy remains unclear.

### 1.5.3 Emerging Therapeutic Approaches

Current clinical trials and research investigate the potential benefits of targeted approaches to directly address the issue the disease is presenting rather than alleviate symptoms or prolong life. Targeted gene therapies using virus packaging constructs, small interfering siRNAs, and anti-sense oligonucleotides against numerous targets have been proven useful in animal studies of ALS and FTD<sup>103-106</sup>. For the results to be conclusive and applicable to patients, further research is required. However, for effective treatments to be developed, comprehensive knowledge of all molecular pathways involved in disease as well as pathogenesis must be developed.

## 1.6 Pathogenesis of ALS and FTD

### 1.6.1 Protein Aggregation and Inclusions

Aggregated proteins, which ultimately form large microscopic inclusions, are the pathological hallmark of neurodegenerative diseases including ALS/FTD<sup>107</sup>. Cytosolic proteins are generally amphipathic, meaning that they are normally hydrophilic on their exterior interacting surfaces, with hydrophobic cores. When misfolded, these cores are exposed and allowed to interact, resulting in an accumulation of abnormally functioning proteins. Functional proteins that normally interact with the misfolded proteins may also be pulled into these inclusions<sup>88</sup>. When aggregated, these proteins exhibit low solubility due to their abnormal interactions, tending to precipitate out in the cytoplasm of cells<sup>88, 108</sup>.

One of the proteins found to be involved in pathology across 97% of ALS cases and 45% of FTD cases is transactive response DNA binding protein 43 (TDP-43) (**Figure 1:6**). Rare disease-linked mutations in the TDP-43 gene (*TARDBP*) have also been causally implicated in ALS, however the vast majority of cases of both diseases with TDP-43 pathology do not show *TARDBP* mutations. Similarly, fused in sarcoma (FUS) is found in inclusions in a minority of patients across both diseases, almost exclusively in rare cases presented with inherited disease-causing *FUS* mutations. Exclusive to FTD is pathology involving the protein Tau, encoded by the *MAPT* gene, which is found in inclusions across 45% of all FTD, again with some of these patients, but not all, showing mutation to the *MAPT* gene<sup>26</sup>.

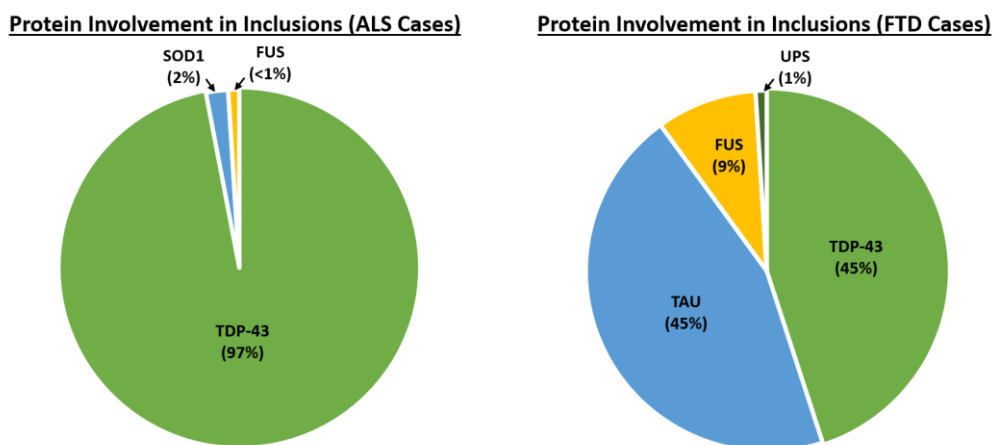


**Figure 1:5 – Major proteins involved in ALS/FTD inclusion pathology:** Proportions of ALS/FTD cases based on the major protein misaccumulated. UPS refers to proteins involved in the ubiquitin proteasome system (Adapted from Ling et al. 2013).

## 1.6.2 Theories of Mechanistic Action

### 1.6.2.1 Dysfunction

#### 1.6.2.1.1 The Unfolded Protein Response and Proteostasis

Protein folding occurs in the endoplasmic reticulum (ER) as part of the protein synthesis pathway. In a normal cellular environment, misfolded proteins are corrected by the unfolded protein response (UPR)<sup>109</sup>. UPR involves a system of ER chaperones that attempt to rectify the issue by stalling the production line and binding immunoglobulin protein (BiP) to the misfolded proteins<sup>110, 111</sup>. In the event of failure, ER-associated degradation (ERAD) is activated by stress proteins that are normally inactively bound to BiP. ERAD involves the misfolded protein being tagged with ubiquitin so that it can be identified by trafficking proteins to be transferred to the proteasome, where it is degraded<sup>109</sup>. If this cannot occur, apoptosis is triggered. In ALS/FTD, misfolded ubiquitinated proteins, some of which may originate from defective ERAD processes and others that are derived from the cytoplasm, accumulate in aggregates and are not cleared, suggesting that the proteasome is unable to degrade them<sup>112</sup>. This is possibly due to insufficient capacity, dysfunction with the machinery/components or being unable to access them within the inclusions<sup>109</sup>.

#### 1.6.2.1.2 Autophagy

Autophagy is the second main process that cells use for degrading aged organelles and proteins. There are three types of autophagy, macro, micro and chaperone-mediated. In macro autophagy, the components designated for degradation are engulfed within a bi-layered membrane (autophagosome) that then fuses to a lysosome (autophagolysosome) that contains enzymes for degradation<sup>113</sup>. In micro autophagy the cytoplasmic contents are directly engulfed by the lysosome, implicating an element of randomness<sup>114</sup>. In chaperone-mediated autophagy, components designated for degradation are escorted directly to the lysosome where they are recruited and engulfed<sup>115</sup>. In ALS/FTD the presence of long-lived protein aggregates suggests that the autophagic machinery is malfunctioning or unable to complete its task. Mutations to several genes implicated in ALS/FTD are related to autophagy (*TBKI*, *OPTN*, *SQSTM1*, *UBQLN2*, *VCP*), implicating functional pathways of autophagy in disease pathogenesis<sup>44, 63, 66, 68, 69</sup>.

#### 1.6.2.1.3 Mitochondrial Dysfunction

Mitochondria are the organelles in the cell responsible for producing energy in the form of ATP from nutrients in the process known as cellular respiration. They also play a crucial role in several other processes such as calcium storage, signalling, apoptosis<sup>116</sup>. By-products of cellular respiration are reactive oxygen species (ROS) such as peroxide and superoxide. These are normally regulated and metabolised to prevent damage to the cell and associated structures within it. In ALS/FTD however ROS levels have been shown to be increased and mitochondria damaged/altered, cumulatively known as oxidative stress<sup>117-119</sup>. Mitochondrial dynamics and structure are compromised and altered in ALS patient motor neurons<sup>118</sup> and in mouse models of ALS<sup>120-122</sup>.

#### 1.6.2.1.4 RNA Metabolism

Numerous genes involved in RNA processing have been implicated in ALS/FTD disease pathology<sup>123</sup>. Inhibition of transcription, defective splicing, interference with mRNA generation and silencing, depletion of RNA binding proteins due to binding to repeat RNAs and negative effects on RNA transport and local translation have all been investigated<sup>26, 123-125</sup>. Mechanisms behind which of these dysfunctions occur are still debated, most likely stemming through a combination of all, as mutations in RNA metabolic protein-encoding genes such as *TARDBP*, *FUS*, *MATR3*, *HNRNPA1* and *HNRNPA2B1* have been directly implicated in disease<sup>40, 41, 61, 65</sup>.

#### 1.6.2.1.5 DNA Damage Repair

Oxidation is hypothesised to be the main cause of DNA damage in neurodegenerative diseases such as ALS/FTD<sup>126</sup>. This type of damage has been shown in both patients and animal models of the disease through increased levels of the oxidation damage marker 8-hydroxy-2'-deoxyguanosine (8-OHdG)<sup>127-129</sup>. The onset of cellular stress due to mitochondrial and ER-stress proteins, ultimately leading to oxidative stress is the most likely explanation for this damage<sup>130</sup>. Failure in the homeostatic processes that normally keep DNA damage in check would not be unlikely considering the various other dysfunctions in disease that have convincing evidence supporting them. Further, 8-oxoguanine DNA glycosylase, an enzyme responsible for clearing 8-OHdG, exhibited impaired activity in the

mitochondria of spinal motor neurons from ALS patients<sup>131</sup>. Mice exhibiting deficiencies in DNA-damage repair pathways also exhibited age-related degeneration of motor neurons<sup>132</sup>.

### 1.6.2.2 Transport Defects

#### 1.6.2.2.1 Axonal/Cytoskeletal Transport

Axonal transport dysfunction refers to the inability for a neuron to maintain transport between cell body and synapse, both retrograde (towards the cell body) and anterograde (away from the cell body)<sup>133</sup>. This process is crucial to ensure long-lived proteins are recycled and connections for travel are maintained between alternate ends of the cell. In human motor neurons these axons can extend up to a metre in length and consist of almost the entirety of the cells volume<sup>134</sup>. This transport network relies on microtubule networks with dynein proteins responsible for retrograde transport and kinesin proteins responsible for anterograde transport<sup>133</sup>. Kinesin mutations in *Drosophila* have been shown to cause ALS phenotypes and ALS-associated mutations in transgenic mice and isolated squid neurons have been shown to disrupt axonal transport<sup>134-137</sup>. Various ALS/FTD genes such as *PFN*, *TUBA4A*, *NEFH*, *MAPT* and *DCTN1* are involved in pathways that directly relate to axonal transport, therefore implicating potential defects in disease<sup>37, 42, 47, 67, 73</sup>.

#### 1.6.2.2.2 Nucleocytoplasmic Transport

The presence of normally nuclear proteins such as TDP-43 and FUS in the cytoplasm in disease pathology has led to discussion regarding nucleocytoplasmic transport<sup>138</sup>. There are no known disease-linked mutations in the TDP-43 nuclear localisation sequence (NLS), which suggests that other mechanisms, such as defects in transport machinery responsible for shuttling between the nucleus and cytoplasm, may be affected in disease to cause cytoplasmic TDP-43 accumulation. However, mutations in the NLS sequence of the gene coding for FUS have been implicated in disease, directly implicating this mechanism in pathogenesis of FUS-linked disease<sup>139</sup>. Investigations have implicated various nuclear transport factors such as transportin-1 to be involved in inclusion-pathology<sup>140, 141</sup>. Due to the increase in relevance of nucleocytoplasmic transport, it is proposed to be the bridge to explain

the loss of nuclear function and cytoplasmic toxic gain of function that occurs to crucial proteins such as TDP-43 and FUS in ALS/FTD<sup>138, 142</sup>.

#### 1.6.2.2.3 Vesicular Transport

Vesicular transport defects are encompassed within many of the previously discussed mechanisms such as axonal transport, autophagy and proteostasis<sup>26, 143</sup>. These defects involve membrane-bound vesicles responsible for trafficking molecules to designated compartments. Typically, this includes shuttling of a protein required for degradation from a compartment such as the ER or a distal location such as a synapse<sup>109</sup>. The proteins affected include cytoskeletal, vesicle tether proteins and recognition molecules bound within vesicles themselves. Recently vesicular transport dysfunction has also been implicated Golgi-vesicle transport, highlighting defects in COPI and COPII transport vesicles, shuttles responsible for Golgi-ER transport, in ALS<sup>144, 145</sup>.

#### 1.6.2.3 Neuroinflammation, Glial Cells and Glutamate excitotoxicity

Neuroinflammation is a process that is mediated by activated glial cells such as astrocytes and microglia<sup>146</sup>. These cells are activated due to interpreting damage signals from neurons, stimulating the release of proinflammatory cytokines such as tumour necrosis factor (TNF) and interleukins<sup>146, 147</sup>. In neurodegeneration, these damage and proinflammatory signals subsist, resulting in a positive feedback loop where more activation signals are sent to activate glial cells thus repeating the process<sup>146</sup>.

Astrocytes are activated in degeneration/death of neurons, and if combined with the positive feedback loop, exhibit astrogliosis, which is an abnormal presence of astrocytes<sup>146, 148</sup>. This neuroprotective mechanism attempts to restore homeostatic balance, however the loss of astrocytic EAAT2/GLT1 transporters in astrocytes has shown to impair glutamate reuptake in ALS patient tissues, and transgenic ALS rats and mice<sup>149-152</sup>.

Astrogliosis in turn can induce another implicated mechanism known as glutamate excitotoxicity, where the degenerating neurons are overstimulated due to excessive extracellular glutamate, leading to further degeneration and death<sup>153</sup>. Glutamate excitotoxicity occurs through influx of calcium ions

which then have impacts throughout cellular mechanisms such as mitochondrial function, ROS metabolism, cytoskeleton formation, DNA metabolism<sup>153, 154</sup>. Therefore, astrocytes can regulate neuron vulnerability to excitotoxicity, such as by modulation of GluR2 expression in motor neurons<sup>155</sup>.

## 1.7 TDP-43

### 1.7.1 Background and Structure of TDP-43

TDP-43 is a nuclear DNA-RNA binding protein that is involved in the regulation of protein synthesis, typically during transcription<sup>125</sup>. TDP-43 is involved in alternate-splicing and transcriptional regulation/repression with more than 40,000 mRNA binding targets<sup>26</sup>.

TDP-43 is a 43kDa, 414 amino acid residue protein with four functionally distinct regions; a nuclear localisation sequence (NLS) that targets it to the nucleus of cells, where it performs many of its functions; two RNA-recognition motifs (RRM1/2) that are important for RNA-binding function; a glycine-rich region that has been shown to be particularly important for protein-protein interactions<sup>156</sup>(**Figure 1:7**).

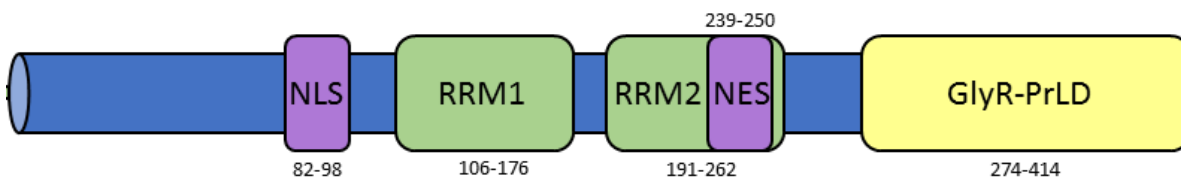


**Figure 1:6 – Protein Structure of TDP-43:** Primary sequence structure of TDP-43 highlighting the four crucial domains for function; the nuclear localisation sequence (NLS), RNA-recognition motifs 1 and 2 (RRM1/2) and the glycine rich prion-like domain (GlyR-PrLD). A nuclear export signal (NES) is also present, which is involved in shuttling of TDP-43 to the cytoplasm.

In TDP-43 pathology the protein mislocalises to the cytoplasm where it is abnormally phosphorylated, ubiquitinated, acetylated and cleaved regardless of whether there is an underlying mutation in *TARDBP* or not<sup>112, 157, 158</sup>. Nuclear TDP-43 clearance as well as formation of abnormal protein aggregates indicates that both loss of normal TDP-43 function and a toxic gain of function may occur related to TDP-43 in ALS and FTD<sup>143</sup>.

## 1.7.2 Role of TDP-43 in Disease

### 1.7.2.1 Nuclear/Cytoplasmic Location

As stated, TDP-43 is predominately nuclear, occasionally shuttling to the cytoplasm where it is then re-localised to the nucleus through detection of its NLS<sup>159</sup>. In pathology, the protein mislocalises to the cytoplasm where it is found predominately aggregated in protein inclusions<sup>143</sup> (**Figure 1.8**). No known mutations have been discovered within the NLS in human cases, therefore implicating other driving factors towards the accumulation of TDP-43 in the cytoplasm. However, in cell and animal models of disease, mutation of the critical lysine K82/arginine R83/lysine K84 residues within the NLS to the functionally inactive alanine (Ala/A) results in cytoplasmic accumulation of TDP-43 reminiscent of that seen in human pathology<sup>160, 161</sup>. This suggests that in model systems the K82A/R83A/K84A mutant TDP-43 is able to recapitulate the pathology formed by as-yet unknown up-stream mechanisms in human disease.

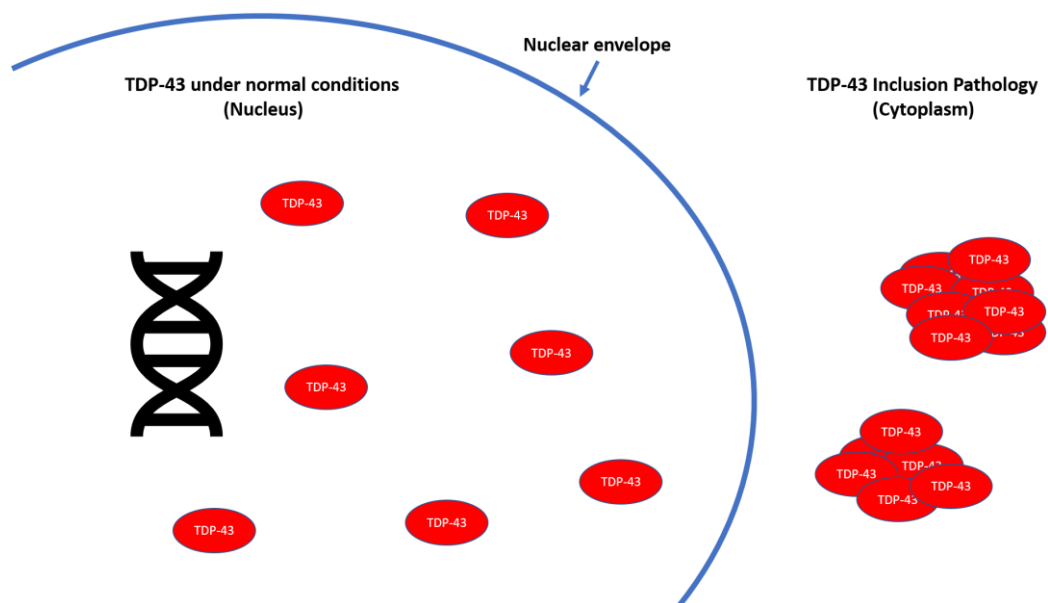


**Figure 1:7 - TDP-43 Mislocalisation and Aggregation in ALS/FTD:** In ALS/FTD, TDP-43 aggregates in the cytoplasm together with other proteins, including misfolded proteins.

### 1.7.2.2 RNA-binding

TDP-43 binds to and regulates expression of thousands of different RNA transcripts, and interactions with RNA are vital for both the normal function of TDP-43 and also for its cytoplasmic localisation. Accumulation of TDP-43 in the cytoplasm can occur under conditions of cellular distress leading to the formation of protein and RNA-containing cytoplasmic stress granules. RNA-binding through the RRM domains is a critical factor in neuronal degeneration in ALS models<sup>162</sup>. TDP-43 binding of RNA is determined by four phenylalanine (Phe/F) residues within the RRMs, and mutation of these F residues to structurally similar but RNA-binding deficient leucine (Leu/L), namely F147L, F149L, F229L and F231L, results in aggregation of the protein<sup>158, 160</sup>. Post-translational modifications of TDP-43, such as phosphorylation and acetylation, which are hallmarks of ALS and FTD pathology, can also compromise the RNA-binding capacity of TDP-43<sup>157, 158</sup>.

### 1.7.2.3 Post-translational modification of TDP-43

#### 1.7.2.3.1 Acetylation

Acetylation has been shown to act as a functional switch for TDP-43, inhibiting the RNA-binding ability of the protein by blocking access to the RRM domains<sup>158</sup>. Acetylation sites in TDP-43 occur on lysine (Lys/K) residues, namely K145 and K192<sup>158, 159</sup>. These residues can be mutated into glycine (Gly/Q) via substitution point mutation, to mimic permanent acetylation through a structural conformation change. Such K145Q/K192Q mutations inhibit TDP-43 function and stimulate protein aggregation, similar to that seen in human disease, suggesting that acetylation at these sites is important in human pathology<sup>158, 159</sup>.

#### 1.7.2.3.2 Phosphorylation

Phosphorylated TDP-43 is characteristic of TDP-43 disease pathology<sup>157</sup>. Phosphorylation sites are serine (Ser/S) and threonine (Thr/T) residues, many of which are in the glycine rich domain, a region that has been shown to be structurally important to protein-protein interactions of TDP-43<sup>163</sup>. The most notable phosphorylation sites in TDP-43 are S403/S404 and S409/S410, and phospho-specific antibodies directed against these residues specifically detect post-translationally modified aggregated TDP-43 found exclusively in disease tissue<sup>164, 165</sup>.

#### 1.7.2.3.3 Ubiquitination

Ubiquitination solicits the degradation of misfolded/abnormal proteins<sup>109</sup>. In ALS/FTD disease pathology, TDP-43, as well as other proteins contained within inclusions are found to be ubiquitinated<sup>112</sup>. This characteristic demonstrates that the protein has been marked for degradation by the proteasome, suggesting that cellular mechanisms have recognised the abnormalities occurring in pathology<sup>109</sup>. Whether or not ubiquitination of TDP-43 plays a causative role in formation of pathology remains unclear.

#### 1.7.2.3.4 Cleavage-fragment

The presence of truncated fragments of TDP-43 have also been implicated in disease pathology<sup>166, 167</sup>. Two C-terminal fragments of approximately 25 and 35kDa are generated from caspase cleavage of TDP-43 at residues 220 and 90 respectively<sup>168</sup>. These fragments, particularly the 25kDa fragment, lose crucial protein domains such as the NLS and RRM sites. Studies have proposed this as a prerequisite for total TDP-43 mislocalisation, although similar to ubiquitination, the role of C-terminal cleaved of TDP-43 in disease pathogenesis remains debated.

## 1.8 Animal Models of ALS and FTD

### 1.8.1 Rodent Models

Animal models have been crucial to the development in understanding of ALS and FTD. One of the first ALS animal models was the SOD1<sup>G93A</sup> mouse, a point substitution mutation of glycine to alanine at the 93<sup>rd</sup> residue of SOD1<sup>169</sup>. Many models began to follow with the discovery of new genes such as *TARDBP*, and new mutations, generated in both rats and mice<sup>161, 170-172</sup>. Due to variation and limitations in models, conflicting points are often raised, such as the TDP-43<sup>A315T</sup> mutation, a mutation that confers disease phenotype on mice but does not exhibit cytoplasmic aggregate TDP-43 pathology<sup>173</sup>. Recently, Walker and colleagues (2015) developed new transgenic mice that do exhibit cytoplasmic TDP-43 inclusion pathology and an ALS-like phenotype<sup>174</sup>. The mice express human TDP-43, with artificial K82A/R83A/K84A/ NLS-site mutations that drive cytoplasmic localisation, under the control of the neurofilament heavy-chain promoter to select for brain and spinal cord neuronal expression, induced by a doxycycline suppression system<sup>174</sup>.

### 1.8.2 Cell Models

#### 1.8.2.1 SH-SY5Y cells

The SH-SY5Y human neuroblastoma cell-line is a useful model in the study of neurodegenerative disorders<sup>175</sup>. Features that make it desirable include the human derived nature, neuronal-like, immortalised and easy to transfect, leading to routine use for studies of Parkinson's disease, Alzheimer's disease, ALS and other neurodegenerative disorders<sup>176-180</sup>. Experiments investigating the various mechanisms involved in neurodegeneration such as ER and oxidative stress are common<sup>181, 182</sup>. Studies providing insight into the effects of phosphorylated and ubiquitinated TDP-43 on protein aggregation and cellular stress have been performed using SH-SY5Y cells<sup>183, 184</sup>. Recently, Liu and colleagues (2017) demonstrated the role of endocytosis in the regulation of TDP-43 toxicity and turnover with the use of SH-SY5Y cells<sup>185</sup>. Due to the ease of locating literature that has utilised the cells, many optimisation experiments and reviews have been performed to determine their validity<sup>177,</sup>

<sup>179, 186</sup>.

#### *1.8.2.2 NSC-34 cells*

The NSC-34 cell-line is a hybrid mouse neuroblastoma combined with mouse spinal cord. Due to this it exhibits several properties that are akin to motor-neurons. This has led to extensive use in the field of ALS, including studies investigating implicated neurodegenerative mechanisms such as protein aggregation<sup>187-189</sup>. In the context of TDP-43 pathology, NSC-34 cells are widely used for studies of mislocalisation, aggregation and cellular dysfunction<sup>190-192</sup>. Recently, Correria and colleagues (2015) demonstrated the inducing effects of inflammation on TDP-43 mislocalisation and aggregation<sup>190</sup>. However, a recent study has described them as unsuitable for the role of studying glutamate-mediated excitotoxicity in ALS due to observing no effects of glutamate on their survival and morphology<sup>193</sup>.

#### *1.8.2.3 Neuro-2A cells*

The Neuro-2a cell-line is derived from a mouse neuroblastoma<sup>194</sup>. It has been used widely in ALS/FTD studies to demonstrate neurodegeneration associated with particular ALS/FTD mutations, such as the GGGGCC repeat expansion found in the first region of the C9ORF72 gene<sup>195</sup>. Conclusive co-localisation studies testing mutants of UBQLN2 with TDP-43 and FUS inclusions have also incorporated the use of Neuro-2a cells<sup>68</sup>. They are also commonly used as subjects for neurotoxicity studies for novel compounds as well as neurodegenerative diseases<sup>196, 197</sup>.

#### *1.8.2.4 Primary mouse neurons*

Primary neuronal cells are harvested from the embryos of mice, and as they are unmodified genuine neural cells they would more closely resemble a real system compared to cell-lines<sup>198</sup>. Difficulty arises when attempting to work with them as they are significantly more difficult to transfect and do not replicate as cell-lines do<sup>199</sup>. Despite this, they are routinely used for neurodegeneration and ALS studies as they are more representative model than cell-lines<sup>198, 200</sup>.

In combination with lentiviral use, effectively modelled systems that closely resemble human pathology can be formulated<sup>201</sup>. Lentiviral vectors allow the targeting of desired gene expression to the central nervous system, a tool with greater efficiency than previously described transfection methods.

They are commonly used in neurodegeneration studies such as in Parkinson's disease and have even shown potential to be used as a treatment delivery system for neurodegenerative diseases<sup>202-204</sup>.

#### *1.8.2.5 Neuronal induced pluripotent stem cells*

Patient-derived neuronal induced pluripotent stem cells (iPSCs) are the most accurate cell model developed, as they can be harvested from patients and even differentiated into motor neurons<sup>205, 206</sup>. As well as model use, they have the potential to be used for personalised medicine as well as develop foundations for drug discovery platforms for treatment of neurodegenerative diseases<sup>207</sup>. The drawback that arises with their use is efficiency, reprogramming cells after extraction can take months, a process which is heavily resource dependent requiring a cocktail of growth factors<sup>205</sup>. However, the future further use of iPSCs in ALS and FTD studies offers a potential high-impact advance in the field.

## 1.9 Proteomics in ALS/FTD

Proteomics-based approaches to elucidate and understand disease mechanism have been beneficial in context of ALS/FTD<sup>26</sup>. They have allowed identification of one of the most prevalent components of the pathology in both diseases, TDP-43 within inclusions is present in 97% of ALS cases as-well as 45% of FTD cases<sup>112, 208, 209</sup>. Mass spectrometry is one of the primary methods utilised, the instrument detects the mass over charge (m/z) ratio of peptides. The identified proteolytic peptides are then searched in expansive databases to identify their respective proteins. The method has been implemented in studies of cerebrospinal fluid (CSF), plasma and patient cells in ALS as well as various neurodegenerative disorders<sup>210, 211</sup>. Proteomics has also been used to investigate biomarkers within the biofluids of patients for various neurodegenerative diseases<sup>212, 213</sup>. Investigative studies into ALS patients to identify biomarkers have also been performed, however further research is required for conclusive results<sup>214</sup>.

Mass spectrometric analysis has been used to identify abnormalities in protein composition within patients brains exhibiting TDP-43 pathology<sup>211</sup>. In ALS/FTD proteomics has been used to study the hallmark phosphorylation and ubiquitination of pathological TDP-43 to identify these modification sites<sup>124, 211</sup>. A global analysis of the interactors of TDP-43 using proteomics has also been performed, identifying two distinct groups of interactors, nuclear RNA metabolism proteins and cytoplasmic mRNA translation proteins<sup>125</sup>. However, only a subset of these were verified with co-immunoprecipitation, demonstrating room for improvement. This study identified a strong association of TDP-43 with RNA splicing, with RNA-dependent and independent interactions, as well as cytoplasmic translation machinery<sup>125</sup>

To our knowledge, no large-scale proteomic studies targeted exclusively towards the protein inclusions containing TDP-43 have been performed. Previous studies have investigated either entire populations of cells or identified singular proteins involved within inclusions through alternate methods such as Western blotting and immunohistochemistry<sup>215-217</sup>. This thesis will address this gap in

knowledge in the ALS/FTD field by performing a proteomic-based study to identify the different proteins that are present within TDP-43 pathology, by examining a range of cytoplasmic and post-translational modification mimic human TDP-43 proteins in neuronal cell culture and an established ALS mouse-model that presents with TDP-43 pathology.

## 2. Aims

---

### Hypothesis:

This suggests that in model systems the K82A/R83A/K84A mutant TDP-43 is able to recapitulate the pathology formed by as-yet unknown up-stream mechanisms in human disease. Proteins involved in TDP-43 inclusion pathology will provide insight into potential mechanisms that are affected in ALS and FTD.

### Aim:

To overall aim of this thesis is to identify the suite of proteins that are present in TDP-43 pathology related to ALS and FTD.

To achieve this aim, the project was divided into several technical components (**Figure 2:1**)

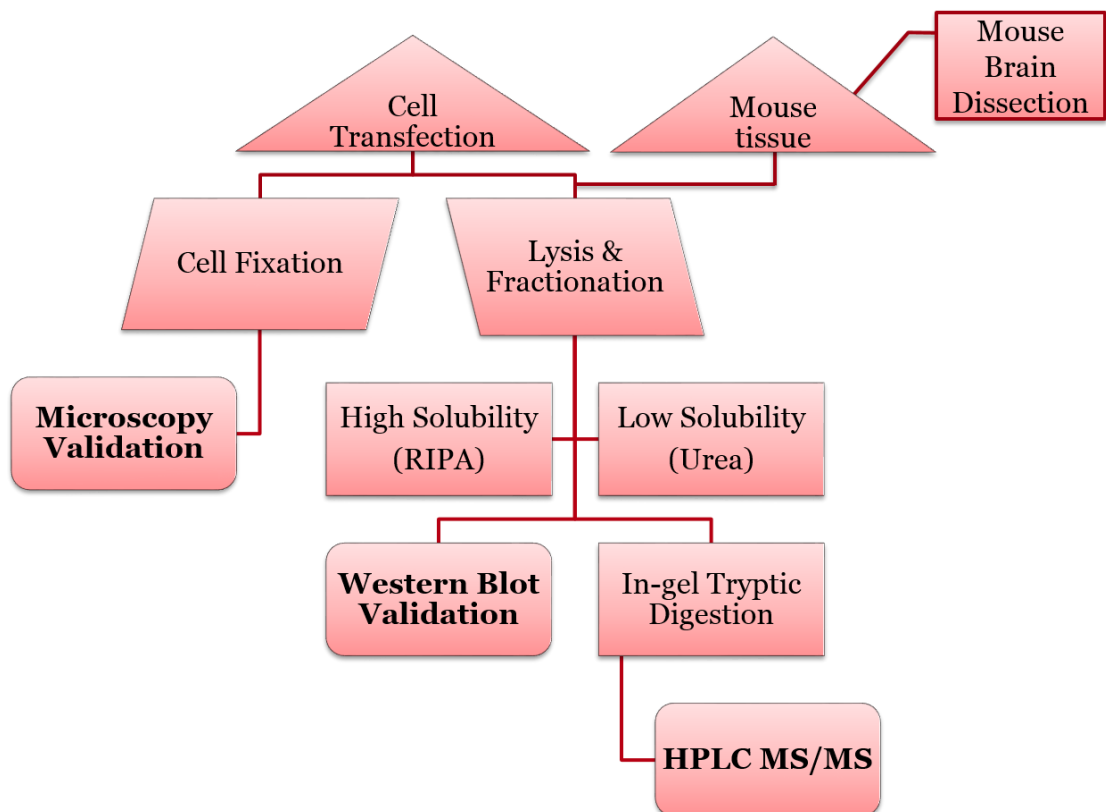


**Figure 2:1 – Workflow Demonstrating the Techniques used in this Thesis**

- Aim 1: To express and characterise in NSC-34 and SH-SY5Y cells both human TDP-43 wildtype (WT) and disease-mimicking mutants: cytoplasmic mislocalisation  $\Delta$ NLS (K82A,R83A,K84A), RNA-binding deficient 4FL (F147L,F149L,F229L,F231L), cytoplasmic mislocalisation RNA-binding deficient  $\Delta$ NLS+4FL(K82A,R83A,K84A, F147L,F149L,F229L,F231L) and cytoplasmic mislocalisation acetylation mimic  $\Delta$ NLS+2KQ (K82A,R83A,K84A,K145Q,K192Q), using immunocytochemistry and immunofluorescence microscopy.
  
- Aim 2: To develop a biochemical fractionation method to specifically isolate low-solubility proteins, typical of aggregated forms found in ALS and FTD pathology.
  
- Aim 3: To identify the low-solubility proteins that are potentially involved in ALS/FTD pathology, using proteomics analysis of NSC-34 and SH-SY5Y cell-line models expressing the various forms of human TDP-43, as well brain tissues isolated from the human TDP-43 transgenic (NEFH-tTA/tetO-h TDP-43 $\Delta$ NLS) mouse model of disease.

# 3. Methods

---

## 3.1 General Reagent Preparation / Materials

### 3.1.1 Reagent Preparation

#### RIPA Buffer

For 1x RIPA buffer with final composition of 50 mM Tris, 150 mM NaCl, 1% NP-40 substitute, 5 mM EDTA, 0.5% sodium deoxycholate, 0.1% sodium dodecyl sulphate (SDS), and 1 mM PMSF, the following were dissolved in a final volume of 10 mL dH<sub>2</sub>O:

0.12 g Tris

0.172 g NaCl

0.1 mL NP-40

0.0372 g EDTA

0.05 g sodium deoxycholate

0.01 g SDS

20 µL PMSF from stock of 250 mg PMSF (50 mM) in 2.87 mL DMSO

PMSF, phosphatase inhibitor cocktail (Roche, 1 tablet per 10 mL) and protease inhibitor cocktail (Roche, 1 tablet per 10 mL) were added to the buffer immediately prior to use.

#### Western blot sample buffer

4x Laemmli buffer, 10x Nu-Page reducing agent and appropriate sample buffer (RIPA/Urea) to adjust loading volumes to be identical.

### Urea Buffer

For 1x Urea buffer with final composition of 7 M Urea, 2 M Thiourea, 4% CHAPS, 30 mM Tris, the following were dissolved in a final volume of 50 mL dH<sub>2</sub>O

22 g Urea

8 g Thiourea

2 g CHAPS

0.18 g Tris

### Luria-Bertani (LB) medium

20 g LB powder mix (Lennox) was dissolved in 1 L milliQ water and pH adjusted to 7.0 by addition of 5 M NaOH, and the solution was autoclaved in a liquid cycle. Autoclaved medium was stored at room temperature until use.

### Luria-Bertani Agar

20 g LB powder mix (Lennox) and 15 g agar were dissolved in 1 L milliQ water and pH adjusted to 7.0 by addition of 5 M NaOH, and the solution was autoclaved in a liquid cycle. Autoclaved medium was stored at room temperature until use.

### 1x Tris-Buffered Saline (TBS)

1.21 g Tris and 8.8 g NaCl were dissolved in 1 L milliQ water

For TBS with Tween 20 (TBS-T), 0.5 mL of Tween-20 was added to the mix prior to dissolving in a final volume of 1 L milliQ water

### 3.1.2 Plasmids and DNA Constructs

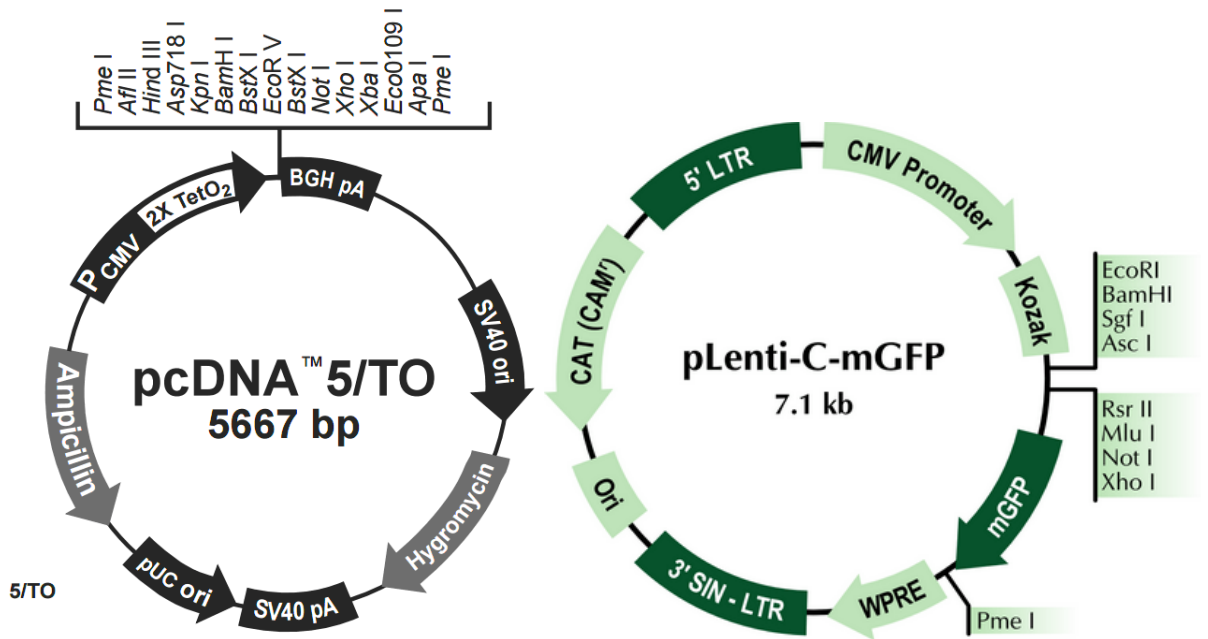


**Figure 3:1 – pcDNA 5/TO and pLenti-C-mGFP Plasmid Constructs:** The two plasmid constructs pcDNA 5/TO and pLenti-C-mGFP that were originally retrieved from Thermo Fisher Scientific and Origene respectively.

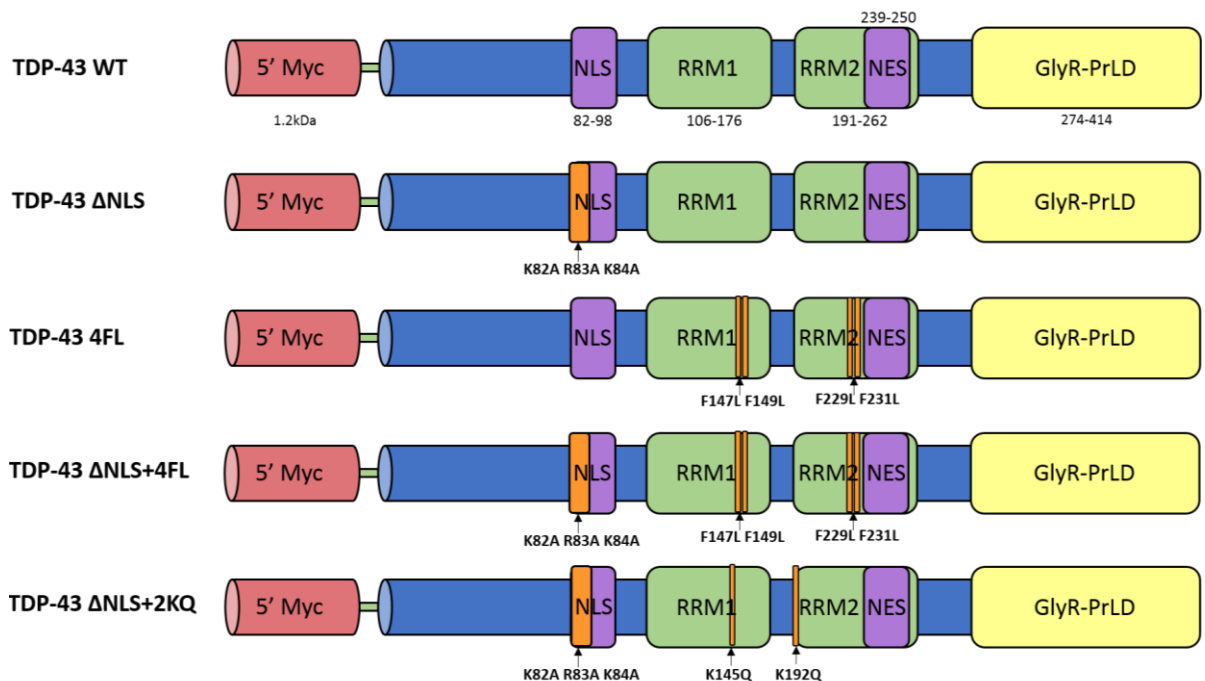


**Figure 3:2 – Human TDP-43 Myc Mutants:** Human TDP-43 mutants generated and supplied by Virginia Lee (University of Pennsylvania) and Todd Cohen (University of North Carolina). See **Table 3:1** for more information.

## 3.2 DNA Preparation

### 3.2.1 DNA Constructs

5'myc-tagged human wildtype TDP-43 cytoplasmic mislocalised ( $\Delta$ NLS) and RNA-binding deficient (4FL), contained within the pcDNA5/TO vector were a gift from Virginia Lee (Centre for Neurodegenerative Research, University of Pennsylvania)<sup>218</sup>. 5'myc-tagged cytoplasmic mislocalised RNA-binding deficient ( $\Delta$ NLS+4FL) and cytoplasmic mislocalised acetylation mimic ( $\Delta$ NLS+2KQ) human TDP-43 constructs contained within the pcDNA5/TO vector were a gift from Dr Todd Cohen (University of North Carolina)<sup>158</sup> (**Table 3:1**).

pLenti-C-mGFP (to express mGFP alone) and human wildtype TDP-43-mGFP pLenti (to express human wildtype TDP-43 with mGFP tag on the C terminus) vectors were purchased from Origene and were provided by Assoc Prof Anna King (University of Tasmania). Mutations to the human wildtype TDP-43-mGFP pLenti vector were introduced by site-directed mutagenesis and sequences were verified by restriction enzyme digestion and vector flanking region and insert target DNA sequencing (Genscript) to generate vectors  $\Delta$ NLS, 4FL, 2KQ,  $\Delta$ NLS+4FL and  $\Delta$ NLS+2KQ (**Table 3:1**).

**Table 3:1 – Human TDP-43 Constructs Used in this Thesis:** The human TDP-43 constructs used in this thesis that were either inserted into the pcDNA5/TO vector or pLenti-C-mGFP vector

Construct ID	Vector	Tag	Human TDP-43	Mutation Sites	Antibiotic / Selection	Source
AKW018	pcDNA5/TO	5'myc	Wild-type	n/a	Ampicillin / Hygromycin	Virginia Lee (UPENN)
AKW004	pcDNA5/TO	5'myc	ΔNLS	K82A, R83A, K84A	Ampicillin / Hygromycin	Virginia Lee (UPENN)
AKW017	pcDNA5/TO	5'myc	4FL	F147L, F149L, F229L, F231L	Ampicillin / Hygromycin	Virginia Lee (UPENN)
AKW020	pcDNA5/TO	5'myc	ΔNLS+4FL	K82A, R83A, K84A, F147L, F149L, F229L, F231L	Ampicillin / Hygromycin	Todd Cohen (UNC)
AKW021	pcDNA5/TO	5'myc	ΔNLS+2KQ	K82A, R83A, K84A, K145Q, K192Q	Ampicillin / Hygromycin	Todd Cohen (UNC)
AKW034	pLenti-C-mGFP	mGFP	Empty vector		Chloramphenicol	Origene, Anna King (UTAS)
AKW035	pLenti-C-mGFP	mGFP	Wild-type	n/a	Chloramphenicol	Origene, Anna King (UTAS)
AKW038	pLenti-C-mGFP	mGFP	ΔNLS	K82A, R83A, K84A	Chloramphenicol	Origene, Genscript
AKW039	pLenti-C-mGFP	mGFP	4FL	F147L, F149L, F229L, F231L	Chloramphenicol	Origene, Genscript
AKW040	pLenti-C-mGFP	mGFP	2KQ	K145Q, K192Q	Chloramphenicol	Origene, Genscript
AKW043	pLenti-C-mGFP	mGFP	ΔNLS+4FL	K82A, R83A, K84A, F147L, F149L, F229L, F231L	Chloramphenicol	Origene, Genscript
AKW044	pLenti-C-mGFP	mGFP	ΔNLS+2KQ	K82A, R83A, K84A, K145Q, K192Q	Chloramphenicol	Origene, Genscript

### 3.2.2 Transformation

50  $\mu$ L of Alpha-select gold competent *Escherichia coli* cells (Bioline) were thawed on ice and then gently mixed ~100 ng of DNA from each construct and incubated for 30 minutes on ice. To stimulate DNA uptake and permeabilise cell membranes for transformation, the cells were heat-shocked at 42°C for 45 seconds followed by a further incubation period on ice for 2 minutes. The cells were then diluted with S.O.C media (1:6, Thermo Fisher Scientific) and shaken horizontally at 37°C for 1 hour. The newly transformed cells were spread onto either ampicillin (AMP, Sigma-Aldrich, 100  $\mu$ g/mL) or chloramphenicol (CAM, Sigma-Aldrich, 25  $\mu$ g/mL) coated Luria Bertani (LB) medium agar plates for pcDNA5/TO and pLenti-C-mGFP constructs, respectively. The streaked LB agar plates were then inverted and incubated at 37°C overnight to allow growth of transformed bacteria colonies.

### 3.2.3 Maxi-prep DNA Preparation

A single colony from each plate was selected and inoculated into 5 mL of LB media broth with appropriate antibiotic selection (100  $\mu$ g/mL AMP or 25  $\mu$ g/mL CAM), followed by a 6-hour incubation at 37°C on a rotating shaker. An aliquot of this starter culture was then diluted 1:1000 in fresh LB media broth with appropriate selection (100  $\mu$ g/mL AMP or 25  $\mu$ g/mL CAM) in a 500 mL flask, leaving 3/4 of the volume of the flask as air to allow space for respiration. The flask was left overnight (14-16 hours) at 37°C on a rotating shaker.

Bacterial cells were harvested via centrifugation in a Sorvall Lynx 4000 at 6000 *g* for 15 minutes at 4°C. DNA was extracted using a Maxi-plus plasmid prep kit (Qiagen), following manufacturers protocol. Briefly, the cell pellet was resuspended in Buffer P1, lysed with Buffer P2 to release DNA and neutralised with Buffer S3. The cell debris was then filtered out through QIAfilter cartridge and Buffer BB was added to the filtrate. The filtered lysate was then passed through a Qiagen Plasmid *Plus* spin column under 300 mbar vacuum pressure, which bound the DNA via anion-exchange. The column was washed with Buffer ETR and Buffer PE and the DNA was eluted with 200  $\mu$ L of dH<sub>2</sub>O.

### 3.2.4 Calculation of DNA Concentration

DNA concentration was measured via absorbance, using a NanoDrop 2000 spectrophotometer (Thermo Fisher Scientific). To assess purity, 260 nm/0 nm as well as 260 nm/230 nm values were calculated. Acceptable levels were  $1.8 \pm 0.1$  (260/280) and  $2.2 \pm 0.1$  (260/230).

### 3.3 Mammalian Cell Culture

#### 3.3.1 Cell Lines

SH-SY5Y cells were a gift from Assoc Prof. Julie Atkin and were sourced from ATCC (#CRL-2266).

NSC-34 cells were a gift from Assoc Prof. Julie Atkin and were sourced from Professor Neil Cashman (University of Toronto, Ontario, Canada). Short Tandem Repeat DNA profiling was not used to confirm cell line identity, although this approach may be useful in future studies.

#### 3.3.2 Cell Growth and Routine Passage

Cells were grown in Dulbecco's Modified Eagle Medium (DMEM) + 10% (v/v) foetal bovine serum (FBS) (Sigma-Aldrich, SAFC Biosciences) at 37°C, 5% CO<sub>2</sub>. Cells were routinely grown in the absence of antibiotic/antimycotic to allow detection of contamination and prevent masking of deficiencies in aseptic technique. Cells were routinely passaged every 4-5 days (prior to reaching confluency) to ensure continued growth. To passage cells, the media was removed, cells were washed with phosphate-buffered saline (PBS, Life Technologies) and incubated for ~2 minutes at 37°C, 5% CO<sub>2</sub> in Trypsin/EDTA (Sigma-Aldrich) solution until cells visibly detached. Cells were then suspended in DMEM+10% FBS (v/v) and centrifuged at 1500 g for 5 minutes. The cell pellet was resuspended in DMEM + 10% FBS (v/v) and a 1:10 aliquot of this suspension was seeded into a new flask containing fresh DMEM + 10% FBS (v/v). A total of 5 biological replicates between the passage number range of 8 and 12 were used in this study.

### 3.3.3 Mycoplasma Testing

Bimonthly mycoplasma testing was carried out using a MycoAlert Mycoplasma Detection Kit (Lonza) according to manufacturer's protocol. This test measures ATP luminescence through first lysing cells and converting ADP to ATP (Substrate A) followed by addition of a luciferase enzyme (Substrate B) to convert the ATP signal to light. Media samples from cells growing for at least two days were taken and combined with Substrate A from the kit onto a white-walled 96-well plate (Corning). A baseline luminescence reading across the visible spectrum was then taken in triplicates using a PHERAstar FS (BMG Labtech). Addition of Substrate B containing the luciferase then allowed a second luminescence reading to be taken. The ratio produced from the comparison of these values was an indicator of whether cells were contaminated with mycoplasma. Cells with a ratio less than 0.9 were regarded as negative for mycoplasma contamination and those with a ratio greater than 1.2 were regarded as positive for mycoplasma contamination. Samples that returned values of 0.9-1.2 were regarded as inconclusive and were retested.

### 3.3.4 Long-term Storage of Cell Lines

1mL aliquots of cells (approximately  $3 \times 10^6$  cells prior to seeding) were diluted to a final concentration of 10% Dimethyl sulfoxide (v/v, DMSO, Sigma-Aldrich) in cryogenic vials and frozen overnight in a CoolCell (Sigma-Aldrich) at  $-80^{\circ}\text{C}$  according to manufacturer's protocol. 24 hours post-freezing, the cryogenic vials were transferred to long-term vapour phase liquid nitrogen storage ( $\sim 190^{\circ}\text{C}$ ). When thawed, cells were immediately suspended in DMEM + 10% FBS (v/v) and centrifuged at 1500 g for 5 minutes. The cell pellet was resuspended in fresh DMEM + 10% FBS (v/v) and a 1:5 aliquot of this suspension was seeded into a new flask containing fresh DMEM + 10% FBS (v/v).

### 3.3.5 Cell Density

Cells were counted manually using a Hauser phase contrast hemocytometer (Thermo Fisher Scientific) according to manufacturer's protocol. To do this, a 1:10 dilution of cells in DMEM + 10% FBS (v/v) were diluted 1:1 with Trypan Blue (Sigma-Aldrich). The number of cells in a total of 8

cubic millimetre squares were counted and averaged. This value was then utilised in the following formula to calculate the density of cells per millilitre in the current suspension.

$$\text{Cell density} = \text{Average cell count} \times 20 \text{ (dilution factor)} \times 10 \times 1000 \text{ (conversion to mL)}$$

To calculate the required volume for a desired cell density the classic dilution equation was utilised and rearranged:

$$C_1V_1 = C_2V_2$$

$$\text{Volume of cells required} = \frac{\text{Desired cell density}}{\text{Calculated cell density}} \times 1000 \text{ (conversion to } \mu\text{L)}$$

Optimisation experiments were performed with 4 different concentrations of cells ( $1 \times 10^6$ ,  $1.5 \times 10^6$ ,  $2 \times 10^6$  and  $2.5 \times 10^6$ ) grown in 100 mm treated culture dishes (Corning). At the 48-hour time-point images of these cells were captured at 4x magnification and a concentration of  $2 \times 10^6$  cells was identified as suitable for desired 70-80% confluency after 48 hours (**Results 4.1.1**).

### 3.3.6 Transfection

$2 \times 10^6$  cells were plated on 100 mm treated culture dishes in DMEM + 10% FBS and incubated for 46-50 hours at 37°C and 5% CO<sub>2</sub>. After this time, cells were approximately 70-80% confluent. 25  $\mu\text{L}$  of Lipofectamine 2000 was brought up to a total volume of 350  $\mu\text{L}$  with Opti-MEM media (Life Technologies) and left to incubate for 10 minutes at room temperature. 7.5  $\mu\text{g}$  of prepared DNA was brought up to a total volume of 300  $\mu\text{L}$  with Opti-MEM media (Life Technologies). These mixtures were then combined and left to incubate at room temperature for 20 minutes. The cell media was then aspirated and the combined mixtures were added dropwise to the cells. Cells were left to incubate like this for 5-7 hours at 37°C and 5% CO<sub>2</sub> before transfection media was completely removed and replaced with fresh DMEM+10% FBS.

### 3.3.7 Cell Harvesting

Following transfection, cells were incubated for another 46-50 hours before they were harvested on ice via scraping with 1 mL ice cold PBS (Life Technologies). The supernatant was collected and the cells were harvested via centrifugation at 1500 g for 5 minutes at 22°C. Cell pellets were resuspended in 1 mL ice cold PBS, transferred to a 1.5 mL Eppendorf tube and centrifuged at 16,000 g in an Eppendorf 5424 benchtop centrifuge for 30 seconds. The PBS was aspirated and the cell pellets were snap frozen on dry ice.

### 3.3.8 Mice

Transgenic TDP-43 rNLS mice (NEFH-tTA × hTDP-43ΔNLS bigenic mice) expressing mutant human TDP-43 in cytoplasm of neurons were bred at the Australian BioResources (Moss Vale, Australia) under specific pathogen-free environment. Monogenic NEFH-rTA mice (stock number #025397) and tetO-hTDP-43ΔNLS mice (stock number #014650) were obtained from the Jackson Laboratory (Bar Harbour, ME, USA)<sup>174</sup>. TDP-43 rNLS mice and litter matched non-bigenic mice were transferred to and housed in the Central Animal Facility at Macquarie University for experiments (AEC Reference No.: 2015/042-8). All animals were housed under identical conditions in a 12-hour light/dark cycle with free access to water and food. Animal experiments were approved by Macquarie University Animal Ethics Committee and adhered to the Australian code of practice for the care and use of animals for scientific purposes. At ~6 weeks of age, mice were removed from doxycycline-containing feed to induce hTDP-43ΔNLS expression. At 4 weeks after doxycycline removal, mice were killed by CO<sub>2</sub> asphyxiation and brains rapidly dissected and snap-frozen on dry ice and stored at -80 °C until processing.

### 3.4 Cell and Mouse Tissue Lysis/Fractionation

Cell lysis was performed in 400  $\mu$ l of radioimmunoprecipitation assay buffer (RIPA, 50 mM Tris, 150 mM NaCl, 1% NP-40 substitute, 5 mM EDTA, 0.5% sodium deoxycholate, 0.1% sodium dodecyl sulphate, 1 mM PMSF in DMSO, phosphatase inhibitor cocktail [Roche] and protease inhibitor cocktail [Roche]). A titanium micro-tip on an ultrasonic homogeniser (Omni International) was utilised at 30% power capacity for two rounds of 10 x 1” bursts, placing on ice between rounds. Homogenised cell lysates were then spun in an Optima Max Ultracentrifuge (Beckman Coulter) at 100,000 g, 4°C for 30 minutes. The supernatant was collected and labelled as the RIPA “soluble” fraction. The cell pellet was subsequently washed with 200  $\mu$ L RIPA buffer, probe sonicated with 10 x 1” bursts followed by ultracentrifugation (2x) as earlier described, to remove as many RIPA-soluble proteins as possible. These supernatants were discarded. A final round of 10 x 1” burst-sonication was performed with urea buffer (7 M Urea, 2 M Thiourea, 4% CHAPS, 30 mM Tris), followed by identical ultracentrifugation and the resulting supernatant was collected as the urea fraction. The tiny pellet that remained was stored at -80°C in the event of further extraction with formic acid for confirmation/further analysis.

The lysis and fractionation method described above was also utilised on fresh-frozen left cortex samples from bigenic rNLS (NEFH-tTA/tetO-hTDP-43 $\Delta$ NLS double transgenic) mice as well as sex- and litter-matched non-bigenic control mice. Weight of the mouse cortex samples was measured prior to use so that proportionate volumes of buffer were used across each sample. 5  $\mu$ L of RIPA buffer was used per mg of tissue followed by 2  $\mu$ L of urea buffer per mg of the original tissue weight.

### 3.5 Protein Quantification

RIPA-soluble fraction samples were diluted 1:5 in RIPA buffer. Quantification was achieved using the Pierce Bicinchoninic Acid (BCA) Assay kit (Thermo Fisher Scientific), following the manufacturers protocol. Samples were run in triplicates alongside known bovine serum albumin (BSA) concentrations (0 mg/mL, 0.1 mg/mL, 0.2 mg/mL, 0.4 mg/mL, 0.5 mg/mL, 1 mg/mL, 2 mg/mL). A 50:1 dilution of Reagents A and B from the assay kit were added to the samples in a clear flat-bottomed 96-well plate, forming a 1:10 dilution of each sample. The samples were then left in a 37°C incubator for half an hour before wavelength readings were taken at 570 nm using a PHERAstar FS (BMG Labtech). The BSA readings were utilised to produce a standard concentration curve. Each measurement was fitted to the standard curve to provide an accurate quantification of protein content. The amount of protein within the Urea-soluble fraction was calculated as a percentage of the protein content of the comparable soluble fraction, since the high percentage of urea buffer prevents the use of standard protein quantification methods such as the BCA assay, and was performed as used routinely in the literature<sup>174, 219</sup>.

### 3.6 Western blotting

#### 3.6.1 Sample Preparation

Using the calculated concentrations, Western blot sample preparation for both the RIPA-soluble and Urea-soluble fractions was performed. As the Urea-soluble fractions could not be quantified due to the incompatibility of the extraction buffer with the assay kit, an estimate of protein content was determined from the RIPA-soluble fractions. This estimate also accounted for the difference in buffer extraction volumes between the two fractions (Urea = 1/4 of RIPA). Each sample included protein, 4x Laemmli buffer, 10x Nu-Page reducing agent and appropriate sample buffer (RIPA/Urea) to adjust loading volumes to be identical. For cell lysate samples, 20 µg for the RIPA-fraction and 30 µg protein-equivalent for the urea-fraction were used. For the mouse tissue samples, 20 µg of RIPA-fraction and 20 µg protein-equivalent of urea-fraction were used.

### 3.6.2 SDS-PAGE

Samples were loaded into 4-15% Criterion TGX precast sodium dodecyl sulphate polyacrylamide gel electrophoresis (SDS-PAGE) gels (Bio-Rad) and electrophoresed at 60V for 10 minutes followed by 130V for an hour. Gels were then rinsed in Trans-blot Turbo Transfer buffer (Bio-Rad) and transferred onto midi nitrocellulose membranes using a Bio-Rad semi-dry turbo transfer pack according to the manufacturer's protocol. Transfer running time was extended to 20 minutes at 2.5 A, 25 V.

### 3.6.3 Protein Visualisation

Following transfer, membranes were washed briefly in 1x Tris-buffered saline (TBS) and blocked in Odyssey Licor blocking buffer (diluted 1:1 with TBS) for one hour at room temperature with gentle shaking. Blots were then incubated in primary antibody (**Table 3:2**) diluted in Odyssey Licor blocking buffer (1:1 TBS + 0.1% Tween-20) at 4°C overnight with gentle shaking. Following primary antibody incubation, membranes were washed for 5 minutes in 1x TBS+0.1% Tween-20 (TBS-T) with gentle shaking at room temperature, followed by 3 x 5-minute washes with TBS with gentle shaking at room temperature to remove residual antibody. Membranes were then incubated in IRDye secondary antibodies (**Table 3:2**; Licor Biosciences), diluted 1:20000 in Odyssey Licor blocking buffer (1:1 TBS + 0.1% Tween-20), with gentle shaking for an hour in the dark at room temperature. Membranes were re-washed for 5 minutes in 1x TBS+0.1% Tween-20 (TBST) with gentle shaking at room temperature, followed by 3 x 5-minute washes with TBS with gentle shaking at room temperature to remove residual antibody. Each membrane was then rinsed with distilled water (dH<sub>2</sub>O) and air-dried in darkness. Membranes were then imaged using a Licor Odyssey CLx and Image Studio Version 5.2, detecting both 680 and 800nm channels.

Post-imaging blots were then re-blocked, re-probed for glyceraldehyde 3-phosphate dehydrogenase (GAPDH) and reimaged using the protocol described. This was done to confirm equal protein loading demonstrated through the uniform presence and measurement of GAPDH levels.

**Table 3:2 – Antibody Dilution Table (WB/ICC):** Identification numbers and concentrations of all antibodies used in Western blotting and immunocytochemistry (ICC).

Antibodies	Clone # or Catalogue #	Species	Stock Concentration (mg/mL)	Dilution (WB/ICC)	Final Concentration (µg/mL)	Use (WB/ICC)
<b>Primary Antibodies</b>						
C-terminal TDP-43 (Total TDP)	C1039	Rabbit	3.27	1:20,000	0.164	Both
Human-specific TDP-43	5014	Mouse	0.51	1:10,000	0.051	WB
Anti-phospho TDP-43 (ser409/ser410)	MABN14	Rat	0.5	1:1,000	0.5	WB
GAPDH	60004-1-Ig	Mouse	1	1:10,000	0.1	WB
C-Myc	9B11	Mouse	n/a	1:1,000	n/a	Both
<b>Secondary Antibodies</b>						
IRDye 680LT Anti-Rabbit	925-68023	Donkey	1	1:20,000	0.05	WB
IRDye 680LT Anti-Mouse	925-68022	Donkey	1	1:20,000	0.05	WB
IRDye 800CW Anti-Mouse	925-32212	Donkey	1	1:20,000	0.05	WB
IRDye 800CW Anti-Rat	925-32219	Goat	1	1:20,000	0.05	WB
Alexa Fluor 488 Anti-Rabbit	A-11008	Goat	2	1:500	4	ICC
Alexa Fluor 594 Anti-Rat	ab150168	Goat	2	1:500	4	ICC
Alexa Fluor 647 Anti-Mouse	A-21235	Goat	2	1:500	4	ICC

### 3.7 Proteomics Optimisation

15 µg protein-equivalent of the urea fraction from NSC-34 cell lysate was prepared for SDS-PAGE in 4x Laemmli buffer, 10x Nu-Page reducing agent and urea buffer to adjust loading volumes to be identical. The sample was loaded into two wells and that were processed identically according to the **Methods 3.7** and **3.8** apart from a single difference. One sample was divided into three fractions at the gel-processing stage (**Method 3.7.3**) to be processed separately and pooled after mass spectrometry analysis.

## 3.8 In-gel Tryptic Digestion

### 3.8.1 Sample Preparation

Protein sample preparation for mass spectrometry included protein, 4x Laemmli buffer, 10x Nu-Page reducing agent and appropriate sample buffer (RIPA/Urea) to adjust loading volumes to be identical. For cell lysate samples, 20 µg for the RIPA-fraction and 30 µg protein-equivalent for the urea-fraction were used. A follow-up experiment used 150 µg protein-equivalent for the urea-fraction from only the WT, dNLS 4FL and dNLS 2KQ TDP-43 cell lysate samples. For the mouse tissue samples, 6-10 µg of RIPA-fraction and 30 µg protein-equivalent of urea-fraction were used.

### 3.8.2 SDS-PAGE

Samples were loaded into 4-15% Criterion TGX precast SDS-PAGE gels (Bio-Rad) and run at 60V for 15-20 minutes until the sample had run approximately a centimetre into the gel. Each gel was then fixed in Coomassie Fixative Solution (40% Methanol, 10% Acetic Acid in dH<sub>2</sub>O) for 10 minutes at room temperature with gentle shaking. Gels were then stained in Colloidal Coomassie Blue (-for 30 minutes at room temperature with gentle shaking. With the appearance of visible bands, gels were de-stained in Coomassie Fixative Solution (40% Methanol 10% Acetic Acid in dH<sub>2</sub>O) for 1-hour at room temperature with gentle shaking.

### 3.8.3 Preparation of Gel Fractions

Each section containing proteins stained with Coomassie was excised with a scalpel and cut into 5 mm squares, ensuring to keep gel pieces from one sample separate to another. Gel pieces were buffer exchanged with 100 mM ammonium bicarbonate for 10 minutes at room temperature, vortexing on addition of buffer. This buffer was removed and replaced with 100mM ammonium bicarbonate and 50% acetonitrile for 20 minutes at room temperature, with intermittent vortexing. This buffer was removed and replaced with 100% acetonitrile for 20 minutes at room temperature with intermittent vortexing to dehydrate the gel pieces. Gel pieces were then reduced with 10 mM dithiothreitol (DTT) for 30 minutes at 55°C. DTT was removed and replaced with 20 mM iodoacetamide (IAA) for 45

minutes in darkness, to alkylate reduced disulphide bonds. The IAA was removed and pieces were again subject to buffer exchange with 100mM ammonium bicarbonate for 10 minutes, followed by 100mM ammonium bicarbonate and 50% acetonitrile for 20 minutes and 100% acetonitrile for 20 minutes. Tryptic digestion was performed with the addition of 12.5 ng/ $\mu$ l of trypsin from porcine (Sigma-Aldrich) suspended in 100 mM ammonium bicarbonate and incubated overnight at 37°C.

### 3.8.4 Peptide Extraction

The next day, gel pieces were suspended in extraction buffer (70% ACN, 2% formic acid in dH<sub>2</sub>O) and vortexed, followed by bath sonication for 10 minutes. This resulted in the tryptic peptides diffusing from the gel. The buffer containing the tryptic peptides was then collected and the process was repeated to ensure all peptides were extracted. Peptides suspended in the extraction buffer were centrifuged at 21,000 g in an Eppendorf 5424 benchtop centrifuge for 30 seconds to ensure they settled to the bottom of the tube. The peptides were then concentrated using an Eppendorf concentrator over the period of 2-4 hours to evaporate off the extraction buffer. The peptides were resuspended in 0.1% Formic acid in dH<sub>2</sub>O to prepare for de-salting using Omix C<sub>18</sub> column-packed Zip-tips (Agilent Technologies).

### 3.8.5 Peptide Desalting

Zip-tips were activated with activation buffer (90% acetonitrile, 0.1% formic acid in dH<sub>2</sub>O). 0.1% formic acid in dH<sub>2</sub>O was washed through the zip-tips twice to equilibrate them for sample loading. Samples were added to the zip-tips where they bound to the C18 column. Zip-tips were washed once again with 0.1% formic acid in dH<sub>2</sub>O, to clear unbound debris. Peptides were eluted with elution buffer (60% ACN, 0.1% formic acid in dH<sub>2</sub>O). Peptides suspended in the elution buffer were spun at 21,000g in an Eppendorf 5424 benchtop centrifuge for 30 seconds to ensure they settled to the bottom of the tube. The peptides were then concentrated using an Eppendorf concentrator over the period of 2-4 hours to evaporate off the elution buffer. To prepare the peptides for loading into a mass spectrometer, they were resuspended in 12  $\mu$ L of 0.1% formic acid in dH<sub>2</sub>O and transferred into glass high-performance liquid chromatography (HPLC) auto-sampler tubes (Waters).

### 3.9 Liquid Chromatograph Electrospray Mass Spectrometry (LC-ESI-MS/MS)

Four biological replicates of the NSC-34 cell-line were run for each construct. For the subsequent experiment utilising a 150 µg estimate from the urea-fraction, a total of 5 biological replicates were incorporated. The mouse tissue experiment incorporated fresh-frozen cortex samples from 5 bigenic rNLS (NEFH-tTA/tetO-hTDP-43ΔNLS double transgenic) mice at 4 weeks after removal of doxycycline (approximately 10 weeks of age) as well as 5 sex- and litter-matched control mice.

Mass spectrometry was accomplished using a Q Exactive Orbitrap system (Thermo Fisher Scientific) coupled to an EASY-nLC HPLC (Thermo Fisher Scientific), both controlled using Xcalibur Version 2.0 system software (Thermo Fisher Scientific). Reversed phase columns were packed with approximately 7 cm (100 µm i.d.) of 100 Å, 5 mM Zorbax C18 resin (Agilent Technologies, CA), in a fused silica capillary with an integrated electrospray tip. Each sample was run for 100 minutes on a 0-50% acetonitrile gradient (0-90 mins = 0-50%, 90-100 mins = 50%-85%) with a flow rate of 300 nL/minute. Ion acquisition scan range between 350-1850 m/z, detecting at a resolution of 70,000 for precursor ions and 17,500 for product ions. Acquisition was performed in positive charge mode, with a focus on doubly charged ions. Automatic gain control (AGC) was set to  $1 \times 10^6$  ions in precursor acquisition mode and  $1 \times 10^5$  ions in product acquisition mode. The mass spectrometer was set to collect for 60 ms in precursor acquisition mode (full MS scan) before selecting the top 10 ions for fragmentation. The top 10 ions in this mode underwent subsequent scanning in product ion acquisition mode (MS/MS scan) for 100 ms with an isolation window of 2.0 m/z.

## 3.10 Fluorescence Microscopy

### 3.10.1 Preparation of Cells on Coverslips

Approximately  $5 \times 10^5$  cells were plated onto 24-well tissue culture treated plates (Corning) in DMEM + 10% FBS with 13mm autoclaved coverslips (Thermo Fisher Scientific). They were then left to incubate for 46-50 hours at 37°C and 5% CO<sub>2</sub>. After this time, cells were approximately 70-80% confluent.

### 3.10.2 Transfection

2 µL of Lipofectamine 2000 was brought up to a total volume of 50 µL with Opti-MEM media (Life Technologies) and left to incubate for 10 minutes at room temperature. 1 µg of prepared DNA was brought up to a total volume of 50 µL with Opti-MEM media (Life Technologies). These mixtures were then combined and left to incubate at room temperature for 20 minutes. The cell media was then aspirated and the combined mixtures were added dropwise to the cells. Cells were left to incubate like this for approximately 16 hours at 37°C and 5% CO<sub>2</sub>, before transfection media was completely removed and replaced with fresh DMEM+10% FBS.

### 3.10.3 Cell Fixation and Immunocytochemistry

After a total period of 46-50 hours post-transfection, cell-coated coverslips were rinsed in PBS and fixed in 4% paraformaldehyde (PFA) in PBS for 15 minutes at room temperature with gentle shaking. The cells were then exposed to 2 x 5-minute washes with PBS at room temperature with gentle shaking to remove excess PFA. After washing, cell-coated coverslips were incubated in PBS + 0.2% Triton for 10 minutes at room temperature with gentle shaking, to permeabilise cell membranes. The cells were again exposed to 2 x 5-minute washes with PBS at room temperature with gentle shaking. Cells were then blocked for 1 hour using 1% BSA + 0.03% Triton in PBS. Primary antibodies (**Table 5:2**) were diluted in 1% BSA + 0.01% Triton in PBS and added to the cells in a humidity chamber for an overnight incubation at 4°C with gentle shaking. The cells were again exposed to 2 x 5-minute washes with PBS at room temperature with gentle shaking to remove excess antibody. Secondary antibodies

(Table 5:2) were diluted in 1% BSA + 0.01% Triton in PBS and added to the cells, which were left to incubate in darkness at room temperature for 1 hour with gentle shaking. The cells were again exposed to 2 x 5-minute washes with PBS at room temperature with gentle shaking to remove excess antibody. The cell-coated coverslips were briefly rinsed in water and mounted onto Series 1 Frosted Microscope Slides (Trajan) using Vector VECTASHIELD mounting medium with DAPI (Abacus ALS). After drying overnight in darkness at room temperature the cells were stored at 4°C and imaged using a Zeiss AxioImager with Zen Version 2 (Blue Edition) software.

## 3.11 Data and Statistical Analysis

### 3.11.1 Proteomics

Proteomic data analysis was performed using Proteome Discoverer Daemon Version 1.3 (Thermo Fisher Scientific). A custom workflow incorporated the use of the Mascot server (Matrix Science) searching the Swiss-Prot database and validating using the Percolator algorithm (Matrix Science). Search parameters included cleavage using trypsin, allowing for up to 2 missed cleavages, 20 ppm mass tolerance for precursor ions and 0.1Da for fragment ions. Modifications allowed were oxidation of methionines, acetylation of protein N-termini and carbamidomethylation of cysteines. Strict false discovery rate (FDR) was set to 1% for reversed peptide searching and relaxed FDR was set to 5%, ignoring results that had a delta correlation more than 0.05. Paired-wise t-tests for comparisons between the bigenic and control mice data utilised the series of R-modules known as the Spectral Counting Reporting and Analysis Program (SCRAPPY), a suite of scripts for the analysis of label-free data<sup>220</sup>. Protein descriptions were retrieved through searching UniProt ID Accession numbers<sup>221</sup>. Gene Ontology of generated protein lists was performed using the Panther Database<sup>222</sup>.

Figures containing Venn diagrams were produced using the online software jvenn, a plugin for the jQuery Javascript library<sup>223</sup>.

### 3.11.2 Immunoblotting

Western blot image-processing for figure generation was produced using ImageJ Version 1.5<sup>224</sup>.

Quantification of Western blots was achieved using Li-Cor Image Studio Lite Version 5.2, normalising values to GAPDH for the RIPA-fraction. This output was then transferred to Graphpad Prism Version 7.02 for Windows, Graphpad Software, La Jolla California USA, [www.graphpad.com](http://www.graphpad.com). Graphpad was utilised for paired t-testing and ANOVA statistical analysis in addition to figure generation. Figure colour scheme for Graphpad output was determined using a previously developed colour-blind scheme<sup>225</sup>.

# 4. Results

## 4.1 Preliminary Optimisation Experiments

### 4.1.1 Determination of Cell Density for Transfection Experiments

To define the best culture conditions for subsequent proteomic studies, NSC-34 cells were plated at four different densities ( $1 \times 10^6$ ,  $1.5 \times 10^6$ ,  $2 \times 10^6$  or  $2.5 \times 10^6$  cells/plate) in 100mm round culture dishes. Cells were considered healthy based on cell morphology (showing flattened regular cellular shape and dendrite outgrowth), by the colour of culture medium (indicating appropriate pH levels by pH-sensitive phenol red dye) and by observation for lack of cell debris in the culture medium. At 48-hours post-plating, cell density varied based upon the initial plating density (shown in panel in **Figure 4:1**).

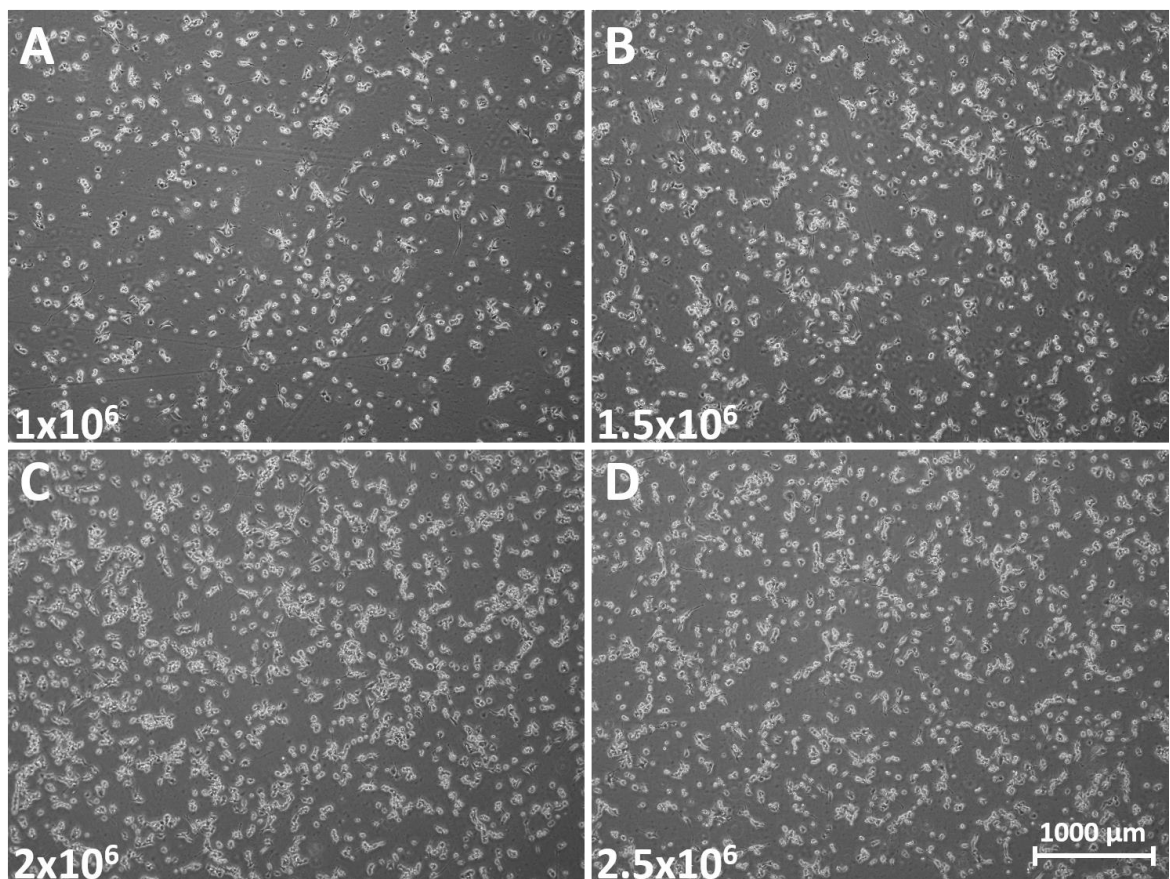


**Figure 4:1 – 100mm Plate Cell Density Optimisation (48 Hours):** 4x Magnification images of NSC-34 cells plated at 4 different densities ( $1 \times 10^6$ ,  $1.5 \times 10^6$ ,  $2 \times 10^6$  or  $2.5 \times 10^6$  cells per 100mm plate) 48 hours post-plating.

The plating density and confluence was deemed ideal based on the finding that after 48 hours, at which point the cell lysates were collected, this starting condition resulted in the presence of many transfected cells but without the cells becoming over-confluent and showing signs of cell death (determined by presence of cellular debris in the medium), as compared to the other chosen cell densities. An initial plating density of  $2 \times 10^6$  cells per plate resulted in a healthy culture of ~70% confluency, which was deemed ideal for subsequent DNA transfection experiments, at the 48-hour time-point. Therefore, a plating density of  $2 \times 10^6$  cells/plate was selected for all subsequent experiments.

#### 4.1.2 Optimisation of Gel-processing Method for Proteomic Studies

Proteomics optimisation was performed as described in **Method 3.7** to determine whether it would be beneficial to perform tryptic digestion and analyse proteomics samples as more than one fraction, a method that may result in more proteins identified. An NSC-34 untransfected cell lysate sample was processed as a singular fraction and the other was divided into three fractions that were processed separately with data pooled after mass spectrometry analysis (**Figure 4:2**).

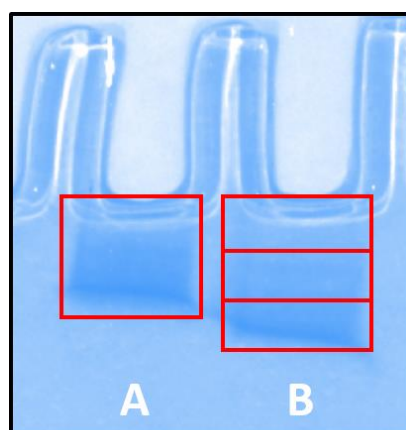


**Figure 4:2 – Proteomics Optimisation Gel Processing:** NSC-34 cell lysate ( $15 \mu\text{g}/\text{lane}$ ) stained with Colloidal Coomassie blue, illustrating **A** – sample to be processed and analysed as a singular fraction or **B** – samples to be processed and analysed separately, to be pooled after mass spectrometry.

For proteomic processing, a total 402 unique proteins were identified in the single-processed fraction, whereas 529 unique proteins were identified in the separately processed fractions that were pooled together (**Figure 4:3**). This is an increase of 31.6% compared to the individually processed fraction. The separately processed fractions did however require more time and triple the amount of resources. Given the substantial number of samples to be processed in experiments, the single processing technique was chosen for subsequent experiments, despite this protocol resulting in fewer protein identifications.

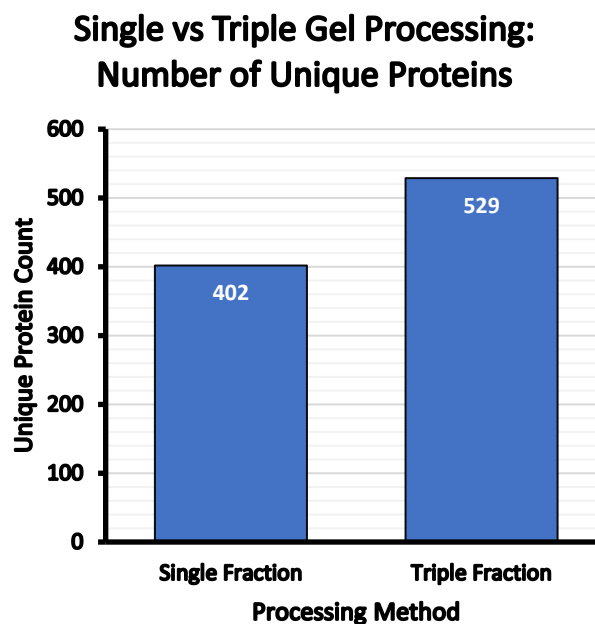


**Figure 4:3 – Single vs Triple Gel Processing: Number of Unique Proteins:** Number of unique proteins identified in the single gel fraction compared to the three gel fractions that were digested and processed individually and pooled for analysis.

## 4.2 Validation of Human TDP-43 pcDNA5/TO Expression by

### Immunocytochemistry

#### 4.2.1 Immunocytochemistry Staining of Human TDP-43 in the pcDNA5/TO vector

Immunohistochemistry was used to validate that human TDP-43 transfections were successful and localised to intended cellular compartments. Human TDP-43 protein did localise to intended compartments: Control untransfected NSC-34 cells exhibited normal nuclear TDP-43, WT transfected cells exhibited nuclear TDP-43,  $\Delta$ NLS transfected cells exhibited cytoplasmic TDP-43, 4FL transfected cells exhibited nuclear TDP-43,  $\Delta$ NLS+4FL cells exhibited cytoplasmic TDP-43 and  $\Delta$ NLS+2KQ transfected cells exhibited cytoplasmic TDP-43 (**Figure 4:4**).

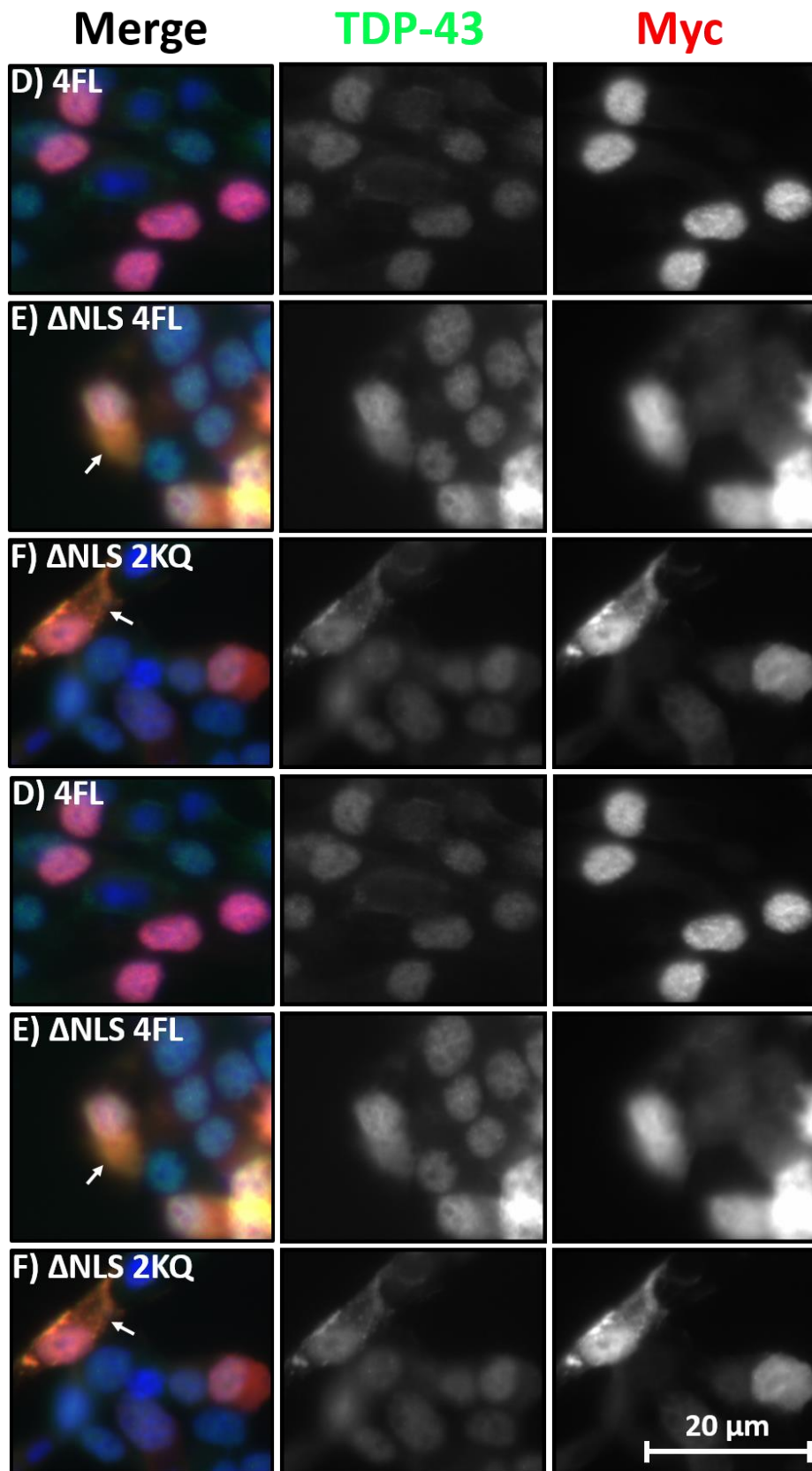


**Figure 4:4 – NSC-34 cells transfected with 5'myc pcDNA5/TO human TDP-43 constructs:**  
Microscope images taken of NSC-34 cells transfected with 5'myc pcDNA5/TO human TDP-43 constructs at 40x magnification, immunostained for **Total TDP-43**, **c-Myc** and **DAPI** (to show **nuclei**). Arrows indicate cytoplasmic TDP-43. Excitation/Emission: **DAPI**: 353 nm/465 nm; **Total TDP-43**: 493 nm/517 nm; **c-Myc**: 653 nm/668 nm. Exposure times DAPI/Alexa Fluor 488/Alexa Fluor 647: Control 20ms/260ms/240ms; WT 20ms/260ms/240ms;  $\Delta$ NLS 40ms/190ms/85ms; 4FL 70ms/800ms/240ms;  $\Delta$ NLS+4FL 40ms/550ms/240ms;  $\Delta$ NLS+2KQ 40ms/550ms/170ms.

#### 4.2.2 Quantification of NSC-34 Transfection Efficiency

Transfection efficiency of these constructs in NSC-34 cells was determined via counting the number of cells that expressed Myc-tagged protein, as determined using the 653 nm/668 nm excitation/emission spectra signal for c-Myc staining (**Figure 4:5**). Using this method, transfection efficiency for the NSC-34 cells used in these experiments was similar between constructs, being between 25% and 35% (n=1 biological replicate, 34-75 cells counted per group).

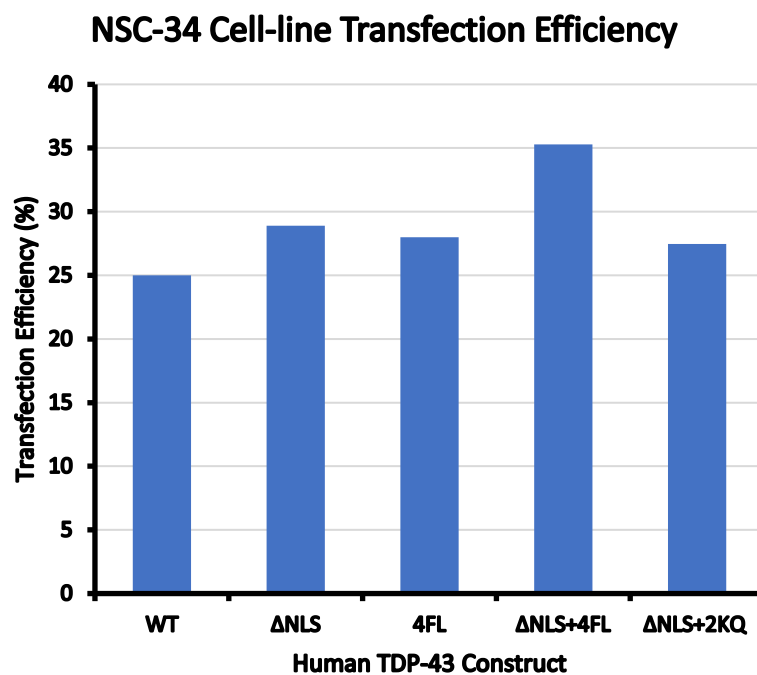


**Figure 4:5 – NSC-34 Cell-line Transfection Efficiency:** Transfection efficiency determined from the number of cells exhibiting c-Myc expression divided by the total cells counted within a given area for 5' myc-tagged human TDP-43 constructs contained within the pcDNA5/TO vector. n=1 biological replicate, counting 34-75 cells counted per group.

### 4.3 Validation of Human TDP-43 pLenti-C-mGFP Expression by

#### Immunocytochemistry

##### 4.3.2 Immunocytochemistry of Human TDP-43 in the pLenti-C-mGFP vector

Expression of the WT  $\Delta$ NLS, 4FL,  $\Delta$ NLS+4FL and  $\Delta$ NLS+2KQ human TDP-43 constructs in the pcDNA5/TO vector was low in the NSC-34 cell-line. As an alternative, these same proteins as well as a 2KQ human TDP-43 construct were expressed with a C-terminal mGFP tag and lacking the myc tag, using the pLenti-C-mGFP vector in SH-SY5Y cells (**Figure 4:6**). As these TDP-43 proteins were tagged with m-GFP, no staining apart from DAPI for nuclei was required to visualise expression. The human TDP-43 proteins localised to their intended compartments within the SH-SY5Y cells: WT cells exhibited normal nuclear TDP-43,  $\Delta$ NLS transfected cells exhibited cytoplasmic TDP-43, 4FL transfected cells exhibited nuclear TDP-43 forming both inclusions and puncta, 2KQ transfected cells exhibited nuclear TDP-43 forming both inclusions and puncta,  $\Delta$ NLS+4FL cells exhibited cytoplasmic TDP-43 forming large inclusions and  $\Delta$ NLS+2KQ transfected cells also exhibited cytoplasmic TDP-43 forming large inclusions.

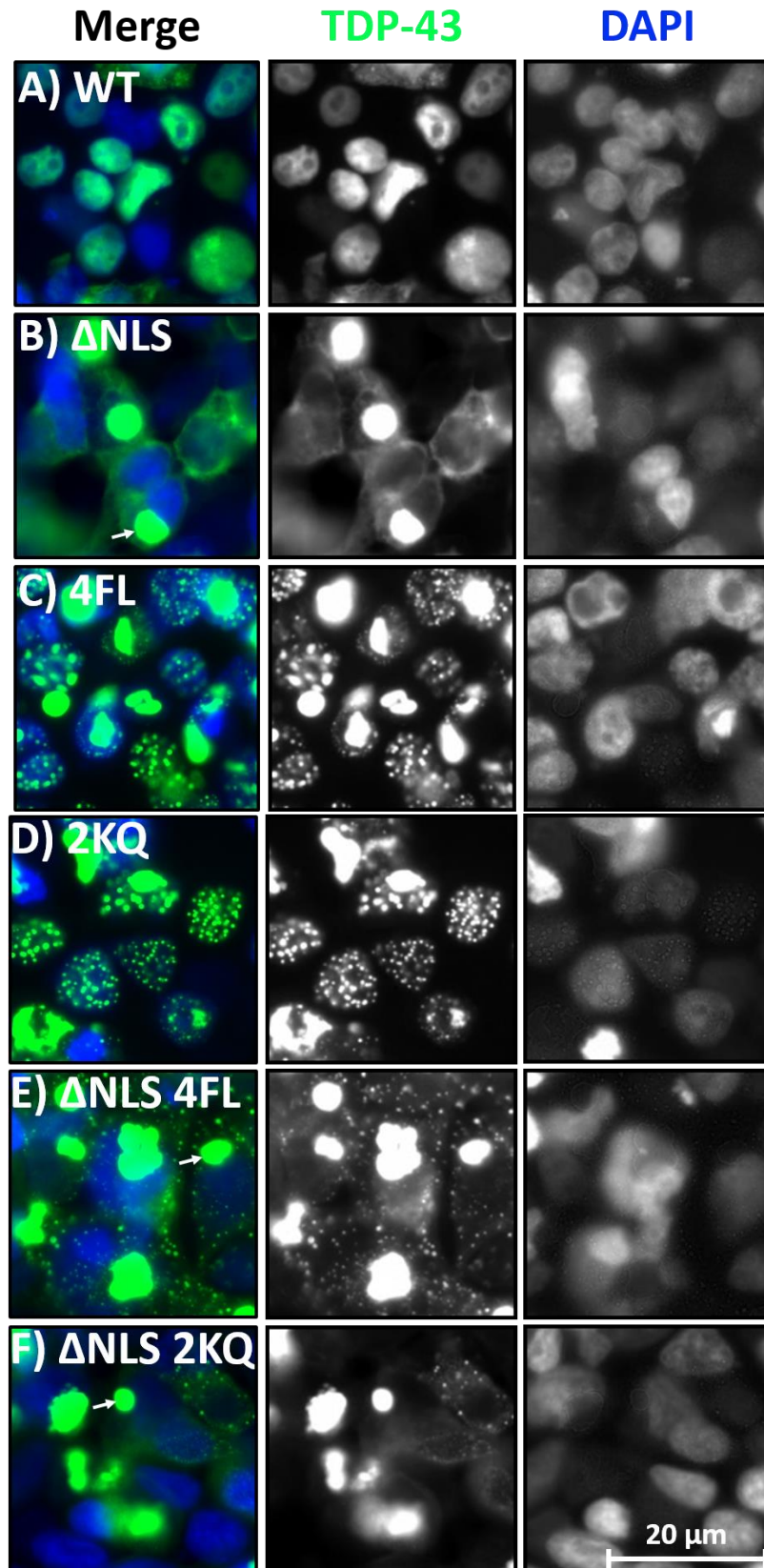


**Figure 4:6 – SH-SY5Y cells transfected with pLenti-c-mGFP human TDP-43 constructs:** SH-SY5Y cells transfected with pLenti-C-mGFP human TDP-43 constructs at 40x magnification. Expressing human TDP-43 mGFP and stained with DAPI (to show nuclei). Arrows indicate cytoplasmic inclusions of hTDP-43-mGFP. Excitation/Emission: DAPI: 353 nm/465 nm; mGFP: 488 nm/509 nm. Exposure times DAPI/eGFP: WT 16ms/46ms; ΔNLS 11ms/16ms; 4FL 5ms/16ms; 2KQ 5ms/16ms ΔNLS+4FL 2.2ms/16ms; ΔNLS+2KQ 2.2ms/16ms.

### 4.3.2 Quantification of SH-SY5Y Transfection Efficiency

Transfection efficiency of these constructs in SH-SY5Y cells was determined via counting the number of mGFP expressing cells, as determined using the 488 nm/509 nm excitation/emission spectra signal for GFP (**Figure 4:7**). Using this method, transfection efficiency for the SH-SY5Y cells used in these experiments was between 50% and 70% (n=1 biological replicate, 104-158 cells counted per group).

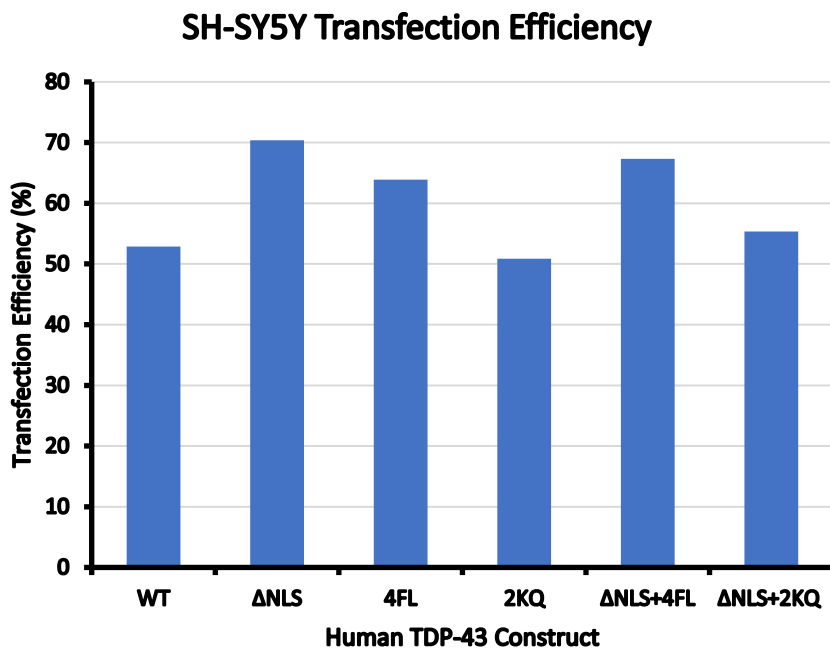


**Figure 4:7 – SH-SY5Y Transfection Efficiency:** Transfection efficiency determined from the amount of cells exhibiting mGFP expression divided by the total cells counted within a given area for pLenti-C-mGFP human TDP-43 constructs. n=1 biological replicate, 104-158 cells counted per group).

In comparison, the SH-SY5Y cell-line demonstrated higher transfection efficiency than the NSC-34 cell-line (**Result 4.2.2**). Due to the time constraints of the project we were unable to determine whether this was a direct result of the vector or the cell-line, or a combination of both.

#### 4.4 Analysis of Urea-soluble Proteins in NSC-34 Transfected Cells

The defining characteristic of human ALS and FTD, is the accumulation of detergent-insoluble proteins into cytoplasmic aggregates in affected neurons. However, although TDP-43 is a recognised major component of this aggregated protein fraction, the other proteins that comprise this pathological pool of proteins remain largely uncharacterised. Identification of these proteins is important, since sequestration into aggregates may result in decrease availability of these proteins to perform their required functions, thus providing insight into disease mechanisms. In addition, a proportion of these proteins could be expected to represent endogenous mechanisms to clear the aggregated TDP-43 protein, and these proteins could thus be potential leads for therapeutic modulation aimed at stimulating clearance of aggregated TDP-43, which may be beneficial for treatment of people living with ALS and FTD.

To isolate the Urea-soluble protein fraction, sequential extraction of mouse cortex tissues coupled with ultracentrifugation was performed (**Methods 3.4**). In this method, RIPA buffer containing the detergents 0.1% SDS, 1% NP-40, as well as 50mM Tris, 150mM NaCl, 5mM EDTA, 0.5% sodium deoxycholate and 1mM PMSF was used to isolate the 'RIPA-soluble' protein fraction, that is the protein fraction taken to represent the normal cellular soluble, non-aggregated proteins. Subsequent washing of the pellet obtained from this step resulted in isolation of protein pellets containing the 'RIPA-insoluble' protein fraction, that is the protein fraction taken to represent the abnormal aggregated proteins. This RIPA-insoluble fraction was subsequently solubilised using harsh denaturing conditions with 7M Urea, 2M Thiourea, 4% CHAPS, 30mM Tris, producing the 'Urea-soluble' protein fraction. The described method is routinely used in the literature to isolate proteins of low detergent solubility, including proteins that are not readily separated from debris during routine extraction protocols<sup>174, 219</sup>.

This method incorporated 4 biological replicates of NSC-34 cells transfected with to express myc-tagged human TDP-43 WT,  $\Delta$ NLS, 4FL,  $\Delta$ NLS+4FL and  $\Delta$ NLS+2KQ as well as untransfected controls for initial 30  $\mu$ g experiments and 5 biological replicates for subsequent 150  $\mu$ g experiments using WT,  $\Delta$ NLS+4FL,  $\Delta$ NLS+2KQ and untransfected controls.

#### 4.4.1 Validation of Human TDP-43 Expression in RIPA-soluble Fraction

Prior to proteomics, verifying that each human TDP-43 was successfully expressed in each sample was required. Transfection success of each sample with human TDP-43 was verified with the detection of c-Myc-tagged human TDP-43 between 37kDa and 50kDa in the RIPA-soluble fraction across 5 biological replicates (**Figure 4:8**). This was validated through the absence of this band from the untransfected control samples. Similar levels of GAPDH proteins were detected at approximately 37kDa across each sample, demonstrating consistency in protein loading and calculations.

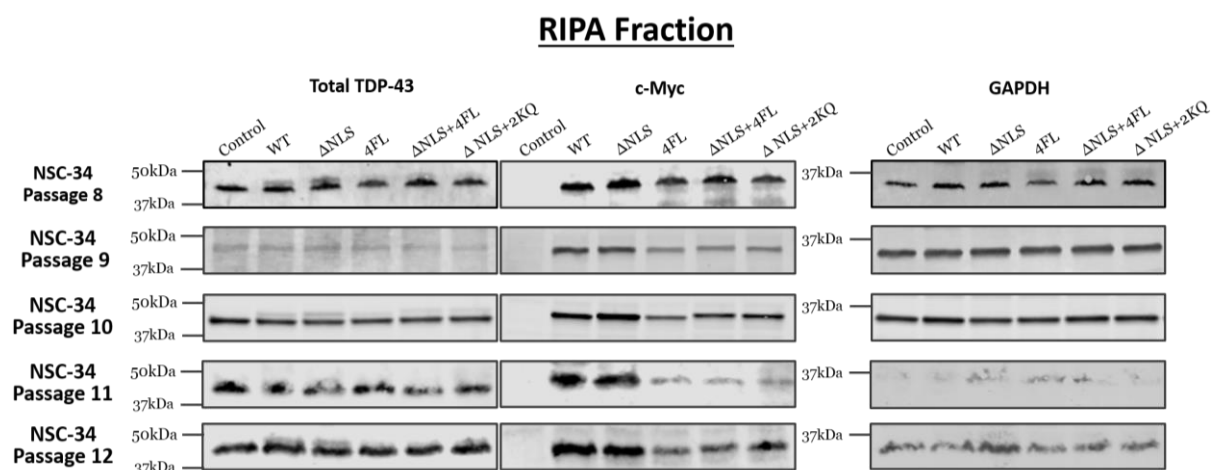


**Figure 4:8 – Total and Myc-tagged TDP-43 in the RIPA-soluble Fraction of NSC-34 Cells:** Western blots of the RIPA-soluble fraction of NSC-34 cell lysate: untransfected control, WT, ΔNLS, 4FL, ΔNLS+4FL and ΔNLS+2KQ transfected myc-tagged human TDP-43 in pcDNA5/TO vector. Probing for C-terminal total TDP-43 (detected in the 680nm channel), myc (transfected myc-tagged human-TDP-43 detected in the 800nm channel) and GAPDH (reprobed and detected in the 680nm channel). n=5 biological replicates.

When quantified using the first 3 biological replicates (as GAPDH signal was inconsistent and therefore not reliably quantifiable in the final 2 replicates), the relative levels of total TDP-43 exhibited a significant decrease in the WT and  $\Delta$ NLS+4FL conditions compared to the control ( $p < 0.05$ ), and no change to the remaining constructs, suggesting a relatively low level of exogenous human TDP-43 protein expression compared to endogenous (**Figure 4:9A**). The likely explanation for this decrease is that accumulated TDP-43 is less soluble, and so is present in a greater proportion in the urea fraction, resulting in an apparent decrease in levels in the RIPA fraction.. However, myc-tagged human TDP-43 was readily detected using the c-Myc antibody. Conversely, the relative levels of 4FL,  $\Delta$ NLS+4FL and  $\Delta$ NLS+2KQ exhibit a downward trend compared to wild-type TDP-43 in this RIPA-soluble fraction, suggesting lower levels of detergent-soluble myc-tagged human TDP-43 with these mutations (**Figure 4:9B**). However, this change was found to be not statistically significant using a one-way ANOVA test with Bonferroni correction.

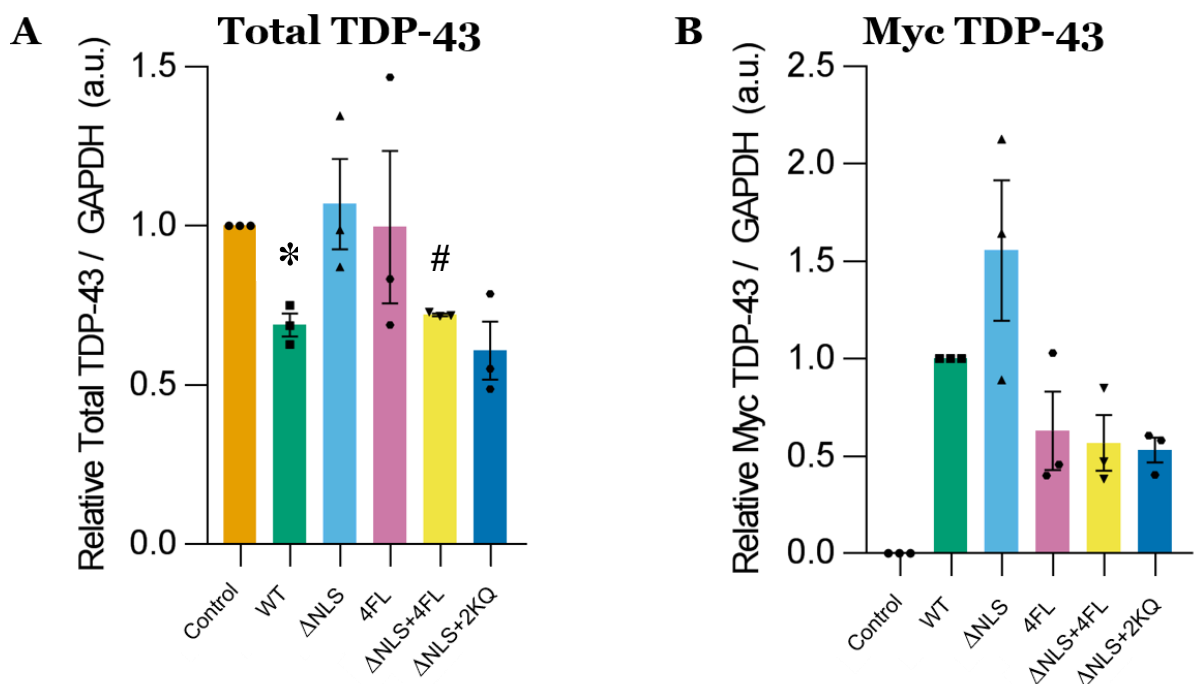


**Figure 4:9 – RIPA Western Blot Quantification of (A) Total and (B) Myc-tagged TDP-43:** Quantification of RIPA-soluble fraction Western blots quantifying (A) Total TDP-43 normalised to control GAPDH and (B) Myc-tagged TDP-43 normalised to WT GAPDH. n=3 biological replicates. a.u. – arbitrary units. \*  $p < 0.05$ ; #  $p < 0.0001$  versus Control.

#### 4.4.2 Validation of Human TDP-43 Expression in Urea-soluble Fraction

In order to confirm that TDP-43 was aggregated and sequestered into inclusions, indicated by decreased solubility, transfection verification of human TDP-43 in each Urea-soluble sample was also required prior to proteomics. Transfection success of each sample with human TDP-43 was verified with the detection of c-Myc-tagged human TDP-43 between 37kDa and 50kDa in the Urea-soluble fraction across 5 biological replicates (**Figure 4:10**). This was validated through the absence of this band from the untransfected control samples. The bands appear to smear in the urea fractions, suggesting post-translational modifications indicative of aggregated TDP-43. GAPDH was not detected in the Urea-soluble fraction as it is all solubilised and removed in the RIPA extraction (not shown).

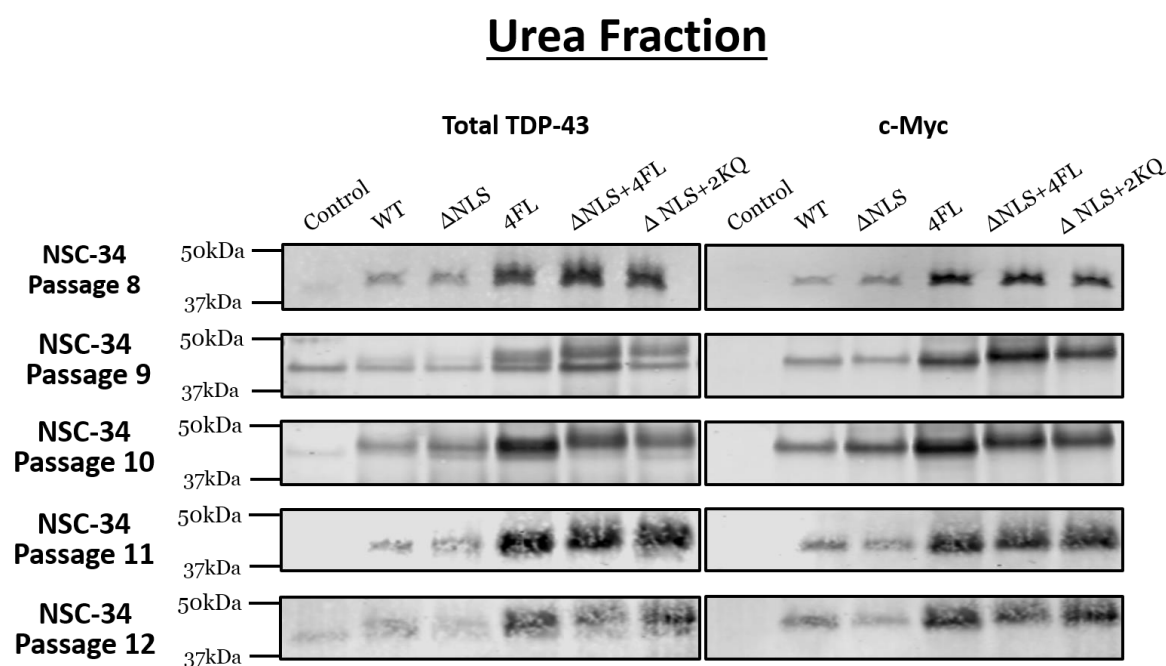


**Figure 4:10 – Total and Myc-tagged TDP-43 in the Urea-soluble Fraction of NSC-34 Cells:** Western blots of the Urea-soluble fraction of NSC-34 cell lysate: untransfected control, WT,  $\Delta$ NLS, 4FL,  $\Delta$ NLS+4FL and  $\Delta$ NLS+2KQ transfected myc-tagged human TDP-43 in pcDNA5/TO vector. Probing for C-terminal total TDP-43 (detected in the 680nm channel) and myc (transfected myc-tagged human-TDP-43 detected in the 800nm channel). n=5 biological replicates.

When quantified using the first 3 biological replicates (therefore not reliably quantifiable in the final 2 replicates), there was a trend towards increased relative levels of total TDP-43 in the 4FL and  $\Delta$ NLS+4FL conditions, exhibiting an upward trend compared to total wild-type TDP-43. The  $\Delta$ NLS+2KQ condition was found to exhibit a statistically significant increase compared to total wild-type TDP-43 ( $p < 0.05$ , **Figure 4:11A**). Likewise, there was a trend towards increased relative levels of these same mutants compared to wild-type TDP-43 when quantified for the signal of the myc tag (**Figure 4:11B**). However, these changes were found to be not statistically significant using a one-way ANOVA test with Bonferroni correction, likely due to low n and variability between experiments.

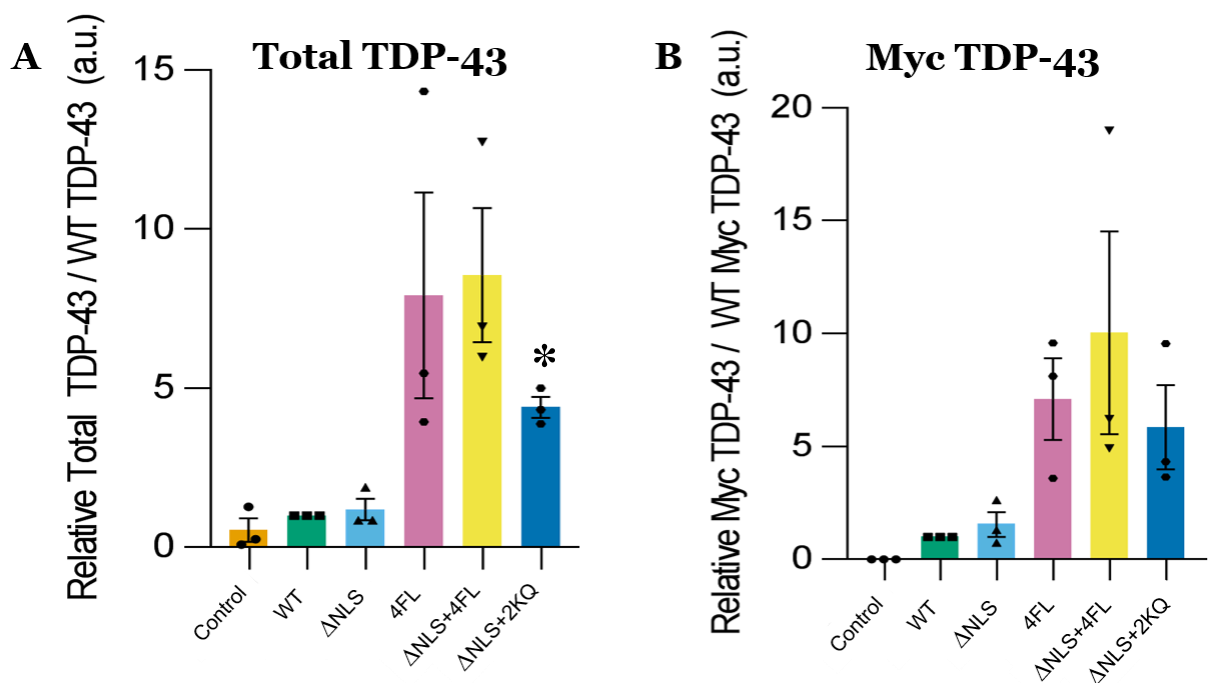


**Figure 4:11 – Urea Western Blot Quantification of (A) Total and (B) Myc-tagged TDP-43:** Quantification of Urea-soluble fraction Western blots quantifying (A) Total TDP-43 normalised to control WT TDP-43 and (B) Myc-tagged TDP-43 normalised to WT myc-tagged TDP-43. n=3 biological replicates. \*  $p < 0.05$  versus WT.

#### 4.4.3 Proteomic Analysis of Transfected Human TDP-43 Urea-soluble Fractions

For initial profiling of the insoluble proteins in TDP-43 pathology derived from NSC-34 cells, proteomic processing (**Methods 3.8/3.9**) using 30  $\mu$ g of protein from each urea-fraction sample was performed. A total of 591 unique proteins were identified across the 4 biological replicates analysed of urea fractions of the NSC-34 cells transfected with no construct, WT,  $\Delta$ NLS, 4FL,  $\Delta$ NLS+4FL and  $\Delta$ NLS+2KQ human TDP-43 mutations. Of these, only 45 (7.6%) of proteins were identified across all 6 conditions. Furthermore, 437 (74%) of the proteins were exclusive to or shared between the  $\Delta$ NLS, 4FL,  $\Delta$ NLS+4FL and  $\Delta$ NLS+2KQ constructs and were not detected in the other conditions (**Figure 4:12**). Human TDP-43 mutants with a loss of functional capacity (4FL,  $\Delta$ NLS+4FL and  $\Delta$ NLS+2KQ) exhibited a greater number of total and exclusive proteins when compared to those with functional capacity (Control, WT,  $\Delta$ NLS) indicating that non-functional TDP-43 is both more insoluble than controls (**Result 4.4.2** – refer to above) and that expression of non-functional TDP-43 increases the cellular burden of other aggregated low-solubility proteins.

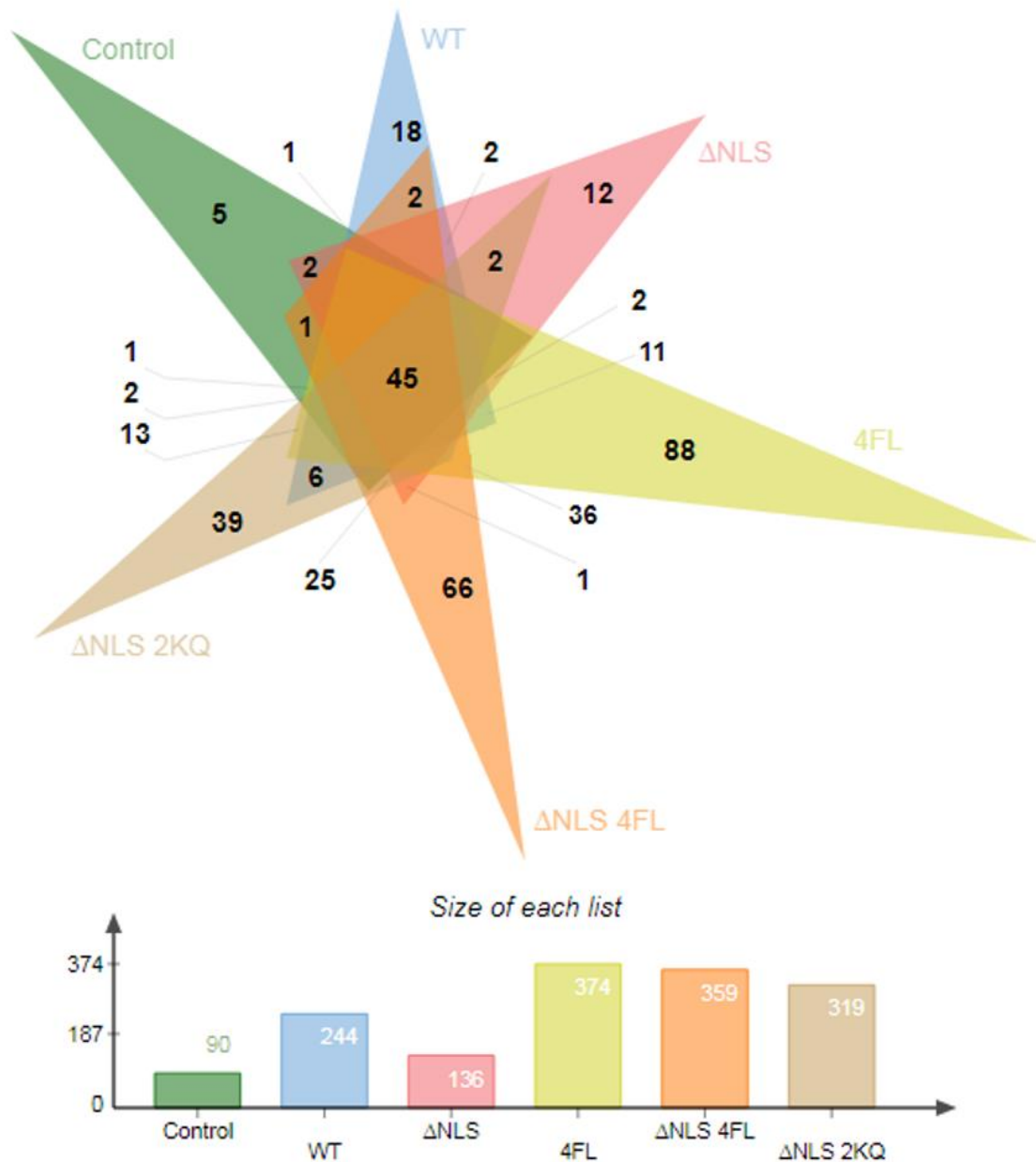


**Figure 4:12 – All Proteins Identified in Urea-soluble Fractions of NSC-34 Cells Transfected with Human TDP-43:** All proteins identified in the Urea-soluble fractions of NSC-34 cells: untransfected control, WT, ΔNLS, 4FL, ΔNLS+4FL, ΔNLS+2KQ human TDP-43 pcDNA5/TO. The top panel shows Venn diagram overlap of the individual proteins detected in each condition with numbers referring to the number of unique proteins in each group. The bottom panel shows the total number of unique proteins detected in any biological replicate for each condition. n=4 biological replicates.

To investigate the type of proteins that are exclusive to the human TDP-43 mutants with loss of functional capacity, a list of the top 10 proteins from the urea fractions of 4FL,  $\Delta$ NLS+4FL and  $\Delta$ NLS+2KQ constructs sorted first by peptide presence across replicates and finally by peptide count is presented in **Table 4:1**. A comprehensive list of all proteins exclusive to or shared between the  $\Delta$ NLS, 4FL,  $\Delta$ NLS+4FL and  $\Delta$ NLS+2KQ constructs, with peptide counts is available in [Appendix A](#). The  $\Delta$ NLS+4FL and  $\Delta$ NLS+2KQ constructs were selected for follow-up experiments as they exhibited cytoplasmic aggregation combined with a predicted loss of functional capacity, similar to human ALS and FTD.

**Table 4:1 – Top 10 Exclusive/Shared Proteins in the Urea-soluble Fractions of  $\Delta$ NLS, 4FL,  $\Delta$ NLS+4FL,  $\Delta$ NLS+2KQ Transfected NSC-34 Cells in the 30  $\mu$ g Experiment:** List of the top 10 proteins found to be exclusive to or shared between the  $\Delta$ NLS, 4FL,  $\Delta$ NLS+4FL and  $\Delta$ NLS+2KQ transfections in the urea-soluble fraction of transfected NSC-34 cells. Sorted by presence across replicates (greatest to least) and peptide count (greatest to least)

UniProt ID	Protein names	NLS Presence (n/4)	4FL Replicate Presence (n/4)	NLS+4FL Replicate Presence (n/4)	NLS+2KQ Replicate Presence (n/4)	Total Replicate Presence (n/16)	Total Peptide Count
P20152	Vimentin	0	3	1	1	5	12
P62492	Ras-related protein Rab-11A (Rab-11)	0	3	1	1	5	8
Q8BUV3	Gephyrin [Includes: Molybdopterin adenylyltransferase (MPT adenylyltransferase) (EC 2.7.7.75) (Domain G); Molybdopterin molybdenumtransferase (MPT Mo-transferase) (EC 2.10.1.1) (Domain E)]	0	2	1	2	5	5
P97807	Fumarate hydratase, mitochondrial (Fumarase) (EC 4.2.1.2) (EF-3)	0	3	1	1	5	5
Q9JJV2	Profilin-2 (Profilin II)	0	3	1	1	5	5
Q8C2Q3	RNA-binding protein 14 (RNA-binding motif protein 14)	0	2	1	1	4	9
Q9Z1Q5	Chloride intracellular channel protein 1 (Nuclear chloride ion channel 27) (NCC27)	0	1	1	2	4	8
Q99K85	Phosphoserine aminotransferase (PSAT) (EC 2.6.1.52) (Endometrial progesterone-induced protein) (EPIP) (Phosphohydroxythreonine aminotransferase)	0	2	1	1	4	8
P29758	Ornithine aminotransferase, mitochondrial (EC 2.6.1.13) (Ornithine--oxo-acid aminotransferase)	0	2	1	1	4	7
P97310	DNA replication licensing factor MCM2 (EC 3.6.4.12) (Minichromosome maintenance protein 2 homolog) (Nuclear protein BM28)	0	2	1	1	4	6

## 4.5 A Greater Number of Proteins are Identified in the Urea-soluble Fraction of Aggregate-Prone Human TDP-43 in Transfected NSC-34 Cells

### 4.5.1 RIPA/Urea Fractionation Isolates Low Solubility Proteins

Subsequent proteomic experiments examined only the untransfected control, WT,  $\Delta$ NLS+4FL and  $\Delta$ NLS+2KQ human TDP-43 samples generated from transfected NSC-34 cells, in order to increase the experimental output and to focus studies on the most aggregation-prone human TDP-43 proteins.

Loading levels of protein for these experiments were increased to 150  $\mu$ g protein per lane for initial SDS-PAGE prior to band extraction for mass spectrometry, with the aim of identifying an even greater number of proteins, and 5 biological replicates for each condition were used.

To confirm that the fractionation method isolated low-solubility proteins in the Urea-soluble fraction that were distinct from those in the RIPA-soluble fraction, an overlay of all proteins identified across all replicates from these samples was generated (**Figure 4:11**). A total of 2857 unique proteins were identified in the RIPA-soluble samples and 1868 unique proteins were identified in the Urea-soluble samples, with an overlap of 1477 proteins. This confirmed the isolation of a distinct population of exclusive Urea-soluble proteins, with 391 proteins (12%) being identified exclusively in the Urea-soluble fraction.

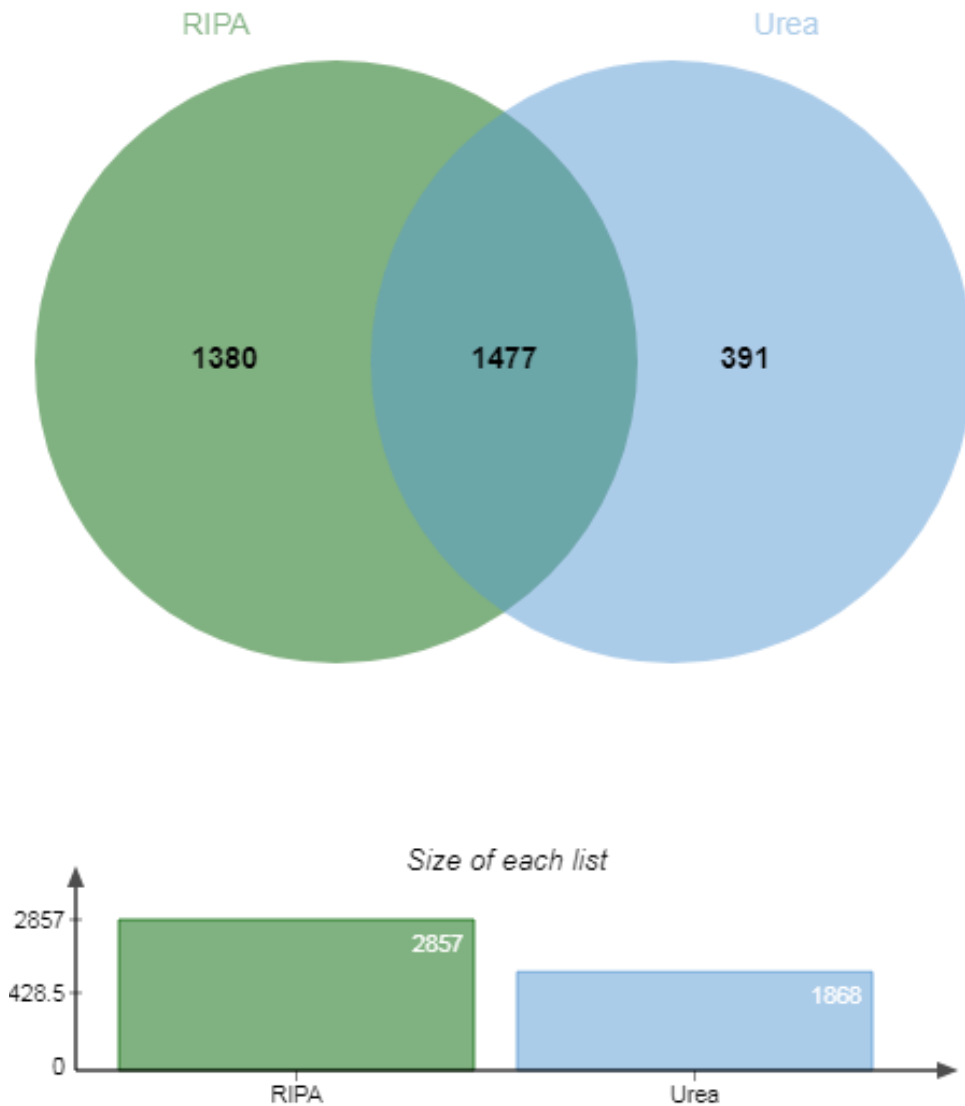


**Figure 4:13 – Total Protein Counts in RIPA/Urea-soluble Fractions for Untransfected, WT,  $\Delta$ NLS+4FL and  $\Delta$ NLS+2KQ Human-TDP-43 Replicates:** Protein counts of all proteins identified in the RIPA and Urea-soluble fractions for untransfected, WT,  $\Delta$ NLS+4FL and  $\Delta$ NLS+2KQ human-TDP-43 NSC-34 samples. Bar chart denotes total protein counts of RIPA and Urea-soluble fractions. n=5 biological replicates.

## 4.5.2 Exclusive Urea-soluble Proteins in Aggregate-prone Human TDP-43 Transfected

### NSC-34 Cells

To then identify the proteins that were exclusive to the aggregate-prone Urea-soluble samples, low-solubility proteins likely involved in inclusions, an overlay of all Urea-soluble proteins identified across the untransfected control, WT,  $\Delta$ NLS+4FL and  $\Delta$ NLS+2KQ human TDP-43 samples was generated (**Figure 4:14**). A total of 1868 unique proteins were identified across the Urea-soluble fractions of the untransfected control, WT,  $\Delta$ NLS+4FL and  $\Delta$ NLS+2KQ human TDP-43 transfections in NSC-34 cells. Of these 715 (38.3%) were identified across all 4 conditions and 458 (24.5%) were exclusive to or shared between the  $\Delta$ NLS+4FL and  $\Delta$ NLS+2KQ samples. Notably, more proteins were detected in the Urea-soluble fraction of the  $\Delta$ NLS+4FL and  $\Delta$ NLS+2KQ samples (1352 and 1317 proteins, respectively) compared to the untransfected control and WT samples (1118 and 1101 proteins, respectively), indicating that the aggregation-prone mutants were indeed causing aggregation of more proteins than the controls.

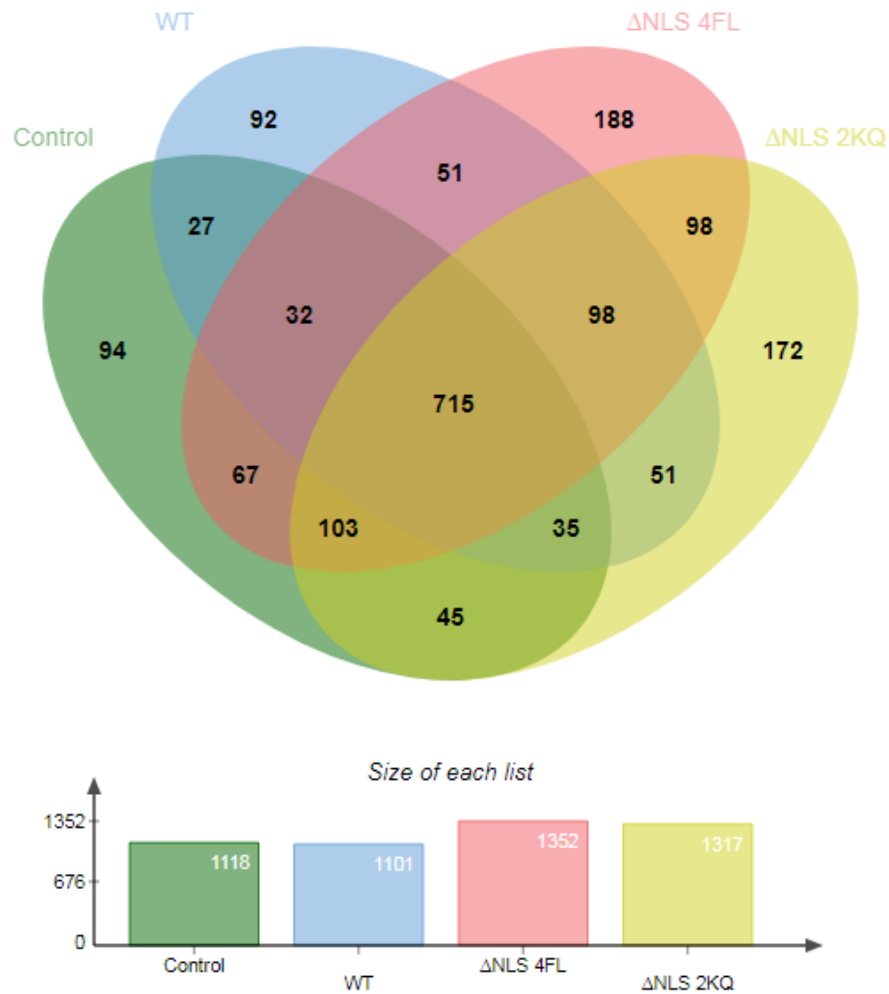


**Figure 4:14 – All Proteins Identified in Urea Fractions of NSC-34 Transfected Cells (150  $\mu$ g)**  
 Protein counts for all proteins identified in the urea fractions of NSC-34 cells: untransfected control, 4FL,  $\Delta$ NLS+4FL,  $\Delta$ NLS+2KQ transfected human TDP-43. Each colour represents a construct and numbers represent the protein counts. Bar charts show the total protein count for a particular construct. n=5 biological replicates.

The 458 proteins exclusive to the aggregate-prone Urea-soluble samples ( $\Delta$ NLS+4FL and  $\Delta$ NLS+2KQ) were deemed to be the low-solubility proteins likely involved in TDP-43 pathology. A list of the top 10 proteins sorted based first on peptide presence across replicates and then by total peptide count is presented in **Table 4:2**. A comprehensive list of all proteins exclusive to or shared between the  $\Delta$ NLS+4FL and  $\Delta$ NLS+2KQ with peptide counts is available in [Appendix B](#).

**Table 4:2 – Top 10 Exclusive/Shared Proteins in the Urea-soluble Fractions of  $\Delta$ NLS+4FL and  $\Delta$ NLS+2KQ Transfected NSC-34 Cells in the 150  $\mu$ g Experiment:**  
List of the top 10 proteins found to be exclusive to or shared between the  $\Delta$ NLS+4FL and  $\Delta$ NLS+2KQ transfections in the urea-soluble fraction of transfected NSC-34 cells. Sorted by exclusivity, replicate presence (greatest to least) and peptide count (greatest to least).

UniProt ID	Protein names	$\Delta$ NLS+4FL Replicate Presence (n/5)	$\Delta$ NLS+2KQ Replicate Presence (n/5)	Total Replicate Presence (n/10)	Total Peptide Count
Q8BKC5	Importin-5 (Imp5) (Importin subunit beta-3) (Karyopherin beta-3) (Ran-binding protein 5) (RanBP5)	2	2	4	12
Q6P5H2	Nestin	2	2	4	11
P63028	Translationally-controlled tumor protein (TCTP) (21 kDa polypeptide) (p21) (p23)	2	2	4	5
P11798	Calcium/calmodulin-dependent protein kinase type II subunit alpha (CaM kinase II subunit alpha) (CaMK-II subunit alpha) (EC 2.7.11.17)	2	2	4	5
Q99LN9	Deoxyhypusine hydroxylase (DOHH) (EC 1.14.99.29) (Deoxyhypusine dioxygenase) (Deoxyhypusine monooxygenase)	2	2	4	4
A2ASS6	Titin (EC 2.7.11.1) (Connectin)	1	2	3	37
Q6NZJ6	Eukaryotic translation initiation factor 4 gamma 1 (eIF-4-gamma 1) (eIF-4G 1) (eIF-4G1)	2	1	3	8
Q9WUK4	Replication factor C subunit 2 (Activator 1 40 kDa subunit) (A1 40 kDa subunit) (Activator 1 subunit 2) (Replication factor C 40 kDa subunit) (RF-C 40 kDa subunit) (RFC40)	2	1	3	6
Q149F3	Eukaryotic peptide chain release factor GTP-binding subunit ERF3B (Eukaryotic peptide chain release factor subunit 3b) (eRF3b) (G1 to S phase transition protein 2 homolog)	1	2	3	5
Q9QY76	Vesicle-associated membrane protein-associated protein B (VAMP-B) (VAMP-associated protein B) (VAP-B) (VAMP-associated protein 33b)	2	1	3	4

#### 4.5.3 Gene Ontology of Urea-soluble Proteins Exclusive to $\Delta$ NLS+4FL and $\Delta$ NLS+2KQ

##### Transfections Reflects Potentially Affected Biological Processes

To identify the types of biological processes that the 458 proteins exclusive to the aggregate-prone Urea-soluble  $\Delta$ NLS+4FL and  $\Delta$ NLS+2KQ transfections are involved in, a gene ontology search using the Panther Database was performed (**Figure 4:15**). These proteins reflected potentially affected biological processes such as nuclear transport, protein localisation, protein transport and RNA metabolic processing.

PANTHER GO-Slim Biological Process	Mus musculus (REF)	
	#	#
<a href="#">nuclear transport</a>	<a href="#">103</a>	<a href="#">12</a>
<a href="#">protein localization</a>	<a href="#">297</a>	<a href="#">17</a>
<a href="#">phosphate-containing compound metabolic process</a>	<a href="#">852</a>	<a href="#">40</a>
↳ <a href="#">metabolic process</a>	<a href="#">6472</a>	<a href="#">200</a>
<a href="#">catabolic process</a>	<a href="#">886</a>	<a href="#">38</a>
<a href="#">protein transport</a>	<a href="#">873</a>	<a href="#">37</a>
<a href="#">RNA metabolic process</a>	<a href="#">1104</a>	<a href="#">46</a>
↳ <a href="#">nucleobase-containing compound metabolic process</a>	<a href="#">2957</a>	<a href="#">100</a>
↳ <a href="#">primary metabolic process</a>	<a href="#">5565</a>	<a href="#">174</a>
<a href="#">nitrogen compound metabolic process</a>	<a href="#">2071</a>	<a href="#">77</a>
<a href="#">cellular component organization</a>	<a href="#">1541</a>	<a href="#">56</a>
↳ <a href="#">cellular component organization or biogenesis</a>	<a href="#">1716</a>	<a href="#">66</a>
<a href="#">cellular process</a>	<a href="#">8252</a>	<a href="#">213</a>
Unclassified	<a href="#">9580</a>	<a href="#">153</a>
<a href="#">regulation of biological process</a>	<a href="#">3059</a>	<a href="#">32</a>
↳ <a href="#">biological regulation</a>	<a href="#">3342</a>	<a href="#">37</a>
<a href="#">response to stimulus</a>	<a href="#">3695</a>	<a href="#">38</a>
<a href="#">sensory perception</a>	<a href="#">1254</a>	<a href="#">6</a>
↳ <a href="#">neurological system process</a>	<a href="#">1653</a>	<a href="#">13</a>
↳ <a href="#">system process</a>	<a href="#">1871</a>	<a href="#">17</a>
↳ <a href="#">single-multicellular organism process</a>	<a href="#">2593</a>	<a href="#">24</a>
↳ <a href="#">multicellular organismal process</a>	<a href="#">2658</a>	<a href="#">24</a>

**Figure 4:15 – Panther Database Gene Ontology of Urea-soluble Proteins Exclusive to the  $\Delta$ NLS+4FL and  $\Delta$ NLS+2KQ human TDP-43 Transfections:** Output from the Panther Database Gene Ontology search generated with input of all 458 protein identifiers that were exclusive to the Urea-soluble fractions from the  $\Delta$ NLS+4FL and  $\Delta$ NLS+2KQ transfections. The first column indicates the biological process implicated, the second column reflects the reference number to that particular set of processes and the third indicates the number of proteins from the input list that were implicated in that process.

#### 4.5.4 Comparison of Preliminary Urea-soluble Protein Identifications to Follow-Up Urea-soluble Protein Identifications

To determine how many proteins were reproducibly identified between the 30  $\mu\text{g}$  and 150  $\mu\text{g}$  experiments, an overlay of all proteins identified in the Urea-soluble replicates for each was produced (**Figure 4:16**). When comparing the 1868 unique proteins from 5 biological replicates of untransfected control, WT,  $\Delta\text{NLS}+4\text{FL}$ ,  $\Delta\text{NLS}+2\text{KQ}$ , from the 150  $\mu\text{g}$  experiment, to the 591 unique proteins from 4 biological replicates of untransfected control, WT,  $\Delta\text{NLS}$ , 4FL,  $\Delta\text{NLS}+4\text{FL}$ ,  $\Delta\text{NLS}+2\text{KQ}$ , from the 30 $\mu\text{g}$  experiment, 87% of the proteins from the 30  $\mu\text{g}$  experiment were reproducibly found in the 150  $\mu\text{g}$  experiment. This demonstrates that most of the proteins found in the 30  $\mu\text{g}$  samples were repetitively found in the 150  $\mu\text{g}$  samples. In addition, in the 150  $\mu\text{g}$  experiments, an additional 1335 proteins were identified, confirming the validity of the approach to use greater amounts of protein to increase overall identifications.

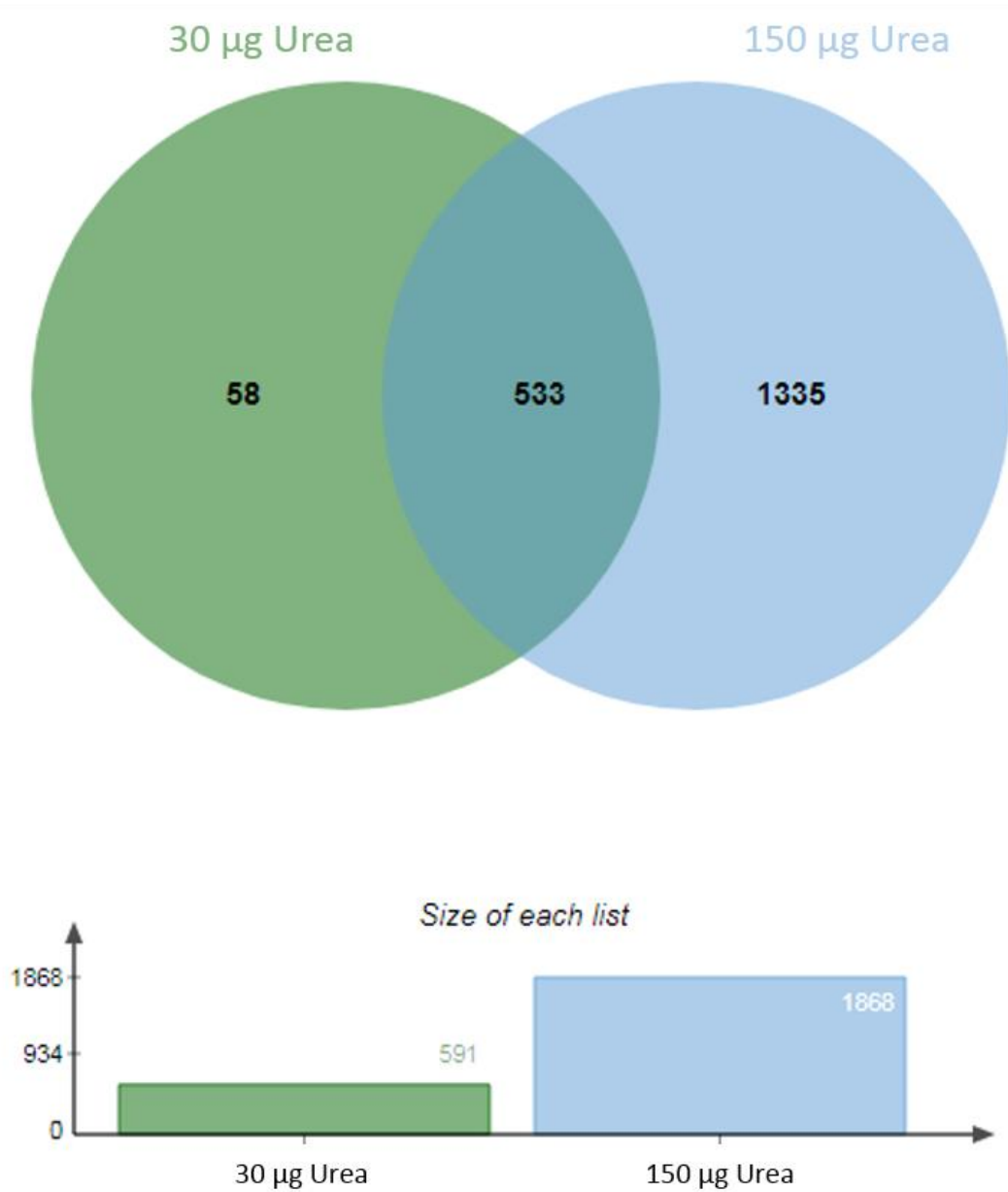


**Figure 4:16 – All Unique Proteins Identified in 30 µg Urea-soluble Replicates vs 150 µg Urea-soluble Replicates :** All unique proteins identified in the 30 µg urea samples (4 replicates; Control, WT, ΔNLS, 4FL, ΔNLS+4FL, ΔNLS+2KQ) as compared to the 150 µg urea samples (5 replicates; Control, WT, ΔNLS+4FL, ΔNLS+2KQ). Numbers represent the total number of proteins detected. Bar charts show the total protein count for the Urea-soluble fraction in each experiment.

Experiments intending to perform the same transfections using SH-SY5Y cells transfected with myc-tagged human TDP-43 WT,  $\Delta$ NLS, 4FL,  $\Delta$ NLS+4FL and  $\Delta$ NLS+2KQ in the pcDNA5/TO vector followed by proteomic analysis were begun, but due to the time constraints of the thesis were not completed.

Subsequent experiments utilising the human TDP-43 mutants WT,  $\Delta$ NLS, 4FL, 2KQ,  $\Delta$ NLS+4FL and  $\Delta$ NLS+2KQ in the pLenti-C-mGFP vector to express in both NSC-34 and SH-SY5Y cells for proteomic analysis were not able to be completed due to the time constraints of the thesis.

## 4.6 Analysis of Urea-soluble Proteins in TDP-43 Transgenic Mice

To isolate the detergent-insoluble protein fraction, sequential extraction of mouse cortex tissues coupled with ultracentrifugation was performed, similar to the method used for cell lysate extractions (**Methods 3.4**). In this method, RIPA buffer containing the detergents 0.1% SDS, 1% NP-40, as well as 50mM Tris, 150mM NaCl, 5mM EDTA, 0.5% sodium deoxycholate and 1mM PMSF was used to isolate the 'RIPA-soluble' protein fraction, that is the protein fraction taken to represent the normal cellular soluble, non-aggregated proteins. Subsequent washing of the pellet obtained from this step resulted in isolation of protein pellets containing the 'RIPA-insoluble' protein fraction, that is the protein fraction taken to represent the abnormal aggregated proteins. This RIPA-insoluble fraction was subsequently solubilised using harsh denaturing conditions with 7M Urea, 2M Thiourea, 4% CHAPS, 30mM Tris, producing the 'Urea-soluble' protein fraction.

This method incorporated left cortex samples from 5 bigenic rNLS (NEFH-tTA/tetO-hTDP-43 $\Delta$ NLS double transgenic) mice as well as 5 sex- and litter-matched control mice at 4 weeks after removal of doxycycline (approximately 10 weeks of age). This is a timepoint previously shown to be early in disease phenotype development and at the start of when pathological TDP-43 begins to accumulate, and prior to dramatic neurodegeneration<sup>174</sup>.

#### 4.6.1 Validation of Human TDP-43 Expression in the RIPA-soluble Fraction of TDP-43

##### Transgenic Mice

To validate the presence of human TDP-43 in the rNLS TDP-43 human transgenic mice, Western blotting using antibodies against human-specific and total TDP-43 was performed. Expression of cytoplasmic targeted human TDP-43 in the transgenic mice was validated through the presence of human TDP-43 specific bands between 37kDa and 50kDa in the RIPA-fraction (**Figure 4:16**). Similar levels of GAPDH proteins were detected at approximately 37kDa across each sample, demonstrating consistency in protein loading and calculations.

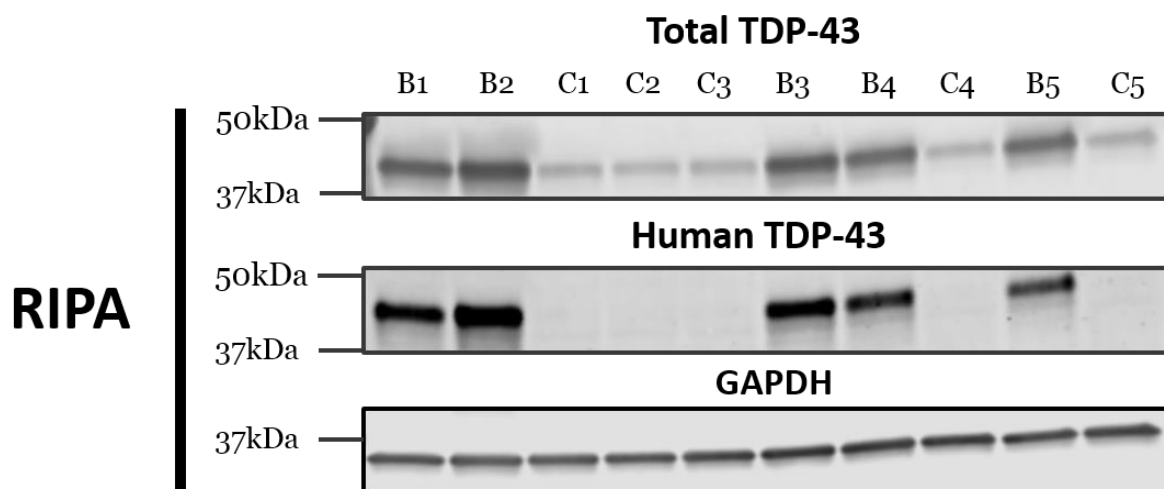


**Figure 4:17 – Total and Human TDP-43 Expression in the RIPA-soluble Fraction of Control and Double Transgenic (NEFH-tTA/tetO-hTDP-43rNLS) Mouse Cortex:** Western blots of mouse left cortex lysate probing for C-terminal total TDP-43(detected in the 680nm channel), human TDP-43 (detected in the 800nm channel) and GAPDH (reprobed and detected in the 680nm channe). B prefix denotes a bigenic rNLS TDP-43 human transgenic mouse whereas a C prefix denotes a littermate non-transgenic control mouse.

#### 4.6.2 Validation of Human TDP-43 Expression in the Urea-soluble Fraction of rNLS TDP-43 Transgenic Mice

As the transgenic mice were confirmed to express human TDP-43, the Urea-soluble fraction was examined to confirm that the aggregated TDP-43 was present in this fraction, as seen in ALS and FTD pathology. Expression of cytoplasmic targeted human TDP-43 in the transgenic mice was validated through the presence of total TDP-43 and phosphorylated TDP-43 specific bands between 37kDa and 50kDa in the urea-fraction (**Figure 4:17**). The bands appear to smear in the urea fractions, suggesting post-translational modifications indicative of aggregating TDP-43, similar to that seen in human disease tissues<sup>112</sup>. Importantly, no to little endogenous mouse TDP-43 was detected in the urea-soluble fraction of control mice despite detectable levels in the RIPA-soluble fraction (Figure 4:16), indicating the specificity of urea-soluble and therefore aggregated TDP-43 to the disease state. Likewise, phosphorylated TDP-43, indicative of pathology, was detected only in the bigenic TDP-43 mice. Not that the main band of the phosphorylated form of TDP-43 is detected at a higher molecular weight of approximately 45 kDa compared to the non-phosphorylated form at approximately 43 kDa. GAPDH was not detected in the Urea-soluble fraction as it is all solubilised and removed in the RIPA extraction.

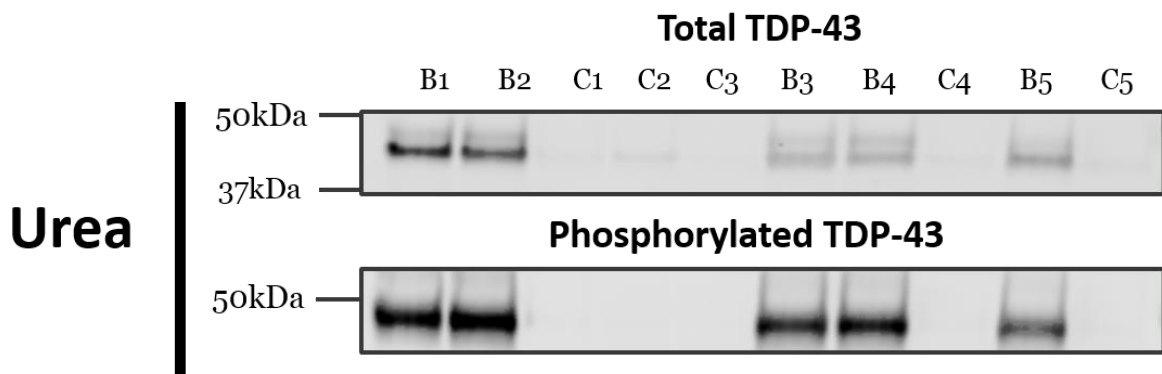


**Figure 4:18 – Total and Human TDP-43 Expression in the Urea-soluble Fraction of Control and Double Transgenic (NEFH-tTA/tetO-hTDP-43 $\Delta$ NLS) Mouse Cortex:** Western blots of mouse left cortex lysate probing for C-terminal total TDP-43 and phosphorylated TDP-43 (S409/410). B prefix denotes a bigenic rNLS TDP-43 human transgenic mouse whereas a C prefix denotes a littermate non-transgenic control mouse.

#### 4.6.3 Proteomic Analysis of Urea-soluble Proteins in rNLS TDP-43 Transgenic Mice

Following confirmation of the pathological TDP-43 content in the rNLS TDP-43 transgenic mice, proteomic studies of the urea-soluble fractions were performed to identify the protein content of pathology reminiscent of ALS and FTD. To demonstrate the biological variation between replicates within the control and rNLS TDP-43 transgenic mice, overlays of all proteins identified in each replicate were generated (**Figure 4:18**).

410 different proteins were identified in the urea fraction for the control mice. Of these, 126 (30.7%) proteins were identified across all 5 biological replicates (**Figure 4:18A**). 562 different proteins were identified in the rNLS TDP-43 human transgenic mice. Of these, 165 (29.5%) proteins were identified across all 5 biological replicates (**Figure 4:18B**). These findings indicate some variation between replicates, but also demonstrate that a core set of urea-soluble proteins were detected in these experiments

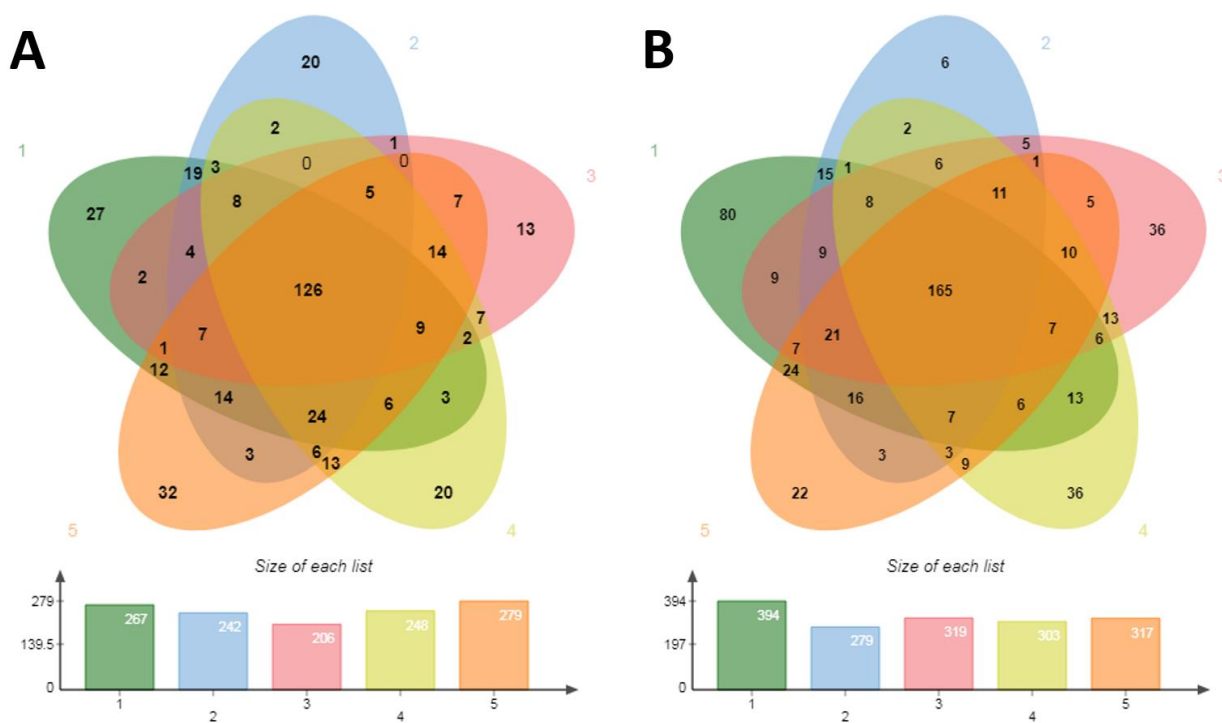


**Figure 4:19 –All Proteins Identified in Urea-soluble Fractions Across 5 Biological Replicates of (A) Control Mice and (B) rNLS TDP-43 Transgenic Mice:** Protein counts for all unique proteins identified in the Urea-soluble fractions of both control (A) and (B) rNLS TDP-43 transgenic mice. Each biologically matched replicate is shown using a different colour and numbers represent the total number of proteins detected that overlap between multiple replicates. Bar charts show the total protein count for each biological replicate. n=5 biological replicates per group.

To determine the proteins that were exclusive to the rNLS TDP-43 transgenic mice in the Urea-soluble fractions, all proteins identified in the Urea-soluble fractions in both control and rNLS TDP-43 transgenic mice were overlaid (**Figure 4:19**). A total of 612 unique proteins were identified in the Urea-soluble fractions, and of these 50 proteins (8.2%) were exclusive to the control mice and whereas 202 (33%) were exclusive to the rNLS TDP-43 transgenic mice, and this subset therefore represents the proteins of interest that are likely associated with aggregated TDP-43 pathology.

Notably, 360 (58.8%) of the proteins overlapped between the Urea-soluble fractions of both groups, indicating a substantial proportion of normal low-solubility proteins in mouse cortex and highlighting the need for comparison of urea-soluble protein content in disease compared to matched control tissues.

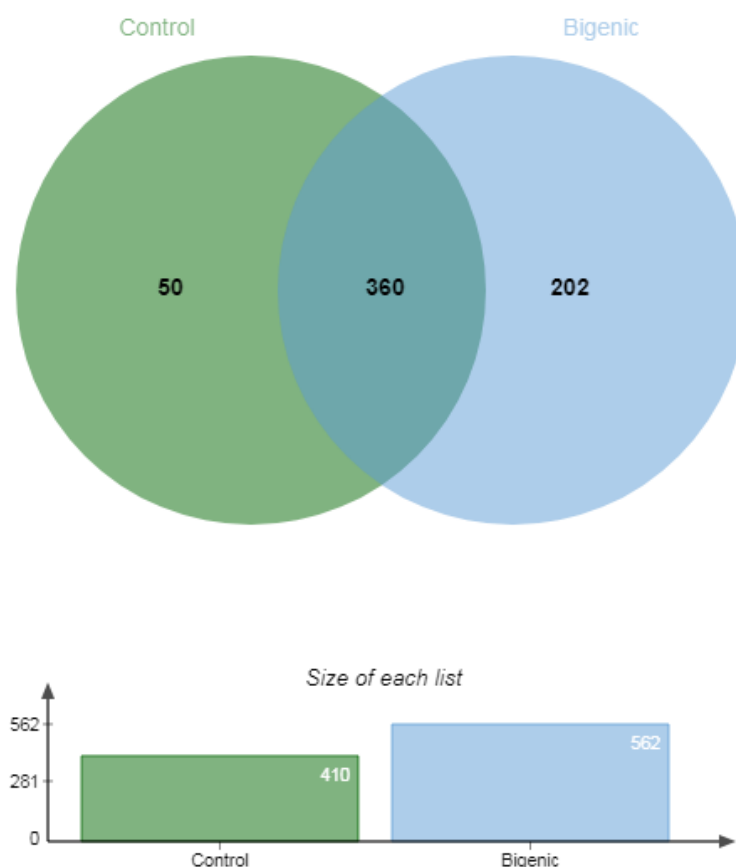


**Figure 4:20 – All Proteins Identified in the Urea-soluble Fractions of Control and rNLS TDP-43 Transgenic Mice:** Protein counts of all proteins identified in the Urea-soluble fractions for both bigenic rNLS TDP-43 transgenic mice as well as litter-matched control mice. Bar charts show the total protein counts for each condition. n=5 biological replicates.

Subsequent data analysis was performed in two parts: firstly to analyse those proteins that were detected exclusively in the rNLS TDP-43 transgenic mice and not in control mice, for which changes in relative abundance cannot be statistically determined, and secondly to analyse the relative abundance changes in rNLS TDP-43 transgenic mice compared to control mice for the urea-soluble proteins that were detected in both groups.

#### 4.6.4 Exclusive Urea-soluble Proteins in rNLS TDP-43 Transgenic Mice

The 202 proteins exclusive to the Urea-soluble fractions from the rNLS TDP-43 transgenic mice are likely involved in TDP-43 pathology. A list of the top 10 proteins sorted based firstly peptide presence across biological replicates and then by total peptide count is presented in **Table 4:3**. A

comprehensive list of all proteins found exclusively in the Urea-soluble fraction of rNLS TDP-43 transgenic mice with peptide counts is available in [Appendix C](#).

**Table 4:3 – Top 10 Exclusive Proteins in the Urea-soluble Fraction of the rNLS TDP-43 Transgenic Mice:** List of the top 10 proteins found exclusively in the Urea-soluble fraction of the rNLS TDP-43 transgenic mice. Sorted by total biological replicate presence and total peptide count (greatest to least).

UniProt ID	Protein names	Biological Replicate Peptide Count					Total Replicate Presence (n/5)	Total Peptide Count
		1	2	3	4	5		
<b>P07901</b>	Heat shock protein HSP 90-alpha (Heat shock 86 kDa) (HSP 86) (HSP86) (Tumor-specific transplantation 86 kDa antigen) (TSTA)	4	5	4	4	6	5	23
<b>P05064</b>	Fructose-bisphosphate aldolase A (EC 4.1.2.13) (Aldolase 1) (Muscle-type aldolase)	5	2	2	1	4	5	14
<b>P30275</b>	Creatine kinase U-type, mitochondrial (EC 2.7.3.2) (Acidic-type mitochondrial creatine kinase) (Mia-CK) (Ubiquitous mitochondrial creatine kinase) (U-MtCK)	2	2	2	3	4	5	13
<b>P97427</b>	Dihydropyrimidinase-related protein 1 (DRP-1) (Collapsin response mediator protein 1) (CRMP-1) (Unc-33-like phosphoprotein 3) (ULIP-3)	4	2	0	2	4	4	12
<b>Q3TXX4</b>	Vesicular glutamate transporter 1 (VGluT1) (Brain-specific Na(+)-dependent inorganic phosphate cotransporter) (Solute carrier family 17 member 7)	2	2	1	2	0	4	7
<b>Q9CQZ5</b>	NADH dehydrogenase [ubiquinone] 1 alpha subcomplex subunit 6 (Complex I-B14) (CI-B14) (NADH-ubiquinone oxidoreductase B14 subunit)	0	1	1	1	2	4	5
<b>B2RSH2</b>	Guanine nucleotide-binding protein G(i) subunit alpha-1 (Adenylate cyclase-inhibiting G alpha protein)	3	4	3	0	0	3	10
<b>Q9CQD1</b>	Ras-related protein Rab-5A	4	3	0	0	3	3	10
<b>P08752</b>	Guanine nucleotide-binding protein G(i) subunit alpha-2 (Adenylate cyclase-inhibiting G alpha protein)	0	4	3	0	2	3	9
<b>Q5SYD0</b>	Unconventional myosin-I $\delta$	3	0	3	0	2	3	8

#### 4.6.5 Gene Ontology of Urea-soluble Proteins Exclusive to rNLS TDP-43 Transgenic Mice

##### Reflects Potentially Affected Biological Processes

To identify the types of biological processes that proteins exclusive to the Urea-soluble fractions of rNLS TDP-43 transgenic mice are involved in, a gene ontology search of all 202 exclusive proteins using the Panther Database was performed (**Figure 4:21**). These proteins reflected potentially affected biological processes such as oxidative phosphorylation, protein complex assemble cellular component morphogenesis and organelle organisation.

	<a href="#">Mus musculus (REF)</a>	
<a href="#">PANTHER GO-Slim Biological Process</a>	#	#
<a href="#">oxidative phosphorylation</a>	<a href="#">48</a>	<a href="#">6</a>
↳ <a href="#">generation of precursor metabolites and energy</a>	<a href="#">227</a>	<a href="#">12</a>
↳ <a href="#">metabolic process</a>	<a href="#">6472</a>	<a href="#">84</a>
<a href="#">protein complex assembly</a>	<a href="#">161</a>	<a href="#">8</a>
↳ <a href="#">protein complex biogenesis</a>	<a href="#">162</a>	<a href="#">8</a>
↳ <a href="#">cellular component biogenesis</a>	<a href="#">548</a>	<a href="#">19</a>
↳ <a href="#">cellular component organization or biogenesis</a>	<a href="#">1716</a>	<a href="#">48</a>
<a href="#">cellular component morphogenesis</a>	<a href="#">433</a>	<a href="#">17</a>
↳ <a href="#">cellular component organization</a>	<a href="#">1541</a>	<a href="#">39</a>
<a href="#">organelle organization</a>	<a href="#">783</a>	<a href="#">19</a>
<a href="#">cellular process</a>	<a href="#">8252</a>	<a href="#">105</a>
Unclassified	<a href="#">9580</a>	<a href="#">56</a>

**Figure 4:21 – Panther Database Gene Ontology of Urea-soluble Proteins Exclusive to the rNLS TDP-43 Transgenic Mice:** Output from the Panther Database Gene Ontology search generated with input of all 202 protein identifiers that were exclusive to the Urea-soluble fractions from the rNLS TDP-43 transgenic mice. The first column indicates the biological process implicated, the second column reflects the reference number to that particular set of processes and the third indicates the number of proteins from the input list that were implicated in that process.

#### 4.6.6 Changed Urea-soluble Proteins in rNLS TDP-43 Transgenic Mice Compared to Control Mice

Using SCRAPPY, a collective series of R-module scripts for the analysis of label-free proteomics data, a paired-wise comparison between both the control and rNLS TDP-43 transgenic Urea-soluble fractions identified 31 proteins that had an increased relative abundance of 1.5x or greater in the rNLS TDP-43 transgenic mice when compared to the control mice (**Table 4:4**). Notably, 13 of these proteins had a >1.5 fold-change with statistically significant difference  $p < 0.05$ . Notably, TDP-43 was detected as having increased abundance in the TDP-43 transgenic mouse urea fraction (**Table 4.4**).

**Table 4:4 – Proteins with Increased Relative Abundance in Urea-soluble Fractions of rNLS TDP-43 Transgenic Mice:** All proteins with a calculated increased fold-change of 1.5x or greater in the rNLS TDP-43 transgenic mice Urea-soluble fractions as compared to the control mice. Total peptide counts refer to the number of peptides found across all 5 biological replicates for that mouse category. P-value is determined from SCRAPPY paired t-test of these peptide counts. Bolded rows indicate proteins with a statistically significant change between rNLS TDP-43 transgenic mice compared to control mice,  $p < 0.05$ ).

Description	Bigenic Total Peptide Count	Control Total Peptide Count	Fold-Change	p.value
Heat shock protein HSP 90-alpha	23	0	8.5	<b>2.35E-08</b>
Fructose-bisphosphate aldolase A	14	0	5.5	<b>0.0001</b>
Creatine kinase U-type, mitochondrial	13	0	5.1	<b>1.07E-06</b>
Cytoplasmic dynein 1 heavy chain 1	39	7	3.7	<b>0.015</b>
Microtubule-associated protein 1A	23	6	2.7	<b>0.018</b>
Protein kinase C gamma type	15	4	2.4	<b>0.027</b>
Creatine kinase B-type	23	7	2.3	<b>0.002</b>
Histone H3.3C	13	3	2.3	0.093
Plectin	40	15	2.2	0.084
Microtubule-associated protein 1B	15	5	2.1	<b>0.032</b>
TAR DNA-binding protein 43	12	4	2.0	0.102
Histone H2B type 1-F/J/L	15	5	1.9	<b>0.014</b>
Myeloid leukemia factor 2	8	2	1.9	0.050
Sodium/potassium-transporting ATPase subunit alpha-2	58	26	1.9	0.104
Transcriptional activator protein Pur-alpha	9	3	1.8	0.097
Synaptophysin	9	3	1.8	<b>0.046</b>
ADP/ATP translocase 1	17	7	1.7	0.111
Ras-related protein Rab-3A	11	4	1.7	0.102
Histone H4	19	8	1.7	0.073
2-oxoglutarate dehydrogenase, mitochondrial	16	7	1.7	0.174

Plasma membrane calcium-transporting ATPase 1	26	12	1.7	0.205
Vimentin	<b>68</b>	<b>34</b>	<b>1.6</b>	<b>0.001</b>
Stress-70 protein, mitochondrial	<b>19</b>	<b>9</b>	<b>1.6</b>	<b>0.038</b>
Solute carrier family 12 member 5	12	5	1.6	0.176
60S ribosomal protein L6	17	8	1.6	0.104
Heat shock protein HSP 90-beta	27	14	1.6	0.138
Glial fibrillary acidic protein	<b>126</b>	<b>66</b>	<b>1.6</b>	<b>0.003</b>
Major vault protein	17	8	1.6	0.106
Citrate synthase, mitochondrial	9	4	1.6	0.138
NADH dehydrogenase [ubiquinone] flavoprotein 1, mitochondrial	35	19	1.5	0.058
GTP-binding nuclear protein Ran	8	3	1.5	0.128

The same paired-wise comparison test between both the control and rNLS TDP-43 transgenic Urea-soluble fractions using SCRAPPY, identified 14 proteins that had a decreased relative abundance of 1.5x or greater in the the rNLS TDP-43 transgenic mice when compared to the control mice (**Table 4:5**). Notably, 5 of these proteins had a >1.5 fold-change with statistically significant difference  $p < 0.05$ .

**Table 4:5 – Proteins with Increased Relative Abundance in Urea-soluble Fractions of rNLS TDP-43 Transgenic Mice:** All proteins with a calculated decreased fold-change of 1.5x or greater in the rNLS TDP-43 transgenic mice Urea-soluble fractions as compared to the control mice. Total peptide counts refer to the number of peptides found across all 5 biological replicates for that mouse category. P-value is determined from SCRAPPY paired t-test of these peptide counts. Bolded rows indicate proteins with a statistically significant change between rNLS TDP-43 transgenic mice compared to control mice,  $p < 0.05$ ).

Description	Bigenic Peptide Count Total	Control Peptide Count Total	Fold-Change	p.value
Oligodendrocyte-myelin glycoprotein	<b>5</b>	<b>12</b>	<b>-3.1</b>	<b>0.01</b>
Neuronal growth regulator 1	<b>5</b>	<b>16</b>	<b>-2.9</b>	<b>0.01</b>
V-type proton ATPase subunit S1	<b>4</b>	<b>10</b>	<b>-2.4</b>	<b>0.03</b>
Actin, alpha cardiac muscle 1	49	84	-2.1	0.09
Alpha-actinin-4	24	40	-1.9	0.12
Homer protein homolog 1	17	30	-1.9	0.06
Alpha-actinin-2	16	27	-1.8	0.71
Spectrin beta chain, non-erythrocytic 1	21	36	-1.8	0.35
Clathrin heavy chain 1	40	62	-1.7	0.05
Tubulin alpha-1A chain	54	70	-1.5	0.16
Voltage-dependent calcium channel subunit alpha-2/delta-1	<b>34</b>	<b>44</b>	<b>-1.5</b>	<b>0.01</b>

<b>Disks large homolog 4</b>	<b>52</b>	<b>68</b>	<b>-1.5</b>	<b>0.01</b>
<b>Pyruvate kinase isozymes M1/M2</b>	12	16	-1.5	0.07

#### 4.7 Comparison of rNLS TDP-43 Transgenic Mice Urea-soluble Exclusive Proteins to Human TDP-43 Mutant Urea-soluble Exclusive Proteins from 30 µg or 150 µg NSC-34 Experiments Implicates Those Involved in TDP-43 Aggregate Pathology

To determine validity between the NSC-34 transfected cell-model and the rNLS TDP-43 transgenic mice, a comparison between all Urea-soluble fraction proteins shared between or exclusive to human TDP-43  $\Delta$ NLS, 4FL,  $\Delta$ NLS+4FL and  $\Delta$ NLS+2KQ from the 30 µg experiment, and all proteins shared between or exclusive to  $\Delta$ NLS+4FL and  $\Delta$ NLS+2KQ from the 150 µg experiment of transfected NSC-34 cells, were overlaid with all Urea-soluble fraction proteins exclusive to the rNLS TDP-43 transgenic mice (**Figure 4:22**). Notably only 1 protein was identified in all 3 experiments. The 32 proteins that overlapped between the 30 µg experiment and rNLS TDP-43 transgenic mice are the most interesting as the 30 µg experiment contained the  $\Delta$ NLS mutant, which directly matches the mutation in the mice. The 13 proteins that overlapped between the 150 µg experiment and rNLS TDP-43 transgenic mice are also interesting, as these would most likely associate with TDP-43 aggregate pathology.

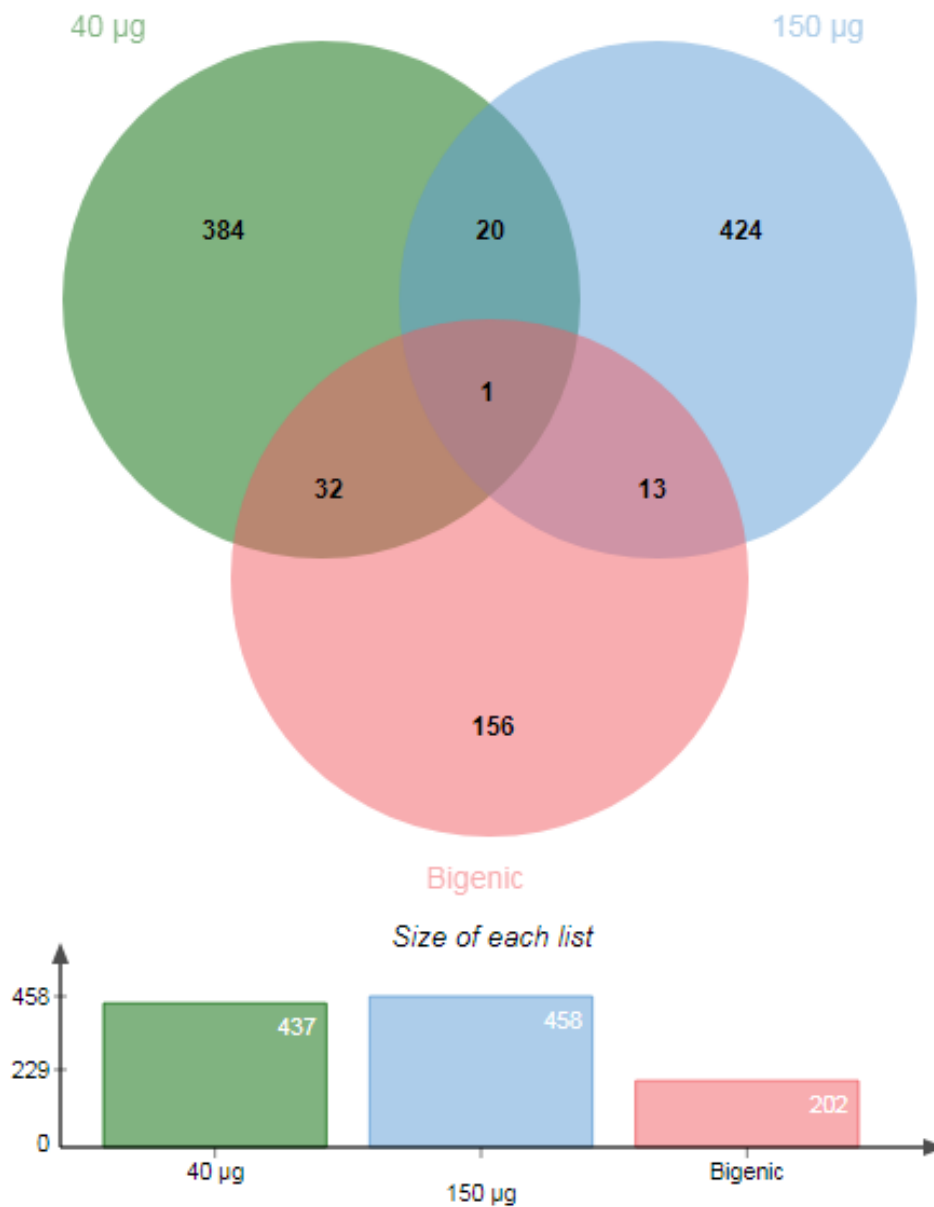


**Figure 4:22 – Total Urea-soluble Fraction Proteins Exclusive to human TDP-43  $\Delta$ NLS, 4FL,  $\Delta$ NLS+4FL and  $\Delta$ NLS+2KQ (30  $\mu$ g),  $\Delta$ NLS+4FL and  $\Delta$ NLS+2KQ (150  $\mu$ g) and rNLS TDP-43 Transgenic Mice:** The total number of Urea-soluble fraction proteins exclusive to the human TDP-43  $\Delta$ NLS, 4FL,  $\Delta$ NLS+4FL and  $\Delta$ NLS+2KQ (30  $\mu$ g) and  $\Delta$ NLS+4FL and  $\Delta$ NLS+2KQ (150  $\mu$ g) NSC-34 transfections compared to the Urea-soluble exclusive proteins from the bigenic TDP-43 mice. Bar charts show the total protein counts for each condition. n=4 biological replicates for the 30  $\mu$ g samples. n=5 biological replicates for the 150  $\mu$ g and bigenic mouse samples.

A list of these 45 proteins that were present in the rNLS TDP-43 transgenic mice and overlap with human TDP-43 mutants from either the 30  $\mu$ g experiment or 150  $\mu$ g experiments of transfected NSC-34 cells is presented in **Table 4:6**.

**Table 4:6 – Replicate Presence of Urea-soluble Proteins Found in rNLS TDP-43 Transgenic Mice That Either Overlap with Urea-soluble Proteins in Human TDP-43 Mutants from the 30  $\mu$ g or 150 $\mu$ g Experiments:** Replicate counts from the Urea-soluble fraction proteins exclusive to the human TDP-43  $\Delta$ NLS, 4FL,  $\Delta$ NLS+4FL and  $\Delta$ NLS+2KQ (30  $\mu$ g) and  $\Delta$ NLS+4FL and  $\Delta$ NLS+2KQ (150  $\mu$ g) NSC-34 transfections as well as the Urea-soluble exclusive proteins from the bigenic TDP-43 mice. n=4 biological replicates for each group in the 30  $\mu$ g samples. n=5 biological replicates for the 150  $\mu$ g and bigenic mouse samples.

Uniprot ID	Protein name	Total 30 $\mu$ g Replicate Presence	Total 150 $\mu$ g Replicate Presence	Total Bigenic Mouse Presence
P40124	Adenylyl cyclase-associated protein 1 (CAP 1)	2	1	1
Q9Z2X1	Heterogeneous nuclear ribonucleoprotein F (hnRNP F) [Cleaved into: Heterogeneous nuclear ribonucleoprotein F, N-terminally processed]	5	0	1
P97807	Fumarate hydratase, mitochondrial (Fumarase) (EC 4.2.1.2) (EF-3)	5	0	2
Q9JJV2	Profilin-2 (Profilin II)	5	0	1
Q62188	Dihydropyrimidinase-related protein 3 (DRP-3) (Unc-33-like phosphoprotein 1) (ULIP-1)	4	0	1
P68373	Tubulin alpha-1C chain (Alpha-tubulin 6) (Alpha-tubulin isotype M-alpha-6) (Tubulin alpha-6 chain) [Cleaved into: Detyrosinated tubulin alpha-1C chain]	3	0	1
P60122	RuvB-like 1 (EC 3.6.4.12) (49 kDa TATA box-binding protein-interacting protein) (49 kDa TBP-interacting protein) (DNA helicase p50) (Pontin 52) (TIP49a)	3	0	1
Q9R1P0	Proteasome subunit alpha type-4 (EC 3.4.25.1) (Macropain subunit C9) (Multicatalytic endopeptidase complex subunit C9) (Proteasome component C9) (Proteasome subunit L)	3	0	1
P35979	60S ribosomal protein L12	3	0	1
Q99JB2	Stomatin-like protein 2, mitochondrial (SLP-2) (mslp2)	2	0	2
P43276	Histone H1.5 (H1 VAR.5) (H1b)	2	0	1
P35293	Ras-related protein Rab-18	2	0	1
P61750	ADP-ribosylation factor 4	2	0	2

<b>P62908</b>	40S ribosomal protein S3 (EC 4.2.99.18)	2	0	3
<b>Q6DFW4</b>	Nucleolar protein 58 (MSSP) (Nucleolar protein 5) (SIK-similar protein)	2	0	2
<b>Q8QZT1</b>	Acetyl-CoA acetyltransferase, mitochondrial (EC 2.3.1.9) (Acetoacetyl-CoA thiolase)	2	0	3
<b>P07901</b>	Heat shock protein HSP 90-alpha (Heat shock 86 kDa) (HSP 86) (HSP86) (Tumor-specific transplantation 86 kDa antigen) (TSTA)	1	0	5
<b>P43277</b>	Histone H1.3 (H1 VAR.4) (H1d)	1	0	1
<b>P63038</b>	60 kDa heat shock protein, mitochondrial (EC 3.6.4.9) (60 kDa chaperonin) (Chaperonin 60) (CPN60) (HSP-65) (Heat shock protein 60) (HSP-60) (Hsp60) (Mitochondrial matrix protein P1)	1	0	2
<b>Q8BGQ7</b>	Alanine--tRNA ligase, cytoplasmic (EC 6.1.1.7) (Alanyl-tRNA synthetase) (AlaRS)	1	0	3
<b>Q3TXS7</b>	26S proteasome non-ATPase regulatory subunit 1 (26S proteasome regulatory subunit RPN2) (26S proteasome regulatory subunit S1)	1	0	1
<b>Q4JIM5</b>	Abelson tyrosine-protein kinase 2 (EC 2.7.10.2) (Abelson murine leukemia viral oncogene homolog 2) (Abelson-related gene protein) (Tyrosine-protein kinase ARG)	1	0	1
<b>Q9CX30</b>	Protein YIF1B (YIP1-interacting factor homolog B)	1	0	1
<b>P35980</b>	60S ribosomal protein L18	1	0	1
<b>P35550</b>	rRNA 2'-O-methyltransferase fibrillar (EC 2.1.1.-) (Histone-glutamine methyltransferase) (Nucleolar protein 1)	1	0	2
<b>Q8CGP6</b>	Histone H2A type 1-H	1	0	1
<b>P53026</b>	60S ribosomal protein L10a (CSA-19) (Neural precursor cell expressed developmentally down-regulated protein 6) (NEDD-6)	1	0	2
<b>Q8K310</b>	Matrin-3	1	0	1
<b>P05064</b>	Fructose-bisphosphate aldolase A (EC 4.1.2.13) (Aldolase 1) (Muscle-type aldolase)	1	0	5
<b>P58252</b>	Elongation factor 2 (EF-2)	1	0	1
<b>P17751</b>	Triosephosphate isomerase (TIM) (EC 5.3.1.1) (Triose-phosphate isomerase)	1	0	2
<b>Q99020</b>	Heterogeneous nuclear ribonucleoprotein A/B (hnRNP A/B) (CArG-binding factor-A) (CBF-A)	1	0	2
<b>P43275</b>	Histone H1.1 (H1 VAR.3) (Histone H1a) (H1a)	1	0	1
<b>Q7TQI3</b>	Ubiquitin thioesterase OTUB1 (EC 3.4.19.12) (Deubiquitinating enzyme OTUB1) (OTU domain-containing	0	2	1

	ubiquitin aldehyde-binding protein 1) (Otubain-1) (Ubiquitin-specific-processing protease OTUB1)			
<b>P16460</b>	Argininosuccinate synthase (EC 6.3.4.5) (Citrulline--aspartate ligase)	0	2	2
<b>Q8K2T1</b>	NmrA-like family domain-containing protein 1	0	2	2
<b>P29387</b>	Guanine nucleotide-binding protein subunit beta-4 (Transducin beta chain 4)	0	2	2
<b>O08788</b>	Dynactin subunit 1 (150 kDa dynein- associated polypeptide) (DAP-150) (DP- 150) (p150-glued)	0	1	2
<b>Q6Q477</b>	Plasma membrane calcium-transporting ATPase 4 (PMCA4) (EC 3.6.3.8)	0	1	1
<b>Q60900</b>	ELAV-like protein 3 (Hu-antigen C) (HuC)	0	1	1
<b>P04627</b>	Serine/threonine-protein kinase A-Raf (EC 2.7.11.1) (Proto-oncogene A-Raf)	0	1	1
<b>Q62465</b>	Synaptic vesicle membrane protein VAT-1 homolog (EC 1.-.-.)	0	1	1
<b>Q8BIF2</b>	RNA binding protein fox-1 homolog 3 (Fox-1 homolog C) (Hexaribonucleotide- binding protein 3) (Fox-3) (Neuronal nuclei antigen) (NeuN antigen)	0	1	1
<b>Q9JII6</b>	Alcohol dehydrogenase [NADP(+)] (EC 1.1.1.2) (Aldehyde reductase) (Aldo-keto reductase family 1 member A1)	0	1	2
<b>Q9Z0E0</b>	Neurochondrin (M-Sema F-associating protein of 75 kDa) (Norbin)	0	1	1
<b>Q60676</b>	Serine/threonine-protein phosphatase 5 (PP5) (EC 3.1.3.16) (Protein phosphatase T) (PPT)	0	1	1

# 5. Discussion

---

The findings presented in this thesis centre around the types of proteins that are involved in the Urea-soluble fractions for either aggregate-prone human TDP-43 transfected in NSC-34 cells (**see below in Discussion 5.1**) or rNLS TDP-43 transgenic mice (**see below in Discussion 5.2**). Proteins within these low-solubility fractions may be either directly involved in ALS or implicated in ALS pathology, and further studies are required to define which, if any, of these proteins play key roles in disease pathogenesis. Many of these identified low-solubility proteins also belong to biological processes that have been implicated in disease pathology. It is now important to consider the functional roles of the identified proteins, which may provide information on changes that occur within neurons with aggregated TDP-43 that could be amenable to modulation for disease treatment.

This study is the first characterisation of TDP-43 insoluble protein aggregates from 5 different human TDP-43 constructs in NSC-34 cells as well as in a mouse model of TDP-43 pathology. We show that across these two models, certain populations of proteins are consistently found. These include:

- Nuclear proteins such as hnRNPs and nucleolar protein 58.
- Mitochondrial proteins such as heat-shock protein 60, fumarate hydratase and acetyl-CoA transferase.
- DNA/RNA-binding proteins such as, 60S ribosomal proteins L12 and L10a, matrin 3, RNA binding protein fox-1 homolog 3, histones H15, H1.3 and H2A.
- Proteins involved in cytoskeletal dynamics such as dihydropyrimidinase-related protein 3, adenylyl cyclase-associated protein 1, tubulin alpha 1-C, profilin 2.
- Proteins involved in transport and vesicle trafficking such as dynactin subunit 1, protein YIF1B.

The functions of these proteins provide insight into potentially affected pathways and mechanisms in ALS pathogenesis, and the most relevant of these can be elucidated through a multiple-model comparison approach.

This project aimed to identify the proteins that are specifically recruited to TDP-43 pathology in disease. To do this, experiments were designed to isolate all insoluble proteins in control conditions (Untransfected/wildtype cells and non-transgenic mice) and compare to disease conditions (cells expressing pathological TDP-43 or TDP-43 transgenic mice). Thus, these experiments are not likely to just isolate proteins found to associate by random aggregation but should determine those proteins that are rendered less soluble specifically in the presence of pathological TDP-43. Further experiments to investigate this in more detail could be performed using sub-cellular fractionation to identify where in the cell this protein aggregation is occurring. In addition, these datasets of proteins detected by these mass spectrometry-based approaches should also be compared to recent work on the super-saturated proteome, which suggested that proteins that are near the level of natural aggregation are more likely to be functionally involved in the pathology of neurodegenerative disease<sup>108</sup>.

## 5.1 Involvement of Urea-soluble Proteins Detected in Aggregate-prone

### $\Delta$ NLS+2KQ and $\Delta$ NLS+4FL Human TDP-43 Transfected NSC-34 Cells in ALS/FTD

Within the list of all 458 Urea-soluble exclusive proteins to the  $\Delta$ NLS+2KQ and  $\Delta$ NLS+4FL human TDP-43 mutants, there are proteins previously shown to be relevant to ALS/FTD mechanisms which are therefore interesting to investigate further. These include: mitochondrial proteins, particularly a few from the TCA-cycle, such as acetyl-CoA acetyltransferase and adenylyl cyclase-associated protein 1; nuclear transport factors, such as Transportin 2 and Importin 5; chaperones such as heat shock 70kDa protein 14 and translationally-controlled tumour protein (TCTP), and; ubiquitin related proteins such as ubiquitin thioesterase and E3 ubiquitin-protein ligase RING2. **Table 5:1** presents a selection of these proteins and illustrates their relevance in the context of ALS pathology. In ALS pathogenesis, various cellular processes are disrupted, some of which involve the described proteins and pathways above, therefore illustrating their potential importance.

**Table 5:1 – Urea-Soluble Proteins in Aggregate-prone human TDP-43 Transfected NSC-34 Cells Reflect Involvement in ALS/FTD:** Urea-soluble proteins present exclusively in the human TDP-43  $\Delta$ NLS+2KQ and  $\Delta$ NLS+4FL from the 150  $\mu$ g NSC-34 experiments. Protein described functions and their relevance to ALS/FTD are in columns 2 and 3 respectively.

Uniprot ID	Protein	Function	Relevance	Reference
<b>Q99M31</b>	Heat shock 70kDa protein 14	Stress chaperone	Elevated in ALS	226
<b>P62858</b>	40S Ribosomal protein S28	Protein synthesis, cell surface receptor, various functions	Interacts with TDP-43, implicated in pathogenic processes	125
<b>P62911</b>	60S ribosomal protein L32	Protein synthesis	Interacts with TDP-43	125
<b>Q9WUK2</b>	eIF-4H	Eukaryotic translation initiation factor	Expression affected by TDP-43	227
<b>Q9QY76</b>	VAPB	Vesicle-ER membrane protein/transport	ALS -causing mutant gene	55
<b>P08228</b>	SOD1	Reactive oxygen species metabolism	ALS-causing mutant gene	121
<b>P63028</b>	TCTP	Ca <sup>2+</sup> binding, apoptosis, microtubule stabilisation	Potential role in ALS	228
<b>Q3U7R1</b>	Synaptotagmin-1	ER-plasma membrane dynamics	Elevated in ALS mice	229
<b>Q99LN9</b>	Deoxyhypusine hydroxylase	RNA translation dynamics	Implicated involvement in ALS	230
<b>Q99LG2</b> <b>Q6P2B1</b>	Transportin 2 and 3	Nuclear Transport	Transportin 1 has been identified in FUS inclusions	140

The identification of highly relevant proteins such as those in **Table 5:1** supports the idea that these low-solubility proteins are likely involved in and sequestered into TDP-43 positive inclusions, therefore implicating them in pathology. Notably, within this list of proteins are potential leads for proteins that may be involved in cellular defence against aggregated TDP-43, such as HSP70. Recently, induction of heat shock proteins was shown to ameliorate TDP-43 aggregation in cell culture models<sup>159</sup>, suggesting that therapeutic modulation of chaperones such as this may be one avenue for removal of pathological TDP-43 from neurons, which may be beneficial in disease.

Also interesting from this list of proteins, is the presence of both VAPB and SOD1 in the low-solubility fraction of aggregation-prone TDP-43 expressing cells. The genes of both VAPB and SOD1 are harbour ALS-causative mutations in a small minority of ALS cases, however the involvement of wildtype VAPB and SOD1 proteins in pathology of sporadic ALS patients lacking these mutations has remained controversial. The finding here that wildtype VAPB and SOD1 can be recruited to the insoluble protein fraction upon TDP-43 aggregation suggests greater overlap in potential disease mechanisms between these rare forms of inherited ALS and the more common sporadic disease with TDP-43 pathology.

We also expect normally insoluble proteins to be present in these Urea-soluble fractions, despite attempting to control against them with the untransfected and WT human TDP-43 samples. This is verified through the presence of cytoskeletal proteins such as Titin and actin filament-associated protein 1-like 2. However, the findings that these proteins were enriched in the urea fractions of cells expressing aggregating TDP-43 suggests that their presence may be associated with pathology formation. Indeed, recently it was shown that proteins that are near the limit of supersaturation and are more likely to aggregate play a key role in forming pathology in ALS<sup>108</sup>.

Gene ontology also supports these conclusions, as the biological processes of nuclear transport, protein localisation, protein transport and mRNA metabolic processing have been all been previously implicated to be affected in ALS/FTD<sup>26, 142, 143</sup>. The findings of this thesis demonstrate that dysfunction of these important cellular functions may be a result of key proteins within these pathways being recruited to the low-solubility fraction upon aggregation of TDP-43, highlighting potential new pathogenic mechanisms in disease

## 5.2 Involvement of Urea-soluble Proteins detected in rNLS TDP-43 Transgenic in ALS/FTD

Within the list of all 202 Urea-soluble exclusive proteins to the rNLS TDP-43 transgenic mice, there are also proteins relevant to ALS/FTD mechanisms and which are therefore interesting for additional investigation. **Table 5:1** presents a selection of these proteins and illustrates their relevance in the context of ALS pathology.

**Table 5:2 – Urea-Soluble Proteins in rNLS TDP-43 Transgenic Mice Reflect Involvement in ALS/FTD:** Urea-soluble proteins present exclusively in the rNLS TDP-43 transgenic mice. Protein described functions and their relevance to ALS/FTD are in columns 2 and 3 respectively.

Uniprot ID	Protein	Function	Relevance	Reference
<b>P46935</b>	E3 ubiquitin-protein ligase NEDD4	Ubiquitin transfer protein/proteostasis	Upregulated in oxidative stress	231
<b>O08788</b>	Dynactin 1	Endosome to Golgi retrograde transport	ALS-causing mutant gene	37
<b>Q8K310</b>	Matrin 3	Transcription/Nuclear matrix protein	ALS-causing mutant gene	41
<b>Q9JJV2</b>	Profilin 2	Cytoskeletal regulator	Mutations in profilin 1 cause ALS	47
<b>Q9CQD1</b>	Ras-related protein Rab-5a	Endosome dynamics	Interacts with ALS2CL, highly homologous to ALS-causing mutant <i>ALS2</i> gene	232
<b>Q4JIM5</b>	Abelson tyrosine-protein kinase 2	Cell survival/growth, cytoskeletal remodelling	Other tyrosine kinases increased in ALS spinal cord	233
<b>P07901</b>	Heat shock protein HSP 90-alpha	Stress chaperone	Elevated in ALS	226
<b>Q9CX30</b>	Protein YIF1B	Golgi vesicle transport	Interacts with the VAPB ALS protein	234
<b>P61750</b>	Arf4	Vesicle transport and cellular stress	Cellular stress responsive protein	235

Again, within this list are several proteins that have been previously implicated in ALS and FTD as rare disease-causing mutations are linked with disease, such as dynactin 1 and matrin 3. For example, the RNA/DNA-binding protein matrin 3 has been previously shown to interact with TDP-43 and in

addition to rare disease-causing mutations, matrin 3 protein is also present within pathology of sporadic ALS patients without matrin 3 mutation<sup>41</sup>. However, whether matrin 3 is involved early on in the process of ALS/FTD-related neurodegeneration *in vivo* has remained unclear. The results of this thesis obtained from rNLS TDP-43 transgenic mouse cortex at 4 weeks of disease, at a timepoint early in the disease process for these mice now show that matrin 3, and other detected proteins, are indeed involved in the protein aggregation related to TDP-43 early in the disease process<sup>174</sup>, suggesting that they may play a role in pathogenesis rather than being simply recruited to pathology in late-stages of disease. Gene ontology also supports these conclusions, as the biological processes of oxidative phosphorylation and protein complex assembly have been previously implicated to be affected in both animal and human studies of ALS/FTD<sup>88, 109, 127-130</sup>

When comparing proteins between the experiments that were performed, several similar-trending hits appear, despite the fact not many proteins overlapped with the Urea-insoluble hits exclusive to the rNLS transgenic mice. Generally mitochondrial proteins, RNA metabolic processing and nuclear/protein transport factors appear across the datasets. Proteins belonging to the same families are also present, such as ADP ribosylation factor 4 present in the rNLS transgenic mice and ADP-ribosylation factor 3 present in the 150 µg Urea-soluble aggregate-prone human TDP-43 NSC-43 transfections accompanied by ADP-ribosylation factor-interacting protein 2 ADP-ribosylation factor-like protein 8A. These factors are responsible for regulating vesicular trafficking and cytoskeletal remodelling, biological processes that have been implicated in ALS/FTD<sup>34, 55, 133-135, 236</sup>. Heterogeneous nuclear ribonucleoproteins (hnRNPs), which are RNA/protein complex proteins involved in transcription and post-transcriptional modifications, are also found across the experimental sample and are implicated in ALS disease pathology, although the top hnRNP hit from this thesis (hnRNP F) has been poorly studied in ALS or FTD and warrants further investigation.<sup>40</sup>

### 5.3 Future Directions

Future research should begin to develop a selection process pipeline to identify the types of proteins in the Urea-soluble fractions that would be most likely be sequestered into inclusions. This could incorporate some of the methods demonstrated here via selecting based on relevance to implicated mechanisms affected in neurodegeneration (such as protein transport/localisation<sup>26</sup>) as well as those that have already been implicated in disease (VAPB or Dynactin 1<sup>37, 55</sup>) or are in the same families as those that have been previously implicated (Transportin 1<sup>140</sup>). These potential hits could then be validated through Western blotting, immunocytochemistry or by the use of selected-reaction monitoring mass spectrometry. Follow-on mechanistic studies of these potential leads to investigate their effect on TDP-43 clearance and aggregation will likely identify disease-related proteins or potential therapeutic avenues.

As peptide counts were not as high or present as expected to provide confidence that the generated lists represent the full complement of low-solubility proteins in these samples, most likely primarily due to the low-abundance nature of this highly-purified Urea-insoluble fraction (which is the entire aim of this stringent biochemical extraction process designed to specifically isolate a small subset of proteins), future work could involve increasing the protein loaded per sample, plating out transfections on larger plates or dividing samples into fractions to be processed separately. In addition, inefficient peptide digestion may also have occurred, and future experiments will be performed to further optimise buffer conditions, protein load and gel processing techniques. Preliminary results in this thesis showed that this method of dividing samples into several fractions did result in increased protein identification (see **Results 4.1.2**), indicating that this is a potential future avenue to identify additional disease-related proteins. Through utilising this method, gradient times could also be shortened due to the lowered complexity of each individual sample as well as providing the benefit of greater sensitivity. Each step of protein preparation pathway for mass spectrometry can facilitate a loss of sample. Future considerations can be made towards the use of alternatives to sources of loss such as ZipTips. The proteomic methodology used for protein quantitation could also be refined, however due to several previously discussed constraints such as the incompatibility of the Urea-soluble fraction

with standard protein quantification methods, it is not possible to utilise this preparation procedure alongside gold standard techniques such as sequential window acquisition of all theoretical mass spectra (SWATH-MS). Incorporating at least one of these procedures would serve to increase the number of hits and matches.

The limitations of this study contribute to how the results can be interpreted, and are therefore worth considering. Neither the cytoplasmic localisation and RNA-binding interruption mutations have been detected in ALS patients, however these were used due to their ability to best represent the histopathology of the human disease in a simplified cell model of disease. The simplicity of the overexpression model does not recapitulate the exact human condition, whereby several systems have become dysfunctional, and this is considered when drawing conclusions from the protein hits. The same concept applies to the mice samples, where several different cell types are present in the homogenised sample. Validating these hits across the samples as well as in human samples would prove beneficial in overcoming these limitations. Overall this study serves as a foundation to a body of work that aims to understand the types of proteins that are involved in disease pathology to develop a basic understanding that can then be adapted and applied to the human condition. In addition, further experiments using other model systems, such as induced pluripotent stem cell-derived motor neurons, which are time-consuming, technically demanding and expensive but which may more closely recapitulate the human disease, are warranted.

Follow up experiments should also investigate the use of the SH-SY5Y cell-line, which was shown in this thesis to have a greater transfection efficiency compared to NSC-34 cells, and may also show an increase in total protein expression level per cell, resulting in increased levels of aggregated TDP-43 protein burden. A greater proportion of cells would be transfected and bearing aggregated TDP-43 would directly increase the number of hits in proteomics by driving more aggressive pathology and recapitulating human disease more closely by development of more abundant as well as large cytoplasmic inclusions (**Results 4.3.2**). Although SH-SY5Y cells are not motor-neuron like, they are human derived, which may also influence the proteome associated with pathology. Selecting an

appropriate model will always involve weighing up benefits and limitations to decide which would be suitable for the experiment being performed. Experiments incorporating SH-SY5Y cells have already begun but due to time limitations in this thesis, have not been included. These subsequent experiments also implement additional replicates to provide validity transfection efficiency results presented in **Figure 4.5** and **Figure 4.7**. Regardless, the efficiency of transfections using these vectors reflects previously published findings, however additional replicates are required for statistical interpretation<sup>237, 238</sup>. As the pLenti-C-mGFP constructs containing human mutants of TDP-43 also appear to produce a high number of inclusions within the cells, proteomic experiments incorporating these constructs would be insightful, given the aims of the study were to characterise aggregate protein-containing inclusions. Due to the limitations

Although these findings focus on proteins exclusive to the Urea-soluble fraction of the described conditions, there is potential that proteins detected across both RIPA and Urea-soluble fractions as well as in control Urea-soluble fractions could also be involved in inclusion pathology through changes in abundance. Further experiments to identify these abundance changes in high-solubility proteins may therefore also be warranted to understand the dynamics of aggregate protein-containing inclusions.

Comparisons of proteins identified in the Urea-soluble fractions of aggregate-prone human TDP-43 transfected NSC-34 cells to the rNLS TDP-43 transgenic mice has also been insightful, as demonstrated, similar families of proteins (ADP-ribosylation factors) are present in both. Comparisons of these proteins to datasets from patient tissue in ALS, as well as other animal generated models would further assist in identifying similarities as well as limitations to these models and to narrow down the suite of proteins that are conclusively involved in ALS/FTD pathology regardless of which specific model is used for experiments. Proteins within the 150  $\mu$ g loss of function and aggregate-prone human TDP-43 NSC-34 dataset, such as VPS4B, also appear to be detected as enriched within patient cortical neurons with knock-down of TDP-43<sup>236</sup>. Future comparisons of the datasets generated

here with previously published and publicly available proteome and gene expression studies in human ALS and different model systems will allow further refinement of the most important TDP-43 pathology-associated proteins.

By streamlining a selection-process it will be possible to identify proteins involved in TDP-43 inclusion pathology. Already these findings are assisting to elucidate disease mechanisms in ALS and FTD, for example, highlighting the involvement of chaperone proteins such as HSP-family proteins and subcellular transport machinery in TDP-43 pathology. Further mechanistic studies aimed at modulating TDP-43 pathology could begin with targeted over-expression and knockdown of the most promising short-listed candidate proteins in cell culture with examination of effects on protein aggregation and neurodegeneration. Since ALS is currently difficult to diagnose, more detailed understanding of the underlying disease mechanisms may also lead to new developments not only in treatments but also in biomarker discovery, such that known disease-linked mechanistic changes within neurons could lead to altered levels of specific proteins within the blood, CSF or urine that could be monitored by methods such as ELISA or mass spectrometry approaches to assist in diagnosis and tracking of disease progression in patients over time. Disease understanding will also identify new targets that could be harnessed to decrease TDP-43 pathology and stimulate neuronal function and survival for treatment of these devastating disease

#### 5.4 Concluding Statements

This thesis has identified a range of proteins that are likely be involved in the composition of TDP-43 inclusions in ALS/FTD, and may therefore be critical factors in disease pathogenesis. This was supported with previous research implicating a subset of the identified proteins as either involved directly in ALS, implicated in ALS, changed in abundance in ALS or as interactors of ALS-implicated proteins. Examination of the biological processes these previously identified proteins as well as the newly identified proteins are involved in will provide insights into disease processes.

Both ALS and FTD are complicated neurodegenerative diseases with no effective treatment. Future studies that employ the research presented in this body of work will begin to elucidate pathological mechanisms to achieve a greater understanding of both diseases with hopes that one day it will be possible to identify effective therapeutics for people living with ALS and FTD.

---

# References

---

1. Rowland LP, Shneider NA. Amyotrophic lateral sclerosis. *New England Journal of Medicine*. 2001;344(22):1688-700.
2. Wijesekera LC, Leigh PN. Amyotrophic lateral sclerosis. *Orphanet Journal of Rare Diseases*. 2009;4:3-.
3. Brain WR, Walton JN. *Brain's diseases of the nervous system*. London: Oxford University Press; 1969.
4. Ince PG, Lowe J, Shaw PJ. Amyotrophic lateral sclerosis: current issues in classification, pathogenesis and molecular pathology. *Neuropathology and applied neurobiology*. 1998;24(2):104-17.
5. Charcot J-M. De la sclérose latérale amyotrophique. *Prog Med*. 1874;23; 24; 29:235-237. 341-232; 453-235.
6. Kumar DR, Aslinia F, Yale SH, Mazza JJ. Jean-Martin Charcot: The Father of Neurology. *Clinical Medicine & Research*. 2011;9(1):46-9.
7. Rowland LP. How amyotrophic lateral sclerosis got its name: The clinical-pathologic genius of Jean-Martin Charcot. *Archives of Neurology*. 2001;58(3):512-5.
8. Charcot J-M. Deuxcas d'atrophie musculaire progressive avec lésions de la substance grise et de faisceaux antérolatéraux de la moelle épinière. *Arch Physiol Norm Pathol*. 1869;1:354-357; 352:628-649; 353:744-757.
9. J C. Sur le paralysie musculaire, progressive, atrophique. *Bull Acad Med*. 1853;18: 490-501. 546-583.
10. Hodges JR. Pick's Disease. In: Burns A, Levy R, editors. *Dementia*. Boston, MA: Springer US; 1994. p. 739-52.
11. Rabinovici GD, Miller BL. Frontotemporal lobar degeneration. *CNS Drugs*. 2010;24(5):375-98.
12. Pick A. Über einen weiteren Symptomenkomplex im Rahmen der Dementia senilis, bedingt durch umschriebene stärkere Hirnatrophie (gemischte Apraxie). *European Neurology*. 1906;19(2):97-108.
13. Alzheimer A. Über eigenartige Krankheitsfälle des späteren Alters. *Zeitschrift für die gesamte Neurologie und Psychiatrie*. 1911;4(1):356-85.
14. Alzheimer A. Über eigenartige Krankheitsfälle des späteren Alters. *History of Psychiatry*. 1991;2(5):74-101.
15. Welfare AloHa. Australian Institute of Health and Welfare National Mortality Database. Canberra, Australian Capital Territory, Australia2013.
16. Chiò A, Logroscino G, Traynor BJ, Collins J, Simeone JC, Goldstein LA, et al. Global Epidemiology of Amyotrophic Lateral Sclerosis: a Systematic Review of the Published Literature. *Neuroepidemiology*. 2013;41(2):118-30.
17. Logroscino G, Traynor BJ, Hardiman O, Chio A, Mitchell D, Swingler RJ, et al. Incidence of amyotrophic lateral sclerosis in Europe. *Journal of neurology, neurosurgery, and psychiatry*. 2010;81(4):385-90.
18. Economics DA. Economic analysis of motor neurone disease in Australia, report for Motor Neurone Disease Australia. Canberra: Deloitte Access Economics; 2015.
19. Robberecht W, Philips T. The changing scene of amyotrophic lateral sclerosis. *Nature Reviews Neuroscience*. 2013;14(4):248-64.
20. Arthur KC, Calvo A, Price TR, Geiger JT, Chiò A, Traynor BJ. Projected increase in amyotrophic lateral sclerosis from 2015 to 2040. *Nature Communications*. 2016;7:12408.
21. Sieben A, Van Langenhove T, Engelborghs S, Martin J-J, Boon P, Cras P, et al. The genetics and neuropathology of frontotemporal lobar degeneration. *Acta neuropathologica*. 2012;124(3):353-72.
22. Bennion Callister J, Pickering-Brown SM. Pathogenesis/genetics of frontotemporal dementia and how it relates to ALS. *Experimental neurology*. 2014;262 Pt B:84-90.
23. Borroni B, Archetti S, Del Bo R, Papetti A, Buratti E, Bonvicini C, et al. TARDBP mutations in frontotemporal lobar degeneration: frequency, clinical features, and disease course. *Rejuvenation research*. 2010;13(5):509-17.

24. Rosso SM, Kamphorst W, de Graaf B, Willemsen R, Ravid R, Niermeijer MF, et al. Familial frontotemporal dementia with ubiquitin-positive inclusions is linked to chromosome 17q21-22. *Brain*. 2001;124(Pt 10):1948-57.
25. Ringholz GM, Appel SH, Bradshaw M, Cooke NA, Mosnik DM, Schulz PE. Prevalence and patterns of cognitive impairment in sporadic ALS. *Neurology*. 2005;65(4):586-90.
26. Ling S-C, Polymenidou M, Cleveland DW. Converging mechanisms in ALS and FTD: Disrupted RNA and protein homeostasis. *Neuron*. 2013;79(3):416-38.
27. McCann EP, Williams KL, Fifita JA, Tarr IS, O'Connor J, Rowe DB, et al. The genotype-phenotype landscape of familial amyotrophic lateral sclerosis in Australia. *Clinical genetics*. 2017.
28. Tan RH, Ke YD, Ittner LM, Halliday GM. ALS/FTLD: experimental models and reality. *Acta neuropathologica*. 2017;133(2):177-96.
29. Hadano S, Hand CK, Osuga H, Yanagisawa Y, Otomo A, Devon RS, et al. A gene encoding a putative GTPase regulator is mutated in familial amyotrophic lateral sclerosis 2. *Nature genetics*. 2001;29(2):166-73.
30. Hand CK, Khoris J, Salachas F, Gros-Louis F, Lopes AA, Mayeux-Portas V, et al. A novel locus for familial amyotrophic lateral sclerosis, on chromosome 18q. *American journal of human genetics*. 2002;70(1):251-6.
31. Sapp PC, Hosler BA, McKenna-Yasek D, Chin W, Gann A, Genise H, et al. Identification of two novel loci for dominantly inherited familial amyotrophic lateral sclerosis. *American journal of human genetics*. 2003;73(2):397-403.
32. Hayward C, Colville S, Swingler RJ, Brock DJ. Molecular genetic analysis of the APEX nuclease gene in amyotrophic lateral sclerosis. *Neurology*. 1999;52(9):1899-901.
33. Greenway MJ, Alexander MD, Ennis S, Traynor BJ, Corr B, Frost E, et al. A novel candidate region for ALS on chromosome 14q11.2. *Neurology*. 2004;63(10):1936-8.
34. Smith BN, Topp SD, Fallini C, Shibata H, Chen H-J, Troakes C, et al. Mutations in the vesicular trafficking protein annexin A11 are associated with amyotrophic lateral sclerosis. *Science Translational Medicine*. 2017;9(388).
35. Elden AC, Kim HJ, Hart MP, Chen-Plotkin AS, Johnson BS, Fang X, et al. Ataxin-2 intermediate-length polyglutamine expansions are associated with increased risk for ALS. *Nature*. 2010;466(7310):1069-75.
36. Mitchell J, Paul P, Chen HJ, Morris A, Payling M, Falchi M, et al. Familial amyotrophic lateral sclerosis is associated with a mutation in D-amino acid oxidase. *Proceedings of the National Academy of Sciences of the United States of America*. 2010;107(16):7556-61.
37. Munch C, Sedlmeier R, Meyer T, Homberg V, Sperfeld AD, Kurt A, et al. Point mutations of the p150 subunit of dynactin (DCTN1) gene in ALS. *Neurology*. 2004;63(4):724-6.
38. Takahashi Y, Fukuda Y, Yoshimura J, Toyoda A, Kurppa K, Moritoyo H, et al. ERBB4 mutations that disrupt the neuregulin-ErbB4 pathway cause amyotrophic lateral sclerosis type 19. *American journal of human genetics*. 2013;93(5):900-5.
39. Chow CY, Landers JE, Bergren SK, Sapp PC, Grant AE, Jones JM, et al. Deleterious variants of FIG4, a phosphoinositide phosphatase, in patients with ALS. *American journal of human genetics*. 2009;84(1):85-8.
40. Kim HJ, Kim NC, Wang YD, Scarborough EA, Moore J, Diaz Z, et al. Mutations in prion-like domains in hnRNPA2B1 and hnRNPA1 cause multisystem proteinopathy and ALS. *Nature*. 2013;495(7442):467-73.
41. Johnson JO, Piro EP, Boehringer A, Chia R, Feit H, Renton AE, et al. Mutations in the Matrin 3 gene cause familial amyotrophic lateral sclerosis. *Nature neuroscience*. 2014;17(5):664-6.
42. Figlewicz DA, Krizus A, Martinoli MG, Meininger V, Dib M, Rouleau GA, et al. Variants of the heavy neurofilament subunit are associated with the development of amyotrophic lateral sclerosis. *Human molecular genetics*. 1994;3(10):1757-61.
43. Al-Chalabi A, Andersen PM, Nilsson P, Chioza B, Andersson JL, Russ C, et al. Deletions of the heavy neurofilament subunit tail in amyotrophic lateral sclerosis. *Human molecular genetics*. 1999;8(2):157-64.

44. Maruyama H, Morino H, Ito H, Izumi Y, Kato H, Watanabe Y, et al. Mutations of optineurin in amyotrophic lateral sclerosis. *Nature*. 2010;465(7295):223-6.
45. Gonzalez-Perez P, Woehlbier U, Chian RJ, Sapp P, Rouleau GA, Leblond CS, et al. Identification of rare protein disulfide isomerase gene variants in amyotrophic lateral sclerosis patients. *Gene*. 2015;566(2):158-65.
46. Woehlbier U, Colombo A, Saaranen MJ, Pérez V, Ojeda J, Bustos FJ, et al. ALS - linked protein disulfide isomerase variants cause motor dysfunction. *The EMBO Journal*. 2016;35(8):845-65.
47. Wu CH, Fallini C, Ticozzi N, Keagle PJ, Sapp PC, Piotrowska K, et al. Mutations in the profilin 1 gene cause familial amyotrophic lateral sclerosis. *Nature*. 2012;488(7412):499-503.
48. Gros-Louis F, Lariviere R, Gowing G, Laurent S, Camu W, Bouchard JP, et al. A frameshift deletion in peripherin gene associated with amyotrophic lateral sclerosis. *The Journal of biological chemistry*. 2004;279(44):45951-6.
49. Chen YZ, Bennett CL, Huynh HM, Blair IP, Puls I, Irobi J, et al. DNA/RNA helicase gene mutations in a form of juvenile amyotrophic lateral sclerosis (ALS4). *American journal of human genetics*. 2004;74(6):1128-35.
50. Al-Saif A, Al-Mohanna F, Bohlega S. A mutation in sigma-1 receptor causes juvenile amyotrophic lateral sclerosis. *Annals of neurology*. 2011;70(6):913-9.
51. Rosen DR, Siddique T, Patterson D, Figlewicz DA, Sapp P, Hentati A, et al. Mutations in Cu/Zn superoxide dismutase gene are associated with familial amyotrophic lateral sclerosis. *Nature*. 1993;362(6415):59-62.
52. Munch C, Rolfs A, Meyer T. Heterozygous S44L missense change of the spastin gene in amyotrophic lateral sclerosis. *Amyotrophic lateral sclerosis : official publication of the World Federation of Neurology Research Group on Motor Neuron Diseases*. 2008;9(4):251-3.
53. Orlicchio A, Babalini C, Borreca A, Patrono C, Massa R, Basaran S, et al. SPATACSIN mutations cause autosomal recessive juvenile amyotrophic lateral sclerosis. *Brain*. 2010;133(Pt 2):591-8.
54. Edens BM, Yan J, Miller N, Deng HX, Siddique T, Ma YC. A novel ALS-associated variant in UBQLN4 regulates motor axon morphogenesis. *eLife*. 2017;6.
55. Nishimura AL, Mitne-Neto M, Silva HC, Richieri-Costa A, Middleton S, Cascio D, et al. A mutation in the vesicle-trafficking protein VAPB causes late-onset spinal muscular atrophy and amyotrophic lateral sclerosis. *American journal of human genetics*. 2004;75(5):822-31.
56. DeJesus-Hernandez M, Mackenzie IR, Boeve BF, Boxer AL, Baker M, Rutherford NJ, et al. Expanded GGGGCC hexanucleotide repeat in noncoding region of C9ORF72 causes chromosome 9p-linked FTD and ALS. *Neuron*. 2011;72(2):245-56.
57. Renton AE, Majounie E, Waite A, Simon-Sanchez J, Rollinson S, Gibbs JR, et al. A hexanucleotide repeat expansion in C9ORF72 is the cause of chromosome 9p21-linked ALS-FTD. *Neuron*. 2011;72(2):257-68.
58. Williams KL, Topp S, Yang S, Smith B, Fifita JA, Warraich ST, et al. CCNF mutations in amyotrophic lateral sclerosis and frontotemporal dementia. *Nat Commun*. 2016;7:11253.
59. Bannwarth S, Ait-El-Mkadem S, Chausseot A, Genin EC, Lacas-Gervais S, Fragaki K, et al. A mitochondrial origin for frontotemporal dementia and amyotrophic lateral sclerosis through CHCHD10 involvement. *Brain*. 2014;137(Pt 8):2329-45.
60. Parkinson N, Ince PG, Smith MO, Highley R, Skibinski G, Andersen PM, et al. ALS phenotypes with mutations in CHMP2B (charged multivesicular body protein 2B). *Neurology*. 2006;67(6):1074-7.
61. Kwiatkowski TJ, Jr., Bosco DA, Leclerc AL, Tamrazian E, Vandenberg CR, Russ C, et al. Mutations in the FUS/TLS gene on chromosome 16 cause familial amyotrophic lateral sclerosis. *Science (New York, NY)*. 2009;323(5918):1205-8.
62. Vance C, Rogelj B, Hortobagyi T, De Vos KJ, Nishimura AL, Sreedharan J, et al. Mutations in FUS, an RNA processing protein, cause familial amyotrophic lateral sclerosis type 6. *Science (New York, NY)*. 2009;323(5918):1208-11.
63. Fecto F, Yan J, Vemula SP, Liu E, Yang Y, Chen W, et al. SQSTM1 mutations in familial and sporadic amyotrophic lateral sclerosis. *Arch Neurol*. 2011;68(11):1440-6.
64. Rubino E, Rainero I, Chio A, Rogaeva E, Galimberti D, Fenoglio P, et al. SQSTM1 mutations in frontotemporal lobar degeneration and amyotrophic lateral sclerosis. *Neurology*. 2012;79(15):1556-62.

65. Sreedharan J, Blair IP, Tripathi VB, Hu X, Vance C, Rogelj B, et al. TDP-43 mutations in familial and sporadic amyotrophic lateral sclerosis. *Science (New York, NY)*. 2008;319(5870):1668-72.
66. Freischmidt A, Wieland T, Richter B, Ruf W, Schaeffer V, Muller K, et al. Haploinsufficiency of TBK1 causes familial ALS and fronto-temporal dementia. *Nature neuroscience*. 2015;18(5):631-6.
67. Smith BN, Ticozzi N, Fallini C, Gkazi AS, Topp S, Kenna KP, et al. Exome-wide rare variant analysis identifies TUBA4A mutations associated with familial ALS. *Neuron*. 2014;84(2):324-31.
68. Deng HX, Chen W, Hong ST, Boycott KM, Gorrie GH, Siddique N, et al. Mutations in UBQLN2 cause dominant X-linked juvenile and adult-onset ALS and ALS/dementia. *Nature*. 2011;477(7363):211-5.
69. Johnson JO, Mandrioli J, Benatar M, Abramzon Y, Van Deerlin VM, Trojanowski JQ, et al. Exome sequencing reveals VCP mutations as a cause of familial ALS. *Neuron*. 2010;68(5):857-64.
70. Watts GD, Wymer J, Kovach MJ, Mehta SG, Mumm S, Darvish D, et al. Inclusion body myopathy associated with Paget disease of bone and frontotemporal dementia is caused by mutant valosin-containing protein. *Nature genetics*. 2004;36(4):377-81.
71. Baker M, Mackenzie IR, Pickering-Brown SM, Gass J, Rademakers R, Lindholm C, et al. Mutations in progranulin cause tau-negative frontotemporal dementia linked to chromosome 17. *Nature*. 2006;442(7105):916-9.
72. Cruts M, Gijselinck I, van der Zee J, Engelborghs S, Wils H, Pirici D, et al. Null mutations in progranulin cause ubiquitin-positive frontotemporal dementia linked to chromosome 17q21. *Nature*. 2006;442(7105):920-4.
73. Hutton M, Lendon CL, Rizzu P, Baker M, Froelich S, Houlden H, et al. Association of missense and 5'-splice-site mutations in tau with the inherited dementia FTDP-17. *Nature*. 1998;393(6686):702-5.
74. Raux G, Gantier R, Thomas-Anterion C, Boulliat J, Verpillat P, Hannequin D, et al. Dementia with prominent frontotemporal features associated with L113P presenilin 1 mutation. *Neurology*. 2000;55(10):1577-8.
75. Brown RH, Al-Chalabi A. Amyotrophic Lateral Sclerosis. *New England Journal of Medicine*. 2017;377(2):162-72.
76. Ferrari R, Kapogiannis D, Huey ED, Momeni P. FTD and ALS: a tale of two diseases. *Current Alzheimer research*. 2011;8(3):273-94.
77. Zarei S, Carr K, Reiley L, Diaz K, Guerra O, Altamirano PF, et al. A comprehensive review of amyotrophic lateral sclerosis. *Surgical Neurology International*. 2015;6:171.
78. Swinnen B, Robberecht W. The phenotypic variability of amyotrophic lateral sclerosis. *Nat Rev Neurol*. 2014;10(11):661-70.
79. Karam C, Scelsa SN, MacGowan DJL. The clinical course of progressive bulbar palsy. *Amyotrophic Lateral Sclerosis*. 2010;11(4):364-8.
80. Kim WK, Liu X, Sandner J, Pasmantier M, Andrews J, Rowland LP, et al. Study of 962 patients indicates progressive muscular atrophy is a form of ALS. *Neurology*. 2009;73(20):1686-92.
81. Gotkine M, Argov Z. Clinical differentiation between primary lateral sclerosis and upper motor neuron predominant amyotrophic lateral sclerosis. *Archives of Neurology*. 2007;64(10):1545-.
82. Tartaglia MC, Rowe A, Findlater K, Orange JB, Grace G, Strong MJ. Differentiation between primary lateral sclerosis and amyotrophic lateral sclerosis: examination of symptoms and signs at disease onset and during follow-up. *Arch Neurol*. 2007;64(2):232-6.
83. Johnson JK, Diehl J, Mendez MF, Neuhaus J, Shapira JS, Forman M, et al. Frontotemporal lobar degeneration: demographic characteristics of 353 patients. *Archives Of Neurology*. 2005;62(6):925-30.
84. Bang J, Spina S, Miller BL. Frontotemporal dementia. *The Lancet*. 2015;386(10004):1672-82.
85. Roberson ED. Frontotemporal dementia. *Current Neurology and Neuroscience Reports*. 2006;6(6):481.
86. Ghosh S, Lippa CF. Clinical Subtypes of Frontotemporal Dementia. *American Journal of Alzheimer's Disease & Other Dementiasr*. 2013;30(7):653-61.

87. Mendez MF, Licht EA, Shapira JS. Changes in Dietary or Eating Behavior in Frontotemporal Dementia Versus Alzheimer's Disease. *American Journal of Alzheimer's Disease & Other Dementias*. 2008;23(3):280-5.
88. Blokhuis AM, Groen EJN, Koppers M, van den Berg LH, Pasterkamp RJ. Protein aggregation in amyotrophic lateral sclerosis. *Acta neuropathologica*. 2013;125(6):777-94.
89. Seeley WW, Carlin DA, Allman JM, Macedo MN, Bush C, Miller BL, et al. Early frontotemporal dementia targets neurons unique to apes and humans. *Annals of neurology*. 2006;60(6):660-7.
90. Seeley WW. Selective functional, regional, and neuronal vulnerability in frontotemporal dementia. *Current opinion in neurology*. 2008;21(6):701-7.
91. Kim EJ, Sidhu M, Gaus SE, Huang EJ, Hof PR, Miller BL, et al. Selective fronto-insular von Economo neuron and fork cell loss in early behavioral variant frontotemporal dementia. *Cerebral cortex (New York, NY : 1991)*. 2012;22(2):251-9.
92. Bensimon G, Lacomblez L, Meininger V. A controlled trial of riluzole in amyotrophic lateral sclerosis. ALS/Riluzole Study Group. *The New England journal of medicine*. 1994;330(9):585-91.
93. Miller RG, Mitchell JD, Moore DH. Riluzole for amyotrophic lateral sclerosis (ALS)/motor neuron disease (MND). *The Cochrane database of systematic reviews*. 2012(3):Cd001447.
94. Dyer AM, Smith A. Riluzole 5 mg/mL oral suspension: for optimized drug delivery in amyotrophic lateral sclerosis. *Drug Design, Development and Therapy*. 2017;11:59-64.
95. Debono MW, Le Guern J, Canton T, Doble A, Pradier L. Inhibition by riluzole of electrophysiological responses mediated by rat kainate and NMDA receptors expressed in *Xenopus* oocytes. *European journal of pharmacology*. 1993;235(2-3):283-9.
96. Wang SJ, Wang KY, Wang WC. Mechanisms underlying the riluzole inhibition of glutamate release from rat cerebral cortex nerve terminals (synaptosomes). *Neuroscience*. 2004;125(1):191-201.
97. Miyaji Y, Yoshimura S, Sakai N, Yamagami H, Egashira Y, Shirakawa M, et al. Effect of Edaravone on Favorable Outcome in Patients with Acute Cerebral Large Vessel Occlusion: Subanalysis of RESCUE-Japan Registry. *Neurologia medico-chirurgica*. 2015;55(3):241-7.
98. Wang HM, Zhang T, Huang JK, Xiang JY, Chen JJ, Fu JL, et al. Edaravone Attenuates the Proinflammatory Response in Amyloid-beta-Treated Microglia by Inhibiting NLRP3 Inflammasome-Mediated IL-1beta Secretion. *Cellular physiology and biochemistry : international journal of experimental cellular physiology, biochemistry, and pharmacology*. 2017;43(3):1113-25.
99. Jiao SS, Yao XQ, Liu YH, Wang QH, Zeng F, Lu JJ, et al. Edaravone alleviates Alzheimer's disease-type pathologies and cognitive deficits. *Proceedings of the National Academy of Sciences of the United States of America*. 2015;112(16):5225-30.
100. Abe K, Itoyama Y, Sobue G, Tsuji S, Aoki M, Doyu M, et al. Confirmatory double-blind, parallel-group, placebo-controlled study of efficacy and safety of edaravone (MCI-186) in amyotrophic lateral sclerosis patients. *Amyotrophic Lateral Sclerosis & Frontotemporal Degeneration*. 2014;15(7-8):610-7.
101. Tanaka M, Akimoto M, Palumbo J, Sakata T. A Double-Blind, Parallel-Group, Placebo-Controlled, 24-Week, Exploratory Study of Edaravone (MCI-186) for the Treatment of Advanced Amyotrophic Lateral Sclerosis (ALS) (P3.191). *Neurology*. 2016;86(16 Supplement).
102. Tanaka M, Sakata T, Palumbo J, Akimoto M. A 24-Week, Phase III, Double-Blind, Parallel-Group Study of Edaravone (MCI-186) for Treatment of Amyotrophic Lateral Sclerosis (ALS) (P3.189). *Neurology*. 2016;86(16 Supplement).
103. Jiang J, Zhu Q, Gendron TF, Saberi S, McAlonis-Downes M, Seelman A, et al. Gain of Toxicity from ALS/FTD-Linked Repeat Expansions in C9ORF72 Is Alleviated by Antisense Oligonucleotides Targeting GGGGCC-Containing RNAs. *Neuron*. 2016;90(3):535-50.
104. Stoica L, Sena-Esteves M. Adeno Associated Viral Vector Delivered RNAi for Gene Therapy of SOD1 Amyotrophic Lateral Sclerosis. *Frontiers in molecular neuroscience*. 2016;9:56.
105. Chen L, Watson C, Morsch M, Cole NJ, Chung RS, Saunders DN, et al. Improving the Delivery of SOD1 Antisense Oligonucleotides to Motor Neurons Using Calcium Phosphate-Lipid Nanoparticles. *Frontiers in neuroscience*. 2017;11:476.

106. Li D, Liu C, Yang C, Wang D, Wu D, Qi Y, et al. Slow intrathecal injection of rAAVrh10 enhances its transduction of spinal cord and therapeutic efficacy in a mutant SOD1 model of ALS. *Neuroscience*. 2017.
107. Scotter EL, Chen H-J, Shaw CE. TDP-43 Proteinopathy and ALS: Insights into Disease Mechanisms and Therapeutic Targets. *Neurotherapeutics : the journal of the American Society for Experimental NeuroTherapeutics*. 2015;12(2):352-63.
108. Ciryam P, Lambert-Smith IA, Bean DM, Freer R, Cid F, Tartaglia GG, et al. Spinal motor neuron protein supersaturation patterns are associated with inclusion body formation in ALS. *Proceedings of the National Academy of Sciences*. 2017;114(20):E3935-E43.
109. Shahheydari H, Ragagnin A, Walker AK, Toth RP, Vidal M, Jagaraj CJ, et al. Protein Quality Control and the Amyotrophic Lateral Sclerosis/Frontotemporal Dementia Continuum. *Frontiers in molecular neuroscience*. 2017;10:119.
110. Walker AK, Atkin JD. Stress signaling from the endoplasmic reticulum: A central player in the pathogenesis of amyotrophic lateral sclerosis. *IUBMB life*. 2011;63(9):754-63.
111. Perri ER, Thomas CJ, Parakh S, Spencer DM, Atkin JD. The Unfolded Protein Response and the Role of Protein Disulfide Isomerase in Neurodegeneration. *Frontiers in cell and developmental biology*. 2015;3:80.
112. Neumann M, Sampathu DM, Kwong LK, Truax AC, Micsenyi MC, Chou TT, et al. Ubiquitinated TDP-43 in frontotemporal lobar degeneration and amyotrophic lateral sclerosis. *Science (New York, NY)*. 2006;314(5796):130-3.
113. Feng Y, He D, Yao Z, Klionsky DJ. The machinery of macroautophagy. *Cell Research*. 2014;24(1):24-41.
114. Li WW, Li J, Bao JK. Microautophagy: lesser-known self-eating. *Cellular and molecular life sciences : CMLS*. 2012;69(7):1125-36.
115. Cuervo AM, Wong E. Chaperone-mediated autophagy: roles in disease and aging. *Cell Res*. 2014;24(1):92-104.
116. Hajnóczky G, Csordás G, Das S, Garcia-Perez C, Saotome M, Sinha Roy S, et al. Mitochondrial calcium signalling and cell death: Approaches for assessing the role of mitochondrial Ca<sup>2+</sup> uptake in apoptosis. *Cell Calcium*. 2006;40(5):553-60.
117. Sasaki S, Horie Y, Iwata M. Mitochondrial alterations in dorsal root ganglion cells in sporadic amyotrophic lateral sclerosis. *Acta neuropathologica*. 2007;114(6):633-9.
118. Sasaki S, Iwata M. Mitochondrial alterations in the spinal cord of patients with sporadic amyotrophic lateral sclerosis. *Journal of neuropathology and experimental neurology*. 2007;66(1):10-6.
119. Said Ahmed M, Hung WY, Zu JS, Hockberger P, Siddique T. Increased reactive oxygen species in familial amyotrophic lateral sclerosis with mutations in SOD1. *Journal of the neurological sciences*. 2000;176(2):88-94.
120. Kong J, Xu Z. Massive mitochondrial degeneration in motor neurons triggers the onset of amyotrophic lateral sclerosis in mice expressing a mutant SOD1. *The Journal of neuroscience : the official journal of the Society for Neuroscience*. 1998;18(9):3241-50.
121. Jaarsma D, Rognoni F, van Duijn W, Verspaget HW, Haasdijk ED, Holstege JC. CuZn superoxide dismutase (SOD1) accumulates in vacuolated mitochondria in transgenic mice expressing amyotrophic lateral sclerosis-linked SOD1 mutations. *Acta neuropathologica*. 2001;102(4):293-305.
122. Tan W, Nanche N, Bogush A, Pedrini S, Trotti D, Pasinelli P. Small peptides against the mutant SOD1/Bcl-2 toxic mitochondrial complex restore mitochondrial function and cell viability in mutant SOD1-mediated ALS. *The Journal of neuroscience : the official journal of the Society for Neuroscience*. 2013;33(28):11588-98.
123. Weishaupt JH, Hyman T, Dikic I. Common Molecular Pathways in Amyotrophic Lateral Sclerosis and Frontotemporal Dementia. *Trends in molecular medicine*. 2016;22(9):769-83.
124. Dammer E, Fallini C, Gozal Y, Duong D, Rossoll W, Xu P, et al. Coaggregation of RNA-Binding Proteins in a Model of TDP-43 Proteinopathy with Selective RGG Motif Methylation and a Role for RRM1 Ubiquitination. *2012*. e38658 p.

125. Freibaum BD, Chitta RK, High AA, Taylor JP. Global analysis of TDP-43 interacting proteins reveals strong association with RNA splicing and translation machinery. *Journal of proteome research*. 2010;9(2):1104-20.
126. Coppedè F. An Overview of DNA Repair in Amyotrophic Lateral Sclerosis. *The Scientific World Journal*. 2011;11:1679-91.
127. Bogdanov M, Brown RH, Matson W, Smart R, Hayden D, O'Donnell H, et al. Increased oxidative damage to DNA in ALS patients. *Free radical biology & medicine*. 2000;29(7):652-8.
128. Aguirre N, Beal MF, Matson WR, Bogdanov MB. Increased oxidative damage to DNA in an animal model of amyotrophic lateral sclerosis. *Free radical research*. 2005;39(4):383-8.
129. Ferrante RJ, Browne SE, Shinobu LA, Bowling AC, Baik MJ, MacGarvey U, et al. Evidence of increased oxidative damage in both sporadic and familial amyotrophic lateral sclerosis. *Journal of neurochemistry*. 1997;69(5):2064-74.
130. Barber SC, Shaw PJ. Oxidative stress in ALS: key role in motor neuron injury and therapeutic target. *Free radical biology & medicine*. 2010;48(5):629-41.
131. Kikuchi H, Furuta A, Nishioka K, Suzuki SO, Nakabeppu Y, Iwaki T. Impairment of mitochondrial DNA repair enzymes against accumulation of 8-oxo-guanine in the spinal motor neurons of amyotrophic lateral sclerosis. *Acta neuropathologica*. 2002;103(4):408-14.
132. de Waard MC, van der Pluijm I, Zuiderveen Borgesius N, Comley LH, Haasdijk ED, Rijksen Y, et al. Age-related motor neuron degeneration in DNA repair-deficient *Ercc1* mice. *Acta neuropathologica*. 2010;120(4):461-75.
133. Encalada SE, Goldstein LS. Biophysical challenges to axonal transport: motor-cargo deficiencies and neurodegeneration. *Annual review of biophysics*. 2014;43:141-69.
134. Hurd DD, Saxton WM. Kinesin Mutations Cause Motor Neuron Disease Phenotypes by Disrupting Fast Axonal Transport in *Drosophila*. *Genetics*. 1996;144(3):1075.
135. Collard JF, Cote F, Julien JP. Defective axonal transport in a transgenic mouse model of amyotrophic lateral sclerosis. *Nature*. 1995;375(6526):61-4.
136. De Vos KJ, Chapman AL, Tennant ME, Manser C, Tudor EL, Lau KF, et al. Familial amyotrophic lateral sclerosis-linked SOD1 mutants perturb fast axonal transport to reduce axonal mitochondria content. *Human molecular genetics*. 2007;16(22):2720-8.
137. Song Y, Nagy M, Ni W, Tyagi NK, Fenton WA, Lopez-Giraldez F, et al. Molecular chaperone Hsp110 rescues a vesicle transport defect produced by an ALS-associated mutant SOD1 protein in squid axoplasm. *Proceedings of the National Academy of Sciences of the United States of America*. 2013;110(14):5428-33.
138. Dormann D, Haass C. TDP-43 and FUS: a nuclear affair. *Trends in neurosciences*. 2011;34(7):339-48.
139. Coady TH, Manley JL. ALS mutations in TLS/FUS disrupt target gene expression. *Genes & Development*. 2015;29(16):1696-706.
140. Takeuchi R, Toyoshima Y, Tada M, Shiga A, Tanaka H, Shimohata M, et al. Transportin 1 accumulates in FUS inclusions in adult-onset ALS without FUS mutation. *Neuropathology and applied neurobiology*. 2013;39(5):580-4.
141. Troakes C, Hortobagyi T, Vance C, Al-Sarraj S, Rogelj B, Shaw CE. Transportin 1 colocalization with Fused in Sarcoma (FUS) inclusions is not characteristic for amyotrophic lateral sclerosis-FUS confirming disrupted nuclear import of mutant FUS and distinguishing it from frontotemporal lobar degeneration with FUS inclusions. *Neuropathology and applied neurobiology*. 2013;39(5):553-61.
142. Boeynaems S, Bogaert E, Van Damme P, Van Den Bosch L. Inside out: the role of nucleocytoplasmic transport in ALS and FTLD. *Acta neuropathologica*. 2016;132(2):159-73.
143. Lee EB, Lee VMY, Trojanowski JQ. Gains or losses: molecular mechanisms of TDP43-mediated neurodegeneration. *Nature Reviews Neuroscience*. 2011;13(1):38-50.
144. Haase G, Rabouille C. Golgi Fragmentation in ALS Motor Neurons. *New Mechanisms Targeting Microtubules, Tethers, and Transport Vesicles*. *Frontiers in neuroscience*. 2015;9:448.
145. Atkin JD, Farg MA, Soo KY, Walker AK, Halloran M, Turner BJ, et al. Mutant SOD1 inhibits ER-Golgi transport in amyotrophic lateral sclerosis. *Journal of neurochemistry*. 2014;129(1):190-204.
146. Komine O, Yamanaka K. Neuroinflammation in motor neuron disease. *Nagoya Journal of Medical Science*. 2015;77(4):537-49.

147. Lasiene J, Yamanaka K. Glial Cells in Amyotrophic Lateral Sclerosis. *Neurology Research International*. 2011;2011:7.
148. Vargas MR, Johnson JA. Astrogliosis in amyotrophic lateral sclerosis: role and therapeutic potential of astrocytes. *Neurotherapeutics : the journal of the American Society for Experimental NeuroTherapeutics*. 2010;7(4):471-81.
149. Rothstein JD, Van Kammen M, Levey AI, Martin LJ, Kuncl RW. Selective loss of glial glutamate transporter GLT-1 in amyotrophic lateral sclerosis. *Annals of neurology*. 1995;38(1):73-84.
150. Fray AE, Ince PG, Banner SJ, Milton ID, Usher PA, Cookson MR, et al. The expression of the glial glutamate transporter protein EAAT2 in motor neuron disease: an immunohistochemical study. *European Journal of Neuroscience*. 1998;10(8):2481-9.
151. Howland DS, Liu J, She Y, Goad B, Maragakis NJ, Kim B, et al. Focal loss of the glutamate transporter EAAT2 in a transgenic rat model of SOD1 mutant-mediated amyotrophic lateral sclerosis (ALS). *Proceedings of the National Academy of Sciences*. 2002;99(3):1604-9.
152. Guo H, Lai L, Butchbach MER, Stockinger MP, Shan X, Bishop GA, et al. Increased expression of the glial glutamate transporter EAAT2 modulates excitotoxicity and delays the onset but not the outcome of ALS in mice. *Human molecular genetics*. 2003;12(19):2519-32.
153. King AE, Woodhouse A, Kirkcaldie MT, Vickers JC. Excitotoxicity in ALS: Overstimulation, or overreaction? *Experimental neurology*. 2016;275 Pt 1:162-71.
154. Blasco H, Mavel S, Corcia P, Gordon PH. The glutamate hypothesis in ALS: pathophysiology and drug development. *Current medicinal chemistry*. 2014;21(31):3551-75.
155. Van Damme P, Bogaert E, Dewil M, Hersmus N, Kiraly D, Scheveneels W, et al. Astrocytes regulate GluR2 expression in motor neurons and their vulnerability to excitotoxicity. *Proceedings of the National Academy of Sciences*. 2007;104(37):14825-30.
156. Ou SH, Wu F, Harrich D, Garcia-Martinez LF, Gaynor RB. Cloning and characterization of a novel cellular protein, TDP-43, that binds to human immunodeficiency virus type 1 TAR DNA sequence motifs. *Journal of virology*. 1995;69(6):3584-96.
157. Hasegawa M, Arai T, Nonaka T, Kametani F, Yoshida M, Hashizume Y, et al. Phosphorylated TDP-43 in frontotemporal lobar degeneration and amyotrophic lateral sclerosis. *Annals of neurology*. 2008;64(1):60-70.
158. Cohen TJ, Hwang AW, Restrepo CR, Yuan C-X, Trojanowski JQ, Lee VMY. An acetylation switch controls TDP-43 function and aggregation propensity. *Nature Communications*. 2015;6:5845.
159. Wang P, Wander CM, Yuan CX, Bereman MS, Cohen TJ. Acetylation-induced TDP-43 pathology is suppressed by an HSF1-dependent chaperone program. *Nat Commun*. 2017;8(1):82.
160. Ayala YM, Zago P, D'Ambrogio A, Xu YF, Petrucelli L, Buratti E, et al. Structural determinants of the cellular localization and shuttling of TDP-43. *Journal of cell science*. 2008;121(Pt 22):3778-85.
161. Igaz LM, Kwong LK, Lee EB, Chen-Plotkin A, Swanson E, Unger T, et al. Dysregulation of the ALS-associated gene TDP-43 leads to neuronal death and degeneration in mice. *The Journal of clinical investigation*. 2011;121(2):726-38.
162. Voigt A, Herholz D, Fiesel FC, Kaur K, Müller D, Karsten P, et al. TDP-43-Mediated Neuron Loss In Vivo Requires RNA-Binding Activity. *PLoS one*. 2010;5(8):e12247.
163. Pesiridis GS, Lee VMY, Trojanowski JQ. Mutations in TDP-43 link glycine-rich domain functions to amyotrophic lateral sclerosis. *Human molecular genetics*. 2009;18(R2):R156-R62.
164. Neumann M, Kwong LK, Lee EB, Kremmer E, Flatley A, Xu Y, et al. Phosphorylation of S409/410 of TDP-43 is a consistent feature in all sporadic and familial forms of TDP-43 proteinopathies. *Acta neuropathologica*. 2009;117(2):137-49.
165. van Eersel J, Ke YD, Gladbach A, Bi M, Götz J, Kril JJ, et al. Cytoplasmic Accumulation and Aggregation of TDP-43 upon Proteasome Inhibition in Cultured Neurons. *PLoS one*. 2011;6(7):e22850.
166. Kabashi E, Valdmanis PN, Dion P, Spiegelman D, McConkey BJ, Vande Velde C, et al. TARDBP mutations in individuals with sporadic and familial amyotrophic lateral sclerosis. *Nature genetics*. 2008;40(5):572-4.
167. Rutherford NJ, Zhang YJ, Baker M, Gass JM, Finch NA, Xu YF, et al. Novel mutations in TARDBP (TDP-43) in patients with familial amyotrophic lateral sclerosis. *PLoS genetics*. 2008;4(9):e1000193.

168. Zhang Y-J, Xu Y-F, Cook C, Gendron TF, Roettges P, Link CD, et al. Aberrant cleavage of TDP-43 enhances aggregation and cellular toxicity. *Proceedings of the National Academy of Sciences*. 2009;106(18):7607-12.
169. Gurney ME. Transgenic-Mouse Model of Amyotrophic Lateral Sclerosis. *New England Journal of Medicine*. 1994;331(25):1721-2.
170. Liu Y-C, Chiang P-M, Tsai K-J. Disease Animal Models of TDP-43 Proteinopathy and Their Pre-Clinical Applications. *International Journal of Molecular Sciences*. 2013;14(10):20079-111.
171. Tsao W, Jeong YH, Lin S, Ling J, Price DL, Chiang P-M, et al. Rodent models of TDP-43: Recent advances. *Brain research*. 2012;1462:26-39.
172. Zhou H, Huang C, Chen H, Wang D, Landel CP, Xia PY, et al. Transgenic Rat Model of Neurodegeneration Caused by Mutation in the TDP Gene. *PLoS genetics*. 2010;6(3):e1000887.
173. Wegorzewska I, Bell S, Cairns NJ, Miller TM, Baloh RH. TDP-43 mutant transgenic mice develop features of ALS and frontotemporal lobar degeneration. *Proceedings of the National Academy of Sciences of the United States of America*. 2009;106(44):18809-14.
174. Walker AK, Spiller KJ, Ge G, Zheng A, Xu Y, Zhou M, et al. Functional recovery in new mouse models of ALS/FTLD after clearance of pathological cytoplasmic TDP-43. *Acta neuropathologica*. 2015;130(5):643-60.
175. Xicoy H, Wieringa B, Martens GJM. The SH-SY5Y cell line in Parkinson's disease research: a systematic review. *Molecular neurodegeneration*. 2017;12:10.
176. Arun P, Moffett JR, Namboodiri AM. Riluzole decreases synthesis of N-acetylaspartate and N-acetylaspartylglutamate in SH-SY5Y human neuroblastoma cells. *Brain research*. 2010;1334:25-30.
177. Lopes FM, Schroder R, da Frota ML, Jr., Zanotto-Filho A, Muller CB, Pires AS, et al. Comparison between proliferative and neuron-like SH-SY5Y cells as an in vitro model for Parkinson disease studies. *Brain research*. 2010;1337:85-94.
178. Nonaka T, Masuda-Suzukake M, Arai T, Hasegawa Y, Akatsu H, Obi T, et al. Prion-like properties of pathological TDP-43 aggregates from diseased brains. *Cell reports*. 2013;4(1):124-34.
179. Krishna A, Biryukov M, Trefois C, Antony PM, Hussong R, Lin J, et al. Systems genomics evaluation of the SH-SY5Y neuroblastoma cell line as a model for Parkinson's disease. *BMC genomics*. 2014;15:1154.
180. Koriyama Y, Furukawa A, Muramatsu M, Takino J, Takeuchi M. Glyceraldehyde caused Alzheimer's disease-like alterations in diagnostic marker levels in SH-SY5Y human neuroblastoma cells. *Scientific reports*. 2015;5:13313.
181. Sala G, Beretta S, Ceresa C, Mattavelli L, Zoia C, Tremolizzo L, et al. Impairment of glutamate transport and increased vulnerability to oxidative stress in neuroblastoma SH-SY5Y cells expressing a Cu,Zn superoxide dismutase typical of familial amyotrophic lateral sclerosis. *Neurochemistry international*. 2005;46(3):227-34.
182. Nakajima A, Tsuji M, Inagaki M, Tamura Y, Kato M, Niiya A, et al. Neuroprotective effects of propofol on ER stress-mediated apoptosis in neuroblastoma SH-SY5Y cells. *European journal of pharmacology*. 2014;725:47-54.
183. Nonaka T, Arai T, Buratti E, Baralle FE, Akiyama H, Hasegawa M. Phosphorylated and ubiquitinated TDP-43 pathological inclusions in ALS and FTLD-U are recapitulated in SH-SY5Y cells. *FEBS letters*. 2009;583(2):394-400.
184. Meyerowitz J, Parker SJ, Vella LJ, Ng DCH, Price KA, Liddell JR, et al. C-Jun N-terminal kinase controls TDP-43 accumulation in stress granules induced by oxidative stress. *Molecular neurodegeneration*. 2011;6:57-.
185. Liu G, Coyne AN, Pei F, Vaughan S, Chaung M, Zarnescu DC, et al. Endocytosis regulates TDP-43 toxicity and turnover. *Nat Commun*. 2017;8(1):2092.
186. Xicoy H, Wieringa B, Martens GJ. The SH-SY5Y cell line in Parkinson's disease research: a systematic review. *Molecular neurodegeneration*. 2017;12(1):10.
187. Pinto S, Cunha C, Barbosa M, Vaz AR, Brites D. Exosomes from NSC-34 Cells Transfected with hSOD1-G93A Are Enriched in miR-124 and Drive Alterations in Microglia Phenotype. *Frontiers in neuroscience*. 2017;11:273.

188. Mishra P-S, Dhull DK, Nalini A, Vijayalakshmi K, Sathyaprabha TN, Alladi PA, et al. Astroglia acquires a toxic neuroinflammatory role in response to the cerebrospinal fluid from amyotrophic lateral sclerosis patients. *Journal of Neuroinflammation*. 2016;13(1):212.
189. Smethurst P, Newcombe J, Troakes C, Simone R, Chen Y-R, Patani R, et al. In vitro prion-like behaviour of TDP-43 in ALS. *Neurobiology of Disease*. 2016;96:236-47.
190. Correia AS, Patel P, Dutta K, Julien JP. Inflammation Induces TDP-43 Mislocalization and Aggregation. *PloS one*. 2015;10(10):e0140248.
191. Gomes C, Escrevente C, Costa J. Mutant superoxide dismutase 1 overexpression in NSC-34 cells: effect of trehalose on aggregation, TDP-43 localization and levels of co-expressed glycoproteins. *Neurosci Lett*. 2010;475(3):145-9.
192. Lu J, Duan W, Guo Y, Jiang H, Li Z, Huang J, et al. Mitochondrial dysfunction in human TDP-43 transfected NSC34 cell lines and the protective effect of dimethoxy curcumin. *Brain research bulletin*. 2012;89(5-6):185-90.
193. Madji Hounoum B, Vourc'h P, Felix R, Corcia P, Patin F, Guéguinou M, et al. NSC-34 Motor Neuron-Like Cells Are Unsuitable as Experimental Model for Glutamate-Mediated Excitotoxicity. *Frontiers in Cellular Neuroscience*. 2016;10:118.
194. Bhat PV, Pandareesh, Khanum F, Tamatam A. Cytotoxic Effects of Ochratoxin A in Neuro-2a Cells: Role of Oxidative Stress Evidenced by N-acetylcysteine. *Frontiers in Microbiology*. 2016;7:1142.
195. Xu Z, Poidevin M, Li X, Li Y, Shu L, Nelson DL, et al. Expanded GGGGCC repeat RNA associated with amyotrophic lateral sclerosis and frontotemporal dementia causes neurodegeneration. *Proceedings of the National Academy of Sciences of the United States of America*. 2013;110(19):7778-83.
196. LePage KT, Dickey RW, Gerwick WH, Jester EL, Murray TF. On the Use of Neuro-2a Neuroblastoma Cells Versus Intact Neurons in Primary Culture for Neurotoxicity Studies. 2005;17(1):27-50.
197. He R-Y, Chao S-H, Tsai Y-J, Lee C-C, Yu C-Y, Gao H-D, et al. Photocontrollable Probe Spatiotemporally Induces Neurotoxic Fibrillar Aggregates and Impairs Nucleocytoplasmic Trafficking. *ACS Nano*. 2017;11(7):6795-807.
198. Schlachetzki JCM, Saliba SW, Oliveira ACPd. Studying neurodegenerative diseases in culture models. *Revista Brasileira de Psiquiatria*. 2013;35:S92-S100.
199. Gordon J, Amini S, White MK. General overview of neuronal cell culture. *Methods in molecular biology (Clifton, NJ)*. 2013;1078:1-8.
200. Haidet-Phillips AM, Hester ME, Miranda CJ, Meyer K, Braun L, Frakes A, et al. Astrocytes from familial and sporadic ALS patients are toxic to motor neurons. *Nat Biotech*. 2011;29(9):824-8.
201. Lundberg C, Bjorklund T, Carlsson T, Jakobsson J, Hantraye P, Deglon N, et al. Applications of lentiviral vectors for biology and gene therapy of neurological disorders. *Current gene therapy*. 2008;8(6):461-73.
202. Martin-Rendon E, Azzouz M, Mazarakis ND. Lentiviral vectors for the treatment of neurodegenerative diseases. *Current opinion in molecular therapeutics*. 2001;3(5):476-81.
203. Kordower JH, Emborg ME, Bloch J, Ma SY, Chu Y, Leventhal L, et al. Neurodegeneration Prevented by Lentiviral Vector Delivery of GDNF in Primate Models of Parkinson's Disease. *Science (New York, NY)*. 2000;290(5492):767.
204. Bensadoun J-C, Déglon N, Tseng JL, Ridet J-L, Zurn AD, Aebischer P. Lentiviral Vectors as a Gene Delivery System in the Mouse Midbrain: Cellular and Behavioral Improvements in a 6-OHDA Model of Parkinson's Disease Using GDNF. *Experimental neurology*. 2000;164(1):15-24.
205. Wilson KD, Wu JC. Induced pluripotent stem cells. *Jama*. 2015;313(16):1613-4.
206. Dimos JT, Rodolfa KT, Niakan KK, Weisenthal LM, Mitsumoto H, Chung W, et al. Induced pluripotent stem cells generated from patients with ALS can be differentiated into motor neurons. *Science (New York, NY)*. 2008;321(5893):1218-21.
207. Pen AE, Jensen UB. Current status of treating neurodegenerative disease with induced pluripotent stem cells. *Acta neurologica Scandinavica*. 2017;135(1):57-72.

208. Arai T, Hasegawa M, Akiyama H, Ikeda K, Nonaka T, Mori H, et al. TDP-43 is a component of ubiquitin-positive tau-negative inclusions in frontotemporal lobar degeneration and amyotrophic lateral sclerosis. *Biochemical and biophysical research communications*. 2006;351(3):602-11.
209. Neumann M, Kwong LK, Sampathu DM, Trojanowski JQ, Lee VY. Tdp-43 proteinopathy in frontotemporal lobar degeneration and amyotrophic lateral sclerosis: Protein misfolding diseases without amyloidosis. *Archives of Neurology*. 2007;64(10):1388-94.
210. Wuolikainen A, Jonsson P, Ahnlund M, Antti H, Marklund SL, Moritz T, et al. Multi-platform mass spectrometry analysis of the CSF and plasma metabolomes of rigorously matched amyotrophic lateral sclerosis, Parkinson's disease and control subjects. *Molecular bioSystems*. 2016;12(4):1287-98.
211. Kametani F, Obi T, Shishido T, Akatsu H, Murayama S, Saito Y, et al. Mass spectrometric analysis of accumulated TDP-43 in amyotrophic lateral sclerosis brains. *Scientific reports*. 2016;6:23281.
212. Andre R, Scahill RI, Haider S, Tabrizi SJ. Biomarker development for Huntington's disease. *Drug discovery today*. 2014;19(7):972-9.
213. Schaffer C, Sarad N, DeCrumpe A, Goswami D, Herrmann S, Morales J, et al. Biomarkers in the Diagnosis and Prognosis of Alzheimer's Disease. *Journal of laboratory automation*. 2015;20(5):589-600.
214. Conraux L, Pech C, Guerraoui H, Loyaux D, Ferrara P, Guillemot JC, et al. Plasma peptide biomarker discovery for amyotrophic lateral sclerosis by MALDI-TOF mass spectrometry profiling. *PloS one*. 2013;8(11):e79733.
215. Gozal YM, Dammer EB, Duong DM, Cheng D, Gearing M, Rees HD, et al. Proteomic analysis of hippocampal dentate granule cells in frontotemporal lobar degeneration: application of laser capture technology. *Frontiers in neurology*. 2011;2:24.
216. Tanaka Y, Hasegawa M. Profilin 1 mutants form aggregates that induce accumulation of prion-like TDP-43. *Prion*. 2016;10(4):283-9.
217. Igaz LM, Kwong LK, Xu Y, Truax AC, Uryu K, Neumann M, et al. Enrichment of C-Terminal Fragments in TAR DNA-Binding Protein-43 Cytoplasmic Inclusions in Brain but not in Spinal Cord of Frontotemporal Lobar Degeneration and Amyotrophic Lateral Sclerosis. *The American Journal of Pathology*. 2008;173(1):182-94.
218. Winton MJ, Igaz LM, Wong MM, Kwong LK, Trojanowski JQ, Lee VM-Y. Disturbance of Nuclear and Cytoplasmic TAR DNA-binding Protein (TDP-43) Induces Disease-like Redistribution, Sequestration, and Aggregate Formation. *Journal of Biological Chemistry*. 2008;283(19):13302-9.
219. Walker AK, Tripathy K, Restrepo CR, Ge G, Xu Y, Kwong LK, et al. An insoluble frontotemporal lobar degeneration-associated TDP-43 C-terminal fragment causes neurodegeneration and hippocampus pathology in transgenic mice. *Human molecular genetics*. 2015;24(25):7241-54.
220. Neilson KA, Keighley T, Pascovici D, Cooke B, Haynes PA. Label-free quantitative shotgun proteomics using normalized spectral abundance factors. *Methods in molecular biology (Clifton, NJ)*. 2013;1002:205-22.
221. UniProt: the universal protein knowledgebase. *Nucleic Acids Research*. 2017;45(D1):D158-D69.
222. Thomas PD, Campbell MJ, Kejariwal A, Mi H, Karlak B, Daverman R, et al. PANTHER: A Library of Protein Families and Subfamilies Indexed by Function. *Genome Research*. 2003;13(9):2129-41.
223. Bardou P, Mariette J, Escudié F, Djemiel C, Klopp C. jvenn: an interactive Venn diagram viewer. *BMC Bioinformatics*. 2014;15(1):293.
224. Schneider CA, Rasband WS, Eliceiri KW. NIH Image to ImageJ: 25 years of image analysis. *Nature methods*. 2012;9(7):671-5.
225. Wong B. Color blindness. *Nat Meth*. 2011;8(6):441-.
226. Miyazaki D, Nakamura A, Hineno A, Kobayashi C, Kinoshita T, Yoshida K, et al. Elevation of serum heat-shock protein levels in amyotrophic lateral sclerosis. *Neurological sciences : official journal of the Italian Neurological Society and of the Italian Society of Clinical Neurophysiology*. 2016;37(8):1277-81.
227. Yang C, Wang H, Qiao T, Yang B, Aliaga L, Qiu L, et al. Partial loss of TDP-43 function causes phenotypes of amyotrophic lateral sclerosis. *Proceedings of the National Academy of Sciences of the United States of America*. 2014;111(12):E1121-E9.

228. Bae S-Y, Sheverdin V, Maeng J, Lyoo IK, Han P-L, Lee K. Immunohistochemical Localization of Translationally Controlled Tumor Protein in Axon Terminals of Mouse Hippocampal Neurons. *Experimental Neurobiology*. 2017;26(2):82-9.
229. Meyer MA. Identification of 17 Highly Expressed Genes within Mouse Lumbar Spinal Cord Anterior Horn Region from an In-Situ Hybridization Atlas of 3430 Genes: Implications for Motor Neuron Disease. *Neurology International*. 2014;6(2):5367.
230. Osorno C, Smeltzer, Shayna., Zamudio, Frank., Quadri, Zain., Selenica, Maj-Linda. . Stress-induced nucleocytoplasmic shuttling of TDP-43 is controlled by eIF-5A hypusination. USF Health Research Day; University of South Florida, Florida, USA: Byrd Alzheimers Institute; 2017.
231. Kwak Y-D, Wang B, Li JJ, Wang R, Deng Q, Diao S, et al. Upregulation of the E3 ligase NEDD4-1 by Oxidative Stress Degrades IGF-1 Receptor Protein in Neurodegeneration. *The Journal of Neuroscience*. 2012;32(32):10971-81.
232. Hadano S, Otomo A, Suzuki-Utsunomiya K, Kunita R, Yanagisawa Y, Showguchi-Miyata J, et al. ALS2CL, the novel protein highly homologous to the carboxy-terminal half of ALS2, binds to Rab5 and modulates endosome dynamics. *FEBS letters*. 2004;575(1-3):64-70.
233. Hu JH, Zhang H, Wagey R, Krieger C, Pelech SL. Protein kinase and protein phosphatase expression in amyotrophic lateral sclerosis spinal cord. *Journal of neurochemistry*. 2003;85(2):432-42.
234. Kuijpers M, Yu KL, Teuling E, Akhmanova A, Jaarsma D, Hoogenraad CC. The ALS8 protein VAPB interacts with the ER–Golgi recycling protein YIF1A and regulates membrane delivery into dendrites. *The EMBO Journal*. 2013;32(14):2056-72.
235. Reiling JH, Olive AJ, Sanyal S, Carette JE, Brummelkamp TR, Ploegh HL, et al. A Luman/CREB3–ADP-ribosylation factor 4 (ARF4) signaling pathway mediates the response to Golgi stress and susceptibility to pathogens. *Nature cell biology*. 2013;15(12):1473-85.
236. Schwenk BM, Hartmann H, Serdaroglu A, Schludi MH, Hornburg D, Meissner F, et al. TDP-43 loss of function inhibits endosomal trafficking and alters trophic signaling in neurons. *Embo j*. 2016;35(21):2350-70.
237. Walker AK, Farg MA, Bye CR, McLean CA, Horne MK, Atkin JD. Protein disulphide isomerase protects against protein aggregation and is S-nitrosylated in amyotrophic lateral sclerosis. *Brain*. 2010;133(Pt 1):105-16.
238. Walker AK, Soo KY, Sundaramoorthy V, Parakh S, Ma Y, Farg MA, et al. ALS-Associated TDP-43 Induces Endoplasmic Reticulum Stress, Which Drives Cytoplasmic TDP-43 Accumulation and Stress Granule Formation. *PLoS one*. 2013;8(11):e81170.

# Appendices

Appendix A – All proteins identified as either exclusive or shared between the 30 µg Urea-soluble fractions of ΔNLS, 4FL, ΔNLS+4FL and ΔNLS+2KQ human TDP-43 Transfections in NSC-34 Cells

UniProt ID	Protein names	NLS Presence (n/4)	4FL Replicate Presence (n/4)	NLS+4FL Replicate Presence (n/4)	NLS+2KQ Replicate Presence (n/4)	Total Replicate Presence (n/16)	Total Peptide Count
P20152	Vimentin	0	3	1	1	5	12
P62492	Ras-related protein Rab-11A (Rab-11)	0	3	1	1	5	8
Q8BUV3	Gephyrin [Includes: Molybdopterin adenylyltransferase (MPT adenylyltransferase) (EC 2.7.7.75) (Domain G); Molybdopterin molybdenumtransferase (MPT Mo-transferase) (EC 2.10.1.1) (Domain E)]	0	2	1	2	5	5
P97807	Fumarate hydratase, mitochondrial (Fumarase) (EC 4.2.1.2) (EF-3)	0	3	1	1	5	5
Q9JJV2	Profilin-2 (Profilin II)	0	3	1	1	5	5
Q8C2Q3	RNA-binding protein 14 (RNA-binding motif protein 14)	0	2	1	1	4	9
Q9Z1Q5	Chloride intracellular channel protein 1 (Nuclear chloride ion channel 27) (NCC27)	0	1	1	2	4	8
Q99K85	Phosphoserine aminotransferase (PSAT) (EC 2.6.1.52) (Endometrial progesterone-induced protein) (EPIP) (Phosphohydroxythreonine aminotransferase)	0	2	1	1	4	8
P29758	Ornithine aminotransferase, mitochondrial (EC 2.6.1.13) (Ornithine--oxo-acid aminotransferase)	0	2	1	1	4	7
P97310	DNA replication licensing factor MCM2 (EC 3.6.4.12) (Minichromosome maintenance protein 2 homolog) (Nuclear protein BM28)	0	2	1	1	4	6
Q7TPR4	Alpha-actinin-1 (Alpha-actinin cytoskeletal isoform) (F-actin cross-linking protein) (Non-muscle alpha-actinin-1)	0	2	1	1	4	6
Q61024	Asparagine synthetase [glutamine-hydrolyzing] (EC 6.3.5.4) (Glutamine-dependent asparagine synthetase)	0	2	1	1	4	6

UniProt ID	Protein names	NLS Presence (n/4)	4FL Replicate Presence (n/4)	NLS+4FL Replicate Presence (n/4)	NLS+2KQ Replicate Presence (n/4)	Total Replicate Presence (n/16)	Total Peptide Count
<b>Q62188</b>	Dihydropyrimidinase-related protein 3 (DRP-3) (Unc-33-like phosphoprotein 1) (ULIP-1)	0	2	1	1	4	6
<b>O35129</b>	Prohibitin-2 (B-cell receptor-associated protein BAP37) (Repressor of estrogen receptor activity)	0	2	1	1	4	5
<b>Q62189</b>	U1 small nuclear ribonucleoprotein A (U1 snRNP A) (U1-A) (U1A)	0	2	1	1	4	4
<b>Q9QZM0</b>	Ubiquilin-2 (Chap1) (DSK2 homolog) (Protein linking IAP with cytoskeleton 2) (PLIC-2) (Ubiquitin-like product Chap1/Dsk2)	0	1	1	2	4	4
<b>Q61029</b>	Lamina-associated polypeptide 2, isoforms beta/delta/epsilon/gamma (Thymopoietin isoforms beta/delta/epsilon/gamma) (TP beta/delta/epsilon/gamma)	0	2	1	1	4	4
<b>Q61205</b>	Platelet-activating factor acetylhydrolase IB subunit gamma (EC 3.1.1.47) (PAF acetylhydrolase 29 kDa subunit) (PAF-AH 29 kDa subunit) (PAF-AH subunit gamma) (PAFAH subunit gamma)	0	2	1	1	4	4
<b>P42932</b>	T-complex protein 1 subunit theta (TCP-1-theta) (CCT-theta)	0	1	1	1	3	13
<b>P60122</b>	RuvB-like 1 (EC 3.6.4.12) (49 kDa TATA box-binding protein-interacting protein) (49 kDa TBP-interacting protein) (DNA helicase p50) (Pontin 52) (TIP49a)	0	1	1	1	3	7
<b>P57776</b>	Elongation factor 1-delta (EF-1-delta)	0	1	1	1	3	7
<b>Q9DCL9</b>	Multifunctional protein ADE2 [Includes: Phosphoribosylaminoimidazole-succinocarboxamide synthase (EC 6.3.2.6) (SAICAR synthetase); Phosphoribosylaminoimidazole carboxylase (EC 4.1.1.21) (AIR carboxylase) (AIRC)]	0	1	1	1	3	6
<b>Q99KP6</b>	Pre-mRNA-processing factor 19 (EC 2.3.2.27) (Nuclear matrix protein 200) (PRP19/PSO4 homolog) (RING-type E3 ubiquitin transferase PRP19) (Senescence evasion factor)	0	1	1	1	3	5
<b>P19001</b>	Keratin, type I cytoskeletal 19 (Cytokeratin-19) (CK-19) (Keratin-19) (K19)	0	1	1	1	3	5
<b>P67778</b>	Prohibitin (B-cell receptor-associated protein 32) (BAP 32)	0	1	1	1	3	4

UniProt ID	Protein names	NLS Presence (n/4)	4FL Replicate Presence (n/4)	NLS+4FL Replicate Presence (n/4)	NLS+2KQ Replicate Presence (n/4)	Total Replicate Presence (n/16)	Total Peptide Count
<b>Q3U0V1</b>	Far upstream element-binding protein 2 (FUSE-binding protein 2) (KH type-splicing regulatory protein) (KSRP)	0	1	1	1	3	4
<b>Q60931</b>	Voltage-dependent anion-selective channel protein 3 (VDAC-3) (mVDAC3) (Outer mitochondrial membrane protein porin 3)	0	1	1	1	3	3
<b>Q9Z2N8</b>	Actin-like protein 6A (53 kDa BRG1-associated factor A) (Actin-related protein Baf53a) (BRG1-associated factor 53A) (BAF53A)	0	1	1	1	3	3
<b>P97823</b>	Acyl-protein thioesterase 1 (APT-1) (EC 3.1.2.-) (Lysophospholipase 1) (Lysophospholipase I) (LPL-I) (LysoPLA I)	0	1	1	1	3	3
<b>Q9R1P0</b>	Proteasome subunit alpha type-4 (EC 3.4.25.1) (Macropain subunit C9) (Multicatalytic endopeptidase complex subunit C9) (Proteasome component C9) (Proteasome subunit L)	0	1	1	1	3	3
<b>P21107</b>	Tropomyosin alpha-3 chain (Gamma-tropomyosin) (Tropomyosin-3)	0	1	1	1	3	3
<b>Q921M3</b>	Splicing factor 3B subunit 3 (Pre-mRNA-splicing factor SF3b 130 kDa subunit) (SF3b130) (Spliceosome-associated protein 130) (SAP 130)	0	1	1	1	3	3
<b>P35979</b>	60S ribosomal protein L12	0	1	1	1	3	3
<b>Q9R0P5</b>	Destrin (Actin-depolymerizing factor) (ADF) (Sid 23)	0	1	1	1	3	3
<b>Q9Z2X1</b>	Heterogeneous nuclear ribonucleoprotein F (hnRNP F) [Cleaved into: Heterogeneous nuclear ribonucleoprotein F, N-terminally processed]	0	4	1	0	5	8
<b>Q8VDM4</b>	26S proteasome non-ATPase regulatory subunit 2 (26S proteasome regulatory subunit RPN1) (26S proteasome regulatory subunit S2) (26S proteasome subunit p97)	0	4	1	0	5	5
<b>Q9R1Q8</b>	Transgelin-3 (Neuronal protein NP25)	0	3	1	0	4	7
<b>P60229</b>	Eukaryotic translation initiation factor 3 subunit E (eIF3e) (Eukaryotic translation initiation factor 3 subunit 6) (MMTV integration site 6) (Mammary tumor-associated protein INT-6) (Viral integration site protein INT-6) (eIF-3 p48)	0	2	0	2	4	7

UniProt ID	Protein names	NLS Presence (n/4)	4FL Replicate Presence (n/4)	NLS+4FL Replicate Presence (n/4)	NLS+2KQ Replicate Presence (n/4)	Total Replicate Presence (n/16)	Total Peptide Count
<b>Q9D2G2</b>	Dihydrolipoyllysine-residue succinyltransferase component of 2-oxoglutarate dehydrogenase complex, mitochondrial (EC 2.3.1.61) (2-oxoglutarate dehydrogenase complex component E2) (OGDC-E2) (Dihydrolipoamide succinyltransferase component of 2-oxoglutarate dehydrogenase complex) (E2K)	0	3	1	0	4	6
<b>Q7TMK9</b>	Heterogeneous nuclear ribonucleoprotein Q (hnRNP Q) (Glycine- and tyrosine-rich RNA-binding protein) (GRY-RBP) (NS1-associated protein 1) (Synaptotagmin-binding, cytoplasmic RNA-interacting protein) (pp68)	0	3	1	0	4	6
<b>Q8VEM8</b>	Phosphate carrier protein, mitochondrial (Phosphate transport protein) (PTP) (Solute carrier family 25 member 3)	0	3	1	0	4	5
<b>Q6NZC7</b>	SEC23-interacting protein	0	3	0	1	4	4
<b>Q62167</b>	ATP-dependent RNA helicase DDX3X (EC 3.6.4.13) (D1Pas1-related sequence 2) (DEAD box RNA helicase DEAD3) (mDEAD3) (DEAD box protein 3, X-chromosomal) (Embryonic RNA helicase)	0	2	1	0	3	6
<b>P08249</b>	Malate dehydrogenase, mitochondrial (EC 1.1.1.37)	0	0	1	2	3	6
<b>Q61937</b>	Nucleophosmin (NPM) (Nucleolar phosphoprotein B23) (Nucleolar protein NO38) (Numatrin)	0	0	1	2	3	6
<b>Q8VDW0</b>	ATP-dependent RNA helicase DDX39A (EC 3.6.4.13) (DEAD box protein 39)	0	2	1	0	3	6
<b>Q9ERU9</b>	E3 SUMO-protein ligase RanBP2 (EC 6.3.2.-) (Ran-binding protein 2) (RanBP2)	0	2	1	0	3	5
<b>Q8BG32</b>	26S proteasome non-ATPase regulatory subunit 11 (26S proteasome regulatory subunit RPN6) (26S proteasome regulatory subunit S9) (26S proteasome regulatory subunit p44.5)	0	2	1	0	3	5
<b>Q6PFR5</b>	Transformer-2 protein homolog alpha (TRA-2 alpha) (TRA2-alpha) (Transformer-2 protein homolog A)	0	2	1	0	3	5

UniProt ID	Protein names	NLS Presence (n/4)	4FL Replicate Presence (n/4)	NLS+4FL Replicate Presence (n/4)	NLS+2KQ Replicate Presence (n/4)	Total Replicate Presence (n/16)	Total Peptide Count
Q8JZQ9	Eukaryotic translation initiation factor 3 subunit B (eIF3b) (Eukaryotic translation initiation factor 3 subunit 9) (eIF-3-eta) (eIF3 p116)	0	2	1	0	3	4
Q99LF4	tRNA-splicing ligase RtcB homolog (EC 6.5.1.3) (Focal adhesion-associated protein) (FAAP)	0	2	1	0	3	4
P54775	26S proteasome regulatory subunit 6B (26S proteasome AAA-ATPase subunit RPT3) (CIP21) (MB67-interacting protein) (MIP224) (Proteasome 26S subunit ATPase 4) (Tat-binding protein 7) (TBP-7)	0	0	1	2	3	4
Q9JK92	Heat shock protein beta-8 (HspB8) (Alpha-crystallin C chain) (Small stress protein-like protein HSP22)	0	0	1	2	3	3
Q8BTW3	Exosome complex component MTR3 (Exosome component 6) (mRNA transport regulator 3 homolog)	0	2	1	0	3	3
Q8BJW6	Eukaryotic translation initiation factor 2A (eIF-2A) [Cleaved into: Eukaryotic translation initiation factor 2A, N-terminally processed]	0	2	1	0	3	3
Q91YR1	Twinfilin-1 (Protein A6)	0	2	1	0	3	3
P61082	NEDD8-conjugating enzyme Ubc12 (EC 6.3.2.-) (NEDD8 carrier protein) (NEDD8 protein ligase) (Ubiquitin-conjugating enzyme E2 M)	0	0	1	2	3	3
Q6NZJ6	Eukaryotic translation initiation factor 4 gamma 1 (eIF-4-gamma 1) (eIF-4G 1) (eIF-4G1)	0	2	0	1	3	3
P80316	T-complex protein 1 subunit epsilon (TCP-1-epsilon) (CCT-epsilon)	0	0	1	1	2	7
P62814	V-type proton ATPase subunit B, brain isoform (V-ATPase subunit B 2) (Endomembrane proton pump 58 kDa subunit) (Vacuolar proton pump subunit B 2)	0	1	1	0	2	5
Q61584	Fragile X mental retardation syndrome-related protein 1 (mFxr1p)	0	1	1	0	2	5
Q3TWW8	Serine/arginine-rich splicing factor 6 (Pre-mRNA-splicing factor SRP55) (Splicing factor, arginine/serine-rich 6)	0	1	1	0	2	4
Q9D051	Pyruvate dehydrogenase E1 component subunit beta, mitochondrial (PDHE1-B) (EC 1.2.4.1)	0	1	1	0	2	4

UniProt ID	Protein names	NLS Presence (n/4)	4FL Replicate Presence (n/4)	NLS+4FL Replicate Presence (n/4)	NLS+2KQ Replicate Presence (n/4)	Total Replicate Presence (n/16)	Total Peptide Count
<b>P70398</b>	Probable ubiquitin carboxyl-terminal hydrolase FAF-X (EC 3.4.19.12) (Deubiquitinating enzyme FAF-X) (Fat facets homolog) (Fat facets protein-related, X-linked) (Ubiquitin carboxyl-terminal hydrolase FAM) (Ubiquitin thioesterase FAF-X) (Ubiquitin-specific protease 9, X chromosome) (Ubiquitin-specific-processing protease FAF-X)	0	1	1	0	2	4
<b>Q9R0E1</b>	Procollagen-lysine,2-oxoglutarate 5-dioxygenase 3 (EC 1.14.11.4) (Lysyl hydroxylase 3) (LH3)	0	0	1	1	2	4
<b>P49025</b>	Citron Rho-interacting kinase (CRIK) (EC 2.7.11.1) (Rho-interacting, serine/threonine-protein kinase 21)	0	1	0	1	2	4
<b>Q8BL97</b>	Serine/arginine-rich splicing factor 7 (Splicing factor, arginine/serine-rich 7)	0	0	1	1	2	4
<b>O08599</b>	Syntaxin-binding protein 1 (Protein unc-18 homolog 1) (Unc18-1) (Protein unc-18 homolog A) (Unc-18A)	0	1	1	0	2	4
<b>Q64737</b>	Trifunctional purine biosynthetic protein adenosine-3 [Includes: Phosphoribosylamine--glycine ligase (EC 6.3.4.13) (Glycinamide ribonucleotide synthetase) (GARS) (Phosphoribosylglycinamide synthetase); Phosphoribosylformylglycinamide cyclo-ligase (EC 6.3.3.1) (AIR synthase) (AIRS) (Phosphoribosyl-aminoimidazole synthetase); Phosphoribosylglycinamide formyltransferase (EC 2.1.2.2) (5'-phosphoribosylglycinamide transformylase) (GAR transformylase) (GART)]	0	1	1	0	2	4
<b>P28658</b>	Ataxin-10 (Brain protein E46) (Spinocerebellar ataxia type 10 protein homolog)	0	1	1	0	2	4
<b>Q76MZ3</b>	Serine/threonine-protein phosphatase 2A 65 kDa regulatory subunit A alpha isoform (PP2A subunit A isoform PR65-alpha) (PP2A subunit A isoform R1-alpha)	0	0	1	1	2	4
<b>P17918</b>	Proliferating cell nuclear antigen (PCNA) (Cyclin)	0	0	1	1	2	4

UniProt ID	Protein names	NLS Presence (n/4)	4FL Replicate Presence (n/4)	NLS+4FL Replicate Presence (n/4)	NLS+2KQ Replicate Presence (n/4)	Total Replicate Presence (n/16)	Total Peptide Count
<b>Q9CZY3</b>	Ubiquitin-conjugating enzyme E2 variant 1 (UEV-1) (CROC-1)	0	1	1	0	2	3
<b>P70318</b>	Nucleolysin TIAR (TIA-1-related protein)	0	1	1	0	2	3
<b>Q9CQV8</b>	14-3-3 protein beta/alpha (Protein kinase C inhibitor protein 1) (KCIP-1) [Cleaved into: 14-3-3 protein beta/alpha, N-terminally processed]	0	0	1	1	2	3
<b>Q99MR6</b>	Serrate RNA effector molecule homolog (Arsenite-resistance protein 2)	0	1	1	0	2	3
<b>P57780</b>	Alpha-actinin-4 (Non-muscle alpha-actinin 4)	0	1	0	1	2	3
<b>O55234</b>	Proteasome subunit beta type-5 (EC 3.4.25.1) (Macropain epsilon chain) (Multicatalytic endopeptidase complex epsilon chain) (Proteasome chain 6) (Proteasome epsilon chain) (Proteasome subunit X)	0	1	1	0	2	3
<b>P32067</b>	Lupus La protein homolog (La autoantigen homolog) (La ribonucleoprotein)	0	1	1	0	2	3
<b>Q8R5H1</b>	Ubiquitin carboxyl-terminal hydrolase 15 (EC 3.4.19.12) (Deubiquitinating enzyme 15) (Ubiquitin thioesterase 15) (Ubiquitin-specific-processing protease 15)	0	0	1	1	2	3
<b>O08795</b>	Glucosidase 2 subunit beta (80K-H protein) (Glucosidase II subunit beta) (Protein kinase C substrate 60.1 kDa protein heavy chain) (PKCSH)	0	0	1	1	2	3
<b>P40124</b>	Adenylyl cyclase-associated protein 1 (CAP 1)	0	0	1	1	2	2
<b>Q5U4D9</b>	THO complex subunit 6 homolog (WD repeat-containing protein 58)	0	0	1	1	2	2
<b>P97379</b>	Ras GTPase-activating protein-binding protein 2 (G3BP-2) (GAP SH3 domain-binding protein 2)	0	0	1	1	2	2
<b>O35295</b>	Transcriptional activator protein Pur-beta (Purine-rich element-binding protein B) (Vascular actin single-stranded DNA-binding factor 2 p44 component)	0	1	1	0	2	2
<b>P09055</b>	Integrin beta-1 (Fibronectin receptor subunit beta) (VLA-4 subunit beta) (CD antigen CD29)	0	1	1	0	2	2

UniProt ID	Protein names	NLS Presence (n/4)	4FL Replicate Presence (n/4)	NLS+4FL Replicate Presence (n/4)	NLS+2KQ Replicate Presence (n/4)	Total Replicate Presence (n/16)	Total Peptide Count
<b>Q9D287</b>	Pre-mRNA-splicing factor SPF27 (Breast carcinoma-amplified sequence 2 homolog) (DNA amplified in mammary carcinoma 1 protein)	0	1	1	0	2	2
<b>P08553</b>	Neurofilament medium polypeptide (NF-M) (160 kDa neurofilament protein) (Neurofilament 3) (Neurofilament triplet M protein)	0	0	1	1	2	2
<b>Q99JB2</b>	Stomatin-like protein 2, mitochondrial (SLP-2) (mslp2)	0	1	0	1	2	2
<b>Q8BMP6</b>	Golgi resident protein GCP60 (Acyl-CoA-binding domain-containing protein 3) (Golgi complex-associated protein 1) (GOCAP1) (Golgi phosphoprotein 1) (GOLPH1) (PBR- and PKA-associated protein 7) (Peripheral benzodiazepine receptor-associated protein PAP7)	0	1	1	0	2	2
<b>Q9D1G1</b>	Ras-related protein Rab-1B	0	1	1	0	2	2
<b>O88487</b>	Cytoplasmic dynein 1 intermediate chain 2 (Cytoplasmic dynein intermediate chain 2) (Dynein intermediate chain 2, cytosolic) (DH IC-2)	0	0	1	1	2	2
<b>Q91VD9</b>	NADH-ubiquinone oxidoreductase 75 kDa subunit, mitochondrial (EC 1.6.5.3) (EC 1.6.99.3) (Complex I-75kD) (CI-75kD)	0	0	1	1	2	2
<b>Q9D2M8</b>	Ubiquitin-conjugating enzyme E2 variant 2 (Ubc-like protein MMS2)	0	0	1	1	2	2
<b>O35326</b>	Serine/arginine-rich splicing factor 5 (Delayed-early protein HRS) (Pre-mRNA-splicing factor SRP40) (Splicing factor, arginine/serine-rich 5)	0	1	0	1	2	2
<b>Q9D1R9</b>	60S ribosomal protein L34	0	1	1	0	2	2
<b>P62334</b>	26S proteasome regulatory subunit 10B (26S proteasome AAA-ATPase subunit RPT4) (Proteasome 26S subunit ATPase 6) (Proteasome subunit p42)	0	1	1	0	2	2
<b>Q78PY7</b>	Staphylococcal nuclease domain-containing protein 1 (100 kDa coactivator) (p100 co-activator)	0	0	1	1	2	2
<b>P21995</b>	Embigin (Teratocarcinoma glycoprotein Gp-70)	0	0	1	1	2	2
<b>Q91UZ5</b>	Inositol monophosphatase 2 (IMP 2) (IMPase 2) (EC 3.1.3.25) (Inositol-1(or 4)-monophosphatase 2) (Myo-inositol monophosphatase A2)	0	0	1	1	2	2

UniProt ID	Protein names	NLS Presence (n/4)	4FL Replicate Presence (n/4)	NLS+4FL Replicate Presence (n/4)	NLS+2KQ Replicate Presence (n/4)	Total Replicate Presence (n/16)	Total Peptide Count
<b>Q9D7G0</b>	Ribose-phosphate pyrophosphokinase 1 (EC 2.7.6.1) (Phosphoribosyl pyrophosphate synthase I) (PRS-I)	0	0	1	1	2	2
<b>Q9DBZ5</b>	Eukaryotic translation initiation factor 3 subunit K (eIF3k) (Eukaryotic translation initiation factor 3 subunit 12) (eIF-3 p25)	0	0	1	1	2	2
<b>Q60973</b>	Histone-binding protein RBBP7 (Histone acetyltransferase type B subunit 2) (Nucleosome-remodeling factor subunit RBAP46) (Retinoblastoma-binding protein 7) (RBBP-7) (Retinoblastoma-binding protein p46)	0	1	0	1	2	2
<b>Q8C5C9</b>	TPA-induced transmembrane protein homolog	0	1	0	1	2	2
<b>Q62193</b>	Replication protein A 32 kDa subunit (RP-A p32) (Replication factor A protein 2) (RF-A protein 2) (Replication protein A 34 kDa subunit) (RP-A p34)	0	1	0	1	2	2
<b>P24288</b>	Branched-chain-amino-acid aminotransferase, cytosolic (BCAT(c)) (EC 2.6.1.42) (Protein ECA39)	0	1	0	1	2	2
<b>P61957</b>	Small ubiquitin-related modifier 2 (SUMO-2) (SMT3 homolog 2) (Ubiquitin-like protein SMT3B) (Smt3B)	0	1	0	1	2	2
<b>Q8BTM8</b>	Filamin-A (FLN-A) (Actin-binding protein 280) (ABP-280) (Alpha-filamin) (Endothelial actin-binding protein) (Filamin-1) (Non-muscle filamin)	0	1	0	1	2	2
<b>P60710</b>	Actin, cytoplasmic 1 (Beta-actin) [Cleaved into: Actin, cytoplasmic 1, N-terminally processed]	4	0	0	0	4	89
<b>P99024</b>	Tubulin beta-5 chain	3	0	0	0	3	86
<b>P43274</b>	Histone H1.4 (H1 VAR.2) (H1e)	3	0	0	0	3	78
<b>P03975</b>	IgE-binding protein	3	0	0	0	3	72
<b>P15331</b>	Peripherin	3	0	0	0	3	46
<b>P68373</b>	Tubulin alpha-1C chain (Alpha-tubulin 6) (Alpha-tubulin isotype M-alpha-6) (Tubulin alpha-6 chain) [Cleaved into: Detyrosinated tubulin alpha-1C chain]	3	0	0	0	3	34

UniProt ID	Protein names	NLS Presence (n/4)	4FL Replicate Presence (n/4)	NLS+4FL Replicate Presence (n/4)	NLS+2KQ Replicate Presence (n/4)	Total Replicate Presence (n/16)	Total Peptide Count
P56480	ATP synthase subunit beta, mitochondrial (EC 3.6.3.14)	3	0	0	0	3	27
Q3TTY5	Keratin, type II cytoskeletal 2 epidermal (Cytokeratin-2e) (CK-2e) (Epithelial keratin-2e) (Keratin-2 epidermis) (Keratin-2e) (K2e) (Type-II keratin Kb2)	3	0	0	0	3	20
P60335	Poly(rC)-binding protein 1 (Alpha-CP1) (Heterogeneous nuclear ribonucleoprotein E1) (hnRNP E1)	3	0	0	0	3	12
Q63844	Mitogen-activated protein kinase 3 (MAP kinase 3) (MAPK 3) (EC 2.7.11.24) (ERT2) (Extracellular signal-regulated kinase 1) (ERK-1) (Insulin-stimulated MAP2 kinase) (MAP kinase isoform p44) (p44-MAPK) (MNK1) (Microtubule-associated protein 2 kinase) (p44-ERK1)	3	0	0	0	3	12
Q9DBY8	Nuclear valosin-containing protein-like (NVLp) (Nuclear VCP-like protein)	0	3	0	0	3	4
Q3UV17	Keratin, type II cytoskeletal 2 oral (Keratin-76) (K76) (Type-II keratin Kb9)	3	0	0	0	3	4
P15864	Histone H1.2 (H1 VAR.1) (H1c)	2	0	0	0	2	68
P63260	Actin, cytoplasmic 2 (Gamma-actin) [Cleaved into: Actin, cytoplasmic 2, N-terminally processed]	2	0	0	0	2	66
P11499	Heat shock protein HSP 90-beta (Heat shock 84 kDa) (HSP 84) (HSP84) (Tumor-specific transplantation 84 kDa antigen) (TSTA)	2	0	0	0	2	55
P43276	Histone H1.5 (H1 VAR.5) (H1b)	2	0	0	0	2	54
P16858	Glyceraldehyde-3-phosphate dehydrogenase (GAPDH) (EC 1.2.1.12) (Peptidyl-cysteine S-nitrosylase GAPDH) (EC 2.6.99.-)	2	0	0	0	2	48
P20029	78 kDa glucose-regulated protein (GRP-78) (Heat shock 70 kDa protein 5) (Immunoglobulin heavy chain-binding protein) (BiP)	2	0	0	0	2	40
P38647	Stress-70 protein, mitochondrial (75 kDa glucose-regulated protein) (GRP-75) (Heat shock 70 kDa protein 9) (Mortalin) (Peptide-binding protein 74) (PBP74) (p66 MOT)	2	0	0	0	2	36
P54116	Erythrocyte band 7 integral membrane protein (Protein 7.2b) (Stomatin)	2	0	0	0	2	35

UniProt ID	Protein names	NLS Presence (n/4)	4FL Replicate Presence (n/4)	NLS+4FL Replicate Presence (n/4)	NLS+2KQ Replicate Presence (n/4)	Total Replicate Presence (n/16)	Total Peptide Count
<b>P10126</b>	Elongation factor 1-alpha 1 (EF-1-alpha-1) (Elongation factor Tu) (EF-Tu) (Eukaryotic elongation factor 1 A-1) (eEF1A-1)	2	0	0	0	2	33
<b>P0CG49</b>	Polyubiquitin-B [Cleaved into: Ubiquitin]	2	0	0	0	2	32
<b>Q921F2</b>	TAR DNA-binding protein 43 (TDP-43)	2	0	0	0	2	27
<b>Q60597</b>	2-oxoglutarate dehydrogenase, mitochondrial (EC 1.2.4.2) (2-oxoglutarate dehydrogenase complex component E1) (OGDC-E1) (Alpha-ketoglutarate dehydrogenase)	2	0	0	0	2	23
<b>P48678</b>	Prelamin-A/C [Cleaved into: Lamin-A/C]	2	0	0	0	2	22
<b>P27773</b>	Protein disulfide-isomerase A3 (EC 5.3.4.1) (58 kDa glucose-regulated protein) (58 kDa microsomal protein) (p58) (Disulfide isomerase ER-60) (Endoplasmic reticulum resident protein 57) (ER protein 57) (ERp57) (Endoplasmic reticulum resident protein 60) (ER protein 60) (ERp60)	2	0	0	0	2	21
<b>Q61990</b>	Poly(rC)-binding protein 2 (Alpha-CP2) (CTBP) (CBP) (Putative heterogeneous nuclear ribonucleoprotein X) (hnRNP X)	2	0	0	0	2	18
<b>Q9CQ48</b>	NudC domain-containing protein 2	2	0	0	0	2	13
<b>Q8CGK3</b>	Lon protease homolog, mitochondrial (EC 3.4.21.53) (Lon protease-like protein) (LONP) (Mitochondrial ATP-dependent protease Lon) (Serine protease 15)	2	0	0	0	2	12
<b>Q99K10</b>	Aconitate hydratase, mitochondrial (Aconitase) (EC 4.2.1.3) (Citrate hydro-lyase)	2	0	0	0	2	12
<b>P35278</b>	Ras-related protein Rab-5C	2	0	0	0	2	12
<b>Q5SF07</b>	Insulin-like growth factor 2 mRNA-binding protein 2 (IGF2 mRNA-binding protein 2) (IMP-2) (IGF-II mRNA-binding protein 2) (VICKZ family member 2)	2	0	0	0	2	12
<b>P63323</b>	40S ribosomal protein S12	2	0	0	0	2	11
<b>Q8VEK3</b>	Heterogeneous nuclear ribonucleoprotein U (hnRNP U) (Scaffold attachment factor A) (SAF-A)	2	0	0	0	2	11

UniProt ID	Protein names	NLS Presence (n/4)	4FL Replicate Presence (n/4)	NLS+4FL Replicate Presence (n/4)	NLS+2KQ Replicate Presence (n/4)	Total Replicate Presence (n/16)	Total Peptide Count
P46471	26S proteasome regulatory subunit 7 (26S proteasome AAA-ATPase subunit RPT1) (Proteasome 26S subunit ATPase 2) (Protein MSS1)	2	0	0	0	2	10
Q9CZ13	Cytochrome b-c1 complex subunit 1, mitochondrial (Complex III subunit 1) (Core protein I) (Ubiquinol-cytochrome-c reductase complex core protein 1)	2	0	0	0	2	10
P17182	Alpha-enolase (EC 4.2.1.11) (2-phospho-D-glycerate hydro-lyase) (Enolase 1) (Non-neural enolase) (NNE)	2	0	0	0	2	9
Q04447	Creatine kinase B-type (EC 2.7.3.2) (B-CK) (Creatine kinase B chain)	2	0	0	0	2	7
P09242	Alkaline phosphatase, tissue-nonspecific isozyme (AP-TNAP) (TNSALP) (EC 3.1.3.1) (Alkaline phosphatase 2) (Alkaline phosphatase liver/bone/kidney isozyme)	2	0	0	0	2	7
P62264	40S ribosomal protein S14	2	0	0	0	2	7
Q6PB66	Leucine-rich PPR motif-containing protein, mitochondrial (130 kDa leucine-rich protein) (LRP 130) (mLRP130)	0	2	0	0	2	6
B2RQC6	CAD protein [Includes: Glutamine-dependent carbamoyl-phosphate synthase (EC 6.3.5.5); Aspartate carbamoyltransferase (EC 2.1.3.2); Dihydroorotase (EC 3.5.2.3)]	2	0	0	0	2	5
P70168	Importin subunit beta-1 (Karyopherin subunit beta-1) (Nuclear factor p97) (Pore targeting complex 97 kDa subunit) (PTAC97) (SCG)	2	0	0	0	2	5
Q6ZWU9	40S ribosomal protein S27	2	0	0	0	2	5
Q9Z2K1	Keratin, type I cytoskeletal 16 (Cytokeratin-16) (CK-16) (Keratin-16) (K16)	0	2	0	0	2	5
O55143	Sarcoplasmic/endoplasmic reticulum calcium ATPase 2 (SERCA2) (SR Ca(2+)-ATPase 2) (EC 3.6.3.8) (Calcium pump 2) (Calcium-transporting ATPase sarcoplasmic reticulum type, slow twitch skeletal muscle isoform) (Endoplasmic reticulum class 1/2 Ca(2+) ATPase)	0	2	0	0	2	5
P29341	Polyadenylate-binding protein 1 (PABP-1) (Poly(A)-binding protein 1)	0	2	0	0	2	5
Q9Z1X4	Interleukin enhancer-binding factor 3	0	2	0	0	2	5

UniProt ID	Protein names	NLS Presence (n/4)	4FL Replicate Presence (n/4)	NLS+4FL Replicate Presence (n/4)	NLS+2KQ Replicate Presence (n/4)	Total Replicate Presence (n/16)	Total Peptide Count
P61750	ADP-ribosylation factor 4	2	0	0	0	2	4
P50446	Keratin, type II cytoskeletal 6A (Cytokeratin-6A) (CK-6A) (Keratin-6-alpha) (mK6-alpha) (Keratin-6A) (K6A)	0	0	2	0	2	4
Q9CZM2	60S ribosomal protein L15	2	0	0	0	2	4
P62192	26S proteasome regulatory subunit 4 (P26s4) (26S proteasome AAA-ATPase subunit RPT2) (Proteasome 26S subunit ATPase 1)	0	2	0	0	2	4
P35293	Ras-related protein Rab-18	0	2	0	0	2	3
P17156	Heat shock-related 70 kDa protein 2 (Heat shock protein 70.2)	2	0	0	0	2	3
Q62318	Transcription intermediary factor 1-beta (TIF1-beta) (E3 SUMO-protein ligase TRIM28) (EC 2.3.2.27) (KRAB-A-interacting protein) (KRIP-1) (RING-type E3 ubiquitin transferase TIF1-beta) (Tripartite motif-containing protein 28)	0	2	0	0	2	3
Q9Z1Q9	Valine--tRNA ligase (EC 6.1.1.9) (Protein G7a) (Valyl-tRNA synthetase) (ValRS)	0	2	0	0	2	3
Q68FL6	Methionine--tRNA ligase, cytoplasmic (EC 6.1.1.10) (Methionyl-tRNA synthetase) (MetRS)	0	2	0	0	2	3
Q922R8	Protein disulfide-isomerase A6 (EC 5.3.4.1) (Thioredoxin domain-containing protein 7)	0	0	0	2	2	2
Q60972	Histone-binding protein RBBP4 (Chromatin assembly factor 1 subunit C) (CAF-1 subunit C) (Chromatin assembly factor I p48 subunit) (CAF-I 48 kDa subunit) (CAF-I p48) (Nucleosome-remodeling factor subunit RBAP48) (Retinoblastoma-binding protein 4) (RBBP-4) (Retinoblastoma-binding protein p48)	0	0	0	2	2	2
P67984	60S ribosomal protein L22 (Heparin-binding protein HBp15)	0	2	0	0	2	2
Q9DB05	Alpha-soluble NSF attachment protein (SNAP-alpha) (N-ethylmaleimide-sensitive factor attachment protein alpha)	0	0	0	2	2	2

UniProt ID	Protein names	NLS Presence (n/4)	4FL Replicate Presence (n/4)	NLS+4FL Replicate Presence (n/4)	NLS+2KQ Replicate Presence (n/4)	Total Replicate Presence (n/16)	Total Peptide Count
P11440	Cyclin-dependent kinase 1 (CDK1) (EC 2.7.11.22) (EC 2.7.11.23) (Cell division control protein 2 homolog) (Cell division protein kinase 1) (p34 protein kinase)	0	2	0	0	2	2
O08756	3-hydroxyacyl-CoA dehydrogenase type-2 (EC 1.1.1.35) (17-beta-hydroxysteroid dehydrogenase 10) (17-beta-HSD 10) (EC 1.1.1.51) (3-hydroxy-2-methylbutyryl-CoA dehydrogenase) (EC 1.1.1.178) (3-hydroxyacyl-CoA dehydrogenase type II) (Endoplasmic reticulum-associated amyloid beta-peptide-binding protein) (Mitochondrial ribonuclease P protein 2) (Mitochondrial RNase P protein 2) (Type II HADH)	0	2	0	0	2	2
P0C0S6	Histone H2A.Z (H2A/z)	0	2	0	0	2	2
P62908	40S ribosomal protein S3 (EC 4.2.99.18)	0	2	0	0	2	2
Q8CG76	Aflatoxin B1 aldehyde reductase member 2 (EC 1.1.1.n11) (Succinic semialdehyde reductase) (SSA reductase)	0	2	0	0	2	2
Q9DCW4	Electron transfer flavoprotein subunit beta (Beta-ETF)	0	2	0	0	2	2
Q6DFW4	Nucleolar protein 58 (MSSP) (Nucleolar protein 5) (SIK-similar protein)	0	2	0	0	2	2
P61222	ATP-binding cassette sub-family E member 1 (RNase L inhibitor) (Ribonuclease 4 inhibitor) (RNS4I)	0	2	0	0	2	2
Q2TBE6	Phosphatidylinositol 4-kinase type 2-alpha (EC 2.7.1.67) (Phosphatidylinositol 4-kinase type II-alpha)	0	2	0	0	2	2
Q8VDP4	Cell cycle and apoptosis regulator protein 2 (Cell division cycle and apoptosis regulator protein 2)	0	2	0	0	2	2
Q8QZT1	Acetyl-CoA acetyltransferase, mitochondrial (EC 2.3.1.9) (Acetoacetyl-CoA thiolase)	0	2	0	0	2	2
P43277	Histone H1.3 (H1 VAR.4) (H1d)	1	0	0	0	1	57
P68372	Tubulin beta-4B chain (Tubulin beta-2C chain)	1	0	0	0	1	54

UniProt ID	Protein names	NLS Presence (n/4)	4FL Replicate Presence (n/4)	NLS+4FL Replicate Presence (n/4)	NLS+2KQ Replicate Presence (n/4)	Total Replicate Presence (n/16)	Total Peptide Count
P63017	Heat shock cognate 71 kDa protein (Heat shock 70 kDa protein 8)	1	0	0	0	1	52
P07901	Heat shock protein HSP 90-alpha (Heat shock 86 kDa) (HSP 86) (HSP86) (Tumor-specific transplantation 86 kDa antigen) (TSTA)	1	0	0	0	1	42
Q9D0E1	Heterogeneous nuclear ribonucleoprotein M (hnRNP M)	1	0	0	0	1	40
P02535	Keratin, type I cytoskeletal 10 (56 kDa cytokeratin) (Cytokeratin-10) (CK-10) (Keratin, type I cytoskeletal 59 kDa) (Keratin-10) (K10)	1	0	0	0	1	32
P08113	Endoplasmic reticulum resident protein 99 (ERp99) (Heat shock protein 90 kDa beta member 1) (Polymorphic tumor rejection antigen 1) (Tumor rejection antigen gp96)	1	0	0	0	1	32
Q03265	ATP synthase subunit alpha, mitochondrial	1	0	0	0	1	25
P43275	Histone H1.1 (H1 VAR.3) (Histone H1a) (H1a)	1	0	0	0	1	24
P17742	Peptidyl-prolyl cis-trans isomerase A (PPIase A) (EC 5.2.1.8) (Cyclophilin A) (Cyclosporin A-binding protein) (Rotamase A) (SP18) [Cleaved into: Peptidyl-prolyl cis-trans isomerase A, N-terminally processed]	1	0	0	0	1	23
O88569	Heterogeneous nuclear ribonucleoproteins A2/B1 (hnRNP A2/B1)	1	0	0	0	1	22
O70133	ATP-dependent RNA helicase A (EC 3.6.4.13) (DEAH box protein 9) (mHEL-5) (Nuclear DNA helicase II) (NDH II) (RNA helicase A) (RHA)	1	0	0	0	1	21
Q9ERD7	Tubulin beta-3 chain	1	0	0	0	1	20
P63038	60 kDa heat shock protein, mitochondrial (EC 3.6.4.9) (60 kDa chaperonin) (Chaperonin 60) (CPN60) (HSP-65) (Heat shock protein 60) (HSP-60) (Hsp60) (Mitochondrial matrix protein P1)	1	0	0	0	1	20
Q91V92	ATP-citrate synthase (EC 2.3.3.8) (ATP-citrate (pro-S-)-lyase) (Citrate cleavage enzyme)	1	0	0	0	1	19
P61979	Heterogeneous nuclear ribonucleoprotein K (hnRNP K)	1	0	0	0	1	19
P58252	Elongation factor 2 (EF-2)	1	0	0	0	1	19

UniProt ID	Protein names	NLS Presence (n/4)	4FL Replicate Presence (n/4)	NLS+4FL Replicate Presence (n/4)	NLS+2KQ Replicate Presence (n/4)	Total Replicate Presence (n/16)	Total Peptide Count
P10853	Histone H2B type 1-F/J/L (H2B 291A)	1	0	0	0	1	18
Q8BMF4	Dihydrolipoyllysine-residue acetyltransferase component of pyruvate dehydrogenase complex, mitochondrial (EC 2.3.1.12) (Dihydrolipoamide acetyltransferase component of pyruvate dehydrogenase complex) (Pyruvate dehydrogenase complex component E2) (PDC-E2) (PDCE2)	1	0	0	0	1	18
P62827	GTP-binding nuclear protein Ran (GTPase Ran) (Ras-like protein TC4) (Ras-related nuclear protein)	1	0	0	0	1	17
P53026	60S ribosomal protein L10a (CSA-19) (Neural precursor cell expressed developmentally down-regulated protein 6) (NEDD-6)	1	0	0	0	1	17
Q6ZWX6	Eukaryotic translation initiation factor 2 subunit 1 (Eukaryotic translation initiation factor 2 subunit alpha) (eIF-2-alpha) (eIF-2A) (eIF-2alpha)	1	0	0	0	1	17
Q9D0I9	Arginine--tRNA ligase, cytoplasmic (EC 6.1.1.19) (Arginyl-tRNA synthetase) (ArgRS)	1	0	0	0	1	16
P80313	T-complex protein 1 subunit eta (TCP-1-eta) (CCT-eta)	1	0	0	0	1	16
Q8BFR5	Elongation factor Tu, mitochondrial	1	0	0	0	1	15
P63085	Mitogen-activated protein kinase 1 (MAP kinase 1) (MAPK 1) (EC 2.7.11.24) (ERT1) (Extracellular signal-regulated kinase 2) (ERK-2) (MAP kinase isoform p42) (p42-MAPK) (Mitogen-activated protein kinase 2) (MAP kinase 2) (MAPK 2)	1	0	0	0	1	15
P63101	14-3-3 protein zeta/delta (Protein kinase C inhibitor protein 1) (KCIP-1) (SEZ-2)	1	0	0	0	1	15
Q9D8N0	Elongation factor 1-gamma (EF-1-gamma) (eEF-1B gamma)	1	0	0	0	1	15
O35286	Pre-mRNA-splicing factor ATP-dependent RNA helicase DHX15 (EC 3.6.4.13) (DEAH box protein 15)	1	0	0	0	1	14
Q7TPV4	Myb-binding protein 1A (Myb-binding protein of 160 kDa)	1	0	0	0	1	14
O35737	Heterogeneous nuclear ribonucleoprotein H (hnRNP H) [Cleaved into: Heterogeneous nuclear ribonucleoprotein H, N-terminally processed]	1	0	0	0	1	14

UniProt ID	Protein names	NLS Presence (n/4)	4FL Replicate Presence (n/4)	NLS+4FL Replicate Presence (n/4)	NLS+2KQ Replicate Presence (n/4)	Total Replicate Presence (n/16)	Total Peptide Count
P68254	14-3-3 protein theta (14-3-3 protein tau)	1	0	0	0	1	13
Q9CXW4	60S ribosomal protein L11	1	0	0	0	1	13
Q501J6	Probable ATP-dependent RNA helicase DDX17 (EC 3.6.4.13) (DEAD box protein 17)	1	0	0	0	1	12
Q9WTM5	RuvB-like 2 (EC 3.6.4.12) (p47 protein)	1	0	0	0	1	12
P68040	Receptor of activated protein C kinase 1 (12-3) (Guanine nucleotide-binding protein subunit beta-2-like 1) (Receptor for activated C kinase) (Receptor of activated protein kinase C 1) (p205) [Cleaved into: Receptor of activated protein C kinase 1, N-terminally processed (Guanine nucleotide-binding protein subunit beta-2-like 1, N-terminally processed)]	1	0	0	0	1	11
Q68FD5	Clathrin heavy chain 1	1	0	0	0	1	10
P05202	Aspartate aminotransferase, mitochondrial (mAspAT) (EC 2.6.1.1) (EC 2.6.1.7) (Fatty acid-binding protein) (FABP-1) (Glutamate oxaloacetate transaminase 2) (Kynurenine aminotransferase 4) (Kynurenine aminotransferase IV) (Kynurenine--oxoglutarate transaminase 4) (Kynurenine--oxoglutarate transaminase IV) (Plasma membrane-associated fatty acid-binding protein) (FABPpm) (Transaminase A)	1	0	0	0	1	10
P35279	Ras-related protein Rab-6A (Rab-6)	1	0	0	0	1	10
Q9CR57	60S ribosomal protein L14	1	0	0	0	1	9
Q9D3D9	ATP synthase subunit delta, mitochondrial (F-ATPase delta subunit)	1	0	0	0	1	9
Q8K310	Matrin-3	1	0	0	0	1	9
Q9QZD9	Eukaryotic translation initiation factor 3 subunit I (eIF3i) (Eukaryotic translation initiation factor 3 subunit 2) (TGF-beta receptor-interacting protein 1) (TRIP-1) (eIF-3-beta) (eIF3 p36)	1	0	0	0	1	9
P10854	Histone H2B type 1-M (H2B 291B)	1	0	0	0	1	8

UniProt ID	Protein names	NLS Presence (n/4)	4FL Replicate Presence (n/4)	NLS+4FL Replicate Presence (n/4)	NLS+2KQ Replicate Presence (n/4)	Total Replicate Presence (n/16)	Total Peptide Count
<b>Q8VBT0</b>	Thioredoxin-related transmembrane protein 1 (Thioredoxin domain-containing protein 1)	1	0	0	0	1	8
<b>P05064</b>	Fructose-bisphosphate aldolase A (EC 4.1.2.13) (Aldolase 1) (Muscle-type aldolase)	1	0	0	0	1	8
<b>Q91WJ8</b>	Far upstream element-binding protein 1 (FBP) (FUSE-binding protein 1)	1	0	0	0	1	8
<b>P70372</b>	ELAV-like protein 1 (Elav-like generic protein) (Hu-antigen R) (HuR) (MeIG)	1	0	0	0	1	8
<b>P17751</b>	Triosephosphate isomerase (TIM) (EC 5.3.1.1) (Triose-phosphate isomerase)	1	0	0	0	1	8
<b>Q9CQM9</b>	Glutaredoxin-3 (PKC-interacting cousin of thioredoxin) (PICOT) (PKC-theta-interacting protein) (PKCq-interacting protein) (Thioredoxin-like protein 2)	1	0	0	0	1	7
<b>Q91VC3</b>	Eukaryotic initiation factor 4A-III (eIF-4A-III) (eIF4A-III) (EC 3.6.4.13) (ATP-dependent RNA helicase DDX48) (ATP-dependent RNA helicase eIF4A-3) (DEAD box protein 48) (Eukaryotic translation initiation factor 4A isoform 3) [Cleaved into: Eukaryotic initiation factor 4A-III, N-terminally processed]	1	0	0	0	1	7
<b>Q3U9G9</b>	Lamin-B receptor (Integral nuclear envelope inner membrane protein)	1	0	0	0	1	7
<b>Q8BK67</b>	Protein RCC2	1	0	0	0	1	6
<b>O35130</b>	Ribosomal RNA small subunit methyltransferase NEP1 (EC 2.1.1.-) (18S rRNA (pseudouridine(1248)-N1)-methyltransferase) (18S rRNA Psi1248 methyltransferase) (Nucleolar protein EMG1 homolog) (Protein C2f) (Ribosome biogenesis protein NEP1)	1	0	0	0	1	6
<b>P04104</b>	Keratin, type II cytoskeletal 1 (67 kDa cytokeratin) (Cytokeratin-1) (CK-1) (Keratin-1) (K1) (Type-II keratin Kb1)	1	0	0	0	1	6
<b>Q8K2B3</b>	Succinate dehydrogenase [ubiquinone] flavoprotein subunit, mitochondrial (EC 1.3.5.1) (Flavoprotein subunit of complex II) (Fp)	1	0	0	0	1	5

UniProt ID	Protein names	NLS Presence (n/4)	4FL Replicate Presence (n/4)	NLS+4FL Replicate Presence (n/4)	NLS+2KQ Replicate Presence (n/4)	Total Replicate Presence (n/16)	Total Peptide Count
P80314	T-complex protein 1 subunit beta (TCP-1-beta) (CCT-beta)	1	0	0	0	1	5
Q8CGP6	Histone H2A type 1-H	1	0	0	0	1	5
P35283	Ras-related protein Rab-12 (Rab-13)	1	0	0	0	1	5
P11276	Fibronectin (FN) [Cleaved into: Anastellin]	1	0	0	0	1	5
Q8BGQ7	Alanine--tRNA ligase, cytoplasmic (EC 6.1.1.7) (Alanyl-tRNA synthetase) (AlaRS)	1	0	0	0	1	4
P09103	Protein disulfide-isomerase (PDI) (EC 5.3.4.1) (Cellular thyroid hormone-binding protein) (Endoplasmic reticulum resident protein 59) (ER protein 59) (ERp59) (Prolyl 4-hydroxylase subunit beta) (p55)	0	0	0	1	1	4
P35546	Proto-oncogene tyrosine-protein kinase receptor Ret (EC 2.7.10.1) (Proto-oncogene c-Ret) [Cleaved into: Soluble RET kinase fragment; Extracellular cell-membrane anchored RET cadherin 120 kDa fragment]	1	0	0	0	1	4
Q9DBC7	cAMP-dependent protein kinase type I-alpha regulatory subunit [Cleaved into: cAMP-dependent protein kinase type I-alpha regulatory subunit, N-terminally processed]	1	0	0	0	1	4
Q9Z204	Heterogeneous nuclear ribonucleoproteins C1/C2 (hnRNP C1/C2)	1	0	0	0	1	4
Q922W5	Pyrroline-5-carboxylate reductase 1, mitochondrial (P5C reductase 1) (P5CR 1) (EC 1.5.1.2)	1	0	0	0	1	4
P60766	Cell division control protein 42 homolog (G25K GTP-binding protein)	1	0	0	0	1	4
Q8CFI2	Ubiquitin-conjugating enzyme E2 R1 (EC 2.3.2.23) ((E3-independent) E2 ubiquitin-conjugating enzyme R1) (EC 2.3.2.24) (E2 ubiquitin-conjugating enzyme R1) (Ubiquitin-conjugating enzyme E2-32 kDa complementing) (Ubiquitin-conjugating enzyme E2-CDC34) (Ubiquitin-protein ligase R1)	1	0	0	0	1	4
Q05920	Pyruvate carboxylase, mitochondrial (EC 6.4.1.1) (Pyruvic carboxylase) (PCB)	1	0	0	0	1	4
Q61781	Keratin, type I cytoskeletal 14 (Cytokeratin-14) (CK-14) (Keratin-14) (K14)	1	0	0	0	1	3

UniProt ID	Protein names	NLS Presence (n/4)	4FL Replicate Presence (n/4)	NLS+4FL Replicate Presence (n/4)	NLS+2KQ Replicate Presence (n/4)	Total Replicate Presence (n/16)	Total Peptide Count
Q9WVA4	Transgelin-2 (SM22-beta)	0	0	0	1	1	3
Q8VDN2	Sodium/potassium-transporting ATPase subunit alpha-1 (Na(+)/K(+)-ATPase alpha-1 subunit) (EC 3.6.3.9) (Sodium pump subunit alpha-1)	0	0	1	0	1	3
Q9QXS1	Plectin (PCN) (PLTN) (Plectin-1) (Plectin-6)	0	0	1	0	1	3
Q9JIK5	Nucleolar RNA helicase 2 (EC 3.6.4.13) (DEAD box protein 21) (Gu-alpha) (Nucleolar RNA helicase Gu) (Nucleolar RNA helicase II) (RH II/Gu)	0	1	0	0	1	3
Q91VM5	RNA binding motif protein, X-linked-like-1 (Heterogeneous nuclear ribonucleoprotein G-like 1) (RNA binding motif protein, X chromosome retrogene)	1	0	0	0	1	3
Q00612	Glucose-6-phosphate 1-dehydrogenase X (G6PD) (EC 1.1.1.49)	1	0	0	0	1	3
P40142	Transketolase (TK) (EC 2.2.1.1) (P68)	1	0	0	0	1	3
Q62448	Eukaryotic translation initiation factor 4 gamma 2 (eIF-4-gamma 2) (eIF-4G 2) (eIF4G 2) (Novel APOBEC-1 target 1) (Translation repressor NAT1) (p97)	1	0	0	0	1	3
Q99020	Heterogeneous nuclear ribonucleoprotein A/B (hnRNP A/B) (CARG-binding factor-A) (CBF-A)	1	0	0	0	1	3
Q8BI84	Transport and Golgi organization protein 1 homolog (TANGO1) (Melanoma inhibitory activity protein 3)	0	0	0	1	1	2
O88544	COP9 signalosome complex subunit 4 (SGN4) (Signalosome subunit 4) (JAB1-containing signalosome subunit 4)	0	0	0	1	1	2
P35700	Peroxiredoxin-1 (EC 1.11.1.15) (Macrophage 23 kDa stress protein) (Osteoblast-specific factor 3) (OSF-3) (Thioredoxin peroxidase 2) (Thioredoxin-dependent peroxide reductase 2)	0	0	0	1	1	2
Q62261	Spectrin beta chain, non-erythrocytic 1 (Beta-II spectrin) (Embryonic liver fodrin) (Fodrin beta chain)	0	0	0	1	1	2
P28659	CUGBP Elav-like family member 1 (CELF-1) (50 kDa nuclear polyadenylated RNA-binding protein) (Brain protein F41) (Bruno-like)	0	1	0	0	1	2

UniProt ID	Protein names	NLS Presence (n/4)	4FL Replicate Presence (n/4)	NLS+4FL Replicate Presence (n/4)	NLS+2KQ Replicate Presence (n/4)	Total Replicate Presence (n/16)	Total Peptide Count
	protein 2) (CUG triplet repeat RNA-binding protein 1) (CUG-BP1) (CUG-BP- and ETR-3-like factor 1) (Deadenylation factor CUG-BP) (Deadenylation factor EDEN-BP) (Embryo deadenylation element-binding protein homolog) (EDEN-BP homolog) (RNA-binding protein BRUNOL-2)						
<b>Q9Z1N5</b>	Spliceosome RNA helicase Ddx39b (EC 3.6.4.13) (56 kDa U2AF65-associated protein) (DEAD box protein UAP56) (HLA-B-associated transcript 1 protein)	0	1	0	0	1	2
<b>P05214</b>	Tubulin alpha-3 chain (Alpha-tubulin 3/7) (Alpha-tubulin isotype M-alpha-3/7) (Tubulin alpha-3/alpha-7 chain) [Cleaved into: Detyrosinated tubulin alpha-3 chain]	1	0	0	0	1	2
<b>Q61656</b>	Probable ATP-dependent RNA helicase DDX5 (EC 3.6.4.13) (DEAD box RNA helicase DEAD1) (mDEAD1) (DEAD box protein 5) (RNA helicase p68)	1	0	0	0	1	2
<b>P62270</b>	40S ribosomal protein S18 (Ke-3) (Ke3)	1	0	0	0	1	2
<b>Q922U2</b>	Keratin, type II cytoskeletal 5 (Cytokeratin-5) (CK-5) (Keratin-5) (K5) (Type-II keratin Kb5)	1	0	0	0	1	2
<b>Q62351</b>	Transferrin receptor protein 1 (TR) (TfR) (TfR1) (Trfr) (CD antigen CD71)	0	0	0	1	1	2
<b>Q8CGP0</b>	Histone H2B type 3-B	0	0	1	0	1	2
<b>P16546</b>	Spectrin alpha chain, non-erythrocytic 1 (Alpha-II spectrin) (Fodrin alpha chain)	0	0	1	0	1	2
<b>Q91VR5</b>	ATP-dependent RNA helicase DDX1 (EC 3.6.4.13) (DEAD box protein 1)	0	0	1	0	1	2
<b>Q99M08</b>	Uncharacterized protein C4orf3 homolog	0	0	1	0	1	2
<b>Q8R1Q8</b>	Cytoplasmic dynein 1 light intermediate chain 1 (Dynein light chain A) (DLC-A) (Dynein light intermediate chain 1, cytosolic)	0	0	1	0	1	2
<b>Q8BU30</b>	Isoleucine--tRNA ligase, cytoplasmic (EC 6.1.1.5) (Isoleucyl-tRNA synthetase) (IRS) (IleRS)	0	0	1	0	1	2
<b>Q80XU3</b>	Nuclear ubiquitous casein and cyclin-dependent kinase substrate 1 (JC7)	0	0	1	0	1	2

UniProt ID	Protein names	NLS Presence (n/4)	4FL Replicate Presence (n/4)	NLS+4FL Replicate Presence (n/4)	NLS+2KQ Replicate Presence (n/4)	Total Replicate Presence (n/16)	Total Peptide Count
<b>Q01853</b>	Transitional endoplasmic reticulum ATPase (TER ATPase) (EC 3.6.4.6) (15S Mg(2+)-ATPase p97 subunit) (Valosin-containing protein) (VCP)	0	0	1	0	1	2
<b>Q922J3</b>	CAP-Gly domain-containing linker protein 1 (Cytoplasmic linker protein 170) (CLIP-170) (Restin)	0	1	0	0	1	2
<b>Q61466</b>	SWI/SNF-related matrix-associated actin-dependent regulator of chromatin subfamily D member 1 (60 kDa BRG-1/Brm-associated factor subunit A) (BRG1-associated factor 60A) (BAF60A) (Protein D15KZ1) (SWI/SNF complex 60 kDa subunit)	0	1	0	0	1	2
<b>P49452</b>	Centromere protein C (CENP-C) (Centromere autoantigen C) (Centromere protein C 1) (CENP-C 1)	0	1	0	0	1	2
<b>Q99K48</b>	Non-POU domain-containing octamer-binding protein (NonO protein)	0	1	0	0	1	2
<b>Q922D8</b>	C-1-tetrahydrofolate synthase, cytoplasmic (C1-THF synthase) [Cleaved into: C-1-tetrahydrofolate synthase, cytoplasmic, N-terminally processed] [Includes: Methylenetetrahydrofolate dehydrogenase (EC 1.5.1.5); Methenyltetrahydrofolate cyclohydrolase (EC 3.5.4.9); Formyltetrahydrofolate synthetase (EC 6.3.4.3)]	0	1	0	0	1	2
<b>A2AQ19</b>	RNA polymerase-associated protein RTF1 homolog	0	1	0	0	1	2
<b>P61089</b>	Ubiquitin-conjugating enzyme E2 N (EC 2.3.2.23) (Bendless-like ubiquitin-conjugating enzyme) (E2 ubiquitin-conjugating enzyme N) (Ubc13) (Ubiquitin carrier protein N) (Ubiquitin-protein ligase N)	1	0	0	0	1	2
<b>P62849</b>	40S ribosomal protein S24	1	0	0	0	1	2
<b>P06240</b>	Proto-oncogene tyrosine-protein kinase LCK (EC 2.7.10.2) (Leukocyte C-terminal Src kinase) (LSK) (Lymphocyte cell-specific protein-tyrosine kinase) (p56-LCK)	1	0	0	0	1	2
<b>P86048</b>	60S ribosomal protein L10-like	1	0	0	0	1	2
<b>P34884</b>	Macrophage migration inhibitory factor (MIF) (EC 5.3.2.1) (Delayed early response protein 6) (DER6) (Glycosylation-inhibiting factor) (GIF) (L-	0	0	0	1	1	1

UniProt ID	Protein names	NLS Presence (n/4)	4FL Replicate Presence (n/4)	NLS+4FL Replicate Presence (n/4)	NLS+2KQ Replicate Presence (n/4)	Total Replicate Presence (n/16)	Total Peptide Count
	dopachrome isomerase) (L-dopachrome tautomerase) (EC 5.3.3.12) (Phenylpyruvate tautomerase)						
<b>O35685</b>	Nuclear migration protein nudC (Nuclear distribution protein C homolog) (Silica-induced gene 92 protein) (SIG-92)	0	0	0	1	1	1
<b>Q9JMH6</b>	Thioredoxin reductase 1, cytoplasmic (TR) (EC 1.8.1.9) (Thioredoxin reductase TR1)	0	0	0	1	1	1
<b>Q9CXW2</b>	28S ribosomal protein S22, mitochondrial (MRP-S22) (S22mt)	0	0	0	1	1	1
<b>Q9CQR2</b>	40S ribosomal protein S21	0	0	0	1	1	1
<b>Q64337</b>	Sequestosome-1 (STONE14) (Ubiquitin-binding protein p62)	0	1	0	0	1	1
<b>P54822</b>	Adenylosuccinate lyase (ASL) (EC 4.3.2.2) (Adenylosuccinase) (ASase)	0	0	0	1	1	1
<b>Q9Z1G3</b>	V-type proton ATPase subunit C 1 (V-ATPase subunit C 1) (Vacuolar proton pump subunit C 1)	0	0	0	1	1	1
<b>P59708</b>	Splicing factor 3B subunit 6 (Pre-mRNA branch site protein p14) (SF3b 14 kDa subunit)	0	0	0	1	1	1
<b>P57724</b>	Poly(rC)-binding protein 4 (Alpha-CP4)	0	0	1	0	1	1
<b>P16045</b>	Galectin-1 (Gal-1) (14 kDa lectin) (Beta-galactoside-binding lectin L-14-I) (Galaptin) (Lactose-binding lectin 1) (Lectin galactoside-binding soluble 1) (S-Lac lectin 1)	0	1	0	0	1	1
<b>P30416</b>	Peptidyl-prolyl cis-trans isomerase FKBP4 (PPIase FKBP4) (EC 5.2.1.8) (52 kDa FK506-binding protein) (52 kDa FKBP) (FKBP-52) (59 kDa immunophilin) (p59) (FK506-binding protein 4) (FKBP-4) (FKBP59) (HSP-binding immunophilin) (HBI) (Immunophilin FKBP52) (Rotamase) [Cleaved into: Peptidyl-prolyl cis-trans isomerase FKBP4, N-terminally processed]	0	0	0	1	1	1
<b>O70251</b>	Elongation factor 1-beta (EF-1-beta)	0	0	0	1	1	1
<b>P14211</b>	Calreticulin (CRP55) (Calregulin) (Endoplasmic reticulum resident protein 60) (ERp60) (HACBP)	0	0	0	1	1	1

UniProt ID	Protein names	NLS Presence (n/4)	4FL Replicate Presence (n/4)	NLS+4FL Replicate Presence (n/4)	NLS+2KQ Replicate Presence (n/4)	Total Replicate Presence (n/16)	Total Peptide Count
P51859	Hepatoma-derived growth factor (HDGF)	0	0	0	1	1	1
Q3TXS7	26S proteasome non-ATPase regulatory subunit 1 (26S proteasome regulatory subunit RPN2) (26S proteasome regulatory subunit S1)	0	0	0	1	1	1
Q9WVA3	Mitotic checkpoint protein BUB3 (WD repeat type I transmembrane protein A72.5)	0	0	0	1	1	1
P62627	Dynein light chain roadblock-type 1 (Dynein light chain 2A, cytoplasmic)	0	0	0	1	1	1
Q80SY4	E3 ubiquitin-protein ligase MIB1 (EC 2.3.2.27) (DAPK-interacting protein 1) (DIP-1) (Mind bomb homolog 1) (RING-type E3 ubiquitin transferase MIB1)	0	0	0	1	1	1
Q91ZR2	Sorting nexin-18 (Sorting nexin-associated Golgi protein 1)	0	0	1	0	1	1
Q9DA39	Protein lifeguard 4 (Transmembrane BAX inhibitor motif-containing protein 4) (Z-protein)	0	0	1	0	1	1
Q9CPY7	Cytosol aminopeptidase (EC 3.4.11.1) (Leucine aminopeptidase 3) (LAP-3) (Leucyl aminopeptidase) (Proline aminopeptidase) (EC 3.4.11.5) (Prolyl aminopeptidase)	0	0	1	0	1	1
Q8K019	Bcl-2-associated transcription factor 1 (Btf)	0	0	1	0	1	1
Q9DD03	Ras-related protein Rab-13	0	0	1	0	1	1
E9Q5C9	Nucleolar and coiled-body phosphoprotein 1 (140 kDa nucleolar phosphoprotein) (Nopp140)	0	0	1	0	1	1
Q8CHW4	Translation initiation factor eIF-2B subunit epsilon (eIF-2B GDP-GTP exchange factor subunit epsilon)	0	0	1	0	1	1
Q8C3I8	Protein HGH1 homolog	0	0	1	0	1	1
Q9QYI3	DnaJ homolog subfamily C member 7 (Cytoplasmic CAR retention protein) (CCRP) (MDj11) (Tetratricopeptide repeat protein 2) (TPR repeat protein 2)	0	1	0	0	1	1

UniProt ID	Protein names	NLS Presence (n/4)	4FL Replicate Presence (n/4)	NLS+4FL Replicate Presence (n/4)	NLS+2KQ Replicate Presence (n/4)	Total Replicate Presence (n/16)	Total Peptide Count
<b>Q61701</b>	ELAV-like protein 4 (Hu-antigen D) (HuD) (Paraneoplastic encephalomyelitis antigen HuD)	0	1	0	0	1	1
<b>Q99LE6</b>	ATP-binding cassette sub-family F member 2	0	1	0	0	1	1
<b>Q91Z31</b>	Polypyrimidine tract-binding protein 2 (Brain-enriched polypyrimidine tract-binding protein) (Brain-enriched PTB) (Neural polypyrimidine tract-binding protein) (RRM-type RNA-binding protein brPTB)	0	1	0	0	1	1
<b>Q9JKR6</b>	Hypoxia up-regulated protein 1 (GRP-170) (140 kDa Ca(2+)-binding protein) (CBP-140)	0	1	0	0	1	1
<b>Q7SIG6</b>	Arf-GAP with SH3 domain, ANK repeat and PH domain-containing protein 2 (Development and differentiation-enhancing factor 2) (Paxillin-associated protein with ARF GAP activity 3) (PAG3) (Pyk2 C-terminus-associated protein) (PAP)	0	1	0	0	1	1
<b>Q3UPL0</b>	Protein transport protein Sec31A (SEC31-like protein 1) (SEC31-related protein A)	0	1	0	0	1	1
<b>Q9D7V1</b>	SH2 domain-containing protein 4A	0	1	0	0	1	1
<b>Q9CRB9</b>	MICOS complex subunit Mic19 (Coiled-coil-helix-coiled-coil-helix domain-containing protein 3)	0	0	0	1	1	1
<b>O70475</b>	UDP-glucose 6-dehydrogenase (UDP-Glc dehydrogenase) (UDP-GlcDH) (UDPGDH) (EC 1.1.1.22)	0	0	0	1	1	1
<b>Q9D1Q4</b>	Dolichol-phosphate mannosyltransferase subunit 3 (Dolichol-phosphate mannose synthase subunit 3) (DPM synthase subunit 3) (Dolichyl-phosphate beta-D-mannosyltransferase subunit 3) (Mannose-P-dolichol synthase subunit 3) (MPD synthase subunit 3)	0	0	0	1	1	1
<b>P08556</b>	GTPase NRas (Transforming protein N-Ras)	0	0	0	1	1	1
<b>P61166</b>	Transmembrane protein 258	0	0	0	1	1	1
<b>Q91VR2</b>	ATP synthase subunit gamma, mitochondrial (F-ATPase gamma subunit)	0	0	0	1	1	1

UniProt ID	Protein names	NLS Presence (n/4)	4FL Replicate Presence (n/4)	NLS+4FL Replicate Presence (n/4)	NLS+2KQ Replicate Presence (n/4)	Total Replicate Presence (n/16)	Total Peptide Count
Q61686	Chromobox protein homolog 5 (Heterochromatin protein 1 homolog alpha) (HP1 alpha)	0	0	0	1	1	1
Q3U2C5	E3 ubiquitin-protein ligase RNF149 (EC 2.3.2.27) (Goliath-related E3 ubiquitin-protein ligase 4) (RING finger protein 149) (RING-type E3 ubiquitin transferase RNF149)	0	0	0	1	1	1
Q9D0F6	Replication factor C subunit 5 (Activator 1 36 kDa subunit) (A1 36 kDa subunit) (Activator 1 subunit 5) (Replication factor C 36 kDa subunit) (RFC-C 36 kDa subunit) (RFC36)	0	0	0	1	1	1
Q6PA06	Atlastin-2 (EC 3.6.5.-) (ADP-ribosylation factor-like protein 6-interacting protein 2) (ARL-6-interacting protein 2) (Aip-2)	0	0	0	1	1	1
O35492	Dual specificity protein kinase CLK3 (EC 2.7.12.1) (CDC-like kinase 3)	0	0	0	1	1	1
P40749	Synaptotagmin-4 (Synaptotagmin IV) (SyIV)	0	0	0	1	1	1
Q69ZR2	E3 ubiquitin-protein ligase HECTD1 (EC 2.3.2.26) (HECT domain-containing protein 1) (HECT-type E3 ubiquitin transferase HECTD1) (Protein open mind)	0	0	0	1	1	1
Q62093	Serine/arginine-rich splicing factor 2 (Protein PR264) (Putative myelin regulatory factor 1) (MRF-1) (Splicing component, 35 kDa) (Splicing factor SC35) (SC-35) (Splicing factor, arginine/serine-rich 2)	0	0	1	0	1	1
P83870	PHD finger-like domain-containing protein 5A (PHD finger-like domain protein 5A) (Splicing factor 3B-associated 14 kDa protein) (SF3b14b)	0	0	1	0	1	1
Q80UU9	Membrane-associated progesterone receptor component 2	0	0	1	0	1	1
Q8BL66	Early endosome antigen 1	0	0	1	0	1	1
O55013	Trafficking protein particle complex subunit 3 (BET3 homolog)	0	0	1	0	1	1
P27641	X-ray repair cross-complementing protein 5 (EC 3.6.4.-) (ATP-dependent DNA helicase 2 subunit 2) (ATP-dependent DNA helicase II 80 kDa subunit) (CTC box-binding factor 85 kDa subunit) (CTC85) (CTCBF) (DNA	0	0	1	0	1	1

UniProt ID	Protein names	NLS Presence (n/4)	4FL Replicate Presence (n/4)	NLS+4FL Replicate Presence (n/4)	NLS+2KQ Replicate Presence (n/4)	Total Replicate Presence (n/16)	Total Peptide Count
	repair protein XRCC5) (Ku autoantigen protein p86 homolog) (Ku80) (Nuclear factor IV)						
<b>Q922P9</b>	Putative oxidoreductase GLYR1 (EC 1.-.-.) (Glyoxylate reductase 1 homolog) (Nuclear protein NP60)	0	0	1	0	1	1
<b>Q08943</b>	FACT complex subunit SSRP1 (Facilitates chromatin transcription complex subunit SSRP1) (Recombination signal sequence recognition protein 1) (Structure-specific recognition protein 1) (T160)	0	0	1	0	1	1
<b>Q8VDL4</b>	ADP-dependent glucokinase (ADP-GK) (ADPGK) (EC 2.7.1.147)	0	0	1	0	1	1
<b>O08917</b>	Flotillin-1	0	0	1	0	1	1
<b>Q8CGY8</b>	UDP-N-acetylglucosamine--peptide N-acetylglucosaminyltransferase 110 kDa subunit (EC 2.4.1.255) (O-GlcNAc transferase subunit p110) (O-linked N-acetylglucosamine transferase 110 kDa subunit) (OGT)	0	0	1	0	1	1
<b>Q6ZQ82</b>	Rho GTPase-activating protein 26 (Rho-type GTPase-activating protein 26)	0	0	1	0	1	1
<b>Q9D8Y1</b>	Transmembrane protein 126A	0	0	1	0	1	1
<b>O70378</b>	ER membrane protein complex subunit 8 (Neighbor of COX4)	0	0	1	0	1	1
<b>Q61739</b>	Integrin alpha-6 (CD49 antigen-like family member F) (VLA-6) (CD antigen CD49f) [Cleaved into: Integrin alpha-6 heavy chain; Integrin alpha-6 light chain]	0	0	1	0	1	1
<b>Q8VE95</b>	UPF0598 protein C8orf82 homolog	0	0	1	0	1	1
<b>Q8R146</b>	Acylamino-acid-releasing enzyme (AARE) (EC 3.4.19.1) (Acyl-peptide hydrolase) (APH) (Acylaminoacyl-peptidase)	0	0	1	0	1	1
<b>Q80ZM8</b>	Cardiolipin synthase (CMP-forming) (CLS) (EC 2.7.8.41)	0	0	1	0	1	1
<b>Q6ZPU9</b>	KIF1-binding protein	0	0	1	0	1	1
<b>Q9CQ92</b>	Mitochondrial fission 1 protein (FIS1 homolog) (Tetratricopeptide repeat protein 11) (TPR repeat protein 11)	0	0	1	0	1	1

UniProt ID	Protein names	NLS Presence (n/4)	4FL Replicate Presence (n/4)	NLS+4FL Replicate Presence (n/4)	NLS+2KQ Replicate Presence (n/4)	Total Replicate Presence (n/16)	Total Peptide Count
Q9WTQ5	A-kinase anchor protein 12 (AKAP-12) (Germ cell lineage protein gercelin) (Src-suppressed C kinase substrate) (SSeCKS)	0	0	1	0	1	1
Q9Z2U0	Proteasome subunit alpha type-7 (EC 3.4.25.1) (Proteasome subunit RC6-1)	0	0	1	0	1	1
Q8VEE4	Replication protein A 70 kDa DNA-binding subunit (RP-A p70) (Replication factor A protein 1) (RF-A protein 1)	0	0	1	0	1	1
Q08122	Transducin-like enhancer protein 3 (ESG) (Grg-3)	0	0	1	0	1	1
Q6DVA0	LEM domain-containing protein 2 (Nuclear envelope transmembrane protein 25) (NET25)	0	0	1	0	1	1
Q61553	Fascin (Singed-like protein)	0	0	1	0	1	1
Q8R3Q0	Store-operated calcium entry-associated regulatory factor (SARAF) (SOCE-associated regulatory factor) (Transmembrane protein 66)	0	0	1	0	1	1
P47753	F-actin-capping protein subunit alpha-1 (CapZ alpha-1)	0	0	1	0	1	1
Q8K4G5	Actin-binding LIM protein 1 (abLIM-1) (Actin-binding LIM protein family member 1)	0	0	1	0	1	1
Q8BKC5	Importin-5 (Imp5) (Importin subunit beta-3) (Karyopherin beta-3) (Ran-binding protein 5) (RanBP5)	0	0	1	0	1	1
P17427	AP-2 complex subunit alpha-2 (100 kDa coated vesicle protein C) (Adaptor protein complex AP-2 subunit alpha-2) (Adaptor-related protein complex 2 subunit alpha-2) (Alpha-adaptin C) (Alpha2-adaptin) (Clathrin assembly protein complex 2 alpha-C large chain) (Plasma membrane adaptor HA2/AP2 adaptin alpha C subunit)	0	0	1	0	1	1
O08784	Treacle protein (Treacher Collins syndrome protein homolog)	0	0	1	0	1	1
Q71LX4	Talin-2	0	0	1	0	1	1
O35955	Proteasome subunit beta type-10 (EC 3.4.25.1) (Low molecular mass protein 10) (Macropain subunit MECL-1) (Multicatalytic endopeptidase	0	0	1	0	1	1

UniProt ID	Protein names	NLS Presence (n/4)	4FL Replicate Presence (n/4)	NLS+4FL Replicate Presence (n/4)	NLS+2KQ Replicate Presence (n/4)	Total Replicate Presence (n/16)	Total Peptide Count
	complex subunit MECL-1) (Proteasome MECL-1) (Proteasome subunit beta-2i)						
<b>Q3TLH4</b>	Protein PRRC2C (BAT2 domain-containing protein 1) (HLA-B-associated transcript 2-like 2) (Proline-rich and coiled-coil-containing protein 2C)	0	0	1	0	1	1
<b>P56399</b>	Ubiquitin carboxyl-terminal hydrolase 5 (EC 3.4.19.12) (Deubiquitinating enzyme 5) (Isopeptidase T) (Ubiquitin thioesterase 5) (Ubiquitin-specific-processing protease 5)	0	0	1	0	1	1
<b>Q9D0L8</b>	mRNA cap guanine-N7 methyltransferase (EC 2.1.1.56) (RG7MT1) (mRNA (guanine-N(7)-)-methyltransferase) (mRNA cap methyltransferase)	0	0	1	0	1	1
<b>P11247</b>	Myeloperoxidase (MPO) (EC 1.11.2.2) [Cleaved into: Myeloperoxidase light chain; Myeloperoxidase heavy chain]	0	0	1	0	1	1
<b>Q3V300</b>	Kinesin-like protein KIF22	0	0	1	0	1	1
<b>P04925</b>	Major prion protein (PrP) (PrP27-30) (PrP33-35C) (CD antigen CD230)	0	0	1	0	1	1
<b>O35654</b>	DNA polymerase delta subunit 2 (DNA polymerase delta subunit p50)	0	0	1	0	1	1
<b>Q99J36</b>	THUMP domain-containing protein 1	0	0	1	0	1	1
<b>Q9D172</b>	ES1 protein homolog, mitochondrial	0	0	1	0	1	1
<b>Q99J62</b>	Replication factor C subunit 4 (Activator 1 subunit 4)	0	0	1	0	1	1
<b>Q78DX7</b>	Proto-oncogene tyrosine-protein kinase ROS (EC 2.7.10.1) (Proto-oncogene c-Ros) (Proto-oncogene c-Ros-1) (Receptor tyrosine kinase c-ros oncogene 1) (c-Ros receptor tyrosine kinase)	0	0	1	0	1	1
<b>Q5XJY5</b>	Coatomer subunit delta (Archain) (Delta-coat protein) (Delta-COP)	0	0	1	0	1	1
<b>Q3THS6</b>	S-adenosylmethionine synthase isoform type-2 (AdoMet synthase 2) (EC 2.5.1.6) (Methionine adenosyltransferase 2) (MAT 2)	0	1	0	0	1	1
<b>O88696</b>	ATP-dependent Clp protease proteolytic subunit, mitochondrial (EC 3.4.21.92) (Endopeptidase Clp)	0	1	0	0	1	1

UniProt ID	Protein names	NLS Presence (n/4)	4FL Replicate Presence (n/4)	NLS+4FL Replicate Presence (n/4)	NLS+2KQ Replicate Presence (n/4)	Total Replicate Presence (n/16)	Total Peptide Count
<b>Q8BFZ9</b>	Erlin-2 (Endoplasmic reticulum lipid raft-associated protein 2) (Stomatin-prohibitin-flotillin-HflC/K domain-containing protein 2) (SPFH domain-containing protein 2)	0	1	0	0	1	1
<b>Q9CR21</b>	Acyl carrier protein, mitochondrial (ACP) (CI-SDAP) (NADH-ubiquinone oxidoreductase 9.6 kDa subunit)	0	1	0	0	1	1
<b>Q9CWI3</b>	BRCA2 and CDKN1A-interacting protein	0	1	0	0	1	1
<b>Q99LC5</b>	Electron transfer flavoprotein subunit alpha, mitochondrial (Alpha-ETF)	0	1	0	0	1	1
<b>Q9D0B0</b>	Serine/arginine-rich splicing factor 9 (Splicing factor, arginine/serine-rich 9)	0	1	0	0	1	1
<b>Q3U308</b>	Cytoplasmic tRNA 2-thiolation protein 2	0	1	0	0	1	1
<b>Q99JY0</b>	Trifunctional enzyme subunit beta, mitochondrial (TP-beta) [Includes: 3-ketoacyl-CoA thiolase (EC 2.3.1.16) (Acetyl-CoA acyltransferase) (Beta-ketothiolase)]	0	1	0	0	1	1
<b>Q8CJ67</b>	Double-stranded RNA-binding protein Staufen homolog 2	0	1	0	0	1	1
<b>P50171</b>	Estradiol 17-beta-dehydrogenase 8 (EC 1.1.1.62) (17-beta-hydroxysteroid dehydrogenase 8) (17-beta-HSD 8) (3-ketoacyl-[acyl-carrier-protein] reductase alpha subunit) (KAR alpha subunit) (3-oxoacyl-[acyl-carrier-protein] reductase) (EC 1.1.1.-) (Protein Ke6) (Ke-6) (Testosterone 17-beta-dehydrogenase 8) (EC 1.1.1.239)	0	1	0	0	1	1
<b>O88712</b>	C-terminal-binding protein 1 (CtBP1) (EC 1.1.1.-)	0	1	0	0	1	1
<b>Q4JIM5</b>	Abelson tyrosine-protein kinase 2 (EC 2.7.10.2) (Abelson murine leukemia viral oncogene homolog 2) (Abelson-related gene protein) (Tyrosine-protein kinase ARG)	0	1	0	0	1	1
<b>P26638</b>	Serine--tRNA ligase, cytoplasmic (EC 6.1.1.11) (Seryl-tRNA synthetase) (SerRS) (Seryl-tRNA(Ser/Sec) synthetase)	0	1	0	0	1	1
<b>P0C605</b>	cGMP-dependent protein kinase 1 (cGK 1) (cGK1) (EC 2.7.11.12) (cGMP-dependent protein kinase I) (cGKI)	0	1	0	0	1	1

UniProt ID	Protein names	NLS Presence (n/4)	4FL Replicate Presence (n/4)	NLS+4FL Replicate Presence (n/4)	NLS+2KQ Replicate Presence (n/4)	Total Replicate Presence (n/16)	Total Peptide Count
<b>Q9JMA1</b>	Ubiquitin carboxyl-terminal hydrolase 14 (EC 3.4.19.12) (Deubiquitinating enzyme 14) (Ubiquitin thioesterase 14) (Ubiquitin-specific-processing protease 14)	0	1	0	0	1	1
<b>Q9QY81</b>	Nuclear pore membrane glycoprotein 210 (Nuclear pore protein gp210) (Nuclear envelope pore membrane protein POM 210) (POM210) (Nucleoporin Nup210) (Pore membrane protein of 210 kDa)	0	1	0	0	1	1
<b>Q6P5D8</b>	Structural maintenance of chromosomes flexible hinge domain-containing protein 1	0	1	0	0	1	1
<b>Q09M02</b>	Cytosolic carboxypeptidase-like protein 5 (EC 3.4.17.-) (ATP/GTP-binding protein-like 5)	0	1	0	0	1	1
<b>Q3V3R1</b>	Monofunctional C1-tetrahydrofolate synthase, mitochondrial (EC 6.3.4.3) (Formyltetrahydrofolate synthetase)	0	1	0	0	1	1
<b>Q9CX30</b>	Protein YIF1B (YIP1-interacting factor homolog B)	0	1	0	0	1	1
<b>P81122</b>	Insulin receptor substrate 2 (IRS-2) (4PS)	0	1	0	0	1	1
<b>Q99PU8</b>	Putative ATP-dependent RNA helicase DHX30 (EC 3.6.4.13) (DEAH box protein 30)	0	1	0	0	1	1
<b>Q6ZQ38</b>	Cullin-associated NEDD8-dissociated protein 1 (Cullin-associated and neddylation-dissociated protein 1) (p120 CAND1)	0	1	0	0	1	1
<b>P35980</b>	60S ribosomal protein L18	0	1	0	0	1	1
<b>Q9D1N9</b>	39S ribosomal protein L21, mitochondrial (L21mt) (MRP-L21)	0	1	0	0	1	1
<b>P35550</b>	rRNA 2'-O-methyltransferase fibrillarin (EC 2.1.1.-) (Histone-glutamine methyltransferase) (Nucleolar protein 1)	0	1	0	0	1	1
<b>P07724</b>	Serum albumin	0	1	0	0	1	1
<b>O08573</b>	Galectin-9 (Gal-9)	0	1	0	0	1	1
<b>P62918</b>	60S ribosomal protein L8	0	1	0	0	1	1
<b>P61358</b>	60S ribosomal protein L27	0	1	0	0	1	1

UniProt ID	Protein names	NLS Presence (n/4)	4FL Replicate Presence (n/4)	NLS+4FL Replicate Presence (n/4)	NLS+2KQ Replicate Presence (n/4)	Total Replicate Presence (n/16)	Total Peptide Count
P62717	60S ribosomal protein L18a	0	1	0	0	1	1
Q9JII5	DAZ-associated protein 1 (Deleted in azoospermia-associated protein 1)	0	1	0	0	1	1
P02088	Hemoglobin subunit beta-1 (Beta-1-globin) (Hemoglobin beta-1 chain) (Hemoglobin beta-major chain)	0	1	0	0	1	1
Q9QX47	Protein SON (Negative regulatory element-binding protein) (NRE-binding protein)	0	1	0	0	1	1
P97432	Next to BRCA1 gene 1 protein (Membrane component chromosome 17 surface marker 2 homolog) (Neighbor of BRCA1 gene 1 protein)	0	1	0	0	1	1
Q9JKL4	NADH dehydrogenase [ubiquinone] 1 alpha subcomplex assembly factor 3 (Protein 2P1)	0	1	0	0	1	1
O54988	STE20-like serine/threonine-protein kinase (STE20-like kinase) (mSLK) (EC 2.7.11.1) (Etk4) (STE20-related kinase SMAK) (STE20-related serine/threonine-protein kinase) (STE20-related kinase) (Serine/threonine-protein kinase 2)	0	1	0	0	1	1
Q91VI7	Ribonuclease inhibitor (Ribonuclease/angiogenin inhibitor 1)	0	1	0	0	1	1
P12970	60S ribosomal protein L7a (Surfeit locus protein 3)	0	1	0	0	1	1
P62242	40S ribosomal protein S8	0	1	0	0	1	1
P08030	Adenine phosphoribosyltransferase (APRT) (EC 2.4.2.7)	0	1	0	0	1	1
P62281	40S ribosomal protein S11	0	1	0	0	1	1
Q8VE22	28S ribosomal protein S23, mitochondrial (MRP-S23) (S23mt)	0	1	0	0	1	1
D3YYU8	Obscurin-like protein 1	0	1	0	0	1	1
Q9QXV0	ProSAAS (IA-4) (Proprotein convertase subtilisin/kexin type 1 inhibitor) (Proprotein convertase 1 inhibitor) (pro-SAAS) [Cleaved into: KEP; Big SAAS (b-SAAS); Little SAAS (l-SAAS); Big PEN-LEN (b-PEN-LEN) (SAAS CT(1-49)); PEN; PEN-20; PEN-19; Little LEN (l-LEN); Big LEN (b-LEN) (SAAS CT(25-40))]	0	1	0	0	1	1

UniProt ID	Protein names	NLS Presence (n/4)	4FL Replicate Presence (n/4)	NLS+4FL Replicate Presence (n/4)	NLS+2KQ Replicate Presence (n/4)	Total Replicate Presence (n/16)	Total Peptide Count
P50518	V-type proton ATPase subunit E 1 (V-ATPase subunit E 1) (V-ATPase 31 kDa subunit) (p31) (Vacuolar proton pump subunit E 1)	1	0	0	0	1	1
Q8QZY9	Splicing factor 3B subunit 4	1	0	0	0	1	1
O08553	Dihydropyrimidinase-related protein 2 (DRP-2) (Unc-33-like phosphoprotein 2) (ULIP-2)	1	0	0	0	1	1
P83882	60S ribosomal protein L36a (60S ribosomal protein L44)	1	0	0	0	1	1
Q8BH04	Phosphoenolpyruvate carboxykinase [GTP], mitochondrial (PEPCK-M) (EC 4.1.1.32)	1	0	0	0	1	1
Q9WUK4	Replication factor C subunit 2 (Activator 1 40 kDa subunit) (A1 40 kDa subunit) (Activator 1 subunit 2) (Replication factor C 40 kDa subunit) (RFC-C 40 kDa subunit) (RFC40)	1	0	0	0	1	1
Q9D5U9	MICAL C-terminal-like protein (Mical-cL) (ERK2-binding testicular protein 1) (Ebitein-1)	1	0	0	0	1	1
E9PVA8	eIF-2-alpha kinase activator GCN1 (GCN1 eIF-2-alpha kinase activator homolog) (GCN1-like protein 1) (General control of amino-acid synthesis 1-like protein 1) (Translational activator GCN1)	1	0	0	0	1	1
Q6A058	Armadillo repeat-containing X-linked protein 2	1	0	0	0	1	1

Appendix B – All proteins identified as either exclusive or shared between the 150 µg Urea-soluble fractions of ΔNLS+4FL and ΔNLS+2KQ human TDP-43 Transfections in NSC-34 Cells

UniProt ID	Protein names	ΔNLS+4FL Replicate Presence (n/5)	ΔNLS+2KQ Replicate Presence (n/5)	Total Replicate Presence (n/10)	Total Peptide Count
Q8BKC5	Importin-5 (Imp5) (Importin subunit beta-3) (Karyopherin beta-3) (Ran-binding protein 5) (RanBP5)	2	2	4	12
Q6P5H2	Nestin	2	2	4	11
P63028	Translationally-controlled tumor protein (TCTP) (21 kDa polypeptide) (p21) (p23)	2	2	4	5
P11798	Calcium/calmodulin-dependent protein kinase type II subunit alpha (CaM kinase II subunit alpha) (CaMK-II subunit alpha) (EC 2.7.11.17)	2	2	4	5
Q99LN9	Deoxyhypusine hydroxylase (DOHH) (EC 1.14.99.29) (Deoxyhypusine dioxygenase) (Deoxyhypusine monooxygenase)	2	2	4	4
A2ASS6	Titin (EC 2.7.11.1) (Connectin)	1	2	3	37
Q6NZJ6	Eukaryotic translation initiation factor 4 gamma 1 (eIF-4-gamma 1) (eIF-4G 1) (eIF-4G1)	2	1	3	8
Q9WUK4	Replication factor C subunit 2 (Activator 1 40 kDa subunit) (A1 40 kDa subunit) (Activator 1 subunit 2) (Replication factor C 40 kDa subunit) (RF-C 40 kDa subunit) (RFC40)	2	1	3	6
Q149F3	Eukaryotic peptide chain release factor GTP-binding subunit ERF3B (Eukaryotic peptide chain release factor subunit 3b) (eRF3b) (G1 to S phase transition protein 2 homolog)	1	2	3	5
Q9QY76	Vesicle-associated membrane protein-associated protein B (VAMP-B) (VAMP-associated protein B) (VAP-B) (VAMP-associated protein 33b)	2	1	3	4
P61079	Ubiquitin-conjugating enzyme E2 D3 (EC 2.3.2.23) ((E3-independent) E2 ubiquitin-conjugating enzyme D3) (EC 2.3.2.24) (E2 ubiquitin-conjugating enzyme D3) (Ubiquitin carrier protein D3) (Ubiquitin-conjugating enzyme E2(17)KB 3) (Ubiquitin-conjugating enzyme E2-17 kDa 3) (Ubiquitin-protein ligase D3)	1	2	3	4
Q9WVJ2	26S proteasome non-ATPase regulatory subunit 13 (26S proteasome regulatory subunit RPN9) (26S proteasome regulatory subunit S11) (26S proteasome regulatory subunit p40.5)	1	2	3	4
Q9QYI4	DnaJ homolog subfamily B member 12 (mDj10)	1	2	3	4

UniProt ID	Protein names	$\Delta$ NLS+4FL Replicate Presence (n/5)	$\Delta$ NLS+2KQ Replicate Presence (n/5)	Total Replicate Presence (n/10)	Total Peptide Count
P26516	26S proteasome non-ATPase regulatory subunit 7 (26S proteasome regulatory subunit RPN8) (26S proteasome regulatory subunit S12) (Mov34 protein) (Proteasome subunit p40)	1	2	3	3
Q9D1M0	Protein SEC13 homolog (GATOR complex protein SEC13) (SEC13-like protein 1) (SEC13-related protein)	2	1	3	3
P63168	Dynein light chain 1, cytoplasmic (8 kDa dynein light chain) (DLC8) (Dynein light chain LC8-type 1) (Protein inhibitor of neuronal nitric oxide synthase) (PIN) (mPIN)	1	2	3	3
Q8VCM8	Nicalin (Nicastrin-like protein)	2	1	3	3
Q9CR51	V-type proton ATPase subunit G 1 (V-ATPase subunit G 1) (V-ATPase 13 kDa subunit 1) (Vacuolar proton pump subunit G 1)	2	1	3	3
P97823	Acyl-protein thioesterase 1 (APT-1) (EC 3.1.2.-) (Lysophospholipase 1) (Lysophospholipase I) (LPL-I) (LysoPLA I)	1	2	3	3
Q4FK66	Pre-mRNA-splicing factor 38A	1	2	3	3
Q64525	Histone H2B type 2-B (H2b 616)	1	1	2	22
Q9CW03	Structural maintenance of chromosomes protein 3 (SMC protein 3) (SMC-3) (Basement membrane-associated chondroitin proteoglycan) (Bamacan) (Chondroitin sulfate proteoglycan 6) (Chromosome segregation protein SmcD) (Mad member-interacting protein 1)	1	1	2	8
P30285	Cyclin-dependent kinase 4 (EC 2.7.11.22) (CRK3) (Cell division protein kinase 4) (PSK-J3)	1	1	2	7
Q8BMF3	NADP-dependent malic enzyme, mitochondrial (NADP-ME) (EC 1.1.1.40) (Malic enzyme 3)	1	1	2	5
Q9EPE9	Manganese-transporting ATPase 13A1 (CATP) (EC 3.6.3.-)	1	1	2	5
P08228	Superoxide dismutase [Cu-Zn] (EC 1.15.1.1)	1	1	2	5
Q8CGF7	Transcription elongation regulator 1 (Formin-binding protein 28) (FBP 28) (TATA box-binding protein-associated factor 2S) (Transcription factor CA150) (p144)	1	1	2	5
Q9Z1R2	Large proline-rich protein BAG6 (BAG family molecular chaperone regulator 6) (BCL2-associated athanogene 6) (BAG-6) (HLA-B-associated transcript 3) (Protein Scythe)	1	1	2	5
Q9WUK2	Eukaryotic translation initiation factor 4H (eIF-4H) (Williams-Beuren syndrome chromosomal region 1 protein homolog)	1	1	2	4

UniProt ID	Protein names	$\Delta$ NLS+4FL Replicate Presence (n/5)	$\Delta$ NLS+2KQ Replicate Presence (n/5)	Total Replicate Presence (n/10)	Total Peptide Count
<b>Q7TQI3</b>	Ubiquitin thioesterase OTUB1 (EC 3.4.19.12) (Deubiquitinating enzyme OTUB1) (OTU domain-containing ubiquitin aldehyde-binding protein 1) (Otubain-1) (Ubiquitin-specific-processing protease OTUB1)	1	1	2	4
<b>Q9QYB1</b>	Chloride intracellular channel protein 4 (mc3s5/mtCLIC)	1	1	2	4
<b>P26443</b>	Glutamate dehydrogenase 1, mitochondrial (GDH 1) (EC 1.4.1.3)	1	1	2	4
<b>E9Q5K9</b>	YTH domain-containing protein 1	1	1	2	4
<b>Q8CAY6</b>	Acetyl-CoA acetyltransferase, cytosolic (EC 2.3.1.9) (Cytosolic acetoacetyl-CoA thiolase)	1	1	2	4
<b>Q6PDG5</b>	SWI/SNF complex subunit SMARCC2 (BRG1-associated factor 170) (BAF170) (SWI/SNF complex 170 kDa subunit) (SWI/SNF-related matrix-associated actin-dependent regulator of chromatin subfamily C member 2)	1	1	2	4
<b>Q8BHD7</b>	Polypyrimidine tract-binding protein 3 (Regulator of differentiation 1) (Rod1)	1	1	2	4
<b>Q6PDN3</b>	Myosin light chain kinase, smooth muscle (MLCK) (smMLCK) (EC 2.7.11.18) (Kinase-related protein) (KRP) (Telokin) [Cleaved into: Myosin light chain kinase, smooth muscle, deglutamylated form]	1	1	2	4
<b>Q8K224</b>	RNA cytidine acetyltransferase (EC 2.3.1.-) (18S rRNA cytosine acetyltransferase) (N-acetyltransferase 10)	1	1	2	4
<b>Q9EQU5</b>	Protein SET (Phosphatase 2A inhibitor I2PP2A) (I-2PP2A) (Template-activating factor I) (TAF-I)	1	1	2	4
<b>P13439</b>	Uridine 5'-monophosphate synthase (UMP synthase) [Includes: Orotate phosphoribosyltransferase (OPRTase) (EC 2.4.2.10); Orotidine 5'-phosphate decarboxylase (EC 4.1.1.23) (OMPdecase)]	1	1	2	4
<b>Q99PU8</b>	Putative ATP-dependent RNA helicase DHX30 (EC 3.6.4.13) (DEAH box protein 30)	1	1	2	4
<b>O70439</b>	Syntaxin-7	1	1	2	4
<b>O55013</b>	Trafficking protein particle complex subunit 3 (BET3 homolog)	1	1	2	4
<b>Q9D2R0</b>	Acetoacetyl-CoA synthetase (EC 6.2.1.16)	1	1	2	4

UniProt ID	Protein names	$\Delta$ NLS+4FL Replicate Presence (n/5)	$\Delta$ NLS+2KQ Replicate Presence (n/5)	Total Replicate Presence (n/10)	Total Peptide Count
<b>Q80SW1</b>	S-adenosylhomocysteine hydrolase-like protein 1 (IP3R-binding protein released with inositol 1,4,5-trisphosphate) (Putative adenosylhomocysteinase 2) (S-adenosyl-L-homocysteine hydrolase 2) (AdoHcyase 2)	1	1	2	4
<b>P16460</b>	Argininosuccinate synthase (EC 6.3.4.5) (Citrulline--aspartate ligase)	1	1	2	3
<b>Q80SY4</b>	E3 ubiquitin-protein ligase MIB1 (EC 2.3.2.27) (DAPK-interacting protein 1) (DIP-1) (Mind bomb homolog 1) (RING-type E3 ubiquitin transferase MIB1)	1	1	2	3
<b>Q9Z2I0</b>	Mitochondrial proton/calcium exchanger protein (Leucine zipper-EF-hand-containing transmembrane protein 1)	1	1	2	3
<b>Q9CQJ4</b>	E3 ubiquitin-protein ligase RING2 (EC 2.3.2.27) (RING finger protein 1B) (RING1b) (RING finger protein 2) (RING-type E3 ubiquitin transferase RING2)	1	1	2	3
<b>Q9JJY3</b>	Sphingomyelin phosphodiesterase 3 (EC 3.1.4.12) (Neutral sphingomyelinase 2) (nSMase-2) (nSMase2) (Neutral sphingomyelinase II)	1	1	2	3
<b>Q8BGD9</b>	Eukaryotic translation initiation factor 4B (eIF-4B)	1	1	2	3
<b>Q8C5L3</b>	CCR4-NOT transcription complex subunit 2 (CCR4-associated factor 2)	1	1	2	3
<b>Q8C650</b>	Septin-10	1	1	2	3
<b>P32921</b>	Tryptophan--tRNA ligase, cytoplasmic (EC 6.1.1.2) (Tryptophanyl-tRNA synthetase) (TrpRS) [Cleaved into: T1-TrpRS; T2-TrpRS]	1	1	2	3
<b>Q8K2T1</b>	NmrA-like family domain-containing protein 1	1	1	2	3
<b>O35955</b>	Proteasome subunit beta type-10 (EC 3.4.25.1) (Low molecular mass protein 10) (Macropain subunit MECL-1) (Multicatalytic endopeptidase complex subunit MECL-1) (Proteasome MECL-1) (Proteasome subunit beta-2i)	1	1	2	3
<b>P20108</b>	Thioredoxin-dependent peroxide reductase, mitochondrial (EC 1.11.1.15) (Antioxidant protein 1) (AOP-1) (PRX III) (Perioredoxin-3) (Protein MER5)	1	1	2	3
<b>Q9QZH3</b>	Peptidyl-prolyl cis-trans isomerase E (PPIase E) (EC 5.2.1.8) (Cyclophilin E) (Cyclophilin-33) (Rotamase E)	1	1	2	3
<b>O35114</b>	Lysosome membrane protein 2 (85 kDa lysosomal membrane sialoglycoprotein) (LGP85) (Lysosome membrane protein II) (LIMP II) (Scavenger receptor class B member 2)	1	1	2	3

UniProt ID	Protein names	$\Delta$ NLS+4FL Replicate Presence (n/5)	$\Delta$ NLS+2KQ Replicate Presence (n/5)	Total Replicate Presence (n/10)	Total Peptide Count
<b>Q9QYF1</b>	Retinol dehydrogenase 11 (EC 1.1.1.300) (Androgen-regulated short-chain dehydrogenase/reductase 1) (Cell line MC/9.IL4-derived protein 1) (M42C60) (Prostate short-chain dehydrogenase/reductase 1) (Retinal reductase 1) (RaR1) (Short-chain aldehyde dehydrogenase) (SCALD)	1	1	2	3
<b>Q91XU0</b>	ATPase WRNIP1 (EC 3.6.1.3) (Werner helicase-interacting protein 1)	1	1	2	3
<b>Q9CQ22</b>	Ragulator complex protein LAMTOR1 (Late endosomal/lysosomal adaptor and MAPK and MTOR activator 1) (Lipid raft adaptor protein p18)	1	1	2	3
<b>O70318</b>	Band 4.1-like protein 2 (Generally expressed protein 4.1) (4.1G)	1	1	2	3
<b>O88967</b>	ATP-dependent zinc metalloprotease YME1L1 (EC 3.4.24.-) (ATP-dependent metalloprotease FtsH1) (YME1-like protein 1)	1	1	2	3
<b>O35445</b>	E3 ubiquitin-protein ligase RNF5 (EC 2.3.2.27) (RING finger protein 5) (RING-type E3 ubiquitin transferase RNF5)	1	1	2	3
<b>Q61466</b>	SWI/SNF-related matrix-associated actin-dependent regulator of chromatin subfamily D member 1 (60 kDa BRG-1/Brm-associated factor subunit A) (BRG1-associated factor 60A) (BAF60A) (Protein D15KZ1) (SWI/SNF complex 60 kDa subunit)	1	1	2	3
<b>Q61703</b>	Inter-alpha-trypsin inhibitor heavy chain H2 (ITI heavy chain H2) (ITI-HC2) (Inter-alpha-inhibitor heavy chain 2)	1	1	2	3
<b>Q9DCU6</b>	39S ribosomal protein L4, mitochondrial (L4mt) (MRP-L4)	1	1	2	3
<b>Q3U7R1</b>	Extended synaptotagmin-1 (E-Syt1) (Membrane-bound C2 domain-containing protein)	1	1	2	2
<b>Q9DBS1</b>	Transmembrane protein 43 (Protein LUMA)	1	1	2	2
<b>Q80YV2</b>	Nuclear-interacting partner of ALK (Nuclear-interacting partner of anaplastic lymphoma kinase) (mNIPA) (Zinc finger C3HC-type protein 1)	1	1	2	2
<b>Q99M31</b>	Heat shock 70 kDa protein 14 (NST-1) (hsr.1)	1	1	2	2
<b>Q6PEB6</b>	MOB-like protein phocein (Class II mMOB1) (Mob1 homolog 3) (Mob3) (Mps one binder kinase activator-like 3) (Preimplantation protein 3)	1	1	2	2
<b>Q9WUU7</b>	Cathepsin Z (EC 3.4.18.1)	1	1	2	2

UniProt ID	Protein names	$\Delta$ NLS+4FL Replicate Presence (n/5)	$\Delta$ NLS+2KQ Replicate Presence (n/5)	Total Replicate Presence (n/10)	Total Peptide Count
Q99LG2	Transportin-2 (Karyopherin beta-2b)	1	1	2	2
P29387	Guanine nucleotide-binding protein subunit beta-4 (Transducin beta chain 4)	1	1	2	2
Q91VA6	Polymerase delta-interacting protein 2	1	1	2	2
Q8BHB4	WD repeat-containing protein 3	1	1	2	2
Q9CQ88	Tetraspanin-31 (Tspan-31) (Sarcoma-amplified sequence homolog)	1	1	2	2
O54692	Centromere/kinetochore protein zw10 homolog	1	1	2	2
Q9D7M8	DNA-directed RNA polymerase II subunit RPB4 (RNA polymerase II subunit B4) (DNA-directed RNA polymerase II subunit D)	1	1	2	2
Q99P72	Reticulon-4 (Neurite outgrowth inhibitor) (Nogo protein)	1	1	2	2
Q60960	Importin subunit alpha-5 (Importin alpha-S1) (Karyopherin subunit alpha-1) (Nucleoprotein interactor 1) (NPI-1) (RAG cohort protein 2) (SRP1-beta)	1	1	2	2
P62869	Elongin-B (EloB) (Elongin 18 kDa subunit) (RNA polymerase II transcription factor SIII subunit B) (SIII p18) (Transcription elongation factor B polypeptide 2)	1	1	2	2
Q6P2B1	Transportin-3	1	1	2	2
Q9CR16	Peptidyl-prolyl cis-trans isomerase D (PPIase D) (EC 5.2.1.8) (40 kDa peptidyl-prolyl cis-trans isomerase) (Cyclophilin-40) (CYP-40) (Rotamase D)	1	1	2	2
Q9DBA6	Peroxisomal leader peptide-processing protease (EC 3.4.21.-) (Trypsin domain-containing protein 1) [Cleaved into: Peroxisomal leader peptide-processing protease, 10 kDa form; Peroxisomal leader peptide-processing protease, 49 kDa form]	1	1	2	2
Q9CRC0	Vitamin K epoxide reductase complex subunit 1 (EC 1.17.4.4) (Vitamin K1 2,3-epoxide reductase subunit 1)	1	1	2	2
P61205	ADP-ribosylation factor 3	1	1	2	2
P99027	60S acidic ribosomal protein P2	1	1	2	2
Q9WUU8	TNFAIP3-interacting protein 1 (A20-binding inhibitor of NF-kappa-B activation 1) (ABIN) (ABIN-1) (Nef-associated factor 1) (Naf1) (Virion-associated nuclear shuttling protein) (VAN) (mVAN)	1	1	2	2
Q6NZM9	Histone deacetylase 4 (HD4) (EC 3.5.1.98)	1	1	2	2

UniProt ID	Protein names	$\Delta$ NLS+4FL Replicate Presence (n/5)	$\Delta$ NLS+2KQ Replicate Presence (n/5)	Total Replicate Presence (n/10)	Total Peptide Count
P56382	ATP synthase subunit epsilon, mitochondrial (ATPase subunit epsilon)	1	1	2	2
O88507	Ciliary neurotrophic factor receptor subunit alpha (CNTF receptor subunit alpha) (CNTFR-alpha)	1	1	2	2
Q9QXY9	Peroxisomal biogenesis factor 3 (Peroxin-3) (Peroxisomal assembly protein PEX3)	1	1	2	2
P42669	Transcriptional activator protein Pur-alpha (Purine-rich single-stranded DNA-binding protein alpha)	1	1	2	2
Q59J78	NADH dehydrogenase [ubiquinone] 1 alpha subcomplex assembly factor 2 (Mimitin) (Myc-induced mitochondrial protein) (MMTN) (NDUFA12-like protein)	1	1	2	2
Q80XN0	D-beta-hydroxybutyrate dehydrogenase, mitochondrial (EC 1.1.1.30) (3-hydroxybutyrate dehydrogenase) (BDH)	1	1	2	2
Q9CYN9	Renin receptor (ATPase H(+)-transporting lysosomal accessory protein 2) (ATPase H(+)-transporting lysosomal-interacting protein 2) (Renin/prorenin receptor)	2	0	2	2
O70475	UDP-glucose 6-dehydrogenase (UDP-Glc dehydrogenase) (UDP-GlcDH) (UDPGDH) (EC 1.1.1.22)	2	0	2	2
P10854	Histone H2B type 1-M (H2B 291B)	1	0	1	8
D3YXK2	Scaffold attachment factor B1 (SAF-B1)	1	0	1	3
Q6ZPY7	Lysine-specific demethylase 3B (EC 1.14.11.-) (JmjC domain-containing histone demethylation protein 2B) (Jumonji domain-containing protein 1B)	1	0	1	3
O08550	Histone-lysine N-methyltransferase 2B (Lysine N-methyltransferase 2B) (EC 2.1.1.43) (Myeloid/lymphoid or mixed-lineage leukemia protein 4 homolog) (Trithorax homolog 2) (WW domain-binding protein 7) (WBP-7)	1	0	1	3
O08788	Dynactin subunit 1 (150 kDa dynein-associated polypeptide) (DAP-150) (DP-150) (p150-glued)	1	0	1	3
Q6R891	Neurabin-2 (Neurabin-II) (Protein phosphatase 1 regulatory subunit 9B) (Spinophilin)	1	0	1	3
Q9CPQ1	Cytochrome c oxidase subunit 6C (Cytochrome c oxidase polypeptide VIc)	1	0	1	3
Q8BVQ5	Protein phosphatase methylesterase 1 (PME-1) (EC 3.1.1.89)	1	0	1	2
Q8K354	Carbonyl reductase [NADPH] 3 (EC 1.1.1.184) (NADPH-dependent carbonyl reductase 3)	1	0	1	2
Q9JJW6	Aly/REF export factor 2 (Alyref) (RNA and export factor-binding protein 2)	1	0	1	2

UniProt ID	Protein names	$\Delta$ NLS+4FL Replicate Presence (n/5)	$\Delta$ NLS+2KQ Replicate Presence (n/5)	Total Replicate Presence (n/10)	Total Peptide Count
Q8R3L2	Transcription factor 25 (TCF-25) (Nuclear localized protein 1)	1	0	1	2
Q6P2L7	Protein CASC4 (Cancer susceptibility candidate gene 4 protein homolog)	1	0	1	2
Q8C878	NEDD8-activating enzyme E1 catalytic subunit (EC 6.3.2.-) (NEDD8-activating enzyme E1C) (Ubiquitin-activating enzyme E1C) (Ubiquitin-like modifier-activating enzyme 3) (Ubiquitin-activating enzyme 3)	1	0	1	2
P0C6F1	Dynein heavy chain 2, axonemal (Axonemal beta dynein heavy chain 2) (Ciliary dynein heavy chain 2)	1	0	1	2
P68368	Tubulin alpha-4A chain (Alpha-tubulin 4) (Alpha-tubulin isotype M-alpha-4) (Tubulin alpha-4 chain)	1	0	1	2
Q9CRA8	Exosome complex component RRP46 (Exosome component 5) (Ribosomal RNA-processing protein 46)	1	0	1	2
Q8BGW1	Alpha-ketoglutarate-dependent dioxygenase FTO (EC 1.14.11.-) (Fat mass and obesity-associated protein) (Protein fatso)	1	0	1	2
Q6PHN9	Ras-related protein Rab-35	1	0	1	2
Q9CYN2	Signal peptidase complex subunit 2 (EC 3.4.-.-) (Microsomal signal peptidase 25 kDa subunit) (SPase 25 kDa subunit)	1	0	1	2
Q06185	ATP synthase subunit e, mitochondrial (ATPase subunit e)	1	0	1	2
Q920E5	Farnesyl pyrophosphate synthase (FPP synthase) (FPS) (EC 2.5.1.10) ((2E,6E)-farnesyl diphosphate synthase) (Cholesterol-regulated 39 kDa protein) (CR 39) (Dimethylallyltranstransferase) (EC 2.5.1.1) (Farnesyl diphosphate synthase) (Geranyltranstransferase)	1	0	1	2
Q8VDJ3	Vigilin (High density lipoprotein-binding protein) (HDL-binding protein)	1	0	1	2
Q8K274	Ketosamine-3-kinase (EC 2.7.1.-) (Fructosamine-3-kinase-related protein)	1	0	1	2
P70399	TP53-binding protein 1 (53BP1) (p53-binding protein 1) (p53BP1)	1	0	1	2
Q70IV5	Synemin (Desmuslin)	1	0	1	2
P52912	Nucleolysin TIA-1 (RNA-binding protein TIA-1) (T-cell-restricted intracellular antigen-1) (TIA-1)	1	0	1	2

UniProt ID	Protein names	$\Delta$ NLS+4FL Replicate Presence (n/5)	$\Delta$ NLS+2KQ Replicate Presence (n/5)	Total Replicate Presence (n/10)	Total Peptide Count
Q6P8I4	PEST proteolytic signal-containing nuclear protein (PCNP) (PEST-containing nuclear protein)	1	0	1	2
P84096	Rho-related GTP-binding protein RhoG (Sid 10750)	1	0	1	2
P57110	A disintegrin and metalloproteinase with thrombospondin motifs 8 (ADAM-TS 8) (ADAM-TS8) (ADAMTS-8) (EC 3.4.24.-) (METH-2)	1	0	1	2
P37913	DNA ligase 1 (EC 6.5.1.1) (DNA ligase I) (Polydeoxyribonucleotide synthase [ATP] 1)	1	0	1	2
Q9CQS2	H/ACA ribonucleoprotein complex subunit 3 (Nucleolar protein 10) (Nucleolar protein family A member 3) (snoRNP protein NOP10)	1	0	1	2
Q61335	B-cell receptor-associated protein 31 (BCR-associated protein 31) (Bap31) (p28)	1	0	1	2
Q9WV55	Vesicle-associated membrane protein-associated protein A (VAMP-A) (VAMP-associated protein A) (VAP-A) (33 kDa VAMP-associated protein) (VAP-33)	1	0	1	2
Q68FL4	Putative adenosylhomocysteinase 3 (AdoHcyase 3) (EC 3.3.1.1) (Long-IRBIT) (S-adenosyl-L-homocysteine hydrolase 3) (S-adenosylhomocysteine hydrolase-like protein 2)	1	0	1	2
Q8K4L0	ATP-dependent RNA helicase DDX54 (EC 3.6.4.13) (DEAD box protein 54)	1	0	1	2
Q9JJY4	Probable ATP-dependent RNA helicase DDX20 (EC 3.6.4.13) (Component of gems 3) (DEAD box protein 20) (DEAD box protein DP 103) (Gemin-3) (Regulator of steroidogenic factor 1) (ROSF-1)	1	0	1	2
Q8BZ05	Arf-GAP with Rho-GAP domain, ANK repeat and PH domain-containing protein 2 (Centaurin-delta-1) (Cnt-d1)	1	0	1	2
Q6Q477	Plasma membrane calcium-transporting ATPase 4 (PMCA4) (EC 3.6.3.8)	1	0	1	2
Q9QXV1	Chromobox protein homolog 8 (Polycomb 3 homolog) (Pc3) (mPc3)	1	0	1	2
P62823	Ras-related protein Rab-3C	1	0	1	2
Q8VE22	28S ribosomal protein S23, mitochondrial (MRP-S23) (S23mt)	1	0	1	2
Q9D1B9	39S ribosomal protein L28, mitochondrial (L28mt) (MRP-L28)	1	0	1	1
Q9CY97	RNA polymerase II subunit A C-terminal domain phosphatase SSU72 (CTD phosphatase SSU72) (EC 3.1.3.16)	1	0	1	1
O35841	Apoptosis inhibitor 5 (API-5) (AAC-11)	1	0	1	1
A6H694	Leucine-rich repeat-containing protein 63	1	0	1	1

UniProt ID	Protein names	$\Delta$ NLS+4FL Replicate Presence (n/5)	$\Delta$ NLS+2KQ Replicate Presence (n/5)	Total Replicate Presence (n/10)	Total Peptide Count
Q80VQ1	Leucine-rich repeat-containing protein 1	1	0	1	1
Q99L13	3-hydroxyisobutyrate dehydrogenase, mitochondrial (HIBADH) (EC 1.1.1.31)	1	0	1	1
Q9ERF3	WD repeat-containing protein 61 (Meiotic recombination REC14 protein homolog) [Cleaved into: WD repeat-containing protein 61, N-terminally processed]	1	0	1	1
Q9CX53	Gem-associated protein 6 (Gemin-6)	1	0	1	1
Q8R0G9	Nuclear pore complex protein Nup133 (133 kDa nucleoporin) (Nucleoporin Nup133)	1	0	1	1
Q61647	Hyaluronan synthase 1 (EC 2.4.1.212) (Hyaluronate synthase 1) (Hyaluronic acid synthase 1) (HA synthase 1)	1	0	1	1
Q3U308	Cytoplasmic tRNA 2-thiolation protein 2	1	0	1	1
O54825	Bystin	1	0	1	1
Q9CQJ6	Density-regulated protein (DRP)	1	0	1	1
Q9DAW6	U4/U6 small nuclear ribonucleoprotein Prp4 (U4/U6 snRNP 60 kDa protein) (WD splicing factor Prp4)	1	0	1	1
Q8VDT9	39S ribosomal protein L50, mitochondrial (L50mt) (MRP-L50)	1	0	1	1
Q9JIG8	PRA1 family protein 2	1	0	1	1
Q8K221	Arfaptin-2 (ADP-ribosylation factor-interacting protein 2)	1	0	1	1
Q91YR1	Twinfilin-1 (Protein A6)	1	0	1	1
O35218	Cleavage and polyadenylation specificity factor subunit 2 (Cleavage and polyadenylation specificity factor 100 kDa subunit) (CPSF 100 kDa subunit)	1	0	1	1
Q9D1P4	Cysteine and histidine-rich domain-containing protein 1 (CHORD domain-containing protein 1) (CHORD-containing protein 1) (Chp-1) (Protein morgana)	1	0	1	1
P39447	Tight junction protein ZO-1 (Tight junction protein 1) (Zona occludens protein 1) (Zonula occludens protein 1)	1	0	1	1
Q4FZF3	Probable ATP-dependent RNA helicase DDX49 (EC 3.6.4.13) (DEAD box protein 49)	1	0	1	1
Q8R143	Pituitary tumor-transforming gene 1 protein-interacting protein (Pituitary tumor-transforming gene protein-binding factor) (PBF) (PTTG-binding factor)	1	0	1	1

UniProt ID	Protein names	$\Delta$ NLS+4FL Replicate Presence (n/5)	$\Delta$ NLS+2KQ Replicate Presence (n/5)	Total Replicate Presence (n/10)	Total Peptide Count
Q61941	NAD(P) transhydrogenase, mitochondrial (EC 1.6.1.2) (Nicotinamide nucleotide transhydrogenase) (Pyridine nucleotide transhydrogenase)	1	0	1	1
Q8VCL2	Protein SCO2 homolog, mitochondrial	1	0	1	1
Q60649	Caseinolytic peptidase B protein homolog (EC 3.6.1.3) (Suppressor of potassium transport defect 3)	1	0	1	1
Q8CA72	Gigaxonin	1	0	1	1
P53986	Monocarboxylate transporter 1 (MCT 1) (Solute carrier family 16 member 1)	1	0	1	1
Q9CQF0	39S ribosomal protein L11, mitochondrial (L11mt) (MRP-L11)	1	0	1	1
O88844	Isocitrate dehydrogenase [NADP] cytoplasmic (IDH) (EC 1.1.1.42) (Cytosolic NADP-isocitrate dehydrogenase) (IDP) (NADP(+)-specific ICDH) (Oxalosuccinate decarboxylase)	1	0	1	1
Q8R429	Sarcoplasmic/endoplasmic reticulum calcium ATPase 1 (SERCA1) (SR Ca(2+)-ATPase 1) (EC 3.6.3.8) (Calcium pump 1) (Calcium-transporting ATPase sarcoplasmic reticulum type, fast twitch skeletal muscle isoform) (Endoplasmic reticulum class 1/2 Ca(2+) ATPase)	1	0	1	1
Q99MS8	Tubulin polyglutamylase complex subunit 1 (PGs1) (p32)	1	0	1	1
P14069	Protein S100-A6 (5B10) (Calcyclin) (Prolactin receptor-associated protein) (S100 calcium-binding protein A6)	1	0	1	1
Q80SU3	Zygote arrest protein 1 (Oocyte-specific maternal effect factor)	1	0	1	1
Q9EPL4	Methyltransferase-like protein 9 (DORA reverse strand protein) (DREV)	1	0	1	1
Q64G17	Putative acidic leucine-rich nuclear phosphoprotein 32 family member C	1	0	1	1
Q9Z1T5	Deformed epidermal autoregulatory factor 1 homolog (Nuclear DEAF-1-related transcriptional regulator) (NUDR)	1	0	1	1
Q9QXP6	E3 ubiquitin-protein ligase makorin-1 (EC 2.3.2.27) (RING-type E3 ubiquitin transferase makorin-1)	1	0	1	1
Q8CF66	Ragulator complex protein LAMTOR4 (Late endosomal/lysosomal adaptor and MAPK and MTOR activator 4) [Cleaved into: Ragulator complex protein LAMTOR4, N-terminally processed]	1	0	1	1

UniProt ID	Protein names	ΔNLS+4FL Replicate Presence (n/5)	ΔNLS+2KQ Replicate Presence (n/5)	Total Replicate Presence (n/10)	Total Peptide Count
<b>Q9DCR2</b>	AP-3 complex subunit sigma-1 (AP-3 complex subunit sigma-3A) (Adaptor-related protein complex 3 subunit sigma-1) (Sigma-3A-adaptin) (Sigma3A-adaptin) (Sigma-adaptin 3a)	1	0	1	1
<b>P31938</b>	Dual specificity mitogen-activated protein kinase kinase 1 (MAP kinase kinase 1) (MAPKK 1) (EC 2.7.12.2) (ERK activator kinase 1) (MAPK/ERK kinase 1) (MEK 1)	1	0	1	1
<b>Q9R1Q7</b>	Proteolipid protein 2	1	0	1	1
<b>Q99LJ6</b>	Glutathione peroxidase 7 (GPx-7) (GSHPx-7) (EC 1.11.1.9)	1	0	1	1
<b>Q3UJB9</b>	Enhancer of mRNA-decapping protein 4	1	0	1	1
<b>Q3TMX7</b>	Sulfhydryl oxidase 2 (EC 1.8.3.2) (Quiescin Q6-like protein 1)	1	0	1	1
<b>Q61469</b>	Phospholipid phosphatase 1 (EC 3.1.3.4) (35 kDa PAP) (mPAP) (Hydrogen peroxide-inducible protein 53) (Hic53) (Lipid phosphate phosphohydrolase 1) (PAP2-alpha) (Phosphatidate phosphohydrolase type 2a) (Phosphatidic acid phosphatase 2a) (PAP-2a) (PAP2a)	1	0	1	1
<b>Q62470</b>	Integrin alpha-3 (CD49 antigen-like family member C) (Galactoprotein B3) (GAPB3) (VLA-3 subunit alpha) (CD antigen CD49c) [Cleaved into: Integrin alpha-3 heavy chain; Integrin alpha-3 light chain]	1	0	1	1
<b>Q91UZ5</b>	Inositol monophosphatase 2 (IMP 2) (IMPase 2) (EC 3.1.3.25) (Inositol-1(or 4)-monophosphatase 2) (Myo-inositol monophosphatase A2)	1	0	1	1
<b>Q60900</b>	ELAV-like protein 3 (Hu-antigen C) (HuC)	1	0	1	1
<b>Q9DCN2</b>	NADH-cytochrome b5 reductase 3 (B5R) (Cytochrome b5 reductase) (EC 1.6.2.2) (Diaphorase-1) [Cleaved into: NADH-cytochrome b5 reductase 3 membrane-bound form; NADH-cytochrome b5 reductase 3 soluble form]	1	0	1	1
<b>P63280</b>	SUMO-conjugating enzyme UBC9 (EC 2.3.2.-) (RING-type E3 SUMO transferase UBC9) (SUMO-protein ligase) (Ubiquitin carrier protein 9) (mUBC9) (Ubiquitin carrier protein I) (Ubiquitin-conjugating enzyme E2 I) (Ubiquitin-protein ligase I)	1	0	1	1
<b>P69566</b>	Ran-binding protein 9 (RanBP9) (B-cell antigen receptor Ig beta-associated protein 1) (IBAP-1) (Ran-binding protein M) (RanBPM)	1	0	1	1
<b>Q91Z38</b>	Tetratricopeptide repeat protein 1 (TPR repeat protein 1)	1	0	1	1

UniProt ID	Protein names	ΔNLS+4FL Replicate Presence (n/5)	ΔNLS+2KQ Replicate Presence (n/5)	Total Replicate Presence (n/10)	Total Peptide Count
Q9QVN7	Transcription elongation factor A protein 2 (Protein S-II-T1) (Testis-specific S-II) (Transcription elongation factor S-II protein 2) (Transcription elongation factor TFIIIS.I)	1	0	1	1
Q9D1J3	SAP domain-containing ribonucleoprotein (Nuclear protein Hcc-1)	1	0	1	1
P35803	Neuronal membrane glycoprotein M6-b (M6b)	1	0	1	1
Q921F4	Heterogeneous nuclear ribonucleoprotein L-like	1	0	1	1
O89090	Transcription factor Sp1	1	0	1	1
P26369	Splicing factor U2AF 65 kDa subunit (U2 auxiliary factor 65 kDa subunit) (U2 snRNP auxiliary factor large subunit)	1	0	1	1
O08599	Syntaxin-binding protein 1 (Protein unc-18 homolog 1) (Unc18-1) (Protein unc-18 homolog A) (Unc-18A)	1	0	1	1
Q99P31	Hsp70-binding protein 1 (HspBP1) (Heat shock protein-binding protein 1) (Hsp70-interacting protein 1)	1	0	1	1
Q148V7	LisH domain and HEAT repeat-containing protein KIAA1468	1	0	1	1
O70494	Transcription factor Sp3	1	0	1	1
Q9CZ91	Serum response factor-binding protein 1 (SRF-dependent transcription regulation-associated protein) (p49/STRAP)	1	0	1	1
Q9DCV7	Keratin, type II cytoskeletal 7 (Cytokeratin-7) (CK-7) (Keratin-7) (K7) (Type-II keratin Kb7)	1	0	1	1
Q9CZX9	ER membrane protein complex subunit 4 (Transmembrane protein 85)	1	0	1	1
Q9JIK9	28S ribosomal protein S34, mitochondrial (MRP-S34) (S34mt) (T-complex expressed gene 2 protein)	1	0	1	1
Q80U78	Pumilio homolog 1	1	0	1	1
Q8BHG3	Cell cycle control protein 50B (Transmembrane protein 30B)	1	0	1	1
Q8BXA1	Golgi integral membrane protein 4 (Decapacitation factor 10) (Golgi phosphoprotein 4)	1	0	1	1
Q9CQY5	Magnesium transporter protein 1 (MagT1) (Implantation-associated protein) (IAP)	1	0	1	1
Q60809	CCR4-NOT transcription complex subunit 7 (EC 3.1.13.4) (CCR4-associated factor 1) (CAF-1)	1	0	1	1

UniProt ID	Protein names	$\Delta$ NLS+4FL Replicate Presence (n/5)	$\Delta$ NLS+2KQ Replicate Presence (n/5)	Total Replicate Presence (n/10)	Total Peptide Count
Q6NZB1	Protein arginine N-methyltransferase 6 (EC 2.1.1.319) (Histone-arginine N-methyltransferase PRMT6)	1	0	1	1
Q99JP7	Glutathione hydrolase 7 (EC 3.4.19.13) (Gamma-glutamyltransferase 7) (GGT 7) (EC 2.3.2.2) (Gamma-glutamyltransferase-like 3) (Gamma-glutamyltranspeptidase 7) [Cleaved into: Glutathione hydrolase 7 heavy chain; Glutathione hydrolase 7 light chain]	1	0	1	1
Q3UDR8	Protein YIPF3 (Killer lineage protein 1) (YIP1 family member 3) [Cleaved into: Protein YIPF3, N-terminally processed]	1	0	1	1
Q921W4	Quinone oxidoreductase-like protein 1 (EC 1.-.-) (Quinone oxidoreductase homolog 1) (QOH-1) (Zeta-crystallin homolog)	1	0	1	1
Q3THK7	GMP synthase [glutamine-hydrolyzing] (EC 6.3.5.2) (GMP synthetase) (Glutamine amidotransferase)	1	0	1	1
Q9QZ18	Serine incorporator 1 (Axotomy-induced glyco/Golgi protein 2) (Membrane protein TMS-2) (Tumor differentially expressed protein 1-like) (Tumor differentially expressed protein 2)	1	0	1	1
P35285	Ras-related protein Rab-22A (Rab-22) (Rab-14)	1	0	1	1
Q9D1A2	Cytosolic non-specific dipeptidase (EC 3.4.13.18) (CNDP dipeptidase 2) (Glutamate carboxypeptidase-like protein 1)	1	0	1	1
Q91XV3	Brain acid soluble protein 1 (22 kDa neuronal tissue-enriched acidic protein) (Neuronal axonal membrane protein NAP-22)	1	0	1	1
Q9CZG3	COMM domain-containing protein 8	1	0	1	1
Q6PIP5	NudC domain-containing protein 1	1	0	1	1
P30681	High mobility group protein B2 (High mobility group protein 2) (HMG-2)	1	0	1	1
Q3TDQ1	Dolichyl-diphosphooligosaccharide--protein glycosyltransferase subunit STT3B (Oligosaccharyl transferase subunit STT3B) (STT3-B) (EC 2.4.99.18) (B6dom1 antigen) (Source of immunodominant MHC-associated peptides)	1	0	1	1
Q9WVI9	C-Jun-amino-terminal kinase-interacting protein 1 (JIP-1) (JNK-interacting protein 1) (Islet-brain-1) (IB-1) (JNK MAP kinase scaffold protein 1) (Mitogen-activated protein kinase 8-interacting protein 1)	1	0	1	1

UniProt ID	Protein names	$\Delta$ NLS+4FL Replicate Presence (n/5)	$\Delta$ NLS+2KQ Replicate Presence (n/5)	Total Replicate Presence (n/10)	Total Peptide Count
Q791V5	Mitochondrial carrier homolog 2	1	0	1	1
P62911	60S ribosomal protein L32	1	0	1	1
Q8VCH8	UBX domain-containing protein 4 (Erasin) (UBX domain-containing protein 2)	1	0	1	1
Q6ZWR4	Serine/threonine-protein phosphatase 2A 55 kDa regulatory subunit B beta isoform (PP2A subunit B isoform B55-beta) (PP2A subunit B isoform PR55-beta) (PP2A subunit B isoform R2-beta) (PP2A subunit B isoform beta)	1	0	1	1
Q8C6B9	Active regulator of SIRT1 (40S ribosomal protein S19-binding protein 1) (RPS19-binding protein 1) (S19BP)	1	0	1	1
P58242	Acid sphingomyelinase-like phosphodiesterase 3b (ASM-like phosphodiesterase 3b) (EC 3.1.4.-)	1	0	1	1
Q32NY4	Metal transporter CNNM3 (Ancient conserved domain-containing protein 3) (mACDP3) (Cyclin-M3)	1	0	1	1
Q9DCD0	6-phosphogluconate dehydrogenase, decarboxylating (EC 1.1.1.44)	1	0	1	1
Q3TFQ1	SPRY domain-containing protein 7 (Chronic lymphocytic leukemia deletion region gene 6 protein homolog) (CLL deletion region gene 6 protein homolog)	1	0	1	1
Q8BGX2	Mitochondrial import inner membrane translocase subunit Tim29 (TIM29)	1	0	1	1
O08585	Clathrin light chain A (Lca)	1	0	1	1
Q9D787	Peptidyl-prolyl cis-trans isomerase-like 2 (PPIase) (EC 2.3.2.27) (EC 5.2.1.8) (CYC4) (Cyclophilin-60) (Cyclophilin-like protein Cyp-60) (RING-type E3 ubiquitin transferase isomerase-like 2) (Rotamase PPIL2)	1	0	1	1
Q3UPF5	Zinc finger CCCH-type antiviral protein 1 (ADP-ribosyltransferase diphtheria toxin-like 13) (ARTD13)	1	0	1	1
Q8C181	Muscleblind-like protein 2	1	0	1	1
Q9CSU0	Regulation of nuclear pre-mRNA domain-containing protein 1B (Cell cycle-related and expression-elevated protein in tumor)	1	0	1	1
Q6ZPZ3	Zinc finger CCCH domain-containing protein 4	1	0	1	1
P13595	Neural cell adhesion molecule 1 (N-CAM-1) (NCAM-1) (CD antigen CD56)	1	0	1	1

UniProt ID	Protein names	$\Delta$ NLS+4FL Replicate Presence (n/5)	$\Delta$ NLS+2KQ Replicate Presence (n/5)	Total Replicate Presence (n/10)	Total Peptide Count
Q80WJ7	Protein LYRIC (3D3/LYRIC) (Lysine-rich CEACAM1 co-isolated protein) (Metadherin) (Metastasis adhesion protein)	1	0	1	1
P32443	Homeobox protein MOX-2 (Mesenchyme homeobox 2)	1	0	1	1
Q8CI51	PDZ and LIM domain protein 5 (Enigma homolog) (Enigma-like PDZ and LIM domains protein)	1	0	1	1
P63011	Ras-related protein Rab-3A	1	0	1	1
Q497I4	Keratin, type I cuticular Ha5 (Hair keratin, type I Ha5) (Keratin-35) (K35)	1	0	1	1
P13707	Glycerol-3-phosphate dehydrogenase [NAD(+)], cytoplasmic (GPD-C) (GPDH-C) (EC 1.1.1.8)	1	0	1	1
Q9QYL7	Activator of basal transcription 1	1	0	1	1
P49586	Choline-phosphate cytidyltransferase A (EC 2.7.7.15) (CCT-alpha) (CTP:phosphocholine cytidyltransferase A) (CCT A) (CT A) (Phosphorylcholine transferase A)	1	0	1	1
Q9CZ30	Obg-like ATPase 1 (GTP-binding protein 9)	1	0	1	1
Q3URU2	Paternally-expressed gene 3 protein (ASF-1)	1	0	1	1
Q8BWW3	Eukaryotic peptide chain release factor subunit 1 (Eukaryotic release factor 1) (eRF1)	1	0	1	1
Q9QXB9	Developmentally-regulated GTP-binding protein 2 (DRG-2)	1	0	1	1
Q5EG47	5'-AMP-activated protein kinase catalytic subunit alpha-1 (AMPK subunit alpha-1) (EC 2.7.11.1) (Acetyl-CoA carboxylase kinase) (ACACA kinase) (EC 2.7.11.27) (Hydroxymethylglutaryl-CoA reductase kinase) (HMGCR kinase) (EC 2.7.11.31) (Tau-protein kinase PRKAA1) (EC 2.7.11.26)	1	0	1	1
Q04750	DNA topoisomerase 1 (EC 5.99.1.2) (DNA topoisomerase I)	1	0	1	1
Q80XL6	Acyl-CoA dehydrogenase family member 11 (ACAD-11) (EC 1.3.99.-)	1	0	1	1
Q9WUP7	Ubiquitin carboxyl-terminal hydrolase isozyme L5 (UCH-L5) (EC 3.4.19.12) (Ubiquitin C-terminal hydrolase UCH37) (Ubiquitin thioesterase L5)	1	0	1	1
Q8BKT3	GC-rich sequence DNA-binding factor 2 (GC-rich sequence DNA-binding factor) (Transcription factor 9) (TCF-9)	1	0	1	1
Q9DAW9	Calponin-3 (Calponin, acidic isoform)	1	0	1	1

UniProt ID	Protein names	$\Delta$ NLS+4FL Replicate Presence (n/5)	$\Delta$ NLS+2KQ Replicate Presence (n/5)	Total Replicate Presence (n/10)	Total Peptide Count
P24788	Cyclin-dependent kinase 11B (Cell division cycle 2-like protein kinase 1) (Cell division protein kinase 11) (Cyclin-dependent kinase 11) (EC 2.7.11.22) (Galactosyltransferase-associated protein kinase p58/GTA) (PITSLRE serine/threonine-protein kinase CDC2L1)	1	0	1	1
Q8K363	ATP-dependent RNA helicase DDX18 (EC 3.6.4.13) (DEAD box protein 18)	1	0	1	1
Q9CRT8	Exportin-T (Exportin(tRNA)) (tRNA exportin)	1	0	1	1
Q62425	Cytochrome c oxidase subunit NDUFA4	1	0	1	1
Q9D3R6	Katanin p60 ATPase-containing subunit A-like 2 (Katanin p60 subunit A-like 2) (EC 3.6.4.3) (p60 katanin-like 2)	1	0	1	1
P47955	60S acidic ribosomal protein P1	1	0	1	1
P46096	Synaptotagmin-1 (Synaptotagmin I) (Sytl) (p65)	1	0	1	1
O54988	STE20-like serine/threonine-protein kinase (STE20-like kinase) (mSLK) (EC 2.7.11.1) (Etk4) (STE20-related kinase SMAK) (STE20-related serine/threonine-protein kinase) (STE20-related kinase) (Serine/threonine-protein kinase 2)	1	0	1	1
P28867	Protein kinase C delta type (EC 2.7.11.13) (Tyrosine-protein kinase PRKCD) (EC 2.7.10.2) (nPKC-delta) [Cleaved into: Protein kinase C delta type regulatory subunit; Protein kinase C delta type catalytic subunit (Sphingosine-dependent protein kinase-1) (SDK1)]	1	0	1	1
Q80TL7	Protein MON2 homolog (Protein SF21)	1	0	1	1
P62715	Serine/threonine-protein phosphatase 2A catalytic subunit beta isoform (PP2A-beta) (EC 3.1.3.16)	1	0	1	1
Q497V5	S1 RNA-binding domain-containing protein 1	1	0	1	1
Q91XU3	Phosphatidylinositol 5-phosphate 4-kinase type-2 gamma (EC 2.7.1.149) (Phosphatidylinositol 5-phosphate 4-kinase type II gamma) (PI(5)P 4-kinase type II gamma) (PIP4KII-gamma)	1	0	1	1
P62858	40S ribosomal protein S28	1	0	1	1
Q8BYL4	Tyrosine--tRNA ligase, mitochondrial (EC 6.1.1.1) (Tyrosyl-tRNA synthetase) (TyrRS)	1	0	1	1
P04627	Serine/threonine-protein kinase A-Raf (EC 2.7.11.1) (Proto-oncogene A-Raf)	1	0	1	1
Q8BH74	Nuclear pore complex protein Nup107 (107 kDa nucleoporin) (Nucleoporin Nup107)	1	0	1	1

UniProt ID	Protein names	$\Delta$ NLS+4FL Replicate Presence (n/5)	$\Delta$ NLS+2KQ Replicate Presence (n/5)	Total Replicate Presence (n/10)	Total Peptide Count
Q8BHC4	Dephospho-CoA kinase domain-containing protein	1	0	1	1
Q505B7	Protein archease (Protein ZBTB8OS)	1	0	1	1
Q9CZX0	Elongator complex protein 3 (EC 2.3.1.48)	1	0	1	1
Q9JJI8	60S ribosomal protein L38	1	0	1	1
P83940	Elongin-C (EloC) (Elongin 15 kDa subunit) (RNA polymerase II transcription factor SIII subunit C) (SIII p15) (Stromal membrane-associated protein SMAP1B homolog) (Transcription elongation factor B polypeptide 1)	1	0	1	1
Q8C1A5	Thimet oligopeptidase (EC 3.4.24.15)	1	0	1	1
Q8CBY8	Dynactin subunit 4 (Dynactin subunit p62)	1	0	1	1
Q6IFZ6	Keratin, type II cytoskeletal 1b (Cytokeratin-1B) (CK-1B) (Embryonic type II keratin-1) (Keratin-77) (K77) (Type-II keratin Kb39)	0	3	3	8
P39054	Dynammin-2 (EC 3.6.5.5) (Dynammin UDNM)	0	3	3	6
Q61768	Kinesin-1 heavy chain (Conventional kinesin heavy chain) (Ubiquitous kinesin heavy chain) (UKHC)	0	2	2	5
Q9EQZ7	Regulating synaptic membrane exocytosis protein 2 (Rab-3-interacting molecule 2) (RIM 2) (Rab-3-interacting protein 2)	0	2	2	4
P70699	Lysosomal alpha-glucosidase (EC 3.2.1.20) (Acid maltase)	0	2	2	3
Q8BWY9	Protein CIP2A (Cancerous inhibitor of PP2A) (p90 autoantigen homolog)	0	2	2	3
Q9QWT9	Kinesin-like protein KIFC1	0	2	2	3
Q8K1Z0	Ubiquinone biosynthesis protein COQ9, mitochondrial	0	2	2	2
Q91ZD4	Vang-like protein 2 (Loop-tail protein 1) (Loop-tail-associated protein) (Van Gogh-like protein 2)	0	2	2	2
P35922	Synaptic functional regulator FMR1 (Fragile X mental retardation protein 1 homolog) (FMRP) (Protein FMR-1) (mFmr1p)	0	2	2	2
P40749	Synaptotagmin-4 (Synaptotagmin IV) (SytIV)	0	2	2	2
P16381	Putative ATP-dependent RNA helicase Pl10 (EC 3.6.4.13)	0	1	1	5

UniProt ID	Protein names	$\Delta$ NLS+4FL Replicate Presence (n/5)	$\Delta$ NLS+2KQ Replicate Presence (n/5)	Total Replicate Presence (n/10)	Total Peptide Count
Q8R5C5	Beta-centractin (Actin-related protein 1B) (ARP1B)	0	1	1	5
Q9Z1P7	KN motif and ankyrin repeat domain-containing protein 3 (Ankyrin repeat domain-containing protein 47)	0	1	1	4
P55258	Ras-related protein Rab-8A (Oncogene c-mel)	0	1	1	3
Q924K8	Metastasis-associated protein MTA3	0	1	1	3
Q91VW5	Golgin subfamily A member 4 (tGolgin-1)	0	1	1	3
Q3UVK0	Endoplasmic reticulum metalloproteinase 1 (EC 3.4.-.-) (Felix-ina)	0	1	1	3
P55041	GTP-binding protein GEM (GTP-binding mitogen-induced T-cell protein) (RAS-like protein KIR)	0	1	1	3
Q9Z1D1	Eukaryotic translation initiation factor 3 subunit G (eIF3g) (Eukaryotic translation initiation factor 3 RNA-binding subunit) (eIF-3 RNA-binding subunit) (Eukaryotic translation initiation factor 3 subunit 4) (eIF-3-delta) (eIF3 p42) (eIF3 p44)	0	1	1	3
Q62407	Striated muscle-specific serine/threonine-protein kinase (EC 2.7.11.1) (Aortic preferentially expressed protein 1) (APEG-1)	0	1	1	3
Q61820	GTP-binding nuclear protein Ran, testis-specific isoform	0	1	1	3
P58774	Tropomyosin beta chain (Beta-tropomyosin) (Tropomyosin-2)	0	1	1	3
Q9CQV6	Microtubule-associated proteins 1A/1B light chain 3B (Autophagy-related protein LC3 B) (Autophagy-related ubiquitin-like modifier LC3 B) (MAP1 light chain 3-like protein 2) (MAP1A/MAP1B light chain 3 B) (MAP1A/MAP1B LC3 B) (Microtubule-associated protein 1 light chain 3 beta)	0	1	1	3
P60487	Pyridoxal phosphate phosphatase (PLP phosphatase) (EC 3.1.3.3) (EC 3.1.3.74) (Chronophin)	0	1	1	3
Q9EQQ9	Protein O-GlcNAcase (OGA) (EC 3.2.1.169) (Beta-N-acetylhexosaminidase) (Beta-hexosaminidase) (Bifunctional protein NCOAT) (Meningioma-expressed antigen 5) (N-acetyl-beta-D-glucosaminidase) (EC 3.2.1.52) (N-acetyl-beta-glucosaminidase)	0	1	1	3
Q6IFX2	Keratin, type I cytoskeletal 42 (Cytokeratin-42) (CK-42) (Keratin-17n) (Keratin-42) (K42) (Type I keratin Ka22)	0	1	1	3

UniProt ID	Protein names	$\Delta$ NLS+4FL Replicate Presence (n/5)	$\Delta$ NLS+2KQ Replicate Presence (n/5)	Total Replicate Presence (n/10)	Total Peptide Count
<b>O70503</b>	Very-long-chain 3-oxoacyl-CoA reductase (EC 1.1.1.330) (17-beta-hydroxysteroid dehydrogenase 12) (17-beta-HSD 12) (3-ketoacyl-CoA reductase) (KAR) (Estradiol 17-beta-dehydrogenase 12) (EC 1.1.1.62) (KIK-I)	0	1	1	3
<b>P29788</b>	Vitronectin (VN) (S-protein) (Serum-spreading factor)	0	1	1	3
<b>Q5RI75</b>	Ras and EF-hand domain-containing protein homolog	0	1	1	2
<b>Q80YPO</b>	Cyclin-dependent kinase 3 (EC 2.7.11.22) (Cell division protein kinase 3)	0	1	1	2
<b>P52432</b>	DNA-directed RNA polymerases I and III subunit RPAC1 (DNA-directed RNA polymerase I subunit C) (RNA polymerases I and III subunit AC1) (AC40) (DNA-directed RNA polymerases I and III 40 kDa polypeptide) (RPA40) (RPC40)	0	1	1	2
<b>Q91V12</b>	Cytosolic acyl coenzyme A thioester hydrolase (EC 3.1.2.2) (Acyl-CoA thioesterase 7) (Brain acyl-CoA hydrolase) (BACH) (CTE-IIa) (CTE-II) (Long chain acyl-CoA thioester hydrolase)	0	1	1	2
<b>Q9CYR6</b>	Phosphoacetylglucosamine mutase (PAGM) (EC 5.4.2.3) (Acetylglucosamine phosphomutase) (N-acetylglucosamine-phosphate mutase) (Phosphoglucomutase-3) (PGM 3)	0	1	1	2
<b>P40124</b>	Adenylyl cyclase-associated protein 1 (CAP 1)	0	1	1	2
<b>Q4KWH5</b>	1-phosphatidylinositol 4,5-bisphosphate phosphodiesterase eta-1 (EC 3.1.4.11) (Phosphoinositide phospholipase C-eta-1) (Phospholipase C-eta-1) (PLC-eta-1) (Phospholipase C-like protein 3) (PLC-L3)	0	1	1	2
<b>Q7TMF3</b>	NADH dehydrogenase [ubiquinone] 1 alpha subcomplex subunit 12 (Complex I-B17.2) (CI-B17.2) (CIB17.2) (NADH-ubiquinone oxidoreductase subunit B17.2)	0	1	1	2
<b>Q6A4J8</b>	Ubiquitin carboxyl-terminal hydrolase 7 (EC 3.4.19.12) (Deubiquitinating enzyme 7) (Herpesvirus-associated ubiquitin-specific protease) (mHAUSP) (Ubiquitin thioesterase 7) (Ubiquitin-specific-processing protease 7)	0	1	1	2
<b>P08775</b>	DNA-directed RNA polymerase II subunit RPB1 (RNA polymerase II subunit B1) (EC 2.7.7.6) (DNA-directed RNA polymerase II subunit A) (DNA-directed RNA polymerase III largest subunit)	0	1	1	2
<b>Q58Y75</b>	Adhesion G-protein coupled receptor F3 (G-protein coupled receptor 113) (G-protein coupled receptor PGR23)	0	1	1	2

UniProt ID	Protein names	$\Delta$ NLS+4FL Replicate Presence (n/5)	$\Delta$ NLS+2KQ Replicate Presence (n/5)	Total Replicate Presence (n/10)	Total Peptide Count
Q9CWH5	tRNA (guanine(10)-N2)-methyltransferase homolog (EC 2.1.1.-) (tRNA guanosine-2'-O-methyltransferase TRM11 homolog)	0	1	1	2
Q920L1	Fatty acid desaturase 1 (EC 1.14.19.-) (Delta(5) fatty acid desaturase) (D5D) (Delta(5) desaturase) (Delta-5 desaturase)	0	1	1	2
P97370	Sodium/potassium-transporting ATPase subunit beta-3 (Sodium/potassium-dependent ATPase subunit beta-3) (ATPB-3) (CD antigen CD298)	0	1	1	2
Q9WUA2	Phenylalanine--tRNA ligase beta subunit (EC 6.1.1.20) (Phenylalanyl-tRNA synthetase beta subunit) (PheRS)	0	1	1	2
Q62465	Synaptic vesicle membrane protein VAT-1 homolog (EC 1.-.-.-)	0	1	1	2
O35887	Calumenin (Crocabin)	0	1	1	2
Q9CQE8	UPF0568 protein C14orf166 homolog	0	1	1	2
Q99PG2	Opioid growth factor receptor (OGFr) (Zeta-type opioid receptor)	0	1	1	2
Q9CQQ7	ATP synthase F(0) complex subunit B1, mitochondrial (ATP synthase subunit b) (ATPase subunit b)	0	1	1	2
P99028	Cytochrome b-c1 complex subunit 6, mitochondrial (Complex III subunit 6) (Complex III subunit VIII) (Cytochrome c1 non-heme 11 kDa protein) (Mitochondrial hinge protein) (Ubiquinol-cytochrome c reductase complex 11 kDa protein)	0	1	1	2
P97372	Proteasome activator complex subunit 2 (11S regulator complex subunit beta) (REG-beta) (Activator of multicatalytic protease subunit 2) (Proteasome activator 28 subunit beta) (PA28b) (PA28beta)	0	1	1	2
P59016	Vacuolar protein sorting-associated protein 33B	0	1	1	2
Q9WTI7	Unconventional myosin-Ic (Myosin I beta) (MMI-beta) (MMIb)	0	1	1	2
Q6DVA0	LEM domain-containing protein 2 (Nuclear envelope transmembrane protein 25) (NET25)	0	1	1	2
P00342	L-lactate dehydrogenase C chain (LDH-C) (EC 1.1.1.27) (LDH testis subunit) (LDH-X)	0	1	1	2
Q2NL51	Glycogen synthase kinase-3 alpha (GSK-3 alpha) (EC 2.7.11.26) (Serine/threonine-protein kinase GSK3A) (EC 2.7.11.1)	0	1	1	2

UniProt ID	Protein names	$\Delta$ NLS+4FL Replicate Presence (n/5)	$\Delta$ NLS+2KQ Replicate Presence (n/5)	Total Replicate Presence (n/10)	Total Peptide Count
Q04859	Serine/threonine-protein kinase MAK (EC 2.7.11.1) (Male germ cell-associated kinase) (Protein kinase RCK)	0	1	1	2
Q80VQ0	Aldehyde dehydrogenase family 3 member B1 (EC 1.2.1.5) (Aldehyde dehydrogenase 7)	0	1	1	2
P46467	Vacuolar protein sorting-associated protein 4B (EC 3.6.4.6) (Suppressor of K(+) transport growth defect 1) (Protein SKD1)	0	1	1	2
A2AN08	E3 ubiquitin-protein ligase UBR4 (EC 2.3.2.27) (N-recognin-4) (RING-type E3 ubiquitin transferase UBR4) (Zinc finger UBR1-type protein 1) (p600)	0	1	1	2
Q9R049	E3 ubiquitin-protein ligase AMFR (EC 2.3.2.27) (Autocrine motility factor receptor) (AMF receptor) (RING-type E3 ubiquitin transferase AMFR)	0	1	1	2
P28028	Serine/threonine-protein kinase B-raf (EC 2.7.11.1) (Proto-oncogene B-Raf)	0	1	1	2
A2AIV8	Caspase recruitment domain-containing protein 9	0	1	1	1
Q8VCP8	Adenylate kinase isoenzyme 6 (AK6) (EC 2.7.4.3) (Coilin-interacting nuclear ATPase protein) (Dual activity adenylate kinase/ATPase) (AK/ATPase)	0	1	1	1
Q3URD3	Sarcolemmal membrane-associated protein (Sarcolemmal-associated protein)	0	1	1	1
Q91WU5	Arsenite methyltransferase (EC 2.1.1.137) (Methylarsonite methyltransferase) (S-adenosyl-L-methionine:arsenic(III) methyltransferase)	0	1	1	1
Q61508	Extracellular matrix protein 1 (Secretory component p85)	0	1	1	1
P15508	Spectrin beta chain, erythrocytic (Beta-I spectrin)	0	1	1	1
Q8R311	Endoplasmic reticulum export factor CTAGE5 (cTAGE family member 5)	0	1	1	1
Q9CWU9	Nucleoporin Nup37 (Nup107-160 subcomplex subunit Nup37)	0	1	1	1
Q9QZ88	Vacuolar protein sorting-associated protein 29 (Vesicle protein sorting 29)	0	1	1	1
P26883	Peptidyl-prolyl cis-trans isomerase FKBP1A (PPIase FKBP1A) (EC 5.2.1.8) (12 kDa FK506-binding protein) (12 kDa FKBP) (FKBP-12) (Calstabin-1) (FK506-binding protein 1A) (FKBP-1A) (Immunophilin FKBP12) (Rotamase)	0	1	1	1
Q6ZQ12	Ninein-like protein	0	1	1	1
A9Q751	Cilia- and flagella-associated protein 221 (Primary ciliary dyskinesia protein 1)	0	1	1	1

UniProt ID	Protein names	$\Delta$ NLS+4FL Replicate Presence (n/5)	$\Delta$ NLS+2KQ Replicate Presence (n/5)	Total Replicate Presence (n/10)	Total Peptide Count
Q9CYG7	Mitochondrial import receptor subunit TOM34 (Translocase of outer membrane 34 kDa subunit)	0	1	1	1
Q9JHR7	Insulin-degrading enzyme (EC 3.4.24.56) (Insulin protease) (Insulinase) (Insulysin)	0	1	1	1
Q9QZE7	Translin-associated protein X (Translin-associated factor X)	0	1	1	1
Q9ESP1	Stromal cell-derived factor 2-like protein 1 (SDF2-like protein 1)	0	1	1	1
Q9CWW1	DNA helicase MCM8 (EC 3.6.4.12) (Minichromosome maintenance 8)	0	1	1	1
P63073	Eukaryotic translation initiation factor 4E (eIF-4E) (eIF4E) (mRNA cap-binding protein) (eIF-4F 25 kDa subunit)	0	1	1	1
O88545	COP9 signalosome complex subunit 6 (SGN6) (Signalosome subunit 6) (JAB1-containing signalosome subunit 6)	0	1	1	1
Q6PD26	GPI transamidase component PIG-S (Phosphatidylinositol-glycan biosynthesis class S protein)	0	1	1	1
Q9D365	Adipocyte-related X-chromosome expressed sequence 1 Adipocyte-related X-chromosome expressed sequence 2	0	1	1	1
Q9D855	Cytochrome b-c1 complex subunit 7 (Complex III subunit 7) (Complex III subunit VII) (Ubiquinol-cytochrome c reductase complex 14 kDa protein)	0	1	1	1
Q8BWM0	Prostaglandin E synthase 2 (EC 5.3.99.3) (GATE-binding factor 1) (GBF-1) (Microsomal prostaglandin E synthase 2) (mPGES-2) [Cleaved into: Prostaglandin E synthase 2 truncated form]	0	1	1	1
Q91VH6	Protein MEMO1 (Mediator of ErbB2-driven cell motility 1) (Memo-1)	0	1	1	1
Q8BIF2	RNA binding protein fox-1 homolog 3 (Fox-1 homolog C) (Hexaribonucleotide-binding protein 3) (Fox-3) (Neuronal nuclei antigen) (NeuN antigen)	0	1	1	1
Q7TPD0	Integrator complex subunit 3 (Int3) (SOSS complex subunit A) (Sensor of single-strand DNA complex subunit A) (SOSS-A) (Sensor of ssDNA subunit A)	0	1	1	1

UniProt ID	Protein names	$\Delta$ NLS+4FL Replicate Presence (n/5)	$\Delta$ NLS+2KQ Replicate Presence (n/5)	Total Replicate Presence (n/10)	Total Peptide Count
Q3UA06	Pachytene checkpoint protein 2 homolog (Thyroid hormone receptor interactor 13) (Thyroid receptor-interacting protein 13) (TR-interacting protein 13) (TRIP-13)	0	1	1	1
Q8BH58	TIP41-like protein	0	1	1	1
Q9JII6	Alcohol dehydrogenase [NADP(+)] (EC 1.1.1.2) (Aldehyde reductase) (Aldo-keto reductase family 1 member A1)	0	1	1	1
Q8JZRO	Long-chain-fatty-acid--CoA ligase 5 (EC 6.2.1.3) (Long-chain acyl-CoA synthetase 5) (LACS 5)	0	1	1	1
Q8BIJ6	Isoleucine--tRNA ligase, mitochondrial (EC 6.1.1.5) (Isoleucyl-tRNA synthetase) (IleRS)	0	1	1	1
Q8BMG7	Rab3 GTPase-activating protein non-catalytic subunit (Rab3 GTPase-activating protein 150 kDa subunit) (Rab3-GAP p150) (Rab3-GAP150) (Rab3-GAP regulatory subunit)	0	1	1	1
Q8K4F6	Probable 28S rRNA (cytosine-C(5))-methyltransferase (EC 2.1.1.-) (NOL1/NOP2/Sun domain family member 5) (Williams-Beuren syndrome chromosomal region 20A protein homolog)	0	1	1	1
Q7TT37	Elongator complex protein 1 (ELP1) (IkappaB kinase complex-associated protein) (IKK complex-associated protein)	0	1	1	1
Q62186	Translocon-associated protein subunit delta (TRAP-delta) (Signal sequence receptor subunit delta) (SSR-delta)	0	1	1	1
Q9Z0E0	Neurochondrin (M-Sema F-associating protein of 75 kDa) (Norbin)	0	1	1	1
P47791	Glutathione reductase, mitochondrial (GR) (GRase) (EC 1.8.1.7)	0	1	1	1
P60670	Nuclear protein localization protein 4 homolog (Protein NPL4)	0	1	1	1
Q60676	Serine/threonine-protein phosphatase 5 (PP5) (EC 3.1.3.16) (Protein phosphatase T) (PPT)	0	1	1	1
P46664	Adenylosuccinate synthetase isozyme 2 (AMPSase 2) (AdSS 2) (EC 6.3.4.4) (Adenylosuccinate synthetase, acidic isozyme) (Adenylosuccinate synthetase, liver isozyme) (L-type adenylosuccinate synthetase) (IMP--aspartate ligase 2)	0	1	1	1
Q07813	Apoptosis regulator BAX	0	1	1	1
Q80VJ3	2'-deoxynucleoside 5'-phosphate N-hydrolase 1 (EC 3.2.2.-) (c-Myc-responsive protein Rcl)	0	1	1	1
Q9DBE8	Alpha-1,3/1,6-mannosyltransferase ALG2 (EC 2.4.1.132) (EC 2.4.1.257) (Asparagine-linked glycosylation protein 2 homolog) (GDP-Man:Man(1)GlcNAc(2)-PP-Dol alpha-1,3-	0	1	1	1

UniProt ID	Protein names	$\Delta$ NLS+4FL Replicate Presence (n/5)	$\Delta$ NLS+2KQ Replicate Presence (n/5)	Total Replicate Presence (n/10)	Total Peptide Count
	mannosyltransferase) (GDP-Man:Man(1)GlcNAc(2)-PP-dolichol mannosyltransferase) (GDP-Man:Man(2)GlcNAc(2)-PP-Dol alpha-1,6-mannosyltransferase)				
<b>Q8VEH3</b>	ADP-ribosylation factor-like protein 8A (ADP-ribosylation factor-like protein 10B) (Novel small G protein indispensable for equal chromosome segregation 2)	0	1	1	1
<b>Q8CGF1</b>	Rho GTPase-activating protein 29 (Rho-type GTPase-activating protein 29)	0	1	1	1
<b>Q9WTX5</b>	S-phase kinase-associated protein 1 (Cyclin-A/CDK2-associated protein p19) (S-phase kinase-associated protein 1A) (p19A) (p19skp1)	0	1	1	1
<b>Q91W53</b>	Golgin subfamily A member 7	0	1	1	1
<b>Q8C0L8</b>	Conserved oligomeric Golgi complex subunit 5 (COG complex subunit 5) (Component of oligomeric Golgi complex 5)	0	1	1	1
<b>P35123</b>	Ubiquitin carboxyl-terminal hydrolase 4 (EC 3.4.19.12) (Deubiquitinating enzyme 4) (Ubiquitin thioesterase 4) (Ubiquitin-specific-processing protease 4) (Ubiquitous nuclear protein)	0	1	1	1
<b>Q921I9</b>	Exosome complex component RRP41 (Exosome component 4) (Ribosomal RNA-processing protein 41)	0	1	1	1
<b>Q9JK81</b>	UPF0160 protein MYG1, mitochondrial (Protein Gamm1)	0	1	1	1
<b>Q62426</b>	Cystatin-B (Stefin-B)	0	1	1	1
<b>Q8R1V4</b>	Transmembrane emp24 domain-containing protein 4 (Endoplasmic reticulum stress-response protein 25) (ERS25) (p24 family protein alpha-3) (p24alpha3) (p26)	0	1	1	1
<b>Q8BSP2</b>	Condensin-2 complex subunit H2 (Kleisin-beta) (Non-SMC condensin II complex subunit H2)	0	1	1	1
<b>Q9CQA1</b>	Trafficking protein particle complex subunit 5	0	1	1	1
<b>Q5FWI3</b>	Cell surface hyaluronidase (EC 3.2.1.35) (Transmembrane protein 2)	0	1	1	1
<b>Q99LI2</b>	Chloride channel CLIC-like protein 1	0	1	1	1
<b>Q8C522</b>	Endonuclease domain-containing 1 protein (EC 3.1.30.-)	0	1	1	1
<b>P25322</b>	G1/S-specific cyclin-D1	0	1	1	1
<b>P59325</b>	Eukaryotic translation initiation factor 5 (eIF-5)	0	1	1	1

UniProt ID	Protein names	$\Delta$ NLS+4FL Replicate Presence (n/5)	$\Delta$ NLS+2KQ Replicate Presence (n/5)	Total Replicate Presence (n/10)	Total Peptide Count
Q9Z2X2	26S proteasome non-ATPase regulatory subunit 10 (26S proteasome regulatory subunit p28) (Gankyrin)	0	1	1	1
Q8BI84	Transport and Golgi organization protein 1 homolog (TANGO1) (Melanoma inhibitory activity protein 3)	0	1	1	1
P61327	Protein mago nashi homolog	0	1	1	1
P62838	Ubiquitin-conjugating enzyme E2 D2 (EC 2.3.2.23) ((E3-independent) E2 ubiquitin-conjugating enzyme D2) (EC 2.3.2.24) (E2 ubiquitin-conjugating enzyme D2) (Ubiquitin carrier protein D2) (Ubiquitin-conjugating enzyme E2(17)KB 2) (Ubiquitin-conjugating enzyme E2-17 kDa 2) (Ubiquitin-protein ligase D2)	0	1	1	1
Q9DBG5	Perilipin-3 (Cargo selection protein TIP47) (Mannose-6-phosphate receptor-binding protein 1)	0	1	1	1
Q9WTX8	Mitotic spindle assembly checkpoint protein MAD1 (Mitotic arrest deficient 1-like protein 1) (MAD1-like protein 1)	0	1	1	1
Q8BME9	Cerebellin-4 (Cerebellin-like glycoprotein 1)	0	1	1	1
P11688	Integrin alpha-5 (CD49 antigen-like family member E) (Fibronectin receptor subunit alpha) (Integrin alpha-F) (VLA-5) (CD antigen CD49e) [Cleaved into: Integrin alpha-5 heavy chain; Integrin alpha-5 light chain]	0	1	1	1
O88665	Bromodomain-containing protein 7 (75 kDa bromodomain protein)	0	1	1	1
Q8K1R3	Polyribonucleotide nucleotidyltransferase 1, mitochondrial (EC 2.7.7.8) (3'-5' RNA exonuclease OLD35) (PNPase old-35) (Polynucleotide phosphorylase 1) (PNPase 1) (Polynucleotide phosphorylase-like protein)	0	1	1	1
Q9JJK8	Serine/threonine-protein kinase ATR (EC 2.7.11.1) (Ataxia telangiectasia and Rad3-related protein)	0	1	1	1
Q9JI18	Low-density lipoprotein receptor-related protein 1B (LRP-1B) (Low-density lipoprotein receptor-related protein-deleted in tumor) (LRP-DIT)	0	1	1	1
Q3UHD3	Microtubule-associated tumor suppressor candidate 2 homolog (Cardiac zipper protein) (Microtubule plus-end tracking protein TIP150) (Tracking protein of 150 kDa)	0	1	1	1
Q9CWM4	Prefoldin subunit 1	0	1	1	1

UniProt ID	Protein names	$\Delta$ NLS+4FL Replicate Presence (n/5)	$\Delta$ NLS+2KQ Replicate Presence (n/5)	Total Replicate Presence (n/10)	Total Peptide Count
Q80ZA4	Fibrocystin-L (Polycystic kidney and hepatic disease 1-like protein 1) (PKHD1-like protein 1) (Protein D86)	0	1	1	1
Q8VCU0	Protein angel homolog 1	0	1	1	1
P81066	Iroquois-class homeodomain protein IRX-2 (Homeodomain protein IRXA2) (Iroquois homeobox protein 2) (Iroquois-class homeobox protein Irx6)	0	1	1	1
Q99MD9	Nuclear autoantigenic sperm protein (NASP)	0	1	1	1
P21180	Complement C2 (EC 3.4.21.43) (C3/C5 convertase) [Cleaved into: Complement C2b fragment; Complement C2a fragment]	0	1	1	1
P20612	Guanine nucleotide-binding protein G(t) subunit alpha-1 (Transducin alpha-1 chain)	0	1	1	1
Q5DTU0	Actin filament-associated protein 1-like 2 (AFAP1-like protein 2)	0	1	1	1
Q9JLT2	Trehalase (EC 3.2.1.28) (Alpha, alpha-trehalase) (Alpha, alpha-trehalose glucohydrolase)	0	1	1	1
Q99PP2	Zinc finger protein 318 (Testicular zinc finger protein) (Fragment)	0	1	1	1
Q64518	Sarcoplasmic/endoplasmic reticulum calcium ATPase 3 (SERCA3) (SR Ca(2+)-ATPase 3) (EC 3.6.3.8) (Calcium pump 3)	0	1	1	1
Q924S7	Sprouty-related, EVH1 domain-containing protein 2 (Spred-2)	0	1	1	1
Q9CZW4	Long-chain-fatty-acid--CoA ligase 3 (EC 6.2.1.3) (Long-chain acyl-CoA synthetase 3) (LACS 3)	0	1	1	1
Q9D0S9	Histidine triad nucleotide-binding protein 2, mitochondrial (HINT-2) (EC 3.-.-.-) (HINT-3)	0	1	1	1
Q8C0E3	Tripartite motif-containing protein 47	0	1	1	1
Q8BGE4	Sushi domain-containing protein 6 (Drago)	0	1	1	1
B9EJ86	Oxysterol-binding protein-related protein 8 (ORP-8) (OSBP-related protein 8)	0	1	1	1
Q8K411	Presequence protease, mitochondrial (EC 3.4.24.-) (Pitrilysin metalloproteinase 1)	0	1	1	1
Q61510	E3 ubiquitin/ISG15 ligase TRIM25 (EC 6.3.2.n3) (Estrogen-responsive finger protein) (RING-type E3 ubiquitin transferase) (EC 2.3.2.27) (RING-type E3 ubiquitin transferase TRIM25) (Tripartite motif-containing protein 25) (Ubiquitin/ISG15-conjugating enzyme TRIM25) (Zinc finger protein 147)	0	1	1	1

UniProt ID	Protein names	$\Delta$ NLS+4FL Replicate Presence (n/5)	$\Delta$ NLS+2KQ Replicate Presence (n/5)	Total Replicate Presence (n/10)	Total Peptide Count
O08582	GTP-binding protein 1 (G-protein 1) (GP-1) (GP1)	0	1	1	1
P36916	Guanine nucleotide-binding protein-like 1 (GTP-binding protein MMR1)	0	1	1	1
Q91YD9	Neural Wiskott-Aldrich syndrome protein (N-WASP)	0	1	1	1
O35615	Zinc finger protein ZFPM1 (Friend of GATA protein 1) (FOG-1) (Friend of GATA 1) (Zinc finger protein multitype 1)	0	1	1	1
P23506	Protein-L-isoaspartate(D-aspartate) O-methyltransferase (PIMT) (EC 2.1.1.77) (L-isoaspartyl protein carboxyl methyltransferase) (Protein L-isoaspartyl/D-aspartyl methyltransferase) (Protein-beta-aspartate methyltransferase)	0	1	1	1
Q8BW10	RNA-binding protein NOB1	0	1	1	1
Q9JIF0	Protein arginine N-methyltransferase 1 (EC 2.1.1.319) (Histone-arginine N-methyltransferase PRMT1)	0	1	1	1
Q8K2Z4	Condensin complex subunit 1 (Chromosome condensation-related SMC-associated protein 1) (Chromosome-associated protein D2) (mCAP-D2) (Non-SMC condensin I complex subunit D2) (XCAP-D2 homolog)	0	1	1	1
Q99KD5	Protein unc-45 homolog A (Unc-45A) (Stromal membrane-associated protein 1) (SMAP-1)	0	1	1	1
Q99PG6	Taste receptor type 1 member 1 (G-protein coupled receptor 70)	0	1	1	1
P46978	Dolichyl-diphosphooligosaccharide--protein glycosyltransferase subunit STT3A (Oligosaccharyl transferase subunit STT3A) (STT3-A) (EC 2.4.99.18) (B5) (Integral membrane protein 1)	0	1	1	1
Q8C0N1	Kinesin-like protein KIF2B	0	1	1	1
Q9Z0R9	Fatty acid desaturase 2 (EC 1.14.19.-) (Delta(6) fatty acid desaturase) (D6D) (Delta(6) desaturase) (Delta-6 desaturase)	0	1	1	1
O08747	Netrin receptor UNC5C (Protein unc-5 homolog 3) (Protein unc-5 homolog C) (Rostral cerebellar malformation protein)	0	1	1	1
O35345	Importin subunit alpha-7 (Importin alpha-S2) (Karyopherin subunit alpha-6)	0	1	1	1
Q8BY71	Histone acetyltransferase type B catalytic subunit (EC 2.3.1.48) (Histone acetyltransferase 1)	0	1	1	1
P55264	Adenosine kinase (AK) (EC 2.7.1.20) (Adenosine 5'-phosphotransferase)	0	1	1	1

UniProt ID	Protein names	$\Delta$ NLS+4FL Replicate Presence (n/5)	$\Delta$ NLS+2KQ Replicate Presence (n/5)	Total Replicate Presence (n/10)	Total Peptide Count
Q9D394	Protein RUFY3 (Rap2-interacting protein x) (RIPx) (Single axon-regulated protein 1) (Singar1)	0	1	1	1

Appendix C – All proteins identified as exclusive in the Urea-soluble fractions from the NEFH-tTA/tetO-hTDP-43 rNLS transgenic mice

UniProt ID	Protein names	Biological Replicate Peptide Count					Total Replicate Presence (n/5)	Total Peptide Count
		1	2	3	4	5		
<b>P07901</b>	Heat shock protein HSP 90-alpha (Heat shock 86 kDa) (HSP 86) (HSP86) (Tumor-specific transplantation 86 kDa antigen) (TSTA)	4	5	4	4	6	5	23
<b>P05064</b>	Fructose-bisphosphate aldolase A (EC 4.1.2.13) (Aldolase 1) (Muscle-type aldolase)	5	2	2	1	4	5	14
<b>P30275</b>	Creatine kinase U-type, mitochondrial (EC 2.7.3.2) (Acidic-type mitochondrial creatine kinase) (Mia-CK) (Ubiquitous mitochondrial creatine kinase) (U-MtCK)	2	2	2	3	4	5	13
<b>P97427</b>	Dihydropyrimidinase-related protein 1 (DRP-1) (Collapsin response mediator protein 1) (CRMP-1) (Unc-33-like phosphoprotein 3) (ULIP-3)	4	2	0	2	4	4	12
<b>Q3TXX4</b>	Vesicular glutamate transporter 1 (VGluT1) (Brain-specific Na(+)-dependent inorganic phosphate cotransporter) (Solute carrier family 17 member 7)	2	2	1	2	0	4	7
<b>Q9CQZ5</b>	NADH dehydrogenase [ubiquinone] 1 alpha subcomplex subunit 6 (Complex I-B14) (CI-B14) (NADH-ubiquinone oxidoreductase B14 subunit)	0	1	1	1	2	4	5
<b>B2RSH2</b>	Guanine nucleotide-binding protein G(i) subunit alpha-1 (Adenylate cyclase-inhibiting G alpha protein)	3	4	3	0	0	3	10
<b>Q9CQD1</b>	Ras-related protein Rab-5A	4	3	0	0	3	3	10
<b>P08752</b>	Guanine nucleotide-binding protein G(i) subunit alpha-2 (Adenylate cyclase-inhibiting G alpha protein)	0	4	3	0	2	3	9
<b>Q5SYD0</b>	Unconventional myosin-IId	3	0	3	0	2	3	8
<b>P05201</b>	Aspartate aminotransferase, cytoplasmic (cAspAT) (EC 2.6.1.1) (EC 2.6.1.3) (Cysteine aminotransferase, cytoplasmic) (Cysteine transaminase, cytoplasmic) (cCAT) (Glutamate oxaloacetate transaminase 1) (Transaminase A)	3	0	1	0	2	3	6
<b>Q8BGQ7</b>	Alanine--tRNA ligase, cytoplasmic (EC 6.1.1.7) (Alanyl-tRNA synthetase) (AlaRS)	3	2	1	0	0	3	6

UniProt ID	Protein names	Biological Replicate Peptide Count					Total Replicate Presence (n/5)	Total Peptide Count
		1	2	3	4	5		
A2A8L5	Receptor-type tyrosine-protein phosphatase F (EC 3.1.3.48) (Leukocyte common antigen related) (LAR)	2	0	2	2	0	3	6
Q9DCJ5	NADH dehydrogenase [ubiquinone] 1 alpha subcomplex subunit 8 (Complex I-19kD) (CI-19kD) (Complex I-PGIV) (CI-PGIV) (NADH-ubiquinone oxidoreductase 19 kDa subunit)	0	0	1	1	2	3	4
Q8BX10	Serine/threonine-protein phosphatase PGAM5, mitochondrial (EC 3.1.3.16) (Phosphoglycerate mutase family member 5)	0	0	1	2	1	3	4
Q8QZT1	Acetyl-CoA acetyltransferase, mitochondrial (EC 2.3.1.9) (Acetoacetyl-CoA thiolase)	2	0	1	1	0	3	4
Q5GH67	XK-related protein 4	2	1	1	0	0	3	4
P62908	40S ribosomal protein S3 (EC 4.2.99.18)	0	0	1	1	1	3	3
P15209	BDNF/NT-3 growth factors receptor (EC 2.7.10.1) (GP145-TrkB/GP95-TrkB) (Trk-B) (Neurotrophic tyrosine kinase receptor type 2) (TrkB tyrosine kinase)	1	1	0	0	1	3	3
P63268	Actin, gamma-enteric smooth muscle (Alpha-actin-3) (Gamma-2-actin) (Smooth muscle gamma-actin)	15	12	0	0	0	2	27
P62880	Guanine nucleotide-binding protein G(I)/G(S)/G(T) subunit beta-2 (G protein subunit beta-2) (Transducin beta chain 2)	4	4	0	0	0	2	8
Q8CI94	Glycogen phosphorylase, brain form (EC 2.4.1.1)	0	2	0	5	0	2	7
Q6URW6	Myosin-14 (Myosin heavy chain 14) (Myosin heavy chain, non-muscle IIc) (Non-muscle myosin heavy chain IIc) (NMHC II-C)	0	0	5	2	0	2	7
Q8VCW2	Keratin, type I cytoskeletal 25 (Cytokeratin-25) (CK-25) (Keratin-25) (K25) (Type I inner root sheath-specific keratin-K25irs1) (mIRSa1)	2	0	0	3	0	2	5
P21278	Guanine nucleotide-binding protein subunit alpha-11 (G alpha-11) (G-protein subunit alpha-11)	3	2	0	0	0	2	5
P29387	Guanine nucleotide-binding protein subunit beta-4 (Transducin beta chain 4)	0	0	2	0	3	2	5
Q3UIU2	NADH dehydrogenase [ubiquinone] 1 beta subcomplex subunit 6 (Complex I-B17) (CI-B17) (NADH-ubiquinone oxidoreductase B17 subunit)	2	0	0	0	2	2	4

UniProt ID	Protein names	Biological Replicate Peptide Count					Total Replicate Presence (n/5)	Total Peptide Count
		1	2	3	4	5		
P53026	60S ribosomal protein L10a (CSA-19) (Neural precursor cell expressed developmentally down-regulated protein 6) (NEDD-6)	0	0	0	2	2	2	4
Q8CCK0	Core histone macro-H2A.2 (Histone macroH2A2) (mH2A2)	0	0	0	1	3	2	4
Q9JII6	Alcohol dehydrogenase [NADP(+)] (EC 1.1.1.2) (Aldehyde reductase) (Aldo-keto reductase family 1 member A1)	2	2	0	0	0	2	4
P97807	Fumarate hydratase, mitochondrial (Fumarase) (EC 4.2.1.2) (EF-3)	2	0	0	0	2	2	4
P35550	rRNA 2'-O-methyltransferase fibrillarin (EC 2.1.1.-) (Histone-glutamine methyltransferase) (Nucleolar protein 1)	2	0	0	0	2	2	4
Q3UTJ2	Sorbin and SH3 domain-containing protein 2 (Arg-binding protein 2) (ArgBP2) (Arg/Abl-interacting protein 2)	3	0	0	0	1	2	4
Q99020	Heterogeneous nuclear ribonucleoprotein A/B (hnRNP A/B) (CARG-binding factor-A) (CBF-A)	0	0	2	0	1	2	3
Q9DB20	ATP synthase subunit O, mitochondrial (Oligomycin sensitivity conferral protein) (OSCP)	0	0	0	2	1	2	3
P23927	Alpha-crystallin B chain (Alpha(B)-crystallin) (P23)	0	0	0	1	2	2	3
Q6P1F6	Serine/threonine-protein phosphatase 2A 55 kDa regulatory subunit B alpha isoform (PP2A subunit B isoform B55-alpha) (PP2A subunit B isoform PR55-alpha) (PP2A subunit B isoform R2-alpha) (PP2A subunit B isoform alpha)	2	0	1	0	0	2	3
P11983	T-complex protein 1 subunit alpha (TCP-1-alpha) (CCT-alpha) (Tailless complex polypeptide 1A) (TCP-1-A) (Tailless complex polypeptide 1B) (TCP-1-B)	2	0	0	0	1	2	3
O35405	Phospholipase D3 (PLD 3) (EC 3.1.4.4) (Choline phosphatase 3) (Phosphatidylcholine-hydrolyzing phospholipase D3) (Schwannoma-associated protein 9) (SAM-9)	2	0	0	0	1	2	3
P62881	Guanine nucleotide-binding protein subunit beta-5 (Gbeta5) (Transducin beta chain 5)	1	2	0	0	0	2	3
P16460	Argininosuccinate synthase (EC 6.3.4.5) (Citrulline--aspartate ligase)	2	0	0	0	1	2	3
Q9CQH3	NADH dehydrogenase [ubiquinone] 1 beta subcomplex subunit 5, mitochondrial (Complex I-SGDH) (CI-SGDH) (NADH-ubiquinone oxidoreductase SGDH subunit)	1	0	2	0	0	2	3

UniProt ID	Protein names	Biological Replicate Peptide Count					Total Replicate Presence (n/5)	Total Peptide Count
		1	2	3	4	5		
P17751	Triosephosphate isomerase (TIM) (EC 5.3.1.1) (Triose-phosphate isomerase)	2	0	0	0	1	2	3
Q60803	TNF receptor-associated factor 3 (EC 2.3.2.27) (CD40 receptor-associated factor 1) (CRAF1) (RING-type E3 ubiquitin transferase TRAF3) (TRAFAMN)	1	0	0	1	1	2	3
P27546	Microtubule-associated protein 4 (MAP-4)	1	0	0	0	2	2	3
Q99JB2	Stomatin-like protein 2, mitochondrial (SLP-2) (mslp2)	1	0	1	0	0	2	2
Q3UMR5	Calcium uniporter protein, mitochondrial	1	0	0	0	1	2	2
Q8K3J1	NADH dehydrogenase [ubiquinone] iron-sulfur protein 8, mitochondrial (EC 1.6.5.3) (EC 1.6.99.3) (Complex I-23kD) (CI-23kD) (NADH-ubiquinone oxidoreductase 23 kDa subunit)	0	1	1	0	0	2	2
P67871	Casein kinase II subunit beta (CK II beta) (Phosvitin)	0	1	1	0	0	2	2
Q02257	Junction plakoglobin (Desmoplakin III) (Desmoplakin-3)	0	1	0	0	1	2	2
Q9D6Z1	Nucleolar protein 56 (Nucleolar protein 5A)	0	0	1	1	0	2	2
Q64436	Potassium-transporting ATPase alpha chain 1 (EC 3.6.3.10) (Gastric H(+)/K(+) ATPase subunit alpha) (Proton pump)	0	0	1	1	0	2	2
Q6DFW4	Nucleolar protein 58 (MSSP) (Nucleolar protein 5) (SIK-similar protein)	0	0	0	1	1	2	2
O55125	Protein NipSnap homolog 1 (NipSnap1)	1	1	0	0	0	2	2
O08788	Dynactin subunit 1 (150 kDa dynein-associated polypeptide) (DAP-150) (DP-150) (p150-glued)	1	0	1	0	0	2	2
Q3UBG2	PTB-containing, cubilin and LRP1-interacting protein (P-CLI1) (Phosphotyrosine interaction domain-containing protein 1)	1	0	0	1	0	2	2
P63038	60 kDa heat shock protein, mitochondrial (EC 3.6.4.9) (60 kDa chaperonin) (Chaperonin 60) (CPN60) (HSP-65) (Heat shock protein 60) (HSP-60) (Hsp60) (Mitochondrial matrix protein P1)	1	0	0	1	0	2	2

UniProt ID	Protein names	Biological Replicate Peptide Count					Total Replicate Presence (n/5)	Total Peptide Count
		1	2	3	4	5		
P04370	Myelin basic protein (MBP) (Myelin A1 protein)	1	0	0	0	1	2	2
P68404	Protein kinase C beta type (PKC-B) (PKC-beta) (EC 2.7.11.13)	1	0	0	1	0	2	2
Q9CR68	Cytochrome b-c1 complex subunit Rieske, mitochondrial (EC 1.10.2.2) (Complex III subunit 5) (Cytochrome b-c1 complex subunit 5) (Rieske iron-sulfur protein) (RISP) (Ubiquinol-cytochrome c reductase iron-sulfur subunit) [Cleaved into: Cytochrome b-c1 complex subunit 11 (Complex III subunit IX) (Ubiquinol-cytochrome c reductase 8 kDa protein)]	1	0	1	0	0	2	2
Q8BWF0	Succinate-semialdehyde dehydrogenase, mitochondrial (EC 1.2.1.24) (Aldehyde dehydrogenase family 5 member A1) (NAD(+)-dependent succinic semialdehyde dehydrogenase)	1	0	0	0	1	2	2
Q9QYB8	Beta-adducin (Add97) (Erythrocyte adducin subunit beta)	1	0	0	1	0	2	2
Q8K2T1	NmrA-like family domain-containing protein 1	1	0	0	0	1	2	2
Q9D6R2	Isocitrate dehydrogenase [NAD] subunit alpha, mitochondrial (EC 1.1.1.41) (Isocitric dehydrogenase subunit alpha) (NAD(+)-specific ICDH subunit alpha)	1	1	0	0	0	2	2
Q9WUC3	Lymphocyte antigen 6H (Ly-6H)	1	1	0	0	0	2	2
Q60605	Myosin light polypeptide 6 (17 kDa myosin light chain) (LC17) (Myosin light chain 3) (MLC-3) (Myosin light chain alkali 3) (Myosin light chain A3) (Smooth muscle and nonmuscle myosin light chain alkali 6)	1	0	1	0	0	2	2
P61750	ADP-ribosylation factor 4	1	0	0	0	1	2	2
P68373	Tubulin alpha-1C chain (Alpha-tubulin 6) (Alpha-tubulin isotype M-alpha-6) (Tubulin alpha-6 chain) [Cleaved into: Detyrosinated tubulin alpha-1C chain]	13	0	0	0	0	1	13
Q6Q477	Plasma membrane calcium-transporting ATPase 4 (PMCA4) (EC 3.6.3.8)	6	0	0	0	0	1	6
P07744	Keratin, type II cytoskeletal 4 (Cytokeratin-4) (CK-4) (Cytoskeletal 57 kDa keratin) (Keratin-4) (K4) (Type-II keratin Kb4)	4	0	0	0	0	1	4

UniProt ID	Protein names	Biological Replicate Peptide Count					Total Replicate Presence (n/5)	Total Peptide Count
		1	2	3	4	5		
<b>Q7TMB8</b>	Cytoplasmic FMR1-interacting protein 1 (Specifically Rac1-associated protein 1) (Sra-1)	4	0	0	0	0	1	4
<b>Q8BKZ9</b>	Pyruvate dehydrogenase protein X component, mitochondrial (Dihydrolipoamide dehydrogenase-binding protein of pyruvate dehydrogenase complex) (Lipoyl-containing pyruvate dehydrogenase complex component X)	0	0	0	3	0	1	3
<b>Q62188</b>	Dihydropyrimidinase-related protein 3 (DRP-3) (Unc-33-like phosphoprotein 1) (ULIP-1)	0	0	0	0	3	1	3
<b>Q9QUM9</b>	Proteasome subunit alpha type-6 (EC 3.4.25.1) (Macropain iota chain) (Multicatalytic endopeptidase complex iota chain) (Proteasome iota chain)	0	0	0	0	3	1	3
<b>P58252</b>	Elongation factor 2 (EF-2)	0	0	0	0	3	1	3
<b>P62874</b>	Guanine nucleotide-binding protein G(I)/G(S)/G(T) subunit beta-1 (Transducin beta chain 1)	3	0	0	0	0	1	3
<b>P50396</b>	Rab GDP dissociation inhibitor alpha (Rab GDI alpha) (Guanosine diphosphate dissociation inhibitor 1) (GDI-1)	3	0	0	0	0	1	3
<b>Q6IMF0</b>	Keratin, type II cuticular 87 (Keratin-87) (K87)	3	0	0	0	0	1	3
<b>P55012</b>	Solute carrier family 12 member 2 (Basolateral Na-K-Cl symporter) (Bumetanide-sensitive sodium-(potassium)-chloride cotransporter 1)	3	0	0	0	0	1	3
<b>Q9R0P9</b>	Ubiquitin carboxyl-terminal hydrolase isozyme L1 (UCH-L1) (EC 3.4.19.12) (EC 6.-.-.-) (Neuron cytoplasmic protein 9.5) (PGP 9.5) (PGP9.5) (Ubiquitin thioesterase L1)	0	2	0	0	0	1	2
<b>Q91X78</b>	Erlin-1 (Endoplasmic reticulum lipid raft-associated protein 1) (Protein KE04 homolog) (Stomatin-prohibitin-flotillin-HflC/K domain-containing protein 1) (SPFH domain-containing protein 1)	0	0	2	0	0	1	2
<b>Q3U381</b>	Zinc finger protein 692	0	0	2	0	0	1	2
<b>Q62465</b>	Synaptic vesicle membrane protein VAT-1 homolog (EC 1.-.-.-)	0	0	2	0	0	1	2
<b>P10922</b>	Histone H1.0 (Histone H1') (Histone H1(0)) (MyD196) [Cleaved into: Histone H1.0, N-terminally processed]	0	0	0	2	0	1	2

UniProt ID	Protein names	Biological Replicate Peptide Count					Total Replicate Presence (n/5)	Total Peptide Count
		1	2	3	4	5		
<b>Q8VHH5</b>	Arf-GAP with GTPase, ANK repeat and PH domain-containing protein 3 (AGAP-3) (CRAM-associated GTPase) (CRAG) (Centaurin-gamma-3) (Cnt-g3) (MR1-interacting protein) (MRIP-1)	0	0	0	2	0	1	2
<b>Q9Z2X1</b>	Heterogeneous nuclear ribonucleoprotein F (hnRNP F) [Cleaved into: Heterogeneous nuclear ribonucleoprotein F, N-terminally processed]	0	0	0	2	0	1	2
<b>P43277</b>	Histone H1.3 (H1 VAR.4) (H1d)	0	0	0	2	0	1	2
<b>Q9Z108</b>	Double-stranded RNA-binding protein Staufen homolog 1	0	0	0	2	0	1	2
<b>Q920R6</b>	V-type proton ATPase 116 kDa subunit a isoform 4 (V-ATPase 116 kDa isoform a4) (Vacuolar proton translocating ATPase 116 kDa subunit a isoform 4) (Vacuolar proton translocating ATPase 116 kDa subunit a kidney isoform)	0	0	0	2	0	1	2
<b>P29319</b>	Ephrin type-A receptor 3 (EC 2.7.10.1) (EPH-like kinase 4) (EK4) (mEK4) (Tyrosine-protein kinase TYRO4) (Tyrosine-protein kinase receptor ETK1)	0	0	0	2	0	1	2
<b>Q8CGP6</b>	Histone H2A type 1-H	0	0	0	0	2	1	2
<b>P29391</b>	Ferritin light chain 1 (Ferritin L subunit 1)	0	0	0	0	2	1	2
<b>Q9R1P0</b>	Proteasome subunit alpha type-4 (EC 3.4.25.1) (Macropain subunit C9) (Multicatalytic endopeptidase complex subunit C9) (Proteasome component C9) (Proteasome subunit L)	0	0	0	0	2	1	2
<b>Q60900</b>	ELAV-like protein 3 (Hu-antigen C) (HuC)	2	0	0	0	0	1	2
<b>Q9R118</b>	Serine protease HTRA1 (EC 3.4.21.-) (High-temperature requirement A serine peptidase 1) (Serine protease 11)	2	0	0	0	0	1	2
<b>Q8VDQ8</b>	NAD-dependent protein deacetylase sirtuin-2 (EC 3.5.1.-) (Regulatory protein SIR2 homolog 2) (SIR2-like protein 2) (mSIR2L2)	2	0	0	0	0	1	2
<b>Q6PER3</b>	Microtubule-associated protein RP/EB family member 3 (EB1 protein family member 3) (EBF3) (End-binding protein 3) (EB3) (RP3)	2	0	0	0	0	1	2
<b>P62482</b>	Voltage-gated potassium channel subunit beta-2 (EC 1.1.1.-) (K(+)) channel subunit beta-2) (Kv-beta-2) (Neuroimmune protein F5)	2	0	0	0	0	1	2

UniProt ID	Protein names	Biological Replicate Peptide Count					Total Replicate Presence (n/5)	Total Peptide Count
		1	2	3	4	5		
<b>Q8VCT3</b>	Aminopeptidase B (AP-B) (EC 3.4.11.6) (Arginine aminopeptidase) (Arginyl aminopeptidase) (Cytosol aminopeptidase IV)	2	0	0	0	0	1	2
<b>P10649</b>	Glutathione S-transferase Mu 1 (EC 2.5.1.18) (GST 1-1) (GST class-mu 1) (Glutathione S-transferase GT8.7) (pmGT10)	2	0	0	0	0	1	2
<b>Q6NS60</b>	F-box only protein 41	2	0	0	0	0	1	2
<b>Q61598</b>	Rab GDP dissociation inhibitor beta (Rab GDI beta) (GDI-3) (Guanosine diphosphate dissociation inhibitor 2) (GDI-2)	2	0	0	0	0	1	2
<b>O35495</b>	Cyclin-dependent kinase 14 (EC 2.7.11.22) (Cell division protein kinase 14) (Serine/threonine-protein kinase PFTAIR-1)	2	0	0	0	0	1	2
<b>Q9WU78</b>	Programmed cell death 6-interacting protein (ALG-2-interacting protein 1) (ALG-2-interacting protein X) (E2F1-inducible protein) (Eig2)	2	0	0	0	0	1	2
<b>Q8VBT6</b>	Apolipoprotein B receptor (Apolipoprotein B-100 receptor) (Apolipoprotein B48 receptor) (apoB-48R)	2	0	0	0	0	1	2
<b>Q80TL4</b>	PHD finger protein 24	2	0	0	0	0	1	2
<b>Q8K310</b>	Matrin-3	2	0	0	0	0	1	2
<b>Q9JJV2</b>	Profilin-2 (Profilin II)	1	0	0	0	0	1	1
<b>Q8B XK8</b>	Arf-GAP with GTPase, ANK repeat and PH domain-containing protein 1 (AGAP-1) (Centaurin-gamma-2) (Cnt-g2)	0	1	0	0	0	1	1
<b>Q68FF6</b>	ARF GTPase-activating protein GIT1 (ARF GAP GIT1) (G protein-coupled receptor kinase-interactor 1) (GRK-interacting protein 1)	0	1	0	0	0	1	1
<b>Q7M6Y3</b>	Phosphatidylinositol-binding clathrin assembly protein (Clathrin assembly lymphoid myeloid leukemia) (CALM)	0	1	0	0	0	1	1
<b>Q8BTG7</b>	Protein NDRG4 (N-myc downstream-regulated gene 4 protein) (Protein Ndr4)	0	1	0	0	0	1	1
<b>P48722</b>	Heat shock 70 kDa protein 4L (Heat shock 70-related protein APG-1) (Osmotic stress protein 94)	0	0	1	0	0	1	1

UniProt ID	Protein names	Biological Replicate Peptide Count					Total Replicate Presence (n/5)	Total Peptide Count
		1	2	3	4	5		
<b>Q3UGF1</b>	WD repeat-containing protein 19 (Intraflagellar transport 144 homolog)	0	0	1	0	0	1	1
<b>Q3TWN3</b>	Metal transporter CNNM2 (Ancient conserved domain-containing protein 2) (mACDP2) (Cyclin-M2)	0	0	1	0	0	1	1
<b>Q9CVB6</b>	Actin-related protein 2/3 complex subunit 2 (Arp2/3 complex 34 kDa subunit) (p34-ARC)	0	0	1	0	0	1	1
<b>Q8K341</b>	Alpha-tubulin N-acetyltransferase 1 (Alpha-TAT) (Alpha-TAT1) (TAT) (EC 2.3.1.108) (Acetyltransferase mec-17 homolog)	0	0	1	0	0	1	1
<b>Q3TXS7</b>	26S proteasome non-ATPase regulatory subunit 1 (26S proteasome regulatory subunit RPN2) (26S proteasome regulatory subunit S1)	0	0	1	0	0	1	1
<b>Q8CHK3</b>	Lysophospholipid acyltransferase 7 (LPLAT 7) (EC 2.3.1.-) (1-acylglycerophosphatidylinositol O-acyltransferase) (EC 2.3.1.n4) (Bladder and breast carcinoma-overexpressed gene 1 protein) (Leukocyte receptor cluster member 4) (Lysophosphatidylinositol acyltransferase 1) (LPIAT1) (Membrane-bound O-acyltransferase domain-containing protein 7) (O-acyltransferase domain-containing protein 7) (m-mboa-7)	0	0	1	0	0	1	1
<b>P52503</b>	NADH dehydrogenase [ubiquinone] iron-sulfur protein 6, mitochondrial (Complex I-13kD-A) (CI-13kD-A) (NADH-ubiquinone oxidoreductase 13 kDa-A subunit)	0	0	1	0	0	1	1
<b>P06795</b>	Multidrug resistance protein 1B (EC 3.6.3.44) (ATP-binding cassette sub-family B member 1B) (P-glycoprotein 1) (CD antigen CD243)	0	0	1	0	0	1	1
<b>Q9CPU4</b>	Microsomal glutathione S-transferase 3 (Microsomal GST-3) (EC 2.5.1.18) (Microsomal GST-III)	0	0	1	0	0	1	1
<b>Q9D2P8</b>	Myelin-associated oligodendrocyte basic protein	0	0	1	0	0	1	1
<b>P19096</b>	Fatty acid synthase (EC 2.3.1.85) [Includes: [Acyl-carrier-protein] S-acyltransferase (EC 2.3.1.38); [Acyl-carrier-protein] S-malonyltransferase (EC 2.3.1.39); 3-oxoacyl-[acyl-carrier-protein] synthase (EC 2.3.1.41); 3-oxoacyl-[acyl-carrier-protein] reductase (EC 1.1.1.100); 3-hydroxyacyl-[acyl-carrier-protein] dehydratase (EC 4.2.1.59); Enoyl-[acyl-carrier-protein] reductase (EC 1.3.1.39); Oleoyl-[acyl-carrier-protein] hydrolase (EC 3.1.2.14)]	0	0	1	0	0	1	1

UniProt ID	Protein names	Biological Replicate Peptide Count					Total Replicate Presence (n/5)	Total Peptide Count
		1	2	3	4	5		
<b>Q9CR62</b>	Mitochondrial 2-oxoglutarate/malate carrier protein (OGCP) (Solute carrier family 25 member 11)	0	0	1	0	0	1	1
<b>Q9JM13</b>	Rab5 GDP/GTP exchange factor (Rabex-5)	0	0	1	0	0	1	1
<b>Q9CPP6</b>	NADH dehydrogenase [ubiquinone] 1 alpha subcomplex subunit 5 (Complex I subunit B13) (Complex I-13kD-B) (CI-13kD-B) (NADH-ubiquinone oxidoreductase 13 kDa-B subunit)	0	0	1	0	0	1	1
<b>P39061</b>	Collagen alpha-1(XVIII) chain [Cleaved into: Endostatin]	0	0	0	1	0	1	1
<b>Q8BIF2</b>	RNA binding protein fox-1 homolog 3 (Fox-1 homolog C) (Hexaribonucleotide-binding protein 3) (Fox-3) (Neuronal nuclei antigen) (NeuN antigen)	0	0	0	1	0	1	1
<b>A2BDX3</b>	Adenylyltransferase and sulfurtransferase MOCS3 (Molybdenum cofactor synthesis protein 3) [Includes: Molybdopterin-synthase adenylyltransferase (EC 2.7.7.80) (Adenylyltransferase MOCS3) (Sulfur carrier protein MOCS2A adenylyltransferase); Molybdopterin-synthase sulfurtransferase (EC 2.8.1.11) (Sulfur carrier protein MOCS2A sulfurtransferase) (Sulfurtransferase MOCS3)]	0	0	0	1	0	1	1
<b>Q8BPN8</b>	DmX-like protein 2 (Rabconnectin-3)	0	0	0	1	0	1	1
<b>Q9CQS4</b>	Solute carrier family 25 member 46	0	0	0	1	0	1	1
<b>Q9CXZ1</b>	NADH dehydrogenase [ubiquinone] iron-sulfur protein 4, mitochondrial (Complex I-18 kDa) (CI-18 kDa) (Complex I-AQDQ) (CI-AQDQ) (NADH-ubiquinone oxidoreductase 18 kDa subunit)	0	0	0	1	0	1	1
<b>P43275</b>	Histone H1.1 (H1 VAR.3) (Histone H1a) (H1a)	0	0	0	1	0	1	1
<b>P49817</b>	Caveolin-1	0	0	0	1	0	1	1
<b>Q8C0C7</b>	Phenylalanine--tRNA ligase alpha subunit (EC 6.1.1.20) (Phenylalanyl-tRNA synthetase alpha subunit) (PheRS)	0	0	0	1	0	1	1
<b>Q9DC28</b>	Casein kinase I isoform delta (CKI-delta) (CKId) (EC 2.7.11.1) (Tau-protein kinase CSNK1D) (EC 2.7.11.26)	0	0	0	1	0	1	1

UniProt ID	Protein names	Biological Replicate Peptide Count					Total Replicate Presence (n/5)	Total Peptide Count
		1	2	3	4	5		
Q9JHJ0	Tropomodulin-3 (Ubiquitous tropomodulin) (U-Tmod)	0	0	0	1	0	1	1
Q9QYC0	Alpha-adducin (Erythrocyte adducin subunit alpha)	0	0	0	1	0	1	1
P80317	T-complex protein 1 subunit zeta (TCP-1-zeta) (CCT-zeta-1)	0	0	0	1	0	1	1
Q6ZQ18	Protein EFR3 homolog B	0	0	0	1	0	1	1
P43276	Histone H1.5 (H1 VAR.5) (H1b)	0	0	0	1	0	1	1
P21661	Neuroendocrine convertase 2 (NEC 2) (EC 3.4.21.94) (KEX2-like endoprotease 2) (Prohormone convertase 2) (Proprotein convertase 2) (PC2)	0	0	0	1	0	1	1
Q6P9R4	Rho guanine nucleotide exchange factor 18	0	0	0	0	1	1	1
Q99KJ8	Dynactin subunit 2 (50 kDa dynein-associated polypeptide) (Dynactin complex 50 kDa subunit) (DCTN-50) (Growth cone membrane protein 23-48K) (GMP23-48K) (p50 dynamitin)	0	0	0	0	1	1	1
Q68EF8	Rap guanine nucleotide exchange factor-like 1	0	0	0	0	1	1	1
Q9WU01	KH domain-containing, RNA-binding, signal transduction-associated protein 2 (Sam68-like mammalian protein 1) (SLM-1) (mSLM-1)	0	0	0	0	1	1	1
P40124	Adenylyl cyclase-associated protein 1 (CAP 1)	0	0	0	0	1	1	1
Q5XJV6	Serine/threonine-protein kinase LMTK3 (EC 2.7.11.1) (Apoptosis-associated tyrosine kinase 3) (Lemur tyrosine kinase 3)	0	0	0	0	1	1	1
Q9Z2W0	Aspartyl aminopeptidase (EC 3.4.11.21)	0	0	0	0	1	1	1
Q9CQI6	Coactosin-like protein	0	0	0	0	1	1	1
Q9R0Y5	Adenylate kinase isoenzyme 1 (AK 1) (EC 2.7.4.3) (EC 2.7.4.6) (ATP-AMP transphosphorylase 1) (ATP:AMP phosphotransferase) (Adenylate monophosphate kinase) (Myokinase)	0	0	0	0	1	1	1
Q6WKZ7	Nostrin (Disabled homolog 2-interacting protein 2) (Dab2-interacting protein 2) (Nitric oxide synthase trafficker) (eNOS-trafficking inducer)	0	0	0	0	1	1	1
Q14BI7	ATP-dependent RNA helicase TDRD9 (EC 3.6.4.13) (Tudor domain-containing protein 9)	0	0	0	0	1	1	1

UniProt ID	Protein names	Biological Replicate Peptide Count					Total Replicate Presence (n/5)	Total Peptide Count
		1	2	3	4	5		
Q99LR1	Monoacylglycerol lipase ABHD12 (EC 3.1.1.23) (2-arachidonoylglycerol hydrolase) (Abhydrolase domain-containing protein 12)	1	0	0	0	0	1	1
Q3ULJ0	Glycerol-3-phosphate dehydrogenase 1-like protein (EC 1.1.1.8)	1	0	0	0	0	1	1
Q8K400	Syntaxin-binding protein 5 (Lethal(2) giant larvae protein homolog 3) (Tomosyn-1)	1	0	0	0	0	1	1
Q925N0	Sideroflexin-5	1	0	0	0	0	1	1
Q9CYT6	Adenylyl cyclase-associated protein 2 (CAP 2)	1	0	0	0	0	1	1
Q9D880	Mitochondrial import inner membrane translocase subunit TIM50	1	0	0	0	0	1	1
Q04857	Collagen alpha-1(VI) chain	1	0	0	0	0	1	1
Q920U1	Tight junction protein ZO-2 (Tight junction protein 2) (Zona occludens protein 2) (Zonula occludens protein 2)	1	0	0	0	0	1	1
Q6GQS1	Calcium-binding mitochondrial carrier protein SCaMC-3 (Small calcium-binding mitochondrial carrier protein 3) (Solute carrier family 25 member 23)	1	0	0	0	0	1	1
P47738	Aldehyde dehydrogenase, mitochondrial (EC 1.2.1.3) (AHD-M1) (ALDH class 2) (ALDH-E2) (ALDHI)	1	0	0	0	0	1	1
Q9CPQ8	ATP synthase subunit g, mitochondrial (ATPase subunit g)	1	0	0	0	0	1	1
Q9CX30	Protein YIF1B (YIP1-interacting factor homolog B)	1	0	0	0	0	1	1
Q63959	Potassium voltage-gated channel subfamily C member 3 (KSHIID) (Voltage-gated potassium channel subunit Kv3.3)	1	0	0	0	0	1	1
Q9CZC8	Secernin-1	1	0	0	0	0	1	1
P51660	Peroxisomal multifunctional enzyme type 2 (MFE-2) (17-beta-hydroxysteroid dehydrogenase 4) (17-beta-HSD 4) (D-bifunctional protein) (DBP) (Multifunctional protein 2) (MPF-2) [Cleaved into: (3R)-hydroxyacyl-CoA dehydrogenase (EC 1.1.1.n12); Enoyl-CoA hydratase 2 (EC 4.2.1.107) (EC 4.2.1.119) (3-alpha,7-alpha,12-alpha-trihydroxy-5-beta-cholest-24-enoyl-CoA hydratase)]	1	0	0	0	0	1	1

UniProt ID	Protein names	Biological Replicate Peptide Count					Total Replicate Presence (n/5)	Total Peptide Count
		1	2	3	4	5		
P35293	Ras-related protein Rab-18	1	0	0	0	0	1	1
Q60676	Serine/threonine-protein phosphatase 5 (PP5) (EC 3.1.3.16) (Protein phosphatase T) (PPT)	1	0	0	0	0	1	1
Q61735	Leukocyte surface antigen CD47 (Integrin-associated protein) (IAP) (CD antigen CD47)	1	0	0	0	0	1	1
Q61387	Cytochrome c oxidase subunit 7A-related protein, mitochondrial (Cytochrome c oxidase subunit VIIa-related protein) (Silica-induced gene 81 protein) (SIG-81) (Supercomplex assembly factor I)	1	0	0	0	0	1	1
P35980	60S ribosomal protein L18	1	0	0	0	0	1	1
P17809	Solute carrier family 2, facilitated glucose transporter member 1 (Glucose transporter type 1, erythrocyte/brain) (GLUT-1) (GT1)	1	0	0	0	0	1	1
Q9QZB0	Regulator of G-protein signaling 17 (RGS17) (Regulator of Gz-selective protein signaling 2)	1	0	0	0	0	1	1
Q9JIA1	Leucine-rich glioma-inactivated protein 1	1	0	0	0	0	1	1
P48758	Carbonyl reductase [NADPH] 1 (EC 1.1.1.184) (15-hydroxyprostaglandin dehydrogenase [NADP(+)]) (EC 1.1.1.197) (NADPH-dependent carbonyl reductase 1) (Prostaglandin 9-ketoreductase) (Prostaglandin-E(2) 9-reductase) (EC 1.1.1.189)	1	0	0	0	0	1	1
Q64520	Guanylate kinase (EC 2.7.4.8) (GMP kinase)	1	0	0	0	0	1	1
Q4JIM5	Abelson tyrosine-protein kinase 2 (EC 2.7.10.2) (Abelson murine leukemia viral oncogene homolog 2) (Abelson-related gene protein) (Tyrosine-protein kinase ARG)	1	0	0	0	0	1	1
Q7TQI3	Ubiquitin thioesterase OTUB1 (EC 3.4.19.12) (Deubiquitinating enzyme OTUB1) (OTU domain-containing ubiquitin aldehyde-binding protein 1) (Otubain-1) (Ubiquitin-specific-processing protease OTUB1)	1	0	0	0	0	1	1
P46935	E3 ubiquitin-protein ligase NEDD4 (EC 2.3.2.26) (HECT-type E3 ubiquitin transferase NEDD4) (Neural precursor cell expressed developmentally down-regulated protein 4) (NEDD-4)	1	0	0	0	0	1	1

UniProt ID	Protein names	Biological Replicate Peptide Count					Total Replicate Presence (n/5)	Total Peptide Count
		1	2	3	4	5		
<b>P97358</b>	TATA box-binding protein-associated factor RNA polymerase I subunit B (RNA polymerase I-specific TBP-associated factor 68 kDa) (TAFI68) (TATA box-binding protein-associated factor 1B) (TBP-associated factor 1B) (Transcription initiation factor SL1/TIF-IB subunit B)	1	0	0	0	0	1	1
<b>P60122</b>	RuvB-like 1 (EC 3.6.4.12) (49 kDa TATA box-binding protein-interacting protein) (49 kDa TBP-interacting protein) (DNA helicase p50) (Pontin 52) (TIP49a)	1	0	0	0	0	1	1
<b>P14206</b>	40S ribosomal protein SA (37 kDa laminin receptor precursor) (37LRP) (37 kDa oncofetal antigen) (37/67 kDa laminin receptor) (LRP/LR) (67 kDa laminin receptor) (67LR) (Laminin receptor 1) (LamR) (Laminin-binding protein precursor p40) (LBP/p40) (OFA/iLRP)	1	0	0	0	0	1	1
<b>P35979</b>	60S ribosomal protein L12	1	0	0	0	0	1	1
<b>P19253</b>	60S ribosomal protein L13a (Transplantation antigen P198) (Tum-P198 antigen)	1	0	0	0	0	1	1
<b>Q3UM45</b>	Protein phosphatase 1 regulatory subunit 7 (Protein phosphatase 1 regulatory subunit 22)	1	0	0	0	0	1	1
<b>Q64521</b>	Glycerol-3-phosphate dehydrogenase, mitochondrial (GPD-M) (GPDH-M) (EC 1.1.5.3) (Protein TISP38)	1	0	0	0	0	1	1
<b>P02463</b>	Collagen alpha-1(IV) chain [Cleaved into: Arresten]	1	0	0	0	0	1	1
<b>Q8K596</b>	Sodium/calcium exchanger 2 (Na <sup>+</sup> /Ca <sup>2+</sup> )-exchange protein 2) (Solute carrier family 8 member 2)	1	0	0	0	0	1	1
<b>Q9Z0E0</b>	Neurochondrin (M-Sema F-associating protein of 75 kDa) (Norbin)	1	0	0	0	0	1	1
<b>P16125</b>	L-lactate dehydrogenase B chain (LDH-B) (EC 1.1.1.27) (LDH heart subunit) (LDH-H)	1	0	0	0	0	1	1
<b>Q9JMK2</b>	Casein kinase I isoform epsilon (CKI-epsilon) (CKIe) (EC 2.7.11.1)	1	0	0	0	0	1	1
<b>Q9Z0P5</b>	Twinfilin-2 (A6-related protein) (mA6RP) (Twinfilin-1-like protein)	1	0	0	0	0	1	1
<b>Q9D5W4</b>	Coiled-coil domain-containing protein 81	1	0	0	0	0	1	1

UniProt ID	Protein names	Biological Replicate Peptide Count					Total Replicate Presence (n/5)	Total Peptide Count
		1	2	3	4	5		
<b>P12382</b>	ATP-dependent 6-phosphofructokinase, liver type (ATP-PFK) (PFK-L) (EC 2.7.1.11) (6-phosphofructokinase type B) (Phosphofructo-1-kinase isozyme B) (PFK-B) (Phosphohexokinase)	1	0	0	0	0	1	1
<b>P19137</b>	Laminin subunit alpha-1 (Laminin A chain) (Laminin-1 subunit alpha) (Laminin-3 subunit alpha) (S-laminin subunit alpha) (S-LAM alpha)	1	0	0	0	0	1	1
<b>P04627</b>	Serine/threonine-protein kinase A-Raf (EC 2.7.11.1) (Proto-oncogene A-Raf)	1	0	0	0	0	1	1
<b>P28663</b>	Beta-soluble NSF attachment protein (SNAP-beta) (Brain protein I47) (N-ethylmaleimide-sensitive factor attachment protein beta)	1	0	0	0	0	1	1
<b>Q60952</b>	Centrosome-associated protein CEP250 (250 kDa centrosomal protein) (Cep250) (Centrosomal Nek2-associated protein 1) (C-Nap1) (Centrosomal protein 2) (Intranuclear matrix protein)	1	0	0	0	0	1	1
<b>Q8CGS6</b>	DNA polymerase theta (EC 2.7.7.7) (Chromosome aberrations occurring spontaneously protein 1) (DNA polymerase eta)	1	0	0	0	0	1	1

